Zic2 and *rsph9*: Two genetic controls of neural development and their impact on the vertebrate embryonic brain and craniofacial complex

By

Jessica J. TeSlaa

A dissertation submitted in partial fulfillment of

the requirements for the degree of

Doctor of Philosophy

(Cellular and Molecular Biology)

at the

UNIVERSITY OF WISCONSIN-MADISON

2014

Date of final oral examination: 8/21/2014

The dissertation is approved by the following members of the Final Oral Committee:

Yevgenya Grinblat, Associate Professor, Department of Zoology
Jeff Hardin, Professor, Department of Zoology
Anna Huttenlocher, Professor, Department of Pediatrics
Mary Halloran, Professor, Department of Zoology
Shannon Kenney, Professor, Department of Oncology

Acknowledgements

First and foremost, I have to thank my husband Josh for his unfailing support through many times of need, and for taking care of our son, Maxwell, whenever I had a late night. Thanks also to my parents, Pam and Dale Pierson, for getting me started off right.

Thanks also to Jenya Grinblat, who has been a great research mentor and expansively encouraging of my family life and my forays into teaching while a graduate student.

The past and current members of the Grinblat lab have provided many indispensible services over the years, including but not limited to Nick Sanek, Michael Zhang, Abby Keller, Irina Sedykh, and especially Molly Nyholm. Thanks also to the Halloran lab members for excellent discussions and frequent supplying of reagents.

Finally, thank you to my committee members Jeff Hardin, Anna Huttenlocher, Mary Halloran and Shannon Kenney for their help and feedback over the years.

Table of Contents

Abstract

Achieving the final complexity of the adult brain requires delicate coordination of cellular and tissue rearrangements starting very early during development. Morphogenetic movements, patterning events, and proliferation and differentiation contrive together to generate the neural epithelium surrounding appropriately shaped ventricles filled with circulating cerebrospinal fluid. The work discussed in the following chapters revolves around two disparate aspects of neural development, and how these seemingly peripheral processes impact neurulation, ventricle shaping, and craniofacial development. Initially, both of these projects sprang from previous work examining the role of the *zic* family of transcription factors in regulation of midbrain morphogenesis. As the projects progressed, they became to a greater or lesser degree separated from this initial grounding. In Chapter 2, I discuss the role of the zebrafish *zic2* paralogs in regulating neural crest development, and identify *zic2a* as having parallel roles during craniofacial development. The work presented in Chapter 3 stemmed from a microarray identifying several motile cilia genes as potential *zic* effectors. Although the connection between motile cilia and the *zic* genes became tenuous upon further investigation, it had also become clear that cilia have an interesting role during neurulation and ventricle inflation. In Chapter 3, I demonstrate that *rsph9*, which encodes a structural component of motile cilia, is required for ciliogenesis in the neural tube, and show that Rsph9 knockdown in zebrafish recapitulates some aspects of the human disorder primary ciliary dyskinesia. The microarray itself is discussed in the Appendix.

Chapter 1:

Introduction

The study of embryonic development is one of the oldest scientific disciplines known to man, and study of the brain dates back at least to the ancient Greeks. At the turn of the 15th century, Leonardo da Vinci generated some of the first accurate and detailed drawings of the adult brain and its ventricles, using cadavers and the artistic technique of wax injection (Tascioglu and Tascioglu, 2005). Since then, our knowledge of the brain and its development has advanced through several revolutionary periods. In the 19th century, descriptive embryologists made use of improved microscopy techniques to describe series of carefully staged embryos from different species (Churchill, 1991). The beginning of the 20th century saw experimental embryologists Mangold and Spemann manipulating newt embryos to determine how neural tissue is first induced. Finally, the relatively recent advent of molecular biology ushered in the current era of research into the molecular mechanisms that drive neural development.

Building the final complexity of the adult brain requires delicate coordination of cellular and tissue rearrangements starting very early during development. Early embryonic neural development can be conveniently summarized as the result of tissue morphogenesis, patterning, and growth. These three mechanisms contrive together to generate the neural epithelium, which surrounds ventricles filled with circulating cerebrospinal fluid. The work contained in this thesis covers two disparate aspects of neural development. First, I discuss the *zic* family of transcription factors and how their patterning of the neural crest has widespread effects in the embryo. Second, I characterize the role of the radial spoke head gene *rsph9* and its importance during motile ciliogenesis in the neural tube.

Neural development – from induction to neurulation

The vertebrate neural epithelium is induced from ectodermal tissue when secreted signaling molecules from the organizer (or shield, in zebrafish) such as *chordin* and *noggin* inhibit BMP signaling, which would otherwise promote an epidermal fate (reviewed in Ozair et al., 2012). Specialized tissues including the neural crest and sensory placodes are specified at the lateral and anterior borders of the neural ectoderm. Regionalization of the neural tissue along the anterior-posterior axis requires multiple signaling centers and posteriorizing cues such as Wnt and Fgf, which promote the division of the central nervous system (CNS) into the three primitive brain compartments, the forebrain, midbrain and hindbrain, along with the posterior spinal cord. Patterning along the dorsal-ventral axis is the result of a gradient of secreted signaling molecules emanating from the floorplate (Hedgehog signaling) and roofplate (BMP signaling), which induce combinatorial expression of transcription factors in the neural epithelium.

Meanwhile, the neural epithelium is also undergoing the massive spatial rearrangement termed neurulation, wherein the originally flat sheet of the neural plate is folded up into the neural tube (reviewed in Lowery and Sive, 2004; Harrington et al., 2009). In the anterior neural tube, fated to become the brain, columnarization of the neural ectodermal cells is followed by bending at one or more hinge points and finally closure at the dorsal midline and separation from the overlying ectoderm. The

appropriate patterning events and morphogenetic movements during this time are critical for adult CNS function.

Co-regulation of the embryonic brain and face

The craniofacial complex, which is broadly divided into two parts, has several indispensable functions in vertebrates. The neurocranium houses the brain, while the viscerocranium makes up the jaw and supports the oropharynx (reviewed in Wilkie and Morris-Kay, 2001). Craniofacial structure varies widely among the gnathostomes, but even within a single species there are as many facial shapes as there are individuals. Our faces make us both immediately recognizable as humans, and also differentiate us from one another.

Embryonic brain and craniofacial development are intimately linked, and this relationship often manifests as a tight correlation of brain malformations with craniofacial defects. This is likely true for several reasons. To some extent, the brain provides a physical scaffolding around which the face must be built. On a molecular level, the neural, chondrogenic and facial ectodermal tissues are intimately associated and signal back and forth to one another throughout development, rendering it unlikely that one would escape unharmed when the other is affected in some way (reviewed in Marcucio et al., 2011). For example, in humans with brain malformations such as holoprosencephaly, the most severe neural phenotypes almost always correspond with the worst spectrum of craniofacial abnormalities (Dubourg et al., 2007).

The neural crest

That humans have what we refer to as ‘faces’ is largely thanks to the vertebrate innovation of the neural crest (NC). Much of the craniofacial complex is derived from cranial (cephalic) NC cells, so named because of their origin in the dorsal folds of the mammalian neural epithelium, which look like ‘crests’ as they approach each other at the midline. The first scholarly summary of the NC was published in 1950 by Hörstadius, who collected research conducted since the NC was first described in 1868. Since then, our knowledge of this so-called fourth germ layer has multiplied by leaps and bounds, and today there is a rich landscape of literature examining almost every aspect of NC development.

The NC is a vertebrate-specific population of multipotent cells that arise at the neural plate border during late gastrulation. During the course of neurulation, NC cells undergo an epithelial to mesenchymal transition and delaminate from the basal aspect of the neural tube. They then follow multiple migratory routes towards their endpoint destinations, where they differentiate into numerous cell types that contribute to a wide array of tissues. These include neurons and glia of the peripheral nervous system, pigment cells of the skin, and the cartilage and bone of the craniofacial skeleton, among others (Le Douarin and Kalcheim, 2009).

Neural crest induction and specification

The NC arises at the lateral interface of the neural and non-neural ectoderm, where signals during gastrulation induce a relatively broad region of overlapping medial

neural and lateral ectodermal markers that define the neural plate border (NPB). Expression of these genes is progressively restricted and bilateral domains expressing unique markers of NC become apparent. Secreted molecules from the neural and non-neural ectoderm are vital for NC induction in most organisms, while the role of signaling from the underlying mesoderm seems to vary (it is not required in zebrafish) (reviewed in Stuhlmiller and Garcia-Castro, 2012).

NC development requires both an initial induction signal during gastrulation and subsequent signaling during neurulation to maintain the population. Induction is the result of a combination of Wnt, Fgf and BMP signaling. During gastrulation, BMP signaling must be modulated to a permissive level, allowing a 'zone of competency' to arise at the NPB (Marchal et al., 2009; Steventon et al., 2009). The cohort of NPB genes expressed in and around this region includes *pax3, pax7, msx1,* and *zic1* (Basch et al., 2006; Sato et al., 2005; Tribulo et al., 2003). Canonical Wnt signaling induces expression of some of these NC specifiers, although its requirement for induction is not clear in all organisms (Dorsky et al., 1998; Garcia-Castro et al., 2002). Fgf signaling is similarly capable of inducing early NPB and NC marker genes (Monsoro-Burq et al., 2003; Stuhlmiller and Garcia-Castro, 2012). All three signaling pathways interact with one another in a manner dependent on the organismal context. For example, Fgf signaling can modify both Wnt and BMP signals, although which tissue Fgfs act on is unclear (Hong et al., 2008; Wilson et al., 2000). Subsequently, NC maintenance during neurulation requires reiterated Wnt and BMP signaling (Lewis et al., 2004).

The signaling pathways outlined above induce the expression of transcription factors that delineate the NPB, which in turn promote expression of genes specific to the NC, which in zebrafish include *foxd3*, *sox9b*, *sox10*, and *tfap2a*, among others (Barrallo-Gimeno et al., 2003; Dutton et al., 2001; Li and Cornell, 2007; Stewart et al., 2006). These NC specifiers direct subsequent NC development, including delamination and migration. Changes in adhesion, polarity and motility allow NC cells to undergo an epithelial to mesenchymal transition and migrate away from the NT (reviewed in Clay and Halloran, 2010; Theveneau and Mayor, 2012). Mechanisms promoting NC delamination and initiation of migration include cadherin switching, tight junction dissolution, remodeling of the extracellular matrix, and localized actomyosin contraction. Directed migration is achieved by a variety of chemoattractant/repellent interactions between the NC and surrounding tissues.

The fate of a given NC cell is to some extent dependent on its position of origin along the anterior-posterior and medial-lateral axis of the NT. The spatial sensitivity of cell fate is also intermingled with a temporal aspect of lineage segregation. NC cells emigrating earlier or from different dorsal-ventral aspects of the NT encounter and respond to a different complement of signals than those exiting later. Current models suggest that a mix of pre- and post-migratory, intrinsic and extrinsic influences combine to generate NC cell fate *in vivo* (reviewed in Le Douarin et al., 2004; Takahashi et al., 2013).

It is important to note that while most of the induction signals, NPB, and NC specifier genes are shared among vertebrate species, their hierarchical relationships

may not be identical (reviewed in Stuhlmiller and Garcia-Castro, 2012). Also, the importance of the tissue and its proximity to so many signaling inputs means that NC development must remain robust in the face of variability. A recent study in zebrafish was one of the first to highlight how semi-redundant enhancer elements render expression of NPB genes *pax3* and *zic3* robust in response to varying signaling levels from multiple pathways (Garnett et al., 2012).

The subsequent sections deal specifically with the two NC-derived cell types addressed in Chapter 2: the pigment cells, and the ectomesenchymal cells that contribute to the craniofacial structure. The focus will be on their development in zebrafish, as it has been already been pointed out that the specifics of NC regulation can be quite varied among organisms.

Neural crest contribution to pigment cells

Unlike mammals, which have only melanocytes, zebrafish have two additional types of pigment cells – xanthophores, which are given their yellow color from the presence of pteridines and carotenoids, and iridophores, which are iridescent with reflective platelets (reviewed in Kelsh et al., 2009). Pigment precursors in the cranial NT are generated in response to Wnt signaling, which in zebrafish promotes chromatophore development at the expense of sensory neurons (Dorsky et al., 1998; Lewis et al., 2004). A distinct pathway mediates the development of each class of pigment cell. The NC specifier *sox10* is vital for melanophore specification. In zebrafish, Wnt signaling and *sox10* are both upstream of the chromatophore-specific

mitfa gene, which is itself required for generating the appropriate number of melanocytes (Dorsky et al., 2000; Dutton 2001; Elworthy 2003). Meanwhile, xanthophores alone among the pigment cells are affected by *pax3* knockdown (Minchin and Hughes, 2008; Odenthal et al., 1996).

Differences in the pigment cell genetic program read out as differences in developmental timing. In the zebrafish trunk, melanophores begin migrating earlier and on a different route compared to the xanthophores. Specification and restriction of the pigment cell lineages, particularly melanophores, has important implications for disease. An understanding of the genetic factors driving the formation of differentiated melanocytes from multipotent NC precursors, and when this occurs, will provide insights into the progression of melanoma in the adult. For example, human metastatic melanoma cells seem to respond to environmental cues when transplanted into the chick premigratory NC environment, and undergo reprogramming to a more NC-like state (Kulesa et al., 2006).

Neural crest contribution to craniofacial development

NC cells that contribute to craniofacial structures all originate in the cranial neural tube, at anterior-posterior levels ranging from the diencephalon to the hindbrain. In zebrafish, midbrain NC cells migrate anteriorly to condense in positions where they will contribute to the anterior neurocranium (the ethmoid plate and trabeculae) (Wada et al., 2005). Hindbrain NC cells migrate in three separate streams to populate the pharyngeal arches, which will form the cartilages of the jaw (Meckel's cartilage, hyoid, and branchial

arches) (Schilling and Kimmel, 1994; Schilling and Kimmel, 1997). The chondrogenic NC expresses genes associated with mesenchymal condensations, including *dlx* and *sox9* transcription factors. Mutations disrupting the cephalic neural crest are frequently associated with defects in craniofacial development. Disruption of genes affecting chondrogenic NC specification (*sox9b*, Yan et al., 2005; *dlx2a*, Sperber et al., 2008) and survival (*vgl2a*, Johnson et al., 2011) result in neural crest deficits and craniofacial abnormalities. The interactions between extrinsic pre-migratory signals, cues intrinsic to migratory NC cells, and their post-migratory environment are complex and not well understood. Development of the craniofacial complex offers an important system within which to study these interactions.

Craniofacial development

Facial skeleton development is quite intricate and requires the action of multiple organizing centers. In order to get the job done, the foregut endoderm, the facial ectoderm, the forebrain neural epithelium and the chondrogenic cells themselves engage in signaling crosstalk with many spatial and temporal complexities (reviewed in Szabo-Rogers et al., 2010). For the purposes of this introduction, I will focus on those tissue interactions and signaling pathways that have the most bearing on the studies included herein.

Hedgehog (Hh) signaling is a vital force at many times and places during embryogenesis, but particularly during ventral patterning (reviewed in Lupo et al., 2006). It has a key role in the forebrain, where it is secreted by the ventral diencephalon and

patterns surrounding tissues such as the optic stalk and retina (Chiang et al., 1996). Large-scale zebrafish mutagenesis revealed that many Hh pathway mutants also have craniofacial abnormalities (Brand et al., 1996). Global inhibition of Hh signaling in chick causes cell death in the chondrogenic NC populating the face, while blockade specifically from the neurectoderm disrupts *Shh* expression in the ectoderm and subsequent growth of the frontonasal prominence (Ahlgren and Bronner-Fraser, 1999; Marcucio et al., 2005). Conversely, overactive Hh signaling in the forebrain promotes excessive outgrowth of the fronto-nasal process (Hu and Marcucio, 2009).

Hh signaling is clearly required during craniofacial development, but its ablation has such widespread effects that dissecting its specific roles requires great care. Studies in zebrafish have identified several independent roles for Hh signaling during development of the anterior neurocranium. Genetic mosaic analyses revealed that, during late gastrulation, Hh signaling from the ventral forebrain patterns the roof of the oral epithelium (stomodeum), many hours prior to NC arrival, rendering it competent as a substrate for NC cell condensation (Eberhart et al., 2006). Further experiments suggest that during NC migration, Hh signaling from the ventral forebrain provides a repulsive cue to prevent mixing of ectomesenchymal cells at the midline (Wada et al., 2005). Additionally, after NC migration is complete, Hh signaling from the facial ectoderm and ventral hypothalamus induce chondrification in the ethmoid plate and trabeculae.

Jaw cartilages derived from the pharyngeal arches depend on Hh signaling as well, with early disruption resulting in mandibular defects and late disruption affecting

more posterior cartilages (Schwend and Ahlgren, 2009). Transplantation of wild-type NC into zebrafish *smoothened* mutants rescues some pharyngeal arch defects, indicating a cell-autonomous requirement for Hh in the NC, but further transplant analysis revealed that both the NC and the pharyngeal endoderm are recipients of Hh signaling as well (Swartz et al., 2012).

The optic vesicle is also thought to convey important information during cranial neural crest invasion of the head and arches (reviewed in Kish et al., 2011). During their migration, cranial NC cells come into close contact with the retina and optic stalk structures, making it likely that they exchange some information with one another. Indeed, in eyeless *chokh* mutant zebrafish, NC cells migrating along the dorsal anterior pathway to contribute to the medial ethmoid plate accumulate at the edge of the presumptive eye field, indicating that they lack some vital information (Langenberg et al., 2008). Another study showed that platelet-derived growth factor (PDGF) emanating from the optic stalk region influences the migratory path of NC cells expressing the PDGF receptor (Eberhart et al., 2008). The role of the optic vesicle is possible the least well-studied of those providing migratory cues during development.

Brain malformations associated with craniofacial defects

Holoprosencephaly (HPE) is the most common malformation of the forebrain in humans, and it usually presents with craniofacial malformations (Dubourg et al., 2007). HPE results from a failure of the prosencephalon to fully divide into two hemispheres during the first month of development. It is rare in live births (about 1 in 16,000) but

relatively common among conceptuses (about 1 in 250). The severity of clinical presentation runs a continuum from mild microform, with no appreciable neural anomalies and subtle facial abnormalities, to an alobar forebrain with no hemispheric division and severe craniofacial defects. The brain anomalies present in HPE patients are almost always mirrored by craniofacial defects of comparable severity, with the notable exception of patients with *ZIC2* mutations. More severe phenotypes include cyclopia and facial clefts, while a mildly affected individual may have nothing more abnormal than a single incisor at the midline.

HPE has a complex etiology. At least 13 loci have been identified as susceptible to autosomal dominant mutations that lead to HPE (Roessler and Muenke, 2010). Of these, the most commonly affected is *SHH*, although several other genes in the Hh signaling pathway are implicated, including *PTCH* and *GLI2* (Roessler et al., 1996). Other causally linked genes include *ZIC2* and *SIX3*. However, more than 70% of all HPE cases remain without a distinct genetic cause, leading to the 'multiple hit' theory. This posits that multiple genetic, chromosomal, environmental and metabolic risk factors combine to account for the variability in phenotype observed in patients with HPE.

Zic transcription factors

Transcription factors present as a single gene in protochordates have frequently been expanded through duplications into families of genes in vertebrates. This process is likely a factor in the elaboration of the CNS into the large, complex structure found in

vertebrates. Examples of these important neural transcription factors families include the *Pax*, *Dlx* and *Zic* genes (Shimeld and Holland, 2000).

The *Zic* (*zi*nc finger of the *c*erebellum) genes encode a family of transcription factors, each with five C_2H_2 zinc finger domains, which have vital roles in the developing and adult CNS. *Zic* genes are the vertebrate orthologs of the Drosophila pair-rule gene *opa* (odd-paired, DiNardo and O'Farrell, 1987; Benedyk et al., 1994). The first vertebrate *zic* was identified in a screen for cerebellum-enriched transcripts in the mouse (Aruga et al., 1994). Subsequently, it was determined that, while most vertebrates have five zic genes, zebrafish have seven, due to the whole genome duplication in teleosts (Meyer and Van de Peer, 2005). *Zic*s share high sequence identity in the zinc fingers, with a divergent C-terminal region. They are arranged in the genome in pairs, such that each member of the pair is divergently transcribed away from a shared intergenic regulatory region.

*Zic*s are expressed in highly overlapping but distinct domains in the developing and adult CNS, and as such are expected to have some functional redundancy (reviewed in Merzdorf, 2007). The basic early embryonic functions defined for Zic genes include (1) patterning the neural epithelium, (2) regulating the balance between proliferation and differentiation in neural progenitors, and (3) regulating the morphogenetic movements of neurulation. Zics are important in all of these capacities. For example, neural induction in *Xenopus* is thought to rely on *zic1* (downstream of BMP inhibition) and *zic3* (likely a direct target of Fgf signaling) (Marchal et al., 2009). Zic1 promotes proliferation of neural precursors in the trunk, at the expense of

differentiating neurons (Aruga et al., 2002). Zic2a and Zic5 knockdown in zebrafish causes neurulation defects (Nyholm et al., 2009).

Zics and the neural plate border

Zic function in the vertebrate CNS is at least partially preserved from its role in the protochordates. One Zic gene has been identified in amphioxus, while ascidians appear to have two. In both cases, Zics are expressed in the neural tissue quite early, and ascidians with depleted *HrZicN* do not neurulate appropriately, a defect also observed in vertebrates with disrupted *Zic2* and *Zic5* (Inoue et al., 2004; Wada and Saiga, 2002; Ybot-Gonzalez et al., 2007). There is also evidence that *Zic*s played a role in another vertebrate innovation, the neural crest. Comparison of *Zic* gene expression in the neural plate border region of tunicates and amphioxus with their expression in vertebrates suggests they may have assisted in the specialization and neo-functionalization of this group of cells (Gostling and Shimeld, 2003).

In vertebrates, *Zic* genes are expressed in and participate in defining the neural plate border (NPB) region during late gastrulation and early neurulation. Much of the early work on *Zic* genes and their role at the NPB was done in *Xenopus* embryos. One of the earliest papers showing that *Zic2* expression is a repressor of neuronal differentiation also suggested that this function relates to Zic2's role during NC induction (Brewster et al., 1998). Overexpression of Zic1, Zic2, Zic3 and Zic5 in animal cap explants induces expression of neural crest markers and results in ectopic pigment cells (Nakata et al., 1997; Nakata et al., 1998; Nakata et al., 2000).

To date, the most concentrated efforts have been on dissecting the role of *Zic1* at the *Xenopus* NPB. It was first noted that overexpression of Zic1 and Pax3 induces NC-specific markers in a Wnt-dependent manner during gastrulation (Sato et al., 2005). Several further studies showed that Zic1 and Pax3 regulate other border fates such as pre-placodal cells independently, but their combined action is required for NC specification (de Croze et al., 2011; Hong and Saint-Jeannet, 2007). In fact, in *Xenopus*, Pax3 and Zic1 are thought to be the defining factors sufficient for NC specification, and NC induced by these proteins *in vitro* are capable of appropriate differentiation and migration when transplanted into an embryo (Milet et al., 2012). A pair of recent papers identified many NC-specific genes such as *snail2*, *foxd3* and *twist* as likely direct targets of Zic1 (Bae et al., 2014; Plouhinec et al., 2014)

Study of mouse zic mutants confirmed the role of *Zic*s at the NPB and revealed an additional requirement during forebrain development. Hypomorphic *Zic2* mouse mutants have deficits in some NC-derived structures and highly penetrant HPE (Nagai et al., 1999). This is due at least in part to delayed neurulation. Similarly, the Zic2-null mutant Kumba has reduced numbers of NC cells due to delayed induction, as well as forebrain defects (Elms et al., 2003). *Zic5* mutant mice have a similar reduction in cephalic NC cell number that correlates with craniofacial abnormalities including jaw truncation (Inoue et al., 2004).

Zics regulate forebrain development

The restricted expression of *zic* genes in the embryo, and the role of *Drosophila* homolog *opa* as a pair rule gene required for body pattern, made *ZICs* likely candidates for human malformation syndromes. The first such association was made when *ZIC3* mutations were identified as causing L/R axis defects in humans (Gebbia et al., 1997. *ZIC2*, with its prominent expression in the embryonic brain, was identified as a candidate disease susceptibility gene by virtue of being part of a minimal critical region missing in 13q32 deletion syndrome (Brown et al., 1995). *ZIC2* was subsequently confirmed as the second gene causatively associated with HPE (Brown et al., 1998). *In vitro* analysis of several types of endogenously occurring *ZIC2* mutations revealed that both loss- and gain-of-function mutations are associated with HPE, indicating that any imbalance in ZIC2 transcriptional activity has an effect on neural development (Brown et al., 2005). It is currently thought that up to 9% of HPE patients have *ZIC2* mutations (Roessler et al., 2009; Solomon et al., 2010b).

Unlike HPE associated with genes such as *SHH* and *SIX3*, humans with *ZIC2* mutations almost always have a relatively subtle, although well-defined, set of craniofacial defects. Very few patients have the most severe craniofacial manifestations of HPE. Instead, a less severe phenotype usually includes bitemporal narrowing, upslanting palpebral fissures, and several mild abnormalities of the nose (Mercier et al., 2011; Solomon et al., 2010a). Unusual among the HPE genes, the majority of *ZIC2* mutations are *de novo*, and it is uncommon to find individuals from multiple generations with *ZIC2*-associated HPE. Along with a statistical correlation of *ZIC2* mutations with

the semilobar form of HPE, this suggests that perhaps *ZIC2* mutations are more likely to cause a severe phenotype not compatible with life (Solomon et al., 2010b).

The mouse *Zic2* mutant has provided clues as to one possible mechanism leading to HPE. Zic2 is required during mid-gastrulation for development of the pre-chordal plate, a vital source of Hh signaling (Warr et al., 2008). *Zic1* has also been shown to mediate medial forebrain development in the mouse (Inoue et al., 2007), while Zic1 knockdown in the zebrafish results in phenotypes reminiscent of Hh loss-of-function such as cyclopia and ventral midline defects (Maurus and Harris, 2009). Work in the Grinblat lab has established a role for *zic2a* in the zebrafish forebrain. Although the malformations present in HPE cannot be strictly recapitulated in zebrafish, zic2a morphants do display forebrain deficits such as a smaller prethalamic domain (Sanek and Grinblat, 2008). Zic2a is also expressed in the distal optic stalk, and acts downstream of Hh signaling to non-cell autonomously pattern the optic stalk-retinal border by repressing Hh-induced gene products (Sanek et al., 2009). Specifically, Zic2a restricts expression of Hh signaling targets such as *fgf8a* and *pax2a*.

Neural development – from neurulation to ventricle inflation

A vital step during neurulation is the formation of the open lumen, which is necessary for subsequent shaping of the brain ventricles and their filling with embryonic cerebrospinal fluid (eCSF). In tetrapods, the lumen is formed when the neural folds (from which the NC are actively exiting) meet and fuse at the dorsal midline (reviewed in Lowery and Sive, 2004). In zebrafish, although many of the important cellular

mechanisms are conserved, the lumen opens secondarily within the closed neural rod (Hong and Brewster, 2006). During lumen formation, both fish and tetrapods start to generate the complexity of shape that characterizes the adult brain. Along the dorsal-ventral axis, the neural epithelium bends at medial and lateral hinge points. Along the anterior-posterior axis, the neural tube also develops characteristic constrictions that define the brain ventricles.

Ventricle shape is highly preserved among organisms. The first visible ventricle in the zebrafish is in the midbrain and begins to open at about 18S (18hpf). Subsequently, the fore- and hindbrain ventricles take shape. By 24hpf, the three compartments of the brain each have their own ventricle filled with embryonic CSF. Ventricle formation is an important but neglected step of neural development, as most attention has been focused on the morphogenesis of the neural tube and neural differentiation. Mechanisms driving ventricle inflation are poorly understood, but involve the action of ion pumps (Lowery and Sive, 2009).

Embryonic CSF during neural development

CSF is a secreted fluid containing a complex mixture of macromolecules and ions that fills all four mammalian ventricles, the spinal canal, and the subarachnoid spaces (reviewed in Lehtinen et al., 2013). It is generated by the choroid plexuses, groups of specialized epithelial cells lining the lateral and fourth ventricles. Adult CSF has important homeostatic functions, removing metabolic waste and protecting the brain from injury. Embryonic CSF (eCSF) is very different from adult CSF, and is likely

dynamic in composition throughout development (reviewed in Gato and Desmond, 2009). Compared to adult CSF, eCSF has much higher protein content, and contains growth factors and signaling molecules important for neural development (Lehtinen et al., 2011; Zappaterra et al., 2007). The initial source of eCSF is not clear, since the choroid plexus does not form until well after the ventricles have already filled with CSF. For example, the zebrafish hindbrain choroid plexus is mature at 144hpf, while eCSF can be found in the brain by 24hpf (Garcia-Lecea et al., 2008). Several possible sources of eCSF have been suggested. It may be secreted from the apical surface of all or a subset of neurepithelial cells (Montecinos et al., 2005), or components may be transported across the neural epithelium from the serum (Martin et al., 2006).

Embryonic CSF serves at least two basic functions. First, it provides intracranial pressure that supports the rapid growth of the brain, and its removal causes collapse of the neural epithelium into the ventricles (reviewed in Lowery and Sive, 2009; Chang and Sive, 2012). This same pressure is thought to stimulate proliferation of periventricular cells (Desmond and Jacobson, 1977). Second, eCSF contains trophic factors that direct migration of neurons from the subventricular zone to their final destinations (Sawamoto et al., 2006). This occurs in part because fluid flow generated by ependymal cilia creates a gradient of guidance cues in the CSF.

Hydrocephalus is a disorder of the brain ventricles characterized by abnormal accumulation of CSF, resulting in increased ventricle size. There are three mechanisms that can drive disease progression: generation of excess CSF, impaired reabsorption of CSF, or physical obstruction of the ventricles, usually at the cerebral

aqueduct between the third and fourth ventricle (reviewed in Zhang et al., 2006). Dyskinetic or immotile ependymal cilia are thought to be a primary cause of blockage, but how this occurs is not well understood. Ablation of motile cilia, as in the *foxj1* mutant mouse or the zebrafish *foxj1a* knockdown model, results in hydrocephaly (Brody et al., 2000; Kramer-Zucker et al., 2005). More specific disruption of motile cilia components, such as *Hydin* or *Spag6*, has a similar effect (Davy et al., 2003; Lechtreck et al., 2008; Sapiro et al., 2002). Interestingly, mutations in genes such as *Mdnah5* that cause hydrocephalus the majority of the time in mouse models result in only low-penetrance hydrocephalus in humans (Ibanez-Tallon et al., 2002).

Motile cilia in development

Cilia are microtubule-based organelles that project from the apical surface of most vertebrate cell types. The study of cilia has a long and sometimes ignominious history. Cilia were first described by Anton van Leeuwenhoek in 1675, more than a hundred years before they were given a name. Short, immotile primary cilia were observed on many cell types, but research languished under the belief that they were vestigial and had no purpose. We now know that primary cilia serve numerous vital sensory and signaling functions. Motile cilia have been studied more consistently, if only because their biological function in providing motility seemed obvious from the start.

Classical motile cilia have nine outer microtubule doublets surrounding a central microtubule pair. This in contrast to primary cilia, which lack the central pair. Motile cilia

are relatively long and beat in a planar waveform in order to move a cell about or generate extracellular fluid flow. The details of their structure and the mechanics of beating are still being investigated in the alga *Chlamydomonas reinhardtii*, even as research on motile cilia expands into the much more complex vertebrate organisms.

The best-studied vertebrate tissues with motile cilia have cells sporting large numbers of 9+2 cilia. Multiciliated cells in different organs usually share the common purpose of moving viscous fluid across tissue surfaces (reviewed in Fliegauf et al., 2007). Among these tissues are the brain ependyma and the respiratory and oviductal epithelia. Multiciliated cells have roles in adult homeostasis; for example, clearance of mucus from the airway, and generating the laminar flow of CSF in the ventricles. In the developing embryo, there are a number of other ciliary structures and beating types (reviewed in Choksi et al., 2014). The mammalian node has motile cilia that are vital for establishment of the left-right axis. The majority of these have a 9+0 microtubule arrangement, and beat in a circular rather than planar waveform (Sulik et al., 1994). Cilia with similar 9+0 structure and circular waveform are present in the zebrafish spinal canal (Kramer-Zucker et al., 2005).

In general, it is thought that 9+2 cilia have a planar waveform, while if 9+0 cilia are motile, they beat in a rotational manner. However, the relationship between ciliary structure and waveform is somewhat blurred, and there are examples of atypical ciliary motility. For example, the cilia in zebrafish Kupferr's vesicle are 9+2 but display a rotational waveform (Kramer-Zucker et al., 2005). Both 9+0 and 9+2 cilia have been observed in the mouse node and the zebrafish spinal canal, but thus far only rotational

movement has been reported (Caspary et al., 2007; Sarmah et al., 2007). The converse, a 9+0 cilium with a planar waveform, has not been directly shown, but there are hints that these cilia may exist in the cranial neural epithelium.

Study of the embryo has also made it clear that there are a variety of ciliary arrangements on the cell. Cells of the node and Kupferr's vesicle each have only a single motile cilium. Mouse spinal canal cells are biciliated, with a 9+2 structure, but their beating waveform has not been reported (Luse, 1956). In zebrafish, the pronephric ducts have a mixture of multi- and mono-ciliated cells (Kramer-Zucker et al., 2005). Additionally, cilia are not static entities in the embryo. The developing neural tube presents an increasingly complicated picture of cilia population dynamics. In the *Xenopus* cranial neural tube, ependymal cells begin with elongating monocilia and then gradually become multiciliated (Hagenlocher et al., 2013). In the mouse choroid plexus, a mixture of 9+0 and 9+2 cilia display both planar and rotational beating, and are in fact only transitorily motile during the perinatal period (Narita et al., 2012; Nonami et al., 2013). These studies combine to highlight the changeable nature of ciliary populations, particularly in the brain, and that we have only the barest understanding of how modes of ciliogenesis are regulated during development.

Structure and regulation of motile cilia

The specifics of the 9+2 ciliary structure and how motility is regulated has been extensively studied in the flagellum of the single-celled alga *Chlamydomonas reinhardtii*. Each 9+2 motile cilium has repeating structural units associated specifically with motility

(every 96nm in most organisms). These are composed of four outer dynein arms, three inner dynein arms, one nexin link and three radial spokes (reviewed in Salathe et al., 2007). Outer dynein arms are ATPase-containing complexes anchored to the A microtubule of each outer doublet, and their transient interactions with the B tubule of the neighboring doublet causes the microtubules to slide past one another. The bending that characterizes ciliary beating is generated by asymmetrical dynein activation, while nexin links anchor the filaments to one another. The biology of inner dynein arms is more complex, but they are thought to regulate specific aspects of ciliary beating, rather than being absolutely required for motility.

The exact function of the central pair, its sheath, and radial spokes is unclear. Current models speculate that these structures relay signals to the dynein arms that modulate ciliary beat frequency and waveform. In order to generate fluid flow, cilia have an effective stroke followed by a recovery stroke whose frequency and waveform can have many variations. Mechanisms that regulate both *Chlamydomonas* and mammalian ciliary beating include intracellular calcium concentration, pH, and cAMP-dependent phosphorylation (reviewed in Salathe, 2007). Under physiological conditions, *Chlamydomonas* mutants lacking the radial spoke or central pair have immotile cilia, but motility can be restored by reducing ATP concentration or in the presence of suppressor mutations, indicating that radial spokes are modulators of and not required for ciliary beating (Omoto et al., 1996).

Radial spokes are composed of 23 proteins comprising a stalk, neck and head region, and are currently thought to be specific to 9+2 cilia (reviewed in Pigino and

Ishikawa, 2012). The stalk is stably connected to the outer doublet, near the inner dynein arm, while the head is thought to make transient contact with the central pair. A recent paper showed that obstruction of the radial spoke head-central pair interaction by streptavidin binding paralyzes the *Chlamydomonas* flagellum, while extending the length of radial spokes in mutants lacking spoke head proteins reinstates the collision between the radial spokes and central pair and restores motility (Oda et al., 2014). The current data support a model wherein radial spokes can respond to calcium signaling directly or transduce mechanical stimulation from the central pair, translating this input to the dynein arms by altering their phosphorylation state, and thereby regulating ciliary beating (reviewed Porter and Sale 2000).

Only a few radial spoke proteins have been characterized individually, but those that have are all consistent with this hypothesis. The neck protein RSP2, for example, was identified as a novel kinase that binds calmodulin, lending support to the theory that radial spokes can modulate motility in response to changes in calcium levels (Yang et al., 2004). RSP20, a component of the stalk, belongs to the calmodulin family (Yang et al., 2001). The stalk protein RSP3 and its mammalian homolog *RSPH3* are A-kinase anchor proteins (AKAPs), responsible for not only attaching the radial spoke to the outer doublet, but also for anchoring camp-dependent protein kinase (PKA) to the axoneme and providing a mechanism for cAMP-responsive modulation of ciliary beating (Jivan et al., 2009). The proteins of the spoke head remain perhaps the most mysterious. They have no known domains apart from membrane occupation and recognition nexus (MORN) motifs in RSP1 and RSP10 (Yang et al., 2006). This suggests a relationship

with calcium signaling, but has not been tested experimentally. Much remains to be learned about the role that radial spokes play in motile cilia.

Motile cilia in disease

The first disease link to cilia was established in 1976 when Afzelius published his study of four subjects with Kartagener syndrome. Now we recognize many human ciliopathies, but those involving motile cilia are known as primary ciliary dyskinesia (PCD). PCD is a genetically heterogeneous disorder, usually recessively inherited. Clinical presentation is characterized by a combination of chronic respiratory infections due to impaired mucociliary clearance, left-right axis defects, infertility, and sometimes hydrocephaly, all as a result of defects in motile cilia (reviewed in Knowles et al., 2013a).

A concerted effort has been made in the last several years to identify genetic causes of PCD. In 2013 and 2014 alone, at least ten new genes were identified as mutated in humans with PCD, meaning that there are now 31 genes associated with PCD (Antony et al., 2013; Austin-Tse et al., 2013; Hjeij et al., 2013; Horani et al., 2013; Knowles et al., 2013b; Kott et al., 2013; Moore et al., 2013; Onoufriadas et al., 2014a). These include components of the inner and outer dynein arms, radial spoke and central pair proteins, and cytoplasmic proteins presumed to have functions in ciliary assembly. Thus far, the spoke head components *RSPH1*, *RSPH4A*, and *RSPH9* are the only three radial spoke genes with PCD-causing mutations recovered in humans (Castleman et al., 2009; Knowles et al., 2014; Kott et al., 2013; Zietkiewicz et al., 2012).

Humans with mutations in the radial spoke head genes have a specific set of ciliary defects, including incompletely penetrant alterations in waveform and beat frequency of respiratory epithelial cells (Chilvers et al., 2003). Beating phenotypes are highly variable both between patients and within an individual. Some patients with an *RSPH1* mutation have uniformly immotile cilia, whereas others have normal, slow and immotile cilia within the same airway sample (Kott et al., 2013). Radial spoke head mutations are also associated with a specific type of ciliary ultrastructural problem, the transposition defect (Castleman et al., 2009; Zietkiewicz et al., 2012). This involves loss of the central pair and movement of an outer microtubule doublet into the center of the axoneme, usually at a distal location. This defect is also not fully penetrant, occurring in anywhere from 20-70% of cilia in a given patient, and results in a change in ciliary waveform (Daniels et al., 2013; Kott et al., 2013; Zietkiewicz et al., 2012). Subphenotypic knockdown of Rsph9 in zebrafish results in conversion of some nasal cilia from a planar to a rotational waveform, a phenotype also observed in human airway cells (Castleman et al., 2009; Onoufriadis et al., 2014b).

Although our knowledge of the cellular and molecular mechanisms driving early neural development, and their genetic controls, has expanded hugely in the past few decades, we are just beginning to probe the complexities of brain development. In the following chapters, I present work characterizing two such genetic regulators of early neural development in the zebrafish. In Chapter 2, I show that the *zic2* genes promote neural crest development. I find that *zic2* genes are collectively required for timely neural crest specification and migration, which in turn is important for development of

the jaw and neurocranium. I provide evidence that the requirement for *zic2a* during craniofacial development is dependent on its role in patterning the forebrain and surrounding tissues, and that this requirement is separable from its role during neural crest development. In Chapter 3, I present the first examination of cilia in the cranial neural tube of the zebrafish, and show that depletion of the radial spoke head gene *rsph9* disrupts motile ciliogenesis and ventricle inflation.

References

Afzelius, B. A. 1976. A human syndrome caused by immotile cilia. Science. 193, 317-9.

Ahlgren, S. C. and Bronner-Fraser, M. 1999. Inhibition of sonic hedgehog signaling in vivo results in craniofacial neural crest cell death, Curr Biol. 9, 1304-14.

Antony, D., Becker-Heck, A., Zariwala, M. A., Schmidts, M., Onoufriadis, A., Forouhan, M., Wilson, R., Taylor-Cox, T., Dewar, A., Jackson, C. et al. 2013. Mutations in CCDC39 and CCDC40 are the major cause of primary ciliary dyskinesia with axonemal disorganization and absent inner dynein arms. Hum Mutat. 34, 462-72.

Aruga, J., Tohmonda, T., Homma, S. and Mikoshiba, K. 2002. Zic1 promotes the expansion of dorsal neural progenitors in spinal cord by inhibiting neuronal differentiation. Dev Biol. 244, 329-41.

Aruga, J., Yokota, N., Hashimoto, M., Furuichi, T., Fukuda, M. and Mikoshiba, K. 1994. A novel zinc finger protein, zic, is involved in neurogenesis, especially in the cell lineage of cerebellar granule cells. J Neurochem. 63, 1880-90.

Austin-Tse, C., Halbritter, J., Zariwala, M. A., Gilberti, R. M., Gee, H. Y., Hellman, N., Pathak, N., Liu, Y., Panizzi, J. R., Patel-King, R. S. et al. 2013. Zebrafish Ciliopathy Screen Plus Human Mutational Analysis Identifies C21orf59 and CCDC65 Defects as Causing Primary Ciliary Dyskinesia. Am J Hum Genet. 93, 672-86.

Bae, C. J., Park, B. Y., Lee, Y. H., Tobias, J. W., Hong, C. S. and Saint-Jeannet, J. P. 2014. Identification of Pax3 and Zic1 targets in the developing neural crest, Dev Biol. 386, 473-83.

Barrallo-Gimeno, A., Holzschuh, J., Driever, W. and Knapik, E. W. 2004. Neural crest survival and differentiation in zebrafish depends on mont blanc/tfap2a gene function. Development. 13, 1463-77.

Basch, M. L., Bronner-Fraser, M. and Garcia-Castro, M. I. 2006. Specification of the neural crest occurs during gastrulation and requires Pax7. Nature. 441, 218-22.

Benedyk, M. J., Mullen, J. R. and DiNardo, S. 1994. odd-paired: a zinc finger pair-rule protein required for the timely activation of engrailed and wingless in Drosophila embryos. Genes Dev. 8,105-17.

Brand, M., Heisenberg, C. P., Warga, R. M., Pelegri, F., Karlstrom, R. O., Beuchle, D., Picker, A., Jiang, Y. J., Furutani-Seiki, M., van Eeden, F. J. et al. 1996. Mutations affecting development of the midline and general body shape during zebrafish embryogenesis. Development. 123, 129-42.

Brewster, R., Lee, J. and Ruiz i Altaba, A. 1998. Gli/Zic factors pattern the neural plate by defining domains of cell differentiation. Nature. 393, 579-83.

Brody, S. L., Yan, X. H., Wuerffel, M. K., Song, S. K. and Shapiro, S. D. 2000. Ciliogenesis and left-right axis defects in forkhead factor HFH-4-null mice. Am J Respir Cell Mol Biol. 23, 45-51.

Brown, L., Paraso, M., Arkell, R. and Brown, S. 2005. In vitro analysis of partial loss-of-function ZIC2 mutations in holoprosencephaly: alanine tract expansion modulates DNA binding and transactivation. Hum Mol Genet. 14, 411-20.

Brown, S., Russo, J., Chitayat, D. and Warburton, D. 1995. The 13q- syndrome: the molecular definition of a critical deletion region in band 13q32. Am J Hum Genet. 57, 859-66.

Brown, S. A., Warburton, D., Brown, L. Y., Yu, C. Y., Roeder, E. R., Stengel-Rutkowski, S., Hennekam, R. C. and Muenke, M. 1998. Holoprosencephaly due to mutations in ZIC2, a homologue of Drosophila odd-paired. Nat Genet. 20, 180-3.

Caspary, T., Larkins, C. E. and Anderson, K. V. 2007. The graded response to Sonic Hedgehog depends on cilia architecture. Dev Cell. 12, 767-78.

Castleman, V. H., Romio, L., Chodhari, R., Hirst, R. A., de Castro, S. C., Parker, K. A., Ybot-Gonzalez, P., Emes, R. D., Wilson, S. W., Wallis, C. et al. 2009. Mutations in radial spoke head protein genes RSPH9 and RSPH4A cause primary ciliary dyskinesia with central-microtubular-pair abnormalities. Am J Hum Genet. 84, 197-209.

Chang, J. T. and Sive, H. 2012. Manual drainage of the zebrafish embryonic brain ventricles. J Vis Exp. 70, e4243.

Chiang, C., Litingtung, Y., Lee, E., Young, K. E., Corden, J. L., Westphal, H. and Beachy, P. A. 1996. Cyclopia and defective axial patterning in mice lacking Sonic hedgehog gene function. Nature. 383, 407-13.

Chilvers, M. A., Rutman, A. and O'Callaghan, C. 2003. Ciliary beat pattern is associated with specific ultrastructural defects in primary ciliary dyskinesia. J Allergy Clin Immunol. 112, 518-24.

Choksi, S. P., Lauter, G., Swoboda, P. and Roy, S. 2014. Switching on cilia: transcriptional networks regulating ciliogenesis. Development. 141, 1427-41.

Churchill, F. B. 1991. The rise of classical descriptive embryology. Dev Biol. (NY 1985) 7, 1-29.

Le Douarin, N., Kalcheim, C. 1999. ‘The Neural Crest’, Cambridge University Press.

Clay, M. R. and Halloran, M. C. 2010. Control of neural crest cell behavior and migration:

Insights from live imaging. Cell Adh Migr. 4, 586-94.

Daniels, M. L., Leigh, M. W., Davis, S. D., Armstrong, M. C., Carson, J. L., Hazucha, M., Dell, S. D., Eriksson, M., Collins, F. S., Knowles, M. R. et al. 2013. Founder mutation in RSPH4A identified in patients of Hispanic descent with primary ciliary dyskinesia. Hum Mutat. 34, 1352-6.

Davy, B. E. and Robinson, M. L. 2003. Congenital hydrocephalus in hy3 mice is caused by a frameshift mutation in Hydin, a large novel gene. Hum Mol Genet. 12, 1163-70.

de Croze, N., Maczkowiak, F. and Monsoro-Burq, A. H. 2011. Reiterative AP2a activity controls sequential steps in the neural crest gene regulatory network. Proc Natl Acad Sci USA. 108, 155-60.

Desmond, M. E. and Jacobson, A. G. 1977. Embryonic brain enlargement requires cerebrospinal fluid pressure. Dev Biol. 57, 188-98.

DiNardo, S. and O'Farrell, P. H. 1987. Establishment and refinement of segmental pattern in the Drosophila embryo: spatial control of engrailed expression by pair-rule genes. Genes Dev. 1, 1212-25.

Dorsky, R. I., Moon, R. T. and Raible, D. W. 1998. Control of neural crest cell fate by the Wnt signalling pathway. Nature. 396, 370-3.

Dorsky, R. I., Raible, D. W. and Moon, R. T. 2000. Direct regulation of nacre, a zebrafish MITF homolog required for pigment cell formation, by the Wnt pathway. Genes Dev. 14, 158-62.

Dubourg, C., Bendavid, C., Pasquier, L., Henry, C., Odent, S. and David, V. 2007. Holoprosencephaly. Orphanet J Rare Dis. 2, 8.

Dutton, K. A., Pauliny, A., Lopes, S. S., Elworthy, S., Carney, T. J., Rauch, J., Geisler, R., Haffter, P. and Kelsh, R. N. 2001. Zebrafish colourless encodes sox10 and specifies non-ectomesenchymal neural crest fates. Development. 128, 4113-25.

Eberhart, J. K., He, X., Swartz, M. E., Yan, Y. L., Song, H., Boling, T. C., Kunerth, A. K., Walker, M. B., Kimmel, C. B. and Postlethwait, J. H. 2008. MicroRNA Mirn140 modulates Pdgf signaling during palatogenesis. Nat Genet. 40, 290-8.

Eberhart, J. K., Swartz, M. E., Crump, J. G. and Kimmel, C. B. 2006. Early Hedgehog signaling from neural to oral epithelium organizes anterior craniofacial development. Development. 133, 1069-77.

Elms, P., Siggers, P., Napper, D., Greenfield, A. and Arkell, R. 2003. Zic2 is required for neural crest formation and hindbrain patterning during mouse development. Dev Biol. 264, 391-406.

Elworthy, S., Lister, J. A., Carney, T. J., Raible, D. W. and Kelsh, R. N. 2003. Transcriptional regulation of mitfa accounts for the sox10 requirement in zebrafish melanophore development. Development. 130, 2809-18.

Fliegauf, M., Benzing, T. and Omran, H. 2007. When cilia go bad: cilia defects and ciliopathies. Nat Rev Mol Cell Biol. 8, 880-93.

Garcia-Castro, M. I., Marcelle, C. and Bronner-Fraser, M. 2002. Ectodermal Wnt function as a neural crest inducer. Science. 297, 848-51.

Garcia-Lecea, M., Kondrychyn, I., Fong, S. H., Ye, Z. R. and Korzh, V. 2008. In vivo analysis of choroid plexus morphogenesis in zebrafish. PLoS One. 3, e3090.

Garnett, A. T., Square, T. A. and Medeiros, D. M. 2012. BMP, Wnt and FGF signals are integrated through evolutionarily conserved enhancers to achieve robust expression of Pax3 and Zic genes at the zebrafish neural plate border. Development. 139, 4220-31.

Gato, A. and Desmond, M. E. 2009. Why the embryo still matters: CSF and the neuroepithelium as interdependent regulators of embryonic brain growth, morphogenesis and histiogenesis. Dev Biol. 327, 263-72.

Gebbia, M., Ferrero, G. B., Pilia, G., Bassi, M. T., Aylsworth, A., Penman-Splitt, M., Bird, L. M., Bamforth, J. S., Burn, J., Schlessinger, D. et al. 1997. X-linked situs abnormalities result from mutations in ZIC3. Nat Genet. 17, 305-8.

Gostling, N. J. and Shimeld, S. M. 2003. Protochordate Zic genes define primitive somite compartments and highlight molecular changes underlying neural crest evolution. Evol Dev. 5, 136-44.

Hagenlocher, C., Walentek, P., C, M. L., Thumberger, T. and Feistel, K. 2013. Ciliogenesis and cerebrospinal fluid flow in the developing Xenopus brain are regulated by foxj1. Cilia. 2, 12.

Harrington, M. J., Hong, E. and Brewster, R. 2009. Comparative analysis of neurulation: first impressions do not count. *Mol Reprod Dev.* 76, 954-65.

Hjeij, R., Lindstrand, A., Francis, R., Zariwala, M. A., Liu, X., Li, Y., Damerla, R., Dougherty, G. W., Abouhamed, M., Olbrich, H. et al. 2013. ARMC4 mutations cause primary ciliary dyskinesia with randomization of left/right body asymmetry. Am J Hum Genet. 93, 357-67.

Hong, C. S., Park, B. Y. and Saint-Jeannet, J. P. 2008. Fgf8a induces neural crest indirectly through the activation of Wnt8 in the paraxial mesoderm. Development. 135, 3903-10.

Hong, C. S. and Saint-Jeannet, J. P. 2007. The activity of Pax3 and Zic1 regulates three

distinct cell fates at the neural plate border. Mol Biol Cell. 18, 2192-202.

Hong, E. and Brewster, R. 2006. N-cadherin is required for the polarized cell behaviors that drive neurulation in the zebrafish. Development. 133, 3895-905.

Horani, A., Brody, S. L., Ferkol, T. W., Shoseyov, D., Wasserman, M. G., Ta-shma, A., Wilson, K. S., Bayly, P. V., Amirav, I., Cohen-Cymberknoh, M. et al. 2013. CCDC65 mutation causes primary ciliary dyskinesia with normal ultrastructure and hyperkinetic cilia. PLoS One. 8, e72299.

Hu, D. and Marcucio, R. S. 2009. A SHH-responsive signaling center in the forebrain regulates craniofacial morphogenesis via the facial ectoderm. Development. 136, 107-16.

Ibanez-Tallon, I., Gorokhova, S. and Heintz, N. 2002. Loss of function of axonemal dynein Mdnah5 causes primary ciliary dyskinesia and hydrocephalus. Hum Mol Genet. 11, 715-21.

Inoue, T., Hatayama, M., Tohmonda, T., Itohara, S., Aruga, J. and Mikoshiba, K. 2004. Mouse Zic5 deficiency results in neural tube defects and hypoplasia of cephalic neural crest derivatives. Dev Biol. 270, 146-62.

Inoue, T., Ota, M., Ogawa, M., Mikoshiba, K. and Aruga, J. 2007. Zic1 and Zic3 regulate medial forebrain development through expansion of neuronal progenitors. J Neurosci. 27, 5461-73.

Jivan, A., Earnest, S., Juang, Y. C. and Cobb, M. H. 2009. Radial spoke protein 3 is a mammalian protein kinase A-anchoring protein that binds ERK1/2. J Biol Chem. 284, 29437-45.

Johnson, C. W., Hernandez-Lagunas, L., Feng, W., Melvin, V. S., Williams, T. and Artinger, K. B. 2011. Vgll2a is required for neural crest cell survival during zebrafish craniofacial development. Dev Biol. 357, 269-81.

Kelsh, R. N., Harris, M. L., Colanesi, S. and Erickson, C. A. 2009. Stripes and belly-spots -- a review of pigment cell morphogenesis in vertebrates. Semin Cell Dev Biol. 20, 90-104.

Kish, P. E., Bohnsack, B. L., Gallina, D., Kasprick, D. S. and Kahana, A. 2011. The eye as an organizer of craniofacial development. Genesis. 49, 222-30.

Knowles, M. R., Daniels, L. A., Davis, S. D., Zariwala, M. A. and Leigh, M. W. 2013a. Primary ciliary dyskinesia. Recent advances in diagnostics, genetics, and characterization of clinical disease. Am J Respir Crit Care Med. 188, 913-22.

Knowles, M. R., Ostrowski, L. E., Leigh, M. W., Sears, P. R., Davis, S. D., Wolf, W. E., Hazucha, M. J., Carson, J. L., Olivier, K. N., Sagel, S. D. et al. 2014. Mutations in RSPH1

cause primary ciliary dyskinesia with a unique clinical and ciliary phenotype. Am J Respir Crit Care Med. 189, 707-17.

Knowles, M. R., Ostrowski, L. E., Loges, N. T., Hurd, T., Leigh, M. W., Huang, L., Wolf, W. E., Carson, J. L., Hazucha, M. J., Yin, W. et al. 2013b. Mutations in SPAG1 cause primary ciliary dyskinesia associated with defective outer and inner dynein arms. Am J Hum Genet. 93, 711-20.

Kott, E., Legendre, M., Copin, B., Papon, J. F., Dastot-Le Moal, F., Montantin, G., Duquesnoy, P., Piterboth, W., Amram, D., Bassinet, L. et al. 2013. Loss-of-function mutations in RSPH1 cause primary ciliary dyskinesia with central-complex and radial-spoke defects. Am J Hum Genet. 93, 561-70.

Kramer-Zucker, A. G., Olale, F., Haycraft, C. J., Yoder, B. K., Schier, A. F. and Drummond, I. A. 2005. Cilia-driven fluid flow in the zebrafish pronephros, brain and Kupffer's vesicle is required for normal organogenesis. Development. 132, 1907-21.

Kulesa, P. M., Kasemeier-Kulesa, J. C., Teddy, J. M., Margaryan, N. V., Seftor, E. A., Seftor, R. E. and Hendrix, M. J. 2006. Reprogramming metastatic melanoma cells to assume a neural crest cell-like phenotype in an embryonic microenvironment. Proc Natl Acad Sci USA. 103, 3752-7.

Langenberg, T., Kahana, A., Wszalek, J. A. and Halloran, M. C. 2008. The eye organizes neural crest cell migration. Dev Dyn. 237, 1645-52.

Le Douarin, N. M., Creuzet, S., Couly, G. and Dupin, E. 2004. Neural crest cell plasticity and its limits. Development. 131, 4637-50.

Lechtreck, K. F., Delmotte, P., Robinson, M. L., Sanderson, M. J. and Witman, G. B. 2008. Mutations in Hydin impair ciliary motility in mice. J Cell Biol. 180, 633-43.

Lehtinen, M. K., Bjornsson, C. S., Dymecki, S. M., Gilbertson, R. J., Holtzman, D. M. and Monuki, E. S. 2013. The choroid plexus and cerebrospinal fluid: emerging roles in development, disease, and therapy. J Neurosci. 33, 17553-9.

Lehtinen, M. K., Zappaterra, M. W., Chen, X., Yang, Y. J., Hill, A. D., Lun, M., Maynard, T., Gonzalez, D., Kim, S., Ye, P. et al. 2011. The cerebrospinal fluid provides a proliferative niche for neural progenitor cells. Neuron. 69, 893-905.

Lewis, J. L., Bonner, J., Modrell, M., Ragland, J. W., Moon, R. T., Dorsky, R. I. and Raible, D. W. 2004. Reiterated Wnt signaling during zebrafish neural crest development. Development. 131, 1299-308.

Li, W. and Cornell, R. A. 2007. Redundant activities of Tfap2a and Tfap2c are required for

neural crest induction and development of other non-neural ectoderm derivatives in zebrafish embryos. Dev Biol. 304, 338-54.

Lowery, L. A. and Sive, H. 2004. Strategies of vertebrate neurulation and a re-evaluation of teleost neural tube formation. Mech Dev. 121, 1189-97.

Lowery, L. A. and Sive, H. 2009. Totally tubular: the mystery behind function and origin of the brain ventricular system. Bioessays. 31, 446-58.

Lupo, G., Harris, W. A. and Lewis, K. E. 2006. Mechanisms of ventral patterning in the vertebrate nervous system. Nat Rev Neurosci. 7, 103-14.

Luse, S. A. 1956. Electron microscopic observations of the central nervous system. J Biophys Biochem Cytol. 2, 531-42.

Marchal, L., Luxardi, G., Thome, V. and Kodjabachian, L. 2009. BMP inhibition initiates neural induction via FGF signaling and Zic genes. Proc Natl Acad Sci USA. 106, 17437-42.

Marcucio, R. S., Cordero, D. R., Hu, D. and Helms, J. A. 2005. Molecular interactions coordinating the development of the forebrain and face. Dev Biol. 284, 48-61.

Marcucio, R. S., Young, N. M., Hu, D. and Hallgrimsson, B. 2011. Mechanisms that underlie co-variation of the brain and face. Genesis. 49, 177-89.

Martin, C., Bueno, D., Alonso, M. I., Moro, J. A., Callejo, S., Parada, C., Martin, P., Carnicero, E. and Gato, A. 2006. FGF2 plays a key role in embryonic cerebrospinal fluid trophic properties over chick embryo neuroepithelial stem cells. Dev Biol. 297, 402-16.

Maurus, D. and Harris, W. A. 2009. Zic-associated holoprosencephaly: zebrafish Zic1 controls midline formation and forebrain patterning by regulating Nodal, Hedgehog, and retinoic acid signaling. Genes Dev. 23, 1461-73.

Mercier, S., Dubourg, C., Garcelon, N., Campillo-Gimenez, B., Gicquel, I., Belleguic, M., Ratie, L., Pasquier, L., Loget, P., Bendavid, C. et al. 2011. New findings for phenotype-genotype correlations in a large European series of holoprosencephaly cases. J Med Genet. 48, 752-60.

Merzdorf, C. S. 2007. Emerging roles for zic genes in early development. Dev Dyn. 236, 922-40.

Meyer, A. and Van de Peer, Y. 2005. From 2R to 3R: evidence for a fish-specific genome duplication (FSGD). Bioessays. 27, 937-45.

Milet, C., Maczkowiak, F., Roche, D. D. and Monsoro-Burq, A. H. 2013. Pax3 and Zic1 drive induction and differentiation of multipotent, migratory, and functional neural crest in Xenopus

embryos. Proc Natl Acad Sci USA. 110, 5528-33.

Minchin, J. E. and Hughes, S. M. 2008. Sequential actions of Pax3 and Pax7 drive xanthophore development in zebrafish neural crest. Dev Biol. 317, 508-22.

Monsoro-Burq, A. H., Fletcher, R. B. and Harland, R. M. 2003. Neural crest induction by paraxial mesoderm in Xenopus embryos requires FGF signals. Development. 130, 3111-24.

Montecinos, H. A., Richter, H., Caprile, T. and Rodriguez, E. M. 2005. Synthesis of transthyretin by the ependymal cells of the subcommissural organ. Cell Tissue Res. 320, 487-99.

Moore, D. J., Onoufriadis, A., Shoemark, A., Simpson, M. A., zur Lage, P. I., de Castro, S. C., Bartoloni, L., Gallone, G., Petridi, S., Woollard, W. J. et al. 2013. Mutations in ZMYND10, a gene essential for proper axonemal assembly of inner and outer dynein arms in humans and flies, cause primary ciliary dyskinesia. Am J Hum Genet. 93, 346-56.

Nagai, T., Aruga, J., Minowa, O., Sugimoto, T., Ohno, Y., Noda, T. and Mikoshiba, K. 2000. Zic2 regulates the kinetics of neurulation. Proc Natl Acad Sci USA. 97, 1618-23.

Nakata, K., Koyabu, Y., Aruga, J. and Mikoshiba, K. 2000. A novel member of the Xenopus Zic family, Zic5, mediates neural crest development. Mech Dev. 99, 83-91.

Nakata, K., Nagai, T., Aruga, J. and Mikoshiba, K. 1997. Xenopus Zic3, a primary regulator both in neural and neural crest development. Proc Natl Acad Sci USA. 94, 11980-5.

Nakata, K., Nagai, T., Aruga, J. and Mikoshiba, K. 1998. Xenopus Zic family and its role in neural and neural crest development. Mech Dev. 75, 43-51.

Narita, K., Kawate, T., Kakinuma, N. and Takeda, S. 2010. Multiple primary cilia modulate the fluid transcytosis in choroid plexus epithelium. Traffic. 11, 287-301.

Nonami, Y., Narita, K., Nakamura, H., Inoue, T. and Takeda, S. 2013. Developmental changes in ciliary motility on choroid plexus epithelial cells during the perinatal period. Cytoskeleton (Hoboken). 70, 797-803.

Nyholm, M. K., Abdelilah-Seyfried, S. and Grinblat, Y. 2009. A novel genetic mechanism regulates dorsolateral hinge-point formation during zebrafish cranial neurulation. J Cell Sci. 122, 2137-48.

Oda, T., Yanagisawa, H., Yagi, T. and Kikkawa, M. 2014. Mechanosignaling between central apparatus and radial spokes controls axonemal dynein activity. J Cell Biol. 204, 807-19.

Odenthal, J., Rossnagel, K., Haffter, P., Kelsh, R. N., Vogelsang, E., Brand, M., van Eeden, F.

J., Furutani-Seiki, M., Granato, M., Hammerschmidt, M. et al. 1996. Mutations affecting xanthophore pigmentation in the zebrafish, Danio rerio. Development. 123, 391-8.

Omoto, C. K., Yagi, T., Kurimoto, E. and Kamiya, R. 1996. Ability of paralyzed flagella mutants of Chlamydomonas to move. Cell Motil Cytoskeleton. 33, 88-94.

Onoufriadis, A., Shoemark, A., Munye, M. M., James, C. T., Schmidts, M., Patel, M., Rosser, E. M., Bacchelli, C., Beales, P. L., Scambler, P. J. et al. 2014a. Combined exome and whole-genome sequencing identifies mutations in ARMC4 as a cause of primary ciliary dyskinesia with defects in the outer dynein arm. J Med Genet. 51, 61-7.

Onoufriadis, A., Shoemark, A., Schmidts, M., Patel, M., Jimenez, G., Liu, H., Thomas, B., Dixon, M., Hirst, R. A., Rutman, A. et al. 2014b. Targeted NGS gene panel identifies mutations in RSPH1 causing primary ciliary dyskinesia and a common mechanism for ciliary central pair agenesis due to radial spoke defects. Hum Mol Genet. 23, 3362-74.

Ozair, M. Z., Kintner, C. and Brivanlou, A. H. 2013. Neural induction and early patterning in vertebrates. Wiley Interdiscip Rev Dev Biol. 2, 479-98.

Pigino, G. and Ishikawa, T. 2012. Axonemal radial spokes: 3D structure, function and assembly. Bioarchitecture. 2, 50-58.

Plouhinec, J. L., Roche, D. D., Pegoraro, C., Figueiredo, A. L., Maczkowiak, F., Brunet, L. J., Milet, C., Vert, J. P., Pollet, N., Harland, R. M. et al. 2014. Pax3 and Zic1 trigger the early neural crest gene regulatory network by the direct activation of multiple key neural crest specifiers. Dev Biol. 386, 461-72.

Porter, M. E. and Sale, W. S. 2000. The 9 + 2 axoneme anchors multiple inner arm dyneins and a network of kinases and phosphatases that control motility. *J Cell Biol.* 151, 37-42.

Roessler, E., Belloni, E., Gaudenz, K., Jay, P., Berta, P., Scherer, S. W., Tsui, L. C. and Muenke, M. 1996. Mutations in the human Sonic Hedgehog gene cause holoprosencephaly. Nat Genet. 14, 357-60.

Roessler, E., Lacbawan, F., Dubourg, C., Paulussen, A., Herbergs, J., Hehr, U., Bendavid, C., Zhou, N., Ouspenskaia, M., Bale, S. et al. 2009. The full spectrum of holoprosencephaly-associated mutations within the ZIC2 gene in humans predicts loss-of-function as the predominant disease mechanism. Hum Mutat. 30, E541-54.

Roessler, E. and Muenke, M. 2010. The molecular genetics of holoprosencephaly. Am J Med Genet C Semin Med Genet. 154C, 52-61.

Salathe, M. 2007. Regulation of mammalian ciliary beating. Annu Rev Physiol. 69, 401-22.

Sanek, N. A. and Grinblat, Y. 2008. A novel role for zebrafish zic2a during forebrain development. Dev Biol. 317, 325-35.

Sanek, N. A., Taylor, A. A., Nyholm, M. K. and Grinblat, Y. 2009. Zebrafish zic2a patterns the forebrain through modulation of Hedgehog-activated gene expression. Development. 136, 3791-800.

Sapiro, R., Kostetskii, I., Olds-Clarke, P., Gerton, G. L., Radice, G. L. and Strauss, I. J. 2002. Male infertility, impaired sperm motility, and hydrocephalus in mice deficient in sperm-associated antigen 6. Mol Cell Biol. 22, 6298-305.

Sarmah, B., Winfrey, V. P., Olson, G. E., Appel, B. and Wente, S. R. 2007. A role for the inositol kinase Ipk1 in ciliary beating and length maintenance. Proc Natl Acad Sci USA. 104, 19843-8.

Sato, T., Sasai, N. and Sasai, Y. 2005. Neural crest determination by co-activation of Pax3 and Zic1 genes in Xenopus ectoderm. Development. 132, 2355-63.

Sawamoto, K., Wichterle, H., Gonzalez-Perez, O., Cholfin, J. A., Yamada, M., Spassky, N., Murcia, N. S., Garcia-Verdugo, J. M., Marin, O., Rubenstein, J. L. et al. 2006. New neurons follow the flow of cerebrospinal fluid in the adult brain. Science. 311, 629-32.

Schilling, T. F. and Kimmel, C. B. 1994. Segment and cell type lineage restrictions during pharyngeal arch development in the zebrafish embryo. Development. 120, 483-94.

Schilling, T. F. and Kimmel, C. B. 1997. Musculoskeletal patterning in the pharyngeal segments of the zebrafish embryo. Development. 124, 2945-60.

Schwend, T. and Ahlgren, S. C. 2009. Zebrafish con/disp1 reveals multiple spatiotemporal requirements for Hedgehog-signaling in craniofacial development. BMC Dev Biol. 9, 59.

Shimeld, S. M. and Holland, P. W. 2000. Vertebrate innovations. Proc Natl Acad Sci USA. 97, 4449-52.

Solomon, B. D., Lacbawan, F., Mercier, S., Clegg, N. J., Delgado, M. R., Rosenbaum, K., Dubourg, C., David, V., Olney, A. H., Wehner, L. E. et al. 2010a. Mutations in ZIC2 in human holoprosencephaly: description of a novel ZIC2 specific phenotype and comprehensive analysis of 157 individuals. J Med Genet. 47, 513-24.

Solomon, B. D., Mercier, S., Velez, J. I., Pineda-Alvarez, D. E., Wyllie, A., Zhou, N., Dubourg, C., David, V., Odent, S., Roessler, E. et al. 2010b. Analysis of genotype-phenotype correlations in human holoprosencephaly. Am J Med Genet C Semin Med Genet. 154C, 133-41.

Sperber, S. M., Saxena, V., Hatch, G. and Ekker, M. 2008. Zebrafish dlx2a contributes to hindbrain neural crest survival, is necessary for differentiation of sensory ganglia and functions with dlx1a in maturation of the arch cartilage elements. Dev Biol. 314, 59-70.

Steventon, B., Araya, C., Linker, C., Kuriyama, S. and Mayor, R. 2009. Differential requirements of BMP and Wnt signalling during gastrulation and neurulation define two steps in neural crest induction. Development. 136, 771-9.

Stewart, R. A., Arduini, B. L., Berghmans, S., George, R. E., Kanki, J. P., Henion, P. D. and Look, A. T. 2006. Zebrafish foxd3 is selectively required for neural crest specification, migration and survival. Dev Biol. 292, 174-88.

Stuhlmiller, T. J. and Garcia-Castro, M. I. 2012. Current perspectives of the signaling pathways directing neural crest induction. Cell Mol Life Sci. 69, 3715-37.

Stuhlmiller, T. J. and Garcia-Castro, M. I. 2012. FGF/MAPK signaling is required in the gastrula epiblast for avian neural crest induction. Development. 139, 289-300.

Sulik, K., Dehart, D. B., Iangaki, T., Carson, J. L., Vrablic, T., Gesteland, K. and Schoenwolf, G. C. 1994. Morphogenesis of the murine node and notochordal plate. Dev Dyn. 201, 260-78.

Swartz, M. E., Nguyen, V., McCarthy, N. Q. and Eberhart, J. K. 2012. Hh signaling regulates patterning and morphogenesis of the pharyngeal arch-derived skeleton. Dev Biol. 369, 65-75.

Szabo-Rogers, H. L., Smithers, L. E., Yakob, W. and Liu, K. J. 2010. New directions in craniofacial morphogenesis. Dev Biol. 341, 84-94.

Takahashi, Y., Sipp, D. and Enomoto, H. 2013. Tissue interactions in neural crest cell development and disease. Science. 341, 860-3.

Tascioglu, A.O., Tascioglu, A.B., 2005. Ventricular anatomy: illustrations and concepts from antiquity to Renaissance. Neuroanatomy. 4, 57-63.

Theveneau, E. and Mayor, R. 2012. Neural crest delamination and migration: from epithelium-to-mesenchyme transition to collective cell migration. Dev Biol. 366, 34-54.

Tribulo, C., Aybar, M. J., Nguyen, V. H., Mullins, M. C. and Mayor, R. 2003. Regulation of Msx genes by a Bmp gradient is essential for neural crest specification. Development. 130, 6441-52.

Wada, N., Javidan, Y., Nelson, S., Carney, T. J., Kelsh, R. N. and Schilling, T. F. 2005. Hedgehog signaling is required for cranial neural crest morphogenesis and chondrogenesis at the midline in the zebrafish skull. Development. 132, 3977-88.

Wada, S. and Saiga, H. 2002. HrzicN, a new Zic family gene of ascidians, plays essential roles in the neural tube and notochord development. Development. 129, 5597-608.

Warr, N., Powles-Glover, N., Chappell, A., Robson, J., Norris, D. and Arkell, R. M. 2008. Zic2-associated holoprosencephaly is caused by a transient defect in the organizer region during gastrulation. Hum Mol Genet. 17, 2986-96.

Wilkie, A. O. and Morriss-Kay, G. M. 2001. Genetics of craniofacial development and malformation. Nat Rev Genet. 2, 458-68.

Wilson, S. I., Graziano, E., Harland, R., Jessell, T. M. and Edlund, T. 2000. An early requirement for FGF signalling in the acquisition of neural cell fate in the chick embryo. Curr Biol. 10, 421-9.

Yan, Y. L., Willoughby, J., Liu, D., Crump, J. G., Wilson, C., Miller, C. T., Singer, A., Kimmel, C., Westerfield, M. and Postlethwait, J. H. 2005. A pair of Sox: distinct and overlapping functions of zebrafish sox9 co-orthologs in craniofacial and pectoral fin development. Development. 132, 1069-83.

Yang, P., Diener, D. R., Rosenbaum, J. L. and Sale, W. S. 2001. Localization of calmodulin and dynein light chain LC8 in flagellar radial spokes. J Cell Biol. 153, ß1315-26.

Yang, P., Diener, D. R., Yang, C., Kohno, T., Pazour, G. J., Dienes, J. M., Agrin, N. S., King, S. M., Sale, W. S., Kamiya, R. et al. 2006. Radial spoke proteins of Chlamydomonas flagella. J Cell Sci. 119, 1165-74.

Yang, P., Yang, C. and Sale, W. S. 2004. Flagellar radial spoke protein 2 is a calmodulin binding protein required for motility in Chlamydomonas reinhardtii. Eukaryot Cell. 3, 72-81.

Ybot-Gonzalez, P., Gaston-Massuet, C., Girdler, G., Klingensmith, J., Arkell, R., Greene, N. D. and Copp, A. J. 2007. Neural plate morphogenesis during mouse neurulation is regulated by antagonism of Bmp signaling. Development. 134, 3203-11.

Zappaterra, M. D., Lisgo, S. N., Lindsay, S., Gygi, S. P., Walsh, C. A. and Ballif, B. A. 2007. A comparative proteomic analysis of human and rat embryonic cerebrospinal fluid. J Proteome Res. 6, 3537-48.

Zhang, J., Williams, M. A. and Rigamonti, D. 2006. Genetics of human hydrocephalus. J Neurol. 253, 1255-66.

Zietkiewicz, E., Bukowy-Bieryllo, Z., Voelkel, K., Klimek, B., Dmenska, H., Pogorzelski, A., Sulikowska-Rowinska, A., Rutkiewicz, E. and Witt, M. 2012. Mutations in radial spoke head genes and ultrastructural cilia defects in East-European cohort of primary ciliary dyskinesia patients. PLoS One. 7, e33667.

Chapter 2:

Zebrafish Zic2a and Zic2b regulate neural crest and craniofacial development

The work contained in this chapter was published as follows: Teslaa, J. J., Keller, A. N., Nyholm, M. K. and Grinblat, Y. 2013. Zebrafish Zic2a and Zic2b regulate neural crest and craniofacial development. *Dev Biol.* 380, 73-86.

Abstract

Holoprosencephaly (HPE), the most common malformation of the human forebrain, is associated with defects of the craniofacial skeleton. *ZIC2*, a zinc-finger transcription factor, is strongly linked to HPE and to a characteristic set of dysmorphic facial features in humans. We have previously identified important functions for zebrafish Zic2 in the developing forebrain. Here, we demonstrate that *ZIC2* orthologs *zic2a* and *zic2b* also regulate the forming zebrafish craniofacial skeleton, including the jaw and neurocranial cartilages, and use the zebrafish to study Zic2-regulated processes that may contribute to the complex etiology of HPE. Using temporally controlled Zic2a overexpression, we show that the developing craniofacial cartilages are sensitive to Zic2 elevation prior to 24hpf. This window of sensitivity overlaps the critical expansion and migration of the neural crest (NC) cells, which migrate from the developing neural tube to populate vertebrate craniofacial structures. We demonstrate that *zic2b* influences the induction of NC at the neural plate border, while both *zic2a* and *zic2b* regulate NC migratory onset and strongly contribute to chromatophore development. Both Zic2 depletion and early ectopic Zic2 expression cause moderate, incompletely penetrant mispatterning of the NC-derived jaw precursors at 24hpf, yet by 2dpf these changes in Zic2 expression result in profoundly mispatterned chondrogenic condensations. We attribute this discrepancy to an additional role for Zic2a and Zic2b in patterning the forebrain primordium, an important signaling source during craniofacial development. This hypothesis is supported by evidence that transplanted Zic2-deficient cells can contribute to craniofacial cartilages in a wild-type background. Collectively,

these data suggest that zebrafish Zic2 plays a dual role during craniofacial development, contributing to two disparate aspects of craniofacial morphogenesis: (1) Neural crest induction and migration, and (2) early patterning of tissues adjacent to craniofacial chondrogenic condensations.

Introduction

The complex patterning and morphogenesis of the craniofacial skeleton gives rise to the wide morphological variation in facial structure among vertebrates. Disruptions in normal craniofacial development result in defects ranging from mild dysmorphologies to more severe outcomes, including cleft palate and cyclopia (Wilkie and Morris-Kay, 2001). In humans, dysmorphic facial features and craniofacial defects are often associated with malformations of the brain such as Dandy-Walker malformation (DWM) and HPE (Dubourg et al., 2007; Mademont-Soler et al., 2010). The extent of interdependence between brain and craniofacial morphology, the subject of recent studies, is not fully understood (Le Douarin et al., 2012; Marcucio et al., 2011).

Vertebrate craniofacial development depends heavily on the contribution of chondrogenic precursors from the cephalic NC (Cordero et al., 2010; Minoux and Rijli, 2010). The NC is induced at the border of the neural ectoderm during gastrulation and subsequently exits the neural epithelium and migrates throughout the developing embryo (Milet and Monsoro-Burq, 2012). NC cells from the posterior diencephalon and midbrain contribute to the anterior neurocranial cartilages (Wada et al., 2005), while NC cells from the hindbrain populate the first two pharyngeal arches (PAs) and form the jaw cartilages (Lumsden et al., 1991; Schilling and Kimmel, 1994; Schilling and Kimmel, 1997). Development of the facial complex is disrupted by mutations in genes that regulate NC development and survival, e.g. *arl6ip1* (Tu et al., 2012), *dlx2a* (Sperber et al., 2008), *Myo10* (Nie et al., 2009) *sox9b* (Yan et al., 2005) and *tfap2* genes (Barrallo-Gimeno et al., 2004; Knight et al., 2003; Li and Cornell, 2007).

Establishment of the craniofacial cartilages also relies on appropriate patterning and morphogenesis of surrounding tissues (Szabo-Rogers et al., 2010). Developing craniofacial cartilages receive important patterning cues from neural epithelium (Marcucio et al. 2005; Chong et al., 2012), pharyngeal endoderm (Couly et al., 2002; Haworth et al., 2007; Ruhin et al., 2003), facial ectoderm, (Hu and Marcucio, 2009; Reid et al., 2011) and olfactory placodes (Szabo-Rogers et al., 2009). The NC cells themselves constitute an important piece of this signaling network (Bonilla-Claudio et al., 2012; Jeong et al., 2004). The forebrain, facial ectoderm and pharyngeal endoderm are each a source of Hh signaling, a particularly important patterning cue during craniofacial development. Hh signaling promotes proliferation and differentiation of chondrogenic precursors, and global disruption of Hh signaling causes severe defects in jaw and neurocranial cartilages (Ahlgren and Bronner-Fraser, 1999; Schwend and Ahlgren, 2009; Swartz et al., 2012). In zebrafish, Hh signaling from the ventral forebrain primordium plays a key role in the development of the anterior neurocranium (Wada et al., 2005) and stomodeal ectoderm, which serves as a substrate for chondrogenic NC condensation (Eberhart et al., 2006).

Zic genes encode a family of zinc finger transcription factors with documented roles in NC development and forebrain morphogenesis and patterning (Merzdorf, 2007; Maurus and Harris, 2009). *ZIC2* mutations in humans are linked to HPE and a characteristic craniofacial morphology (Brown et al., 1998; Mercier et al., 2011; Solomon et al., 2010a). Mice homozygous for hypomorphic or null alleles of *Zic2* develop with HPE-like forebrain defects and hypoplastic NC derivatives (Elms et al., 2003; Nagai et

al., 2000; Warr et al., 2008). Homozygous mouse mutants in *Zic5*, a gene closely linked to and co-expressed with *Zic2*, exhibit a shortened mandible, which is fused at the midline (Inoue et al., 2004). Zic2 (Brewster et al., 1998; Nakata et al., 1998) and Zic5 (Nakata et al., 2000) overexpression induces NC genes in *Xenopus*. Whether the craniofacial dysmorphology in mammalian Zic mutants is solely the outcome of Zic regulation of NC generation is unknown.

The zebrafish genome encodes two orthologs of mammalian *ZIC2*, *zic2a* and *zic2b* (Toyama et al., 2004). Our previous work demonstrated a role for *zic2a* during forebrain development (Sanek et al., 2008; Sanek et al., 2009). We showed that Zic2a interacts with the Hh signaling pathway to pattern the diencephalon and optic stalk/retinal interface. In this study, we investigate the roles of the zebrafish *ZIC2* orthologs in craniofacial development. Based on the previously documented role of *zic* genes in NC development and their association with craniofacial dysmorphologies, we hypothesized that Zics regulate early NC lineages that subsequently give rise to craniofacial structures. We find evidence for zebrafish *zic2a* and *zic2b* involvement in early NC induction and migratory onset and demonstrate a requirement for *zic2a* and *zic2b* regulation of the pigment cell lineage. However, *zic* contribution to chondrogenic NC formation may not be the sole cause of the profound craniofacial defects observed in Zic2-depleted and overexpressing embryos. Our data suggest a second, non-cell autonomous role for Zic2a and Zic2b in patterning tissues adjacent to craniofacial cartilages, e.g. the ventral forebrain primordium, which in turn promote post-migratory development of NC-derived chondrogenic precursors.

Material and methods

Zebrafish strains and embryo culture

Adult zebrafish were maintained according to established methods (Westerfield, 2000). Embryos were obtained from natural matings and staged according to Kimmel (Kimmel et al., 1995). The *11XUAS:zic2aYFP* transgene was constructed in the pBH-UAS-mcs-YFP vector backbone, which contains Tol2 sites and a *cmlc2*:Cherry cassette for independent verification of transgene presence (vector provided by M. Nonet; sequence information at http://thalamus.wustl.edu/nonetlab/ResourcesF/Zebrafish.html). Tg(*11XUAS:zic2aYFP;cmlc2:Cherry*) stable transgenics were produced using established methods (Kawakami et al., 2004). The Tg(*hsp70l:Gal4VP16*) line was provided by B. Appel, Vanderbilt University (Inbal et al., 2007; Takada and Appel, 2011)

Knockdown assays

Gene-specific antisense oligonucleotide morpholinos (MO) and standard control MO were purchased from GeneTools (Philomath, OR). The zic2a splice-blocking MO (zic2aMO) and zic2a translation-blocking MOs (zic2aAUGMO and zic2aproxMO), have been described (Nyholm et al., 2007). Zic2b morpholinos were designed against the translational start site (zic2b AUG MO: TATTGACCAAAGAATGCGTAAAGAC) and the exon 1–intron 2 splice donor site (zic2b MO: ATTGAAATAATTACCAGTGTGTGTC) of *zic2b*. MOs were diluted in 1X Danieau buffer (Nasevicius and Ekker, 2000) to 1-2ng/nl (zic2aMO), 6-8ng/nl (zic2aAUG+zic2aproxMO, injected together; henceforth referred to as zic2aAUGMO), 2-4ng/nl (zic2bMO), 4-8ng/nl (zic2b AUG MO) or 3-4ng/nl (conMO).

Injections were carried out at the 1-2 cell stage on a Picospritzer III (Parker Instrumentation) or a PLI100 (Harvard Apparatus). Each injected embryo received 0.5-1nl of either zic2aMO or zic2bMO. Double zic2 morphants were injected twice, with 0.5nl of each MO. To test the efficacy of the zic2bMO, RNA was extracted from embryos injected with zic2bMO and used to generate cDNA using the iScript kit (BioRad). PCR was performed using primers complimentary to sequences in exon 1 (5'-TGGGCGCGTTCAAACTG-3') and exon 3 (5'-ATTGTGCCCGCTGCTGTT-3'). Images show embryos injected with the zic2a or zic2b splice blocking MOs unless noted otherwise.

Overexpression and rescue assays

Zic2aYFP overexpression was achieved by mating the *Tg(hsp70l:Gal4VP16)* line with the *Tg(11XUAS:zic2aYFP)* line. Upon heat shock induction, the resulting double transgenic embryos express Zic2aYFP fusion protein. Heat shocks were administered for one hour in a 37°C water bath. Heat-shocked embryos were allowed to recover at room temperature (25°C) or 29°C for approximately five hours and then sorted for YFP fluorescence. Heat-shocked YFP-negative siblings were used as controls. For rescue experiments using zic2aAUGMO, each clutch obtained from *Tg(hsp70l:Gal4VP16)* x *Tg(11XUAS:zic2aYFP)* pair mating was divided into three sibling groups: (1) uninjected, (2) conMO injected and (3) zic2aAUGMO injected. All embryos were subsequently heat shocked at 10hpf, and sorted for YFP fluorescence 10-12 hours post-heatshock. Note

that YFP fluorescence was not observed in any of the Zic2aAUGMO-injected embryos, consistent with efficient MO-mediated knockdown of Zic2aYFP expression.

In situ hybridization (ISH), histology and Alcian Blue staining

Antisense digoxigenin or fluorescein labeled RNA probes were transcribed using the MAXIscript kit (Ambion) from the following plasmid templates: *apoeb* (Thisse et al., 2001), *col2a1a* (Yan et al., 1995), *dlx2a* (Akimenko et al., 1994), *dlx3b* (Akimenko et al., 1994), *foxd3* (Odenthal and Nusslein-Volhard, 1998), *gch2* (Parichy et al., 2000), *mitfa* (Lister et al., 1999), *nkx2.2a* (Karlstrom et al., 2003), *pax2a* (Hoyle et al., 2004), *pitx2a* (Essner et al., 2000), *ptch2* (Vanderlaan et al., 2005), *sna1b* (Thisse et al., 1995), *sox9a* (Cresko et al., 2003), *sox10* (Dutton et al., 2001), *zic2a* (Grinblat and Sive, 2001) and *zic2b* (a kind gift from Becky Burdine and Alex Schier). Some embryos fixed at 2 and 3dpf were raised in 0.003% phenylthiohydroxyurea (PTU) to prevent pigment formation. ISH was carried out as previously described (Gillhouse et al., 2004). Differential interference contrast (DIC) images were obtained using an Axioskop2 Plus microscope with AxioVision software (Zeiss) or a Leica MZ FLIII with LAS v4.0 software. Stained embryos were embedded in Eponate 12 medium (Ted Pella) and 5-7μm sections were cut with a steel blade on an American Optical Company microtome. Nuclei were counterstained with Neutral Red. For Alcian Blue staining, zebrafish larvae were fixed in 4% paraformaldehyde overnight and stained according to Kimmel et al., 1998. Cartilages were dissected using sharpened tungsten needles and the preparations were flat-mounted in glycerol for imaging.

Transplant assays

Embryos were injected at the 1-cell stage with either conMO or zic2aMO, and transplant donors were injected into the yolk with a mixture of 2% alexa568-dextran/3% biotin-dextran in 0.2M KCl (10,000 MW, lysine fixable, Molecular Probes). Embryos were dechorionated in 0.5X MBS on agarose pads. Cells were removed from the animal pole of sphere-stage donor embryos using finely ground glass capillary tubes with an outer diameter of 100-150μn, and injected into the animal pole of sphere-stage host embryos. The position of labeled donor tissue was examined at 24hpf on a fluorescent microscope. Confocal imaging was carried out on an Olympus FV1000 microscope with FV10-ASW software. Biotin was detected by incubation with an avidin-biotin-HRP complex (VectorLabs) and colorimetric reactions were developed with DAB.

Quantitative real-time PCR

RNA was isolated from embryos using Trizol (Life Technologies) and cDNA was generated with the High Capacity cDNA archive kit from 1ug of input RNA (Applied Biosystems). Each 20ul reaction contained a final concentration of 0.2uM primers, 1X Power SYBR Green dye and 2ul of a 1:20 dilution of template cDNA. Primers designed to amplify a region spanning the exon 2 – exon 3 boundary of *sox10* (IDT) were generated using the PrimerExpress software (Applied Biosystems) and tested for efficiency as in Sanek et al., 2009. qPCR was performed on an Applied Biosystems StepOne Plus machine using the ΔΔCt method. Each of two biological replicates was

loaded with three technical replicates on a single plate. *sox10* primer sequences were 5'-GGCTGCAGGGTCACCATT-3' and 5'-AGGGCTGTGACTCTGACCTGTAG-3', and *ef1*α (used as the reference gene) primer sequences were 5'-CTTCTCAGGCTGACTGTGC-3' and 5'-CCGCTAGCATTACCCTCC-3'.

Results

Zebrafish Zic2 regulates craniofacial development

In humans, mutations in *ZIC2* are associated with HPE and a mild but characteristic set of craniofacial dysmorphologies (Solomon et al., 2010a). Since zebrafish with reduced Zic2a levels display HPE-like forebrain defects (Sanek et al., 2008; Sanek et al., 2009), we asked whether zebrafish *ZIC2* orthologs, *zic2a* and *zic2b*, play roles in craniofacial development. To assess the role of *zic2a*, we injected a previously described *zic2a*-specific antisense morpholino oligonucleotide (zic2aMO) to knock down zebrafish Zic2a (Nyholm et al., 2007) and evaluated the effect on craniofacial cartilages with alcian blue staining at 5dpf (Fig. 1A-F). Zic2a depletion caused hypoplasia of the jaw in 72% of morphants (Fig. 1B). Defects ranged from the relatively mild improperly positioned hyoid arch (Fig. 1B', outlined) to more severely shortened jaw arches, (Fig. 1E). The most strongly affected zic2a morphants exhibited nearly complete deletion of the anterior pharyngeal and neurocranial cartilages (not shown, 20% of morphants).

To investigate a role for *zic2b* during craniofacial development, we designed a *zic2b*-specific splice-blocking morpholino (zic2bMO). Embryos injected with zic2bMO

expressed reduced levels of full-length *zic2b* transcript and developed with neurulation defects comparable to zic2a morphants (Supplemental Fig. 1, Nyholm et al, 2009). Zic2b morphants showed mild craniofacial defects, with 35% displaying slight hypoplasia of the pharyngeal cartilages, while the remainder developed normally (Fig 1C,F). Similar results were obtained using a translation-blocking zic2bMO (data not shown). Together, these results suggest *zic2a* is required for normal craniofacial development, while *zic2b* plays a less critical role in this process (Fig. 1G).

To better understand when Zic2a exerts its effect on craniofacial development, we generated a transgenic line of fish, *Tg(11XUAS:zic2aYFP)*, that allowed temporally controlled overexpression of Zic2aYFP when crossed with the heat-inducible *Tg(hsp70l:Gal4VP16)* line. *Tg(hsp70l:Gal4VP16);Tg(11XUAS:zic2aYFP)* embryos expressed ubiquitous Zic2aYFP upon heat shock (HS) induction. After HS at 10hpf, Zic2aYFP-positive embryos developed with a distinct phenotype compared to their YFP-negative siblings. This phenotype included a shortened anterior-posterior axis, retinal coloboma and neurulation defects consistent with previously published roles of zebrafish *zic2a* in retinal and midbrain morphogenesis (Supplemental Fig. 2; Sanek et al., 2009; Nyholm et al, 2009). In addition, pharyngeal cartilages, which make up the basis of the forming jaw, were strongly affected, with shortening or inversion of the hyoid arch, and reduction of the ceratobranchial cartilages (Fig. 2A,E). HS induction at 14hpf was similarly disruptive, resulting in severely hypoplastic pharyngeal cartilages (Fig. 2B,F). However, when Zic2aYFP was induced at 17hpf, the effects were limited to mild shortening of the mandibular and hyoid elements in 50% of embryos (Fig. 2C,G). HS

induction at 24hpf had no effect on the pharyngeal cartilages (Fig. 2D,H), suggesting that correct Zic2a expression prior to 24hpf is critical for pharyngeal cartilage development.

In addition to its effects on pharyngeal cartilages, Zic2aYFP induction at 10hpf caused abnormal proximity of the neurocranial trabecular cartilages to one another (Fig. 2I,J, asterisk in 2J). This defect was more pronounced after HS induction at 14hpf, with trabeculae fused at the midline (32% of embryos, asterisk in Fig.2L), shortened (21%), or ablated completely (26%, Fig. 2K,L). The medial ethmoid plate was absent in 53% of Zic2a overexpressors (arrow in Fig. 2L). These data show that both pharyngeal and neurocranial cartilages are profoundly affected by Zic2aYFP misexpression before 24hpf, and further support an important role for Zic2a in craniofacial development (Fig. 2M,N).

In order to confirm specificity of the craniofacial defects seen in zic2 morphants and Zic2aYFP-expressing embryos, we used nonoverlapping translation-blocking morpholinos, zic2aAUGMO, to reduce Zic2a levels. Zic2aAUGMO-injected embryos developed with a range of pharyngeal cartilage defects comparable to those observed in Zic2aMO-injected morphants, but with a lower penetrance of these defects (58%, Supplemental Fig. 3). Notably, zic2aAUGMO effectively reduced Zic2aYFP levels and rescued the Zic2aYFP overexpression phenotype in *Tg(hsp70l:Gal4VP16) x Tg(11XUAS:zic2aYFP)* embryos (Supplemental Fig. 4).

To test whether chondrogenesis is disrupted prior to 5dpf in embryos with altered levels of Zic2a, we assayed expression of two chondrogenic markers, *sox9a* and

col2a1a. *Sox9a*, which is required for chondrogenesis and marks the neurocranium and pharyngeal arches at 2dpf, was reduced in the anterior pharyngeal arches of zic2a morphants, and not expressed posterior to PA1 and PA2 (Fig. 3A,B). *Sox9a* is also expressed in the trabecular condensations, which failed to fully elongate in zic2a morphants (Fig. 3C,D). The medial ethmoid plate, visible by 2dpf in control embryos, failed to form in zic2a morphants (arrow in Fig. 3C). *Col2a1a*, the major collagen of cartilage expressed in the neurocranium, reiterated the shortened trabeculae and absence of the medial ethmoid plate in zic2a morphants (Fig. 3E,F). Similarly, following heat shock at 10hpf, Zic2aYFP-expressing embryos did not appropriately establish the bilateral chondrogenic condensations that prefigure the trabeculae (Fig. 3G,H). Collectively, results from knockdown and overexpression studies demonstrate a role for Zic2a in regulating early development of both pharyngeal and neurocranial cartilages, and show that Zic2a functions before 24hpf to correctly pattern craniofacial chondrogenic primordia.

zic2a and zic2b promote cranial neural crest induction and exit from the neural tube

Many of the craniofacial structures that develop abnormally in embryos with altered levels of Zic2 are derived from NC cells. Based on the timing of Zic2 function, we hypothesized that the craniofacial defects in embryos with elevated or depleted Zic2a levels are due to a disruption in NC development. The expression patterns of *zic2a* and *zic2b* are consistent with an early role in NC induction. Both genes are expressed in the anterior neural plate, including the presumptive cranial NC, beginning

at mid-gastrulation (Fig. 4A,B; Grinblat and Sive, 2001; Toyama et al., 2004). *Zic2a* shares a tight border with the non-neural ectodermal marker *dlx3b* through the end of gastrulation (Fig. 4C,D). As somitogenesis begins, *zic2a* levels are reduced in early NC, marked by expression of *foxd3* (Fig. 4E-H), and remain low through at least 5S (data not shown). In contrast, *zic2b* expression in cranial NC primordia overlaps with the NC marker *foxd3* at 1S (Fig. 4I) and continues in the bilateral NC domains from which *zic2a* is excluded through 6S (Fig. 4J,K). In addition, *zic2b* expression extends into the posterior neural keel during early somitogenesis, while *zic2a* expression does not (Fig. 4L).

To determine if the zebrafish *zic2* genes regulate NC induction, we examined early NC marker expression in zic2 morphants. S*na1b* expression levels are unaffected in most zic2a morphants (77% of morphants, Fig. 4M,N), with only 23% of embryos showing a mild reduction in staining. Single knockdown of Zic2b reduced the expression of *sna1b* in 40% of morphant embryos and eliminated it in 34% of zic2b morphants (Fig. 4O), while depleting Zic2a and Zic2b together eliminated *sna1b* expression in most morphants (63%, not shown) and reduced the NC domain in 30% of morphant embryos (30%, Fig. 4P) Similar results were obtained by ISH for *sox9b* (data not shown). These data suggest that *zic2a* and *zic2b* both contribute to the timely induction of the NC and that *zic2b*, whose expression persists longer in the NC, plays a more critical role.

We next asked if Zic2 continues to regulate NC development after induction. In control 18hpf embryos, *sox10* expression marks the cranial NC cells, which have exited

the neural tube and are migrating forward in bilateral streams (Fig. 5A). Injection of zic2aMO or zic2bMO singly resulted in accumulation of *sox10*-expressing cells on the dorsal aspect of the midbrain and hindbrain (Fig. 5B,C). A similar phenotype was observed in embryos injected with both zic2aMO and zic2bMO (Fig. 5D), indicating that both *zic2a* and *zic2b* functions contribute to the timely emigration of cranial NC. Importantly, *sox10* expression did not appear reduced in zic2b morphants, suggesting that cranial NC may recover after an initial delay in induction following Zic2b knockdown.

In contrast to zic2 morphants, dorsal mislocalization of NC cells was not observed after elevation of Zic2a levels in transgenic overexpressors. Both YFP-negative siblings and embryos expressing Zic2aYFP after a 10hpf HS displayed wild-type localization of *sox10*-positive cells, despite the characteristic abnormal neural tube morphology in overexpressors (Fig. 5E,F). The number of *sox10*-positive cells increased in embryos expressing Zic2aYFP (Fig. 5F and Supplemental Fig. 2J,K), as did the overall amount of *sox10* transcript measured by quantitative real-time PCR (Fig. 5G), suggesting expansion in NC cells following Zic2a misexpression. Taken together, these data demonstrate important roles for Zic2 in the timing of cranial NC induction and in neural tube exit and/or migratory onset, with *zic2b* playing a more prominent role in the process of induction.

zic2a and zic2b regulate pigment NC lineages.

In addition to cranial cartilage, the NC forms chromatophores, and defects in facial cartilage often correlate with pigment defects (Schilling et al., 1996). To test whether Zic2 functions in pigment cell formation, we examined expression of several lineage-specific marker genes in zic2a and zic2b morphants. NC cells fated to differentiate into melanophores express the *mitfa* transcription factor at 24hpf (Fig. 6A). While knockdown of Zic2a alone caused only a mild reduction in *mitfa* staining, depletion of Zic2b resulted in a dramatic reduction of melanophore precursors in the trunk (Fig. 6B,C). Double Zic2 knockdown extended the reduction of *mitfa* expression into the cranial region (Fig. 6D). These data indicate that *zic2b* is required to generate the appropriate number of melanophores in the trunk, while *zic2a* and *zic2b* work together to regulate melanophore development in the cranial region.

NC cells fated to become xanthophores express *gch2* at 24hpf (Fig. 6E). In contrast to *mitfa*, *gch2* expression was reduced at all axial levels of zic2a morphants (Fig. 6F). Zic2b depletion again preferentially reduced *gch2* expression in the trunk (Fig. 6G). Double knockdown caused a severe reduction of *gch2* expression in cranial and trunk regions, similar to single Zic2a depletion (Fig. 6H). Double morphants and zic2b single morphants had a distinctive phenotype in the cranial region, where NC cells formed large aggregates (asterisks in Fig. 6C,G). Additionally, many Zic2b-depleted embryos had aberrantly localized pigment cell precursors on the dorsal aspect of the neural tube (asterisk in C inset; see Fig. 5). Transverse sections through the midbrains of *gch2*-stained embryos revealed no difference between control embryos and zic2a morphants (Fig. 6I,J). However, zic2b morphants and double morphants exhibited large

conglomerates of pigment cell precursors, which had exited the neural tube, but migrated abnormally (asterisks in Fig. 6K,L). In addition, some NC cells were extruded into the lumen from the apical surface, rather than exiting the basal side of the neural epithelium (arrow in Fig. 6L). Together, these results argue that *zic2a* and *zic2b* contribute to the regulation of chromatophore development and exit from the neural tube, with differing requirements at cranial and trunk axial levels.

Zic2a and Zic2b functions contribute to the formation of pharyngeal arch primordia

NC-derived jaw precursors migrate from the hindbrain to colonize the pharyngeal arches during normal development (Schilling and Kimmel, 1994). Having shown that *zic2a* and *zic2b* help orchestrate the onset of cranial NC migration, we hypothesized that cells retained in or near the dorsal neural tube of zic2 morphants are fated to contribute to specific NC-derived lineages, including pharyngeal arch primordia. Using *dlx2a* expression as a marker, we determined that migration of the NC cells to the first two pharyngeal arches, PA1 and PA2, remained largely unaltered in zic2 morphants, since no dorsally mislocalized *dlx2a*-positive cells were observed (Fig. 7A-D). However, *dlx2a*-positive PA1 and PA2 were reduced in 30% of zic2a morphants (Fig. 7B). *Dlx2a* expression in the arches was unchanged in zic2b morphants (Fig. 7C). Zic2 double knockdown caused a reduction in the size of PA1 and PA2 (33% of morphants), the posterior pharyngeal arches (24% of morphants, Fig. 7D), or all pharyngeal arches (22% of morphants).

To further probe the role of Zic2 in PA formation, we induced expression of Zic2aYFP at several time points. After induction at 10hpf, mispatterning of *dlx2a* was observed in Zic2aYFP-positive embryos, consisting of an incomplete separation of PA1 and PA2 in 36% of overexpressors (Fig. 7E,F; arrow in 7F). After induction at 14hpf, pharyngeal arch *dlx2a* expression in Zic2aYFP-positive embryos was indistinguishable from that seen in controls (Fig. 7G,H), despite the fact that older siblings had severe and fully penetrant craniofacial defects at 5dpf (see Fig. 2). Collectively, these data argue that the pharyngeal cartilage defects in zic2a morphants and Zic2aYFP overexpressors may not be fully attributable to early defects in NC specification and migratory onset.

To test whether *zic2a* expression is required within the chondrogenic lineage to promote craniofacial cartilage development, we employed cell transplantation assays. Cells transplanted from control morphant donors to control morphant hosts contributed to both the pharyngeal cartilage (Fig. 7I, see arrowheads) and neurocranium (Fig. 7J, see arrowhead) (4/7 embryos, 1 exp., see asterisks in Supplemental Table 1). Similarly, Zic2a-depleted cells transplanted into control hosts contributed to the pharyngeal cartilages (Fig. 7K,K') and the neurocranium (Fig. 7L,L'), but somewhat less frequently than control cells (3/19 embryos, 2 exp., see asterisks in Supplemental Table 2). Control morphant cells transplanted to a zic2a morphant background also contributed to craniofacial cartilages, suggesting that Zic2a isnot required in surrounding cartilage for integration (2/17 embryos, 1 exp., Supplemental Fig. 5 and Supplemental Table 4). Control cell integration into cartilages did not lead to appreciable rescue of the Zic morphant defect. We observed unusual left-right asymmetry of the host pharyngeal

cartilage defects in several embryos (Supplemental Fig. 5D). This asymmetry was not observed in Zic morphants and is suggestive of non-autonomous rescue by control morphant cells when transplanted into tissues surrounding chondrogenic tissues. Due to a broad distribution of donor cells, we could not conclusively determine which surrounding tissue might be involved. Both control and Zic2a-depleted transplanted cells also contributed to NC lineages earlier during development, at 24hpf (asterisks in Supplemental Fig. 5 and Supplemental Tables 3 and 5).

Among wild-type embryos that received Zic2-morphant transplants, several embryos developed with defects in host-derived neurocranium (5/19, 2 exp., asterisks in Fig. 7L, Supplemental Table 2). All of these embryos had significant contributions of Zic morphant cells to adjacent forebrain, while control-to-control transplants showed no craniofacial cartilage defects (7/7, 1exp.). These observations argue against a strict cell-autonomous requirement for Zic2a function, but are consistent with a dual role for Zic2 in the forebrain neuroepithelium and potentially in the chondrogenic NC itself.

Zebrafish Zic2 patterns the ventral forebrain primordium

The proximal environment of the post-migratory NC-derived chondrogenic precursors plays a key role in promoting NC condensation, proliferation and differentiation into cartilage (Szabo-Rogers et al., 2010). Since early defects in NC development may not fully explain the craniofacial anomalies in Zic2-depleted and misexpressing embryos, we hypothesized that Zic2 patterns tissues surrounding the cartilages, and that incorrect signaling from these mispatterned tissues contributes to

the craniofacial defects observed in embryos with disrupted Zic2 levels. Consistent with this hypothesis, previous work in our lab showed that *zic2a* is required for diencephalic development and for modulating Hh signaling in the forebrain (Sanek et al., 2008; Sanek et al., 2009). To extend these studies, we examined forebrain patterning in Zic2b-depleted morphant embryos. A mild deficit in the prethalamic domain dlx2a was observed in 51% of the embryos (Fig. 8A,B, see arrowhead). The prethalamic defect was similar to, but less pronounced, than that seen in zic2a morphants (Fig.8C, Sanek et al., 2007) or in zic2 double morphants (Fig. 8D). The ventral midline of the forebrain primordium, marked by *ptch2* expression, was unaffected by Zic2 depletion (Supp. Fig. 6). This mild forebrain mispatterning correlates with mild craniofacial cartilage defects in zic2b morphants (see Fig. 1).

To further test the correlation between early forebrain patterning deficits and late craniofacial defects, we used temporally controlled Zic2aYFP misexpression. Craniofacial cartilages are strongly affected by Zic2 elevation after 10hpf and 14hpf heat-shocks, and much less so after 17hpf heat-shocks (Fig. 2). Similarly, we have found *dlx2a* expression to be disrupted in the telencephalon and diencephalon of 66% of Zic2aYFP overexpressors after induction at 10hpf (Fig. 8E,F) and in 39% after induction 14 hpf (data not shown). Importantly, ectopic Zic2a expression following a 17hpf heat shock did not cause forebrain patterning defects (data not shown). Together, these data provide correlative support to the hypothesis that aberrantly formed ventral forebrain may contribute to craniofacial deficits in embryos with reduced or elevated Zic2 levels.

Expression of *ptch2*, a critical component and target of Hh signaling (Concordet et al., 1996), was strongly reduced in the ventral midline of the entire brain primordium after Zic2aYFP induction at 10hpf (Fig. 8G,H). Despite this global reduction, expression was maintained in the ZLI, the main source of Hh signaling in the diencephalon (Scholpp et al., 2006). Similarly, expression of *nkx2.2a*, another target of Hh signaling (Barth and Wilson, 1995), was reduced in the ventral midline of the hindbrain (Fig. 8I, J). Thus, the ventral midline of the brain primordium is aberrantly formed upon Zic2aYFP induction, and is likely compromised in its ability to signal to adjacent tissues, under the same experimental conditions that lead to profound craniofacial defects. Notably, the oropharyngeal epithelium, another important source of morphogens during craniofacial development, is mispatterned in zic2a-depleted and misexpressing embryos (Fig. 8K,L and Supplemental Fig. 7). However, this mispatterning is observed later during development only in strongly affected morphants, and may be a consequence of earlier defects in the neuroepithelium. Collectively, these data demonstrate an early role for both Zic2a and Zic2b in patterning the ventral brain primordium that likely contributes to their roles in craniofacial development.

Discussion

Zic2, a highly conserved transcription factor with essential functions during mammalian brain development, is encoded by two genes in the zebrafish genome, *zic2a* and *zic2b*. Data presented here identify a novel requirement for Zic2 during craniofacial development in zebrafish. We show that the forming jaw and neurocranium

are sensitive to artificial elevation of Zic2 levels prior to 24hpf, suggesting an early role for Zic2 in craniofacial development. Since the craniofacial skeleton is largely derived from the NC, we have examined the relative contributions of the two Zic2 orthologs to neural crest formation. We show that Zic2a and Zic2b regulate several aspects of neural crest development, including induction and migratory onset of the pigment lineages, and generation and proper organization of pre-chondrogenic NC that contribute to pharyngeal primordia. Correct morphogenesis of craniofacial cartilages relies on signals from the adjacent neural epithelium where Zic2 plays an important role that likely contributes to its overall function during craniofacial development.

Zic2 and craniofacial development

We have shown that in the zebrafish craniofacial cartilages are disrupted following depletion of the *ZIC2* orthologs *zic2a* and *zic2b*, products of the teleost genome duplication that share an 82.5% amino acid identity with each other (Meyer and Van de Peer, 2005; Toyama et al., 2004; Vandepoele et al., 2004). This phenotype is consistent with craniofacial abnormalities in mouse mutants of *Zic5*, which is co-expressed and co-regulated with *Zic2* (Inoue et al., 2004). Craniofacial defects have not been reported in Zic2 knockout mice, which die during gestation (Elms et al., 2003; Warr et al., 2008); however, human patients with *ZIC2*-associated holoprosencephaly exhibit a characteristic set of mild craniofacial dysmorphologies (Solomon et al., 2010a). Collectively, these observations indicate an evolutionarily conserved role for Zic2 during craniofacial development, the mechanism of which remains to be explored.

The incompletely penetrant reduction of the NC-derived pharyngeal arches in Zic2a-depleted zebrafish embryos is consistent with early NC deficits reported in *Zic2* and *Zic5* mouse mutants (Elms et al., 2003; Inoue et al., 2004; Nagai et al., 2000). However, several lines of evidence argue that these NC deficits do not completely account for the severe craniofacial defects seen in zebrafish embryos with reduced and enhanced levels of Zic2. First, we have demonstrated that *zic2b* plays a more prominent role than *zic2a* in NC induction, while *zic2a* is more critical for craniofacial development. Second, *zic2a* and *zic2b* are expressed in the brain primordium, but not in the pharyngeal arches or the adjacent stomodeum and craniofacial mesenchyme. Third, we have shown that transplanted Zic2a-deficient cells can contribute to migrating NC and to differentiated craniofacial cartilages in a wild-type background, suggesting that Zic2a is not strictly required in the NC-derived chondrogenic lineage. Additionally, our transplant data suggest that defects in host-derived neurocranium (i.e. abnormal trabeculae) are correlated with clusters of Zic2a-depleted transplanted cells in the adjacent ventral forebrain. These data, while not conclusive, are consistent with the hypothesis that Zic2 controls the developing craniofacial cartilages in part via its role in patterning the forebrain.

In support of this hypothesis, we have shown that depletion of Zic2a or Zic2b, or misexpression of Zic2a, lead to mispatterning of the ventral midline of the brain primordium, as well as to craniofacial defects. The timing of heat shock induction experiments shows that craniofacial cartilages are sensitive to disruption by Zic2a relatively early, prior to 24hpf. Ventral forebrain signaling occurring around 10hpf is

required to pattern the zebrafish oral ectoderm (stomodeum) in preparation for the arrival of chondrogenic NC (Eberhart et al., 2006). Intriguingly, the pharyngeal epithelium is mispatterned in Zic2a-depleted embryos, suggesting the possibility that it is compromised in its ability to support differentiation of chondrogenic precursors.

We have also demonstrated a role for Zic2a in the forming optic stalk (see Supplemental Fig. 2; Sanek et al., 2009), which could contribute to its influence over craniofacial development. The retina and optic stalk are sources of several morphogens with roles in craniofacial development such as PDGF, RA, and Shh (Eberhart et al., 2008; Kish et al., 2011). It has been suggested that the eye is critical for directing neural crest migration, and may secrete positive cues for NC cells migrating towards the most anterior neurocranial structures, e.g. the ethmoid plate (Langenberg et al., 2008). In mouse (Brown et al., 2003) and zebrafish, Zic2 is expressed in the optic stalks, and regulates patterning of the retina/optic stalk interface and the adjacent ventral forebrain (Sanek et al., 2009). Compared with the well-supported roles for neural, ectodermal and endodermal signaling centers, little is known about the eye and optic stalk as organizers of NC migration and craniofacial development. Our ongoing efforts to identify optic stalk–specific targets of Zic2a will shed light on the manner in which these tissues contribute to craniofacial morphogenesis.

Early signaling by Shh, one of the key growth factors produced by the ventral midline of the brain primordium (Chiang et al., 1996), controls cell identity and patterning in surrounding tissues (Ingham and Placzek, 2006). Notably, *SHH* is the most commonly mutated gene in HPE patients (Roessler et al., 1996). We have previously

shown that Zic2a is a negative regulator of gene expression downstream of Hh signaling (Sanek et al., 2008; Sanek et al., 2009), and hypothesize that Zic2a interacts with the Hh signaling pathway to regulate patterning of the neural and oropharyngeal epithelia, which subsequently affects craniofacial development. Consistent with this hypothesis, we find that Zic2aYFP overexpression inhibits expression of the Hh signaling target *ptch2*, and that Zic2aYFP overexpressors develop with craniofacial defects similar to those caused by Hh abrogation in zebrafish, namely, hypoplastic pharyngeal cartilages, lack of medial ethmoid plate, and fused trabeculae (Wada et al., 2005; Schwend and Ahlgren, 2009; Swartz et al., 2012).

Fgf and Wnt signaling pathways interact with Zics and play important roles in craniofacial development. Fgf signaling regulates zic5 expression in *Xenopus* (Monsoro-Burq et al., 2003) and interacts with Zic2a during zebrafish optic stalk development (Sanek et al., 2009), and zebrafish *fgf8* mutants develop with craniofacial defects (Albertson and Yelick, 2005). Zebrafish *zic2a* and *zic5* are direct targets of Wnt signaling, which regulates outgrowth of chondrogenic structures (Nyholm et al., 2007; Reid et al., 2011). To fully understand the role of zic genes in craniofacial development, it will be important to determine how Zic2 interacts with these signaling pathways.

Zic2 and neural crest development

Zic genes function at the border of the neural plate to specify NC identity (Brewster et al., 1998; Hong and Saint-Jeannet, 2007; Sato et al., 2005), and Zic2 is required for generation of the appropriate number of NC cells in mice (Elms et al.,

2003). In zebrafish, *zic2a* and *zic2b* are largely co-expressed, except in the early NC, which expresses only *zic2b*. This study represents the first analysis of *zic2b* function in zebrafish, and establishes its role in several aspects of NC development, including NC induction and pigment lineage development.

NC cells undergo comprehensive changes in morphology and adhesion as they exit the basal surface of the neural tube and begin migrating throughout the embryo (Theveneau and Mayor, 2012; Clay and Halloran, 2011). In zebrafish zic2 morphants, we observe distinct defects during this phase of NC development. These include failure to initiate migration away from the neural tube and extrusion of NC cells into the neural tube lumen. There are several mechanisms by which the *zic2* genes may contribute to these aspects of NC development. Canonical Wnt signaling is important during several phases of neural crest development, including induction (Garcia-Castro et al., 2002; Patthey et al., 2009; Steventon et al., 2009), proliferation (Dickinson et al., 1994; Ikeya et al., 1997; Megason and McMahon, 2002) and delamination (Burstyn-Cohen et al., 2004). Our lab has shown that *zic2a* is a direct target of Wnt signaling, and itself promotes proliferation in the dorsal midbrain (Nyholm et al., 2007). A recent report showed that *Xenopus* Zic3 protein suppresses the Wnt/β-catenin signaling pathway (Fujimi et al., 2011). In cell culture, human ZIC2 protein can interact directly with Tcf4 and act as a negative regulator of Wnt signaling (Pourebrahim et al., 2011). Since it is unclear when and in which tissues these interactions occur *in vivo*, it will be important to examine the interaction between Zics and Wnt signaling in the dorsal neural tube, and during NC induction and proliferation.

Canonical Wnt signaling also promotes the specification of pigment cells from within the NC population. *Wnt1*/*Wnt3a* null mice have very depleted pigment cell populations (Ikeya et al., 1997). In zebrafish, Wnt signaling promotes pigment cell formation at the expense of other NC-derived cell types, such as neurons (Dorsky et al., 1998). Both *zic2a* and *zicb* promote development of melanophores and xanthophores in the cranial region. In the trunk, Zic2b acts without contribution from Zic2a to regulate pigment cell development. It will be interesting to test whether either or both zic2 genes interact with the Wnt signaling pathway to regulate the specification of the pigment cell lineages.

Finally, *zic2a* and *zic2b* may regulate adhesion in the dorsal brain. Concomitant depletion of Zic2a and Zic2b causes large aggregations of NC cells to accumulate. Eph/ephrin signaling regulates adhesion in epithelial cells (Dahmann et al., 2011; Pasquale et al., 2005) and is important during NC migration (Kuriyama and Mayor, 2008; Santiago and Erickson, 2002). Zic2 regulates the expression of EphB1 in the mouse forebrain (Garcia-Frigola et al., 2008; Lee et al., 2008) and Zic2a regulates several zebrafish ephrins expressed in the dorsal brain (J.T. and M.N., unpublished observations). Wnt signaling regulates changes in cell adhesion that occur in delaminating NC cells through one of its targets, the zinc-finger transcription factor *ovo1* (Piloto and Schilling, 2010). Given that *zic2a* is also a target of Wnt signaling, it will be important to determine if Zic2 plays a role in regulating the adhesive properties of the dorsal neural tube from which chondrogenic NC cells exit.

Using zebrafish to dissect Zic functions during brain and craniofacial development

How brain and craniofacial morphogenesis are coordinated remains an important outstanding question in developmental biology. The etiologies of brain defects such as HPE and DWM are complex, seldom attributable to a single genetic alteration (Schachter and Krauss, 2008; Solomon et al., 2010b), and the relationship between the neural and craniofacial phenotypes associated with these diseases is not clear. Zic genes are key regulators of both brain and craniofacial development: in mammals, reduced Zic2 levels are causally associated with gross morphological disruptions of forebrain development (HPE) and facial dysmorphology. The closely related ZIC1 and ZIC4 are linked to DWM, a congenital syndrome characterized by cerebellar hypoplasia, as well as craniofacial dysmorphologies reminiscent of those observed in ZIC2-associated HPE patients (Grinberg et al., 2004; Blank et al., 2011). Moreover, ZIC2 mutations have been identified in a patient with DWM (Mademont-Soler et al., 2010). Having determined the relative contributions of Zic2a and Zic2b to forebrain and craniofacial development in zebrafish, we are positioned to answer two important outstanding questions: (1) In which tissues do vertebrate Zics function? and (2) what is the mechanism of their function? These questions will be addressed in future studies through tissue-specific manipulation of Zic function, identification and functional analysis of Zic transcriptional targets, and identification of genetic modifiers of Zic function in zebrafish.

Acknowledgements

We thank Eric Pueschel, Nick Sanek, Jingzhu (Michael) Zhang, Matt Clay and Mary Halloran for valuable discussions throughout the course of this work, Sreelaja Nair for technical advice and Mike Padilla for expert help. We are grateful to Mary Halloran, Bruce Appel, Becky Burdine, Michael Nonet and the Zebrafish International Resource Center for fish lines and plasmids, and Tony Stretton for sharing equipment. This work was funded by grants from NIH and the American Heart Association to Y.G.

References

Ahlgren, S. C., Bronner-Fraser, M., 1999. Inhibition of sonic hedgehog signaling in vivo results in craniofacial neural crest cell death. Curr Biol. 9**,** 1304-14.

Akimenko, M. A., Ekker, M., Wegner, J., Lin, W., Westerfield, M., 1994. Combinatorial expression of three zebrafish genes related to distal-less: part of a homeobox gene code for the head. J Neurosci. 14**,** 3475-86.

Albertson, R. C., Yelick, P. C., 2005. Roles for fgf8 signaling in left-right patterning of the visceral organs and craniofacial skeleton. Dev Biol. 283**,** 310-21.

Barrallo-Gimeno, A., Holzschuh, J., Driever, W., Knapik, E. W., 2004. Neural crest survival and differentiation in zebrafish depends on mont blanc/tfap2a gene function. Development. 131**,** 1463-77.

Barth, K. A., Wilson, S. W., 1995. Expression of zebrafish nk2.2 is influenced by sonic hedgehog/vertebrate hedgehog-1 and demarcates a zone of neuronal differentiation in the embryonic forebrain. Development. 121**,** 1755-68.

Blank, M. C., Grinberg, I., Aryee, E., Laliberte, C., Chizhikov, V. V., Henkelman, R. M., Millen, K. J., 2011. Multiple developmental programs are altered by loss of Zic1 and Zic4 to cause Dandy-Walker malformation cerebellar pathogenesis. Development. 138**,** 1207-16.

Bonilla-Claudio, M., Wang, J., Bai, Y., Klysik, E., Selever, J., Martin, J. F., 2012. Bmp signaling regulates a dose-dependent transcriptional program to control facial skeletal development. Development. 139**,** 709-19.

Brewster, R., Lee, J., Ruiz i Altaba, A., 1998. Gli/Zic factors pattern the neural plate by defining domains of cell differentiation. Nature. 393**,** 579-83.

Brown, L. Y., Kottmann, A. H., Brown, S., 2003. Immunolocalization of Zic2 expression in the developing mouse forebrain. Gene Expr Patterns. 3**,** 361-7.

Brown, S. A., Warburton, D., Brown, L. Y., Yu, C. Y., Roeder, E. R., Stengel-Rutkowski, S., Hennekam, R. C., Muenke, M., 1998. Holoprosencephaly due to mutations in ZIC2, a homologue of Drosophila odd-paired. Nat Genet. 20**,** 180-3.

Burstyn-Cohen, T., Stanleigh, J., Sela-Donenfeld, D., Kalcheim, C., 2004. Canonical Wnt activity regulates trunk neural crest delamination linking BMP/noggin signaling with G1/S transition. Development. 131**,** 5327-39.

Chiang, C., Litingtung, Y., Lee, E., Young, K. E., Corden, J. L., Westphal, H., Beachy, P. A., 1996. Cyclopia and defective axial patterning in mice lacking Sonic hedgehog gene function. Nature. 383**,** 407-13.

Chong, H. J., Young, N. M., Hu, D., Jeong, J., McMahon, A. P., Hallgrimsson, B., Marcucio, R. S., 2012. Signaling by SHH rescues facial defects following blockade in the brain. Dev Dyn. 241**,** 247-56.

Clay, M. R., Halloran, M. C., 2011. Regulation of cell adhesions and motility during initiation of neural crest migration. Curr Opin Neurobiol. 21**,** 17-22.

Concordet, J. P., Lewis, K. E., Moore, J. W., Goodrich, L. V., Johnson, R. L., Scott, M. P., Ingham, P. W., 1996. Spatial regulation of a zebrafish patched homologue reflects the roles of sonic hedgehog and protein kinase A in neural tube and somite patterning. Development. 122**,** 2835-46.

Cordero, D. R., Brugmann, S., Chu, Y., Bajpai, R., Jame, M., Helms, J. A., 2011. Cranial neural crest cells on the move: their roles in craniofacial development. Am J Med Genet A. 155A**,** 270-9.

Couly, G., Creuzet, S., Bennaceur, S., Vincent, C., Le Douarin, N. M., 2002. Interactions between Hox-negative cephalic neural crest cells and the foregut endoderm in patterning the facial skeleton in the vertebrate head. Development. 129**,** 1061-73.

Cresko, W. A., Yan, Y. L., Baltrus, D. A., Amores, A., Singer, A., Rodriguez-Mari, A., Postlethwait, J. H., 2003. Genome duplication, subfunction partitioning, and lineage divergence: Sox9 in stickleback and zebrafish. Dev Dyn. 228, 480-9.

Dahmann, C., Oates, A. C., Brand, M., 2011. Boundary formation and maintenance in tissue development. Nat Rev Genet. 12, 43-55.

Dickinson, M. E., Krumlauf, R., McMahon, A. P., 1994. Evidence for a mitogenic effect of Wnt-1 in the developing mammalian central nervous system. Development. 120, 1453-71.

Dorsky, R. I., Moon, R. T., Raible, D. W., 1998. Control of neural crest cell fate by the Wnt signalling pathway. Nature. 396, 370-3.

Dubourg, C., Bendavid, C., Pasquier, L., Henry, C., Odent, S., David, V., 2007. Holoprosencephaly. Orphanet J Rare Dis. 2, 8.

Dutton, K. A., Pauliny, A., Lopes, S. S., Elworthy, S., Carney, T. J., Rauch, J., Geisler, R., Haffter, P., Kelsh, R. N., 2001. Zebrafish colourless encodes sox10 and specifies non-ectomesenchymal neural crest fates. Development. 128, 4113-25.

Eberhart, J. K., He, X., Swartz, M. E., Yan, Y. L., Song, H., Boling, T. C., Kunerth, A. K., Walker, M. B., Kimmel, C. B., Postlethwait, J. H., 2008. MicroRNA Mirn140 modulates Pdgf signaling during palatogenesis. Nat Genet. 40, 290-8.

Eberhart, J. K., Swartz, M. E., Crump, J. G., Kimmel, C. B., 2006. Early Hedgehog signaling from neural to oral epithelium organizes anterior craniofacial development. Development. 133, 1069-77.

Elms, P., Siggers, P., Napper, D., Greenfield, A., Arkell, R., 2003. Zic2 is required for neural crest formation and hindbrain patterning during mouse development. Dev Biol. 264, 391-406.

Essner, J. J., Branford, W. W., Zhang, J., Yost, H. J., 2000. Mesendoderm and left-right brain, heart and gut development are differentially regulated by pitx2 isoforms. Development. 127, 1081-93.

Fujimi, T. J., Hatayama, M., Aruga, J., 2012. Xenopus Zic3 controls notochord and organizer development through suppression of the Wnt/beta-catenin signaling pathway. Dev Biol. 361, 220-31.

Garcia-Castro, M. I., Marcelle, C., Bronner-Fraser, M., 2002. Ectodermal Wnt function as a neural crest inducer. Science. 297, 848-51.

Garcia-Frigola, C., Carreres, M. I., Vegar, C., Mason, C., Herrera, E., 2008. Zic2 promotes axonal divergence at the optic chiasm midline by EphB1-dependent and -independent mechanisms. Development. 135**,** 1833-41.

Gillhouse, M., Wagner Nyholm, M., Hikasa, H., Sokol, S. Y., Grinblat, Y., 2004. Two Frodo/Dapper homologs are expressed in the developing brain and mesoderm of zebrafish. Dev Dyn. 230**,** 403-9.

Grinberg, I., Northrup, H., Ardinger, H., Prasad, C., Dobyns, W. B., Millen, K. J., 2004. Heterozygous deletion of the linked genes ZIC1 and ZIC4 is involved in Dandy-Walker malformation. Nat Genet. 36**,** 1053-5.

Grinblat, Y., Sive, H., 2001. zic Gene expression marks anteroposterior pattern in the presumptive neurectoderm of the zebrafish gastrula. Dev Dyn. 222**,** 688-93.

Haworth, K. E., Wilson, J. M., Grevellec, A., Cobourne, M. T., Healy, C., Helms, J. A., Sharpe, P. T., Tucker, A. S., 2007. Sonic hedgehog in the pharyngeal endoderm controls arch pattern via regulation of Fgf8 in head ectoderm. Dev Biol. 303**,** 244-58.

Hong, C. S., Saint-Jeannet, J. P., 2007. The activity of Pax3 and Zic1 regulates three distinct cell fates at the neural plate border. Mol Biol Cell. 18**,** 2192-202.

Hoyle, J., Tang, Y. P., Wiellette, E. L., Wardle, F. C., Sive, H., 2004. nlz gene family is required for hindbrain patterning in the zebrafish. Dev Dyn. 229**,** 835-46.

Hu, D., Marcucio, R. S., 2009. A SHH-responsive signaling center in the forebrain regulates craniofacial morphogenesis via the facial ectoderm. Development. 136**,** 107-16.

Ikeya, M., Lee, S. M., Johnson, J. E., McMahon, A. P., Takada, S., 1997. Wnt signalling required for expansion of neural crest and CNS progenitors. Nature. 389**,** 966-70.

Inbal, A., Kim, S. H., Shin, J., Solnica-Krezel, L., 2007. Six3 represses nodal activity to establish early brain asymmetry in zebrafish. Neuron. 55**,** 407-415.

Ingham, P. W., Placzek, M., 2006. Orchestrating ontogenesis: variations on a theme by sonic hedgehog. Nat Rev Genet. 7**,** 841-50.

Inoue, T., Hatayama, M., Tohmonda, T., Itohara, S., Aruga, J., Mikoshiba, K., 2004. Mouse Zic5 deficiency results in neural tube defects and hypoplasia of cephalic neural crest derivatives. Dev Biol. 270**,** 146-62.

Jeong, J., Mao, J., Tenzen, T., Kottmann, A. H., McMahon, A. P., 2004. Hedgehog signaling in the neural crest cells regulates the patterning and growth of facial primordia. Genes Dev. 18**,** 937-51.

Karlstrom, R. O., Tyurina, O. V., Kawakami, A., Nishioka, N., Talbot, W. S., Sasaki, H., Schier, A. F., 2003. Genetic analysis of zebrafish gli1 and gli2 reveals divergent requirements for gli genes in vertebrate development. Development. 130**,** 1549-64.

Kawakami, K., Takeda, H., Kawakami, N., Kobayashi, M., Matsuda, N., Mishina, M., 2004. A transposon-mediated gene trap approach identifies developmentally regulated genes in zebrafish. Developmental Cell. 7**,** 133-144.

Kimmel, C. B., Ballard, W. W., Kimmel, S. R., Ullmann, B., Schilling, T. F., 1995. Stages of embryonic development of the zebrafish. Dev Dyn. 203**,** 253-310.

Kimmel, C. B., Miller, C. T., Kruze, G., Ullmann, B., BreMiller, R. A., Larison, K. D., Snyder, H. C., 1998. The shaping of pharyngeal cartilages during early development of the zebrafish. Dev Biol. 203**,** 245-63.

Kish, P. E., Bohnsack, B. L., Gallina, D., Kasprick, D. S., Kahana, A., 2011. The eye as an organizer of craniofacial development. Genesis. 49**,** 222-30.

Knight, R. D., Nair, S., Nelson, S. S., Afshar, A., Javidan, Y., Geisler, R., Rauch, G. J., Schilling, T. F., 2003. lockjaw encodes a zebrafish tfap2a required for early neural crest development. Development. 130**,** 5755-68.

Kuriyama, S., Mayor, R., 2008. Molecular analysis of neural crest migration. Philos Trans R Soc Lond B Biol Sci. 363**,** 1349-62.

Langenberg, T., Kahana, A., Wszalek, J. A., Halloran, M. C., 2008. The eye organizes neural crest cell migration. Dev Dyn. 237**,** 1645-52.

Le Douarin, N. M., Couly, G., Creuzet, S. E., 2012. The neural crest is a powerful regulator of pre-otic brain development. Dev Biol. 366**,** 74-82.

Lee, R., Petros, T. J., Mason, C. A., 2008. Zic2 regulates retinal ganglion cell axon avoidance of ephrinB2 through inducing expression of the guidance receptor EphB1. J Neurosci. 28**,** 5910-9.

Li, W., Cornell, R.A., 2007. Redundant activities of Tfap2a and Tfap2c are required for neural crest induction and development of other non-neural ectoderm derivatives in zebrafish embryos. Dev Biol. 304, 338-354.

Lister, J. A., Robertson, C. P., Lepage, T., Johnson, S. L., Raible, D. W., 1999. nacre encodes a zebrafish microphthalmia-related protein that regulates neural-crest-derived pigment cell fate. Development. 126**,** 3757-67.

Lumsden, A., Sprawson, N., Graham, A., 1991. Segmental origin and migration of neural crest cells in the hindbrain region of the chick embryo. Development. 113**,** 1281-91.

Mademont-Soler, I., Morales, C., Armengol, L., Soler, A., Sanchez, A., 2010. Description of the smallest critical region for Dandy-Walker malformation in chromosome 13 in a girl with a cryptic deletion related to t(6;13)(q23;q32). Am J Med Genet A. 152A**,** 2308-12.

Marcucio, R. S., Cordero, D. R., Hu, D., Helms, J. A., 2005. Molecular interactions coordinating the development of the forebrain and face. Dev Biol. 284**,** 48-61.

Marcucio, R. S., Young, N. M., Hu, D., Hallgrimsson, B., 2011. Mechanisms that underlie co-variation of the brain and face. Genesis. 49**,** 177-89.

Maurus, D., Harris, W. A., 2009. Zic-associated holoprosencephaly: zebrafish Zic1 controls midline formation and forebrain patterning by regulating Nodal, Hedgehog, and retinoic acid signaling. Genes Dev. 23**,** 1461-73.

Megason, S. G., McMahon, A. P., 2002. A mitogen gradient of dorsal midline Wnts organizes growth in the CNS. Development. 129**,** 2087-98.

Mercier, S., Dubourg, C., Garcelon, N., Campillo-Gimenez, B., Gicquel, I., Belleguic, M., Ratie, L., Pasquier, L., Loget, P., Bendavid, C., Jaillard, S., Rochard, L., Quelin, C., Dupe, V., David, V., Odent, S., 2011. New findings for phenotype-genotype correlations in a large European series of holoprosencephaly cases. J Med Genet. 48**,** 752-60.

Merzdorf, C. S., 2007. Emerging roles for zic genes in early development. Dev Dyn. 236**,** 922-40.

Meyer, A., Van de Peer, Y., 2005. From 2R to 3R: evidence for a fish-specific genome duplication (FSGD). Bioessays. 27**,** 937-45.

Milet, C., Monsoro-Burq, A. H., 2012. Neural crest induction at the neural plate border in vertebrates. Dev Biol. 366**,** 22-33.

Minoux, M., Rijli, F. M., 2010. Molecular mechanisms of cranial neural crest cell migration and patterning in craniofacial development. Development. 137**,** 2605-21.

Monsoro-Burq, A. H., Fletcher, R. B., Harland, R. M., 2003. Neural crest induction by paraxial mesoderm in Xenopus embryos requires FGF signals. Development. 130, 3111-24.

Nagai, T., Aruga, J., Minowa, O., Sugimoto, T., Ohno, Y., Noda, T., Mikoshiba, K., 2000. Zic2 regulates the kinetics of neurulation. Proc Natl Acad Sci U S A. 97, 1618-23.

Nakata, K., Koyabu, Y., Aruga, J., Mikoshiba, K., 2000. A novel member of the Xenopus Zic family, Zic5, mediates neural crest development. Mech Dev. 99, 83-91.

Nakata, K., Nagai, T., Aruga, J., Mikoshiba, K., 1998. Xenopus Zic family and its role in neural and neural crest development. Mech Dev. 75, 43-51.

Nasevicius, A., Ekker, S. C., 2000. Effective targeted gene 'knockdown' in zebrafish. Nat Genet. 26, 216-20.

Nie, S., Kee, Y., Bronner-Fraser, M., 2009. Myosin-X is critical for migratory ability of Xenopus cranial neural crest cells. Dev Biol. 335, 132-42.

Nyholm, M. K., Abdelilah-Seyfried, S., Grinblat, Y., 2009. A novel genetic mechanism regulates dorsolateral hinge-point formation during zebrafish cranial neurulation. J Cell Sci. 122, 2137-48.

Nyholm, M. K., Wu, S. F., Dorsky, R. I., Grinblat, Y., 2007. The zebrafish zic2a-zic5 gene pair acts downstream of canonical Wnt signaling to control cell proliferation in the developing tectum. Development. 134, 735-46.

Odenthal, J., Nusslein-Volhard, C., 1998. fork head domain genes in zebrafish. Dev Genes Evol. 208, 245-58.

Parichy, D. M., Ransom, D. G., Paw, B., Zon, L. I., Johnson, S. L., 2000. An orthologue of the kit-related gene fms is required for development of neural crest-derived xanthophores and a subpopulation of adult melanocytes in the zebrafish, Danio rerio. Development. 127, 3031-44.

Pasquale, E. B., 2005. Eph receptor signalling casts a wide net on cell behaviour. Nat Rev Mol Cell Biol. 6, 462-75.

Patthey, C., Edlund, T., Gunhaga, L., 2009. Wnt-regulated temporal control of BMP exposure directs the choice between neural plate border and epidermal fate. Development. 136, 73-83.

Piloto, S., Schilling, T. F., 2010. Ovo1 links Wnt signaling with N-cadherin localization during neural crest migration. Development. 137**,** 1981-90.

Pourebrahim, R., Houtmeyers, R., Ghogomu, S., Janssens, S., Thelie, A., Tran, H. T., Langenberg, T., Vleminckx, K., Bellefroid, E., Cassiman, J. J., Tejpar, S., 2011. Transcription factor Zic2 inhibits Wnt/beta-catenin protein signaling. J Biol Chem. 286**,** 37732-40.

Reid, B. S., Yang, H., Melvin, V. S., Taketo, M. M., Williams, T., 2011. Ectodermal Wnt/beta-catenin signaling shapes the mouse face. Dev Biol. 349**,** 261-9.

Roessler, E., Belloni, E., Gaudenz, K., Jay, P., Berta, P., Scherer, S. W., Tsui, L. C., Muenke, M., 1996. Mutations in the human Sonic Hedgehog gene cause holoprosencephaly. Nat Genet. 14**,** 357-60.

Sanek, N. A., Grinblat, Y., 2008. A novel role for zebrafish zic2a during forebrain development. Dev Biol. 317**,** 325-35.

Sanek, N. A., Taylor, A. A., Nyholm, M. K., Grinblat, Y., 2009. Zebrafish zic2a patterns the forebrain through modulation of Hedgehog-activated gene expression. Development. 136**,** 3791-800.

Santiago, A., Erickson, C. A., 2002. Ephrin-B ligands play a dual role in the control of neural crest cell migration. Development. 129**,** 3621-32.

Sato, T., Sasai, N., Sasai, Y., 2005. Neural crest determination by co-activation of Pax3 and Zic1 genes in Xenopus ectoderm. Development. 132**,** 2355-63.

Schachter, K. A., Krauss, R. S., 2008. Murine models of holoprosencephaly. Curr Top Dev Biol. 84**,** 139-70.

Schilling, T. F., Kimmel, C. B., 1994. Segment and cell type lineage restrictions during pharyngeal arch development in the zebrafish embryo. Development. 120**,** 483-94.

Schilling, T. F., Kimmel, C. B., 1997. Musculoskeletal patterning in the pharyngeal segments of the zebrafish embryo. Development. 124**,** 2945-60.

Schilling, T. F., Piotrowski, T., Grandel, H., Brand, M., Heisenberg, C. P., Jiang, Y. J., Beuchle, D., Hammerschmidt, M., Kane, D. A., Mullins, M. C., van Eeden, F. J., Kelsh, R. N., Furutani-Seiki, M., Granato, M., Haffter, P., Odenthal, J., Warga, R. M., Trowe, T., Nusslein-Volhard, C., 1996. Jaw and branchial arch mutants in zebrafish I: branchial arches. Development. 123**,** 329-44.

Scholpp, S., Wolf, O., Brand, M., Lumsden, A., 2006. Hedgehog signalling from the zona limitans intrathalamica orchestrates patterning of the zebrafish diencephalon. Development. 133, 855-64.

Schwend, T., Ahlgren, S. C., 2009. Zebrafish con/disp1 reveals multiple spatiotemporal requirements for Hedgehog-signaling in craniofacial development. BMC Dev Biol. 9, 59.

Solomon, B. D., Lacbawan, F., Mercier, S., Clegg, N. J., Delgado, M. R., Rosenbaum, K., Dubourg, C., David, V., Olney, A. H., Wehner, L. E., Hehr, U., Bale, S., Paulussen, A., Smeets, H. J., Hardisty, E., Tylki-Szymanska, A., Pronicka, E., Clemens, M., McPherson, E., Hennekam, R. C., Hahn, J., Stashinko, E., Levey, E., Wieczorek, D., Roeder, E., Schell-Apacik, C. C., Booth, C. W., Thomas, R. L., Kenwrick, S., Cummings, D. A., Bous, S. M., Keaton, A., Balog, J. Z., Hadley, D., Zhou, N., Long, R., Velez, J. I., Pineda-Alvarez, D. E., Odent, S., Roessler, E., Muenke, M., 2010. Mutations in ZIC2 in human holoprosencephaly: description of a novel ZIC2 specific phenotype and comprehensive analysis of 157 individuals. J Med Genet. 47, 513-24.

Solomon, B. D., Mercier, S., Velez, J. I., Pineda-Alvarez, D. E., Wyllie, A., Zhou, N., Dubourg, C., David, V., Odent, S., Roessler, E., Muenke, M., 2010b. Analysis of genotype-phenotype correlations in human holoprosencephaly. Am J Med Genet C Semin Med Genet. 154C, 133-41.

Sperber, S. M., Saxena, V., Hatch, G., Ekker, M., 2008. Zebrafish dlx2a contributes to hindbrain neural crest survival, is necessary for differentiation of sensory ganglia and functions with dlx1a in maturation of the arch cartilage elements. Dev Biol. 314, 59-70.

Steventon, B., Araya, C., Linker, C., Kuriyama, S., Mayor, R., 2009. Differential requirements of BMP and Wnt signalling during gastrulation and neurulation define two steps in neural crest induction. Development. 136, 771-9.

Swartz, M. E., Nguyen, V., McCarthy, N. Q., Eberhart, J. K., 2012. Hh signaling regulates patterning and morphogenesis of the pharyngeal arch-derived skeleton. Dev Biol. 369, 65-75.

Szabo-Rogers, H. L., Geetha-Loganathan, P., Whiting, C. J., Nimmagadda, S., Fu, K., Richman, J. M., 2009. Novel skeletogenic patterning roles for the olfactory pit. Development. 136, 219-29.

Szabo-Rogers, H. L., Smithers, L. E., Yakob, W., Liu, K. J., 2010. New directions in craniofacial morphogenesis. Dev Biol. 341, 84-94.

Takada, N., Appel, B., 2011. swap70 Promotes neural precursor cell cycle exit and oligodendrocyte formation. Molecular and Cellular Neuroscience. 48, 225-235.

Theveneau, E., Mayor, R., 2012. Neural crest delamination and migration: From epithelium-to-mesenchyme transition to collective cell migration. Dev Biol. 366, 34-54.

Thisse, C., Thisse, B., Postlethwait, J. H., 1995. Expression of snail2, a second member of the zebrafish snail family, in cephalic mesendoderm and presumptive neural crest of wild-type and spadetail mutant embryos. Dev Biol. 172, 86-99.

Thisse, B., Pflumio, S., Fürthauer, M., Loppin, B., Heyer, V., Degrave, A., Woehl, R., Lux, A.,Steffan, T., Charbonnier, X.Q. and Thisse, C. (2001) Expression of the zebrafish genome during embryogenesis (NIH R01 RR15402). ZFIN Direct Data Submission (http://zfin.org)

Toyama, R., Gomez, D. M., Mana, M. D., Dawid, I. B., 2004. Sequence relationships and expression patterns of zebrafish zic2 and zic5 genes. Gene Expr Patterns. 4, 345-50.

Tu, C. T., Yang, T. C., Huang, H. Y., Tsai, H. J., 2012. Zebrafish arl6ip1 is required for neural crest development during embryogenesis. PLoS One. 7, e32899.

Vandepoele, K., De Vos, W., Taylor, J. S., Meyer, A., Van de Peer, Y., 2004. Major events in the genome evolution of vertebrates: paranome age and size differ considerably between ray-finned fishes and land vertebrates. Proc Natl Acad Sci U S A. 101, 1638-43.

Vanderlaan, G., Tyurina, O. V., Karlstrom, R. O., Chandrasekhar, A., 2005. Gli function is essential for motor neuron induction in zebrafish. Dev Biol. 282, 550-70.

Wada, N., Javidan, Y., Nelson, S., Carney, T. J., Kelsh, R. N., Schilling, T. F., 2005. Hedgehog signaling is required for cranial neural crest morphogenesis and chondrogenesis at the midline in the zebrafish skull. Development. 132, 3977-88.

Warr, N., Powles-Glover, N., Chappell, A., Robson, J., Norris, D., Arkell, R. M., 2008. Zic2-associated holoprosencephaly is caused by a transient defect in the organizer region during gastrulation. Hum Mol Genet. 17, 2986-96.

Westerfield, M. 2000. The zebrafish book. A guide for the laboratory use of zebrafish (Danio rerio). 4th ed., Univ. of Oregon Press, Eugene.

Wilkie, A. O., Morriss-Kay, G. M., 2001. Genetics of craniofacial development and malformation. Nat Rev Genet. 2, 458-68.

Yan, Y. L., Hatta, K., Riggleman, B., Postlethwait, J. H., 1995. Expression of a type II collagen gene in the zebrafish embryonic axis. Dev Dyn. 203**,** 363-76.

Yan, Y. L., Willoughby, J., Liu, D., Crump, J. G., Wilson, C., Miller, C. T., Singer, A., Kimmel, C., Westerfield, M., Postlethwait, J. H., 2005. A pair of Sox: distinct and overlapping functions of zebrafish sox9 co-orthologs in craniofacial and pectoral fin development. Development. 132**,** 1069-83.

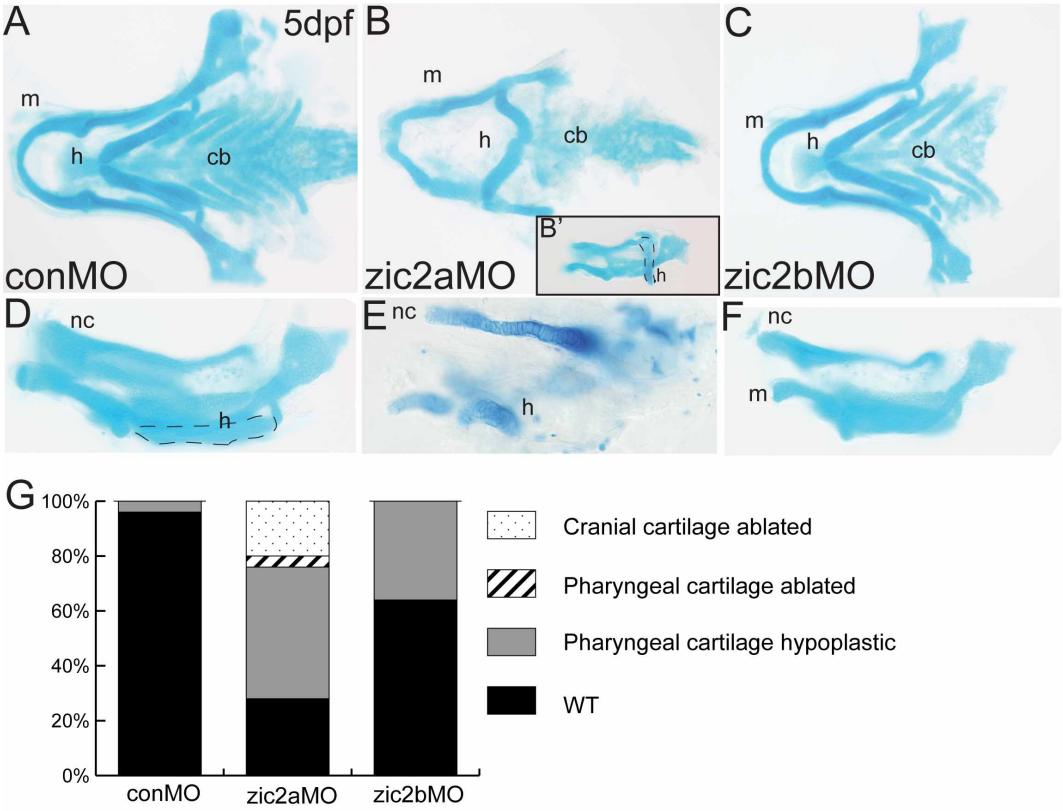

Fig. 1. *Zic2 is required for craniofacial development*. Alcian blue-stained cartilage in zic2 morphants at 5dpf. (A,D) Control morphants have wild-type pharyngeal and neurocranial cartilages (53/55, 6 exp.). (B) Zic2a morphants have variable craniofacial defects, including hypoplastic pharyngeal cartilages and an incorrectly angled hyoid arch (16/54, 5 exp.; outline in 1B'). (E) Severely affected zic2a morphants have more dramatic hypoplasia (10/54, 5 exp.) or ablation of anterior cartilages (11/54, not shown). (C,F) Zic2b morphants are either wild-type (45/70, 6 exp.) or develop shortened mandibular and hyoid arches (25/70, 6 exp.). (G) Penetrance of craniofacial defects in control and morphant embryos. A-C are dorsal views with anterior to the left. D-F are lateral views. Abbreviations: cb – ceratobranchials, h – hyoid, m – mandibular, nc – neurocranium.

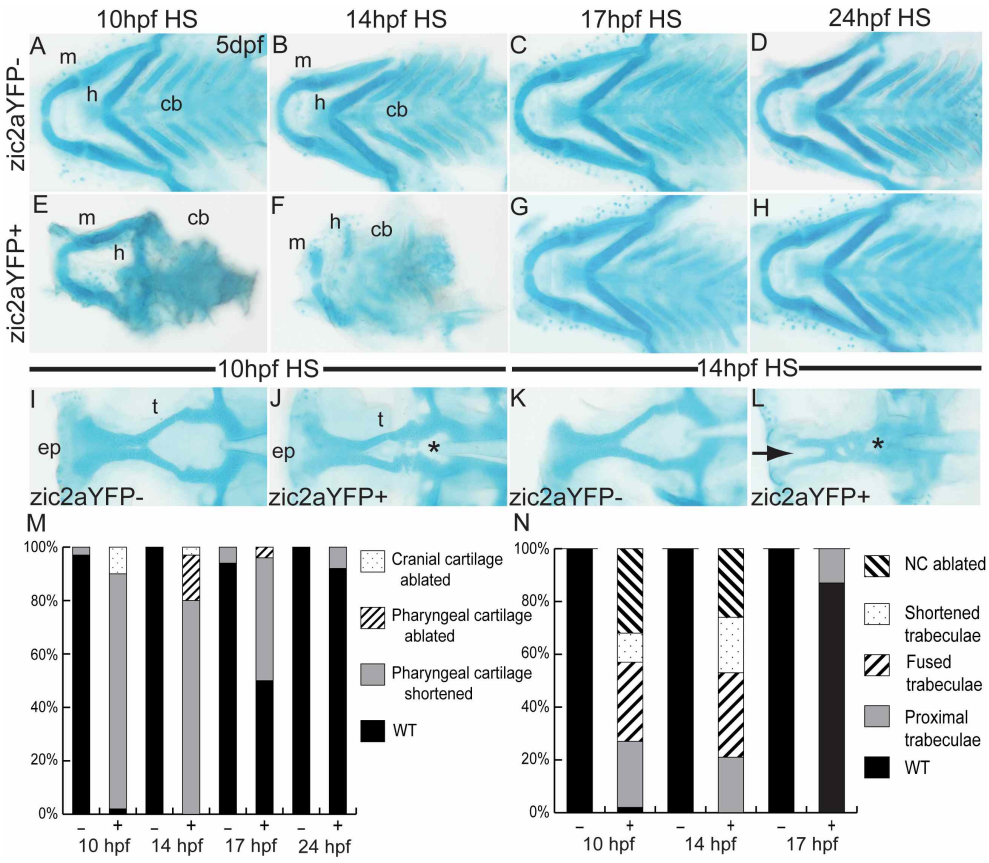

Fig. 2. *Craniofacial development is sensitive to early elevation of Zic2a levels*. Alcian blue-stained cartilage in heat-shocked *Tg(hsp70l:Gal4VP16);Tg(11XUAS:zic2aYFP)* embryos at 5dpf. (A,E) Heat shock (HS)-induced misexpression of Zic2aYFP at 10hpf has a variable effect on craniofacial cartilage, ranging from shortened mandibular and hyoid arches (45/51, 5 exp., shown in 2E) to absence of all anterior cartilages (5/51, 5 exp.). (B,F) Zic2aYFP induction at 14hpf has a similar effect, causing hypoplastic pharyngeal cartilages (29/36, 3 exp., shown in 2F) or ablation (7/36, 3 exp.). (C,G) Zic2aYFP induction at 17hpf causes less penetrant pharyngeal cartilage hypoplasia in overexpressors (12/24, 2 exp.). (D,H) Zic2aYFP induction at 24hpf has no effect on craniofacial cartilage (57/62, 4 exp.). (I,J) 10hpf HS causes a narrowing of the space between trabecular cartilages (13/53, 4 exp., asterisk in 2J) or complete fusion (16/53, 4

exp.). (K,L) Zic2aYPF induction at 14hpf causes fusion of the trabeculae (asterisk in 2L) and absence of the ethmoid plate (10/19, 1 exp., arrow in 2L), or ablation of the entire anterior neurocranium (5/19, 1 exp.). (M,N) Penetrance of cartilage defects following Zic2aYFP induction at specified timepoints. A-H are dissected pharyngeal cartilages, dorsal views, anterior to the left. I-L are dissected neurocranial cartilages, dorsal views, anterior to the left. Abbreviations: cb – ceratobranchials, ep – ethmoid plate, h – hyoid arch, m – mandibular arch, t – trabecular cartilages.

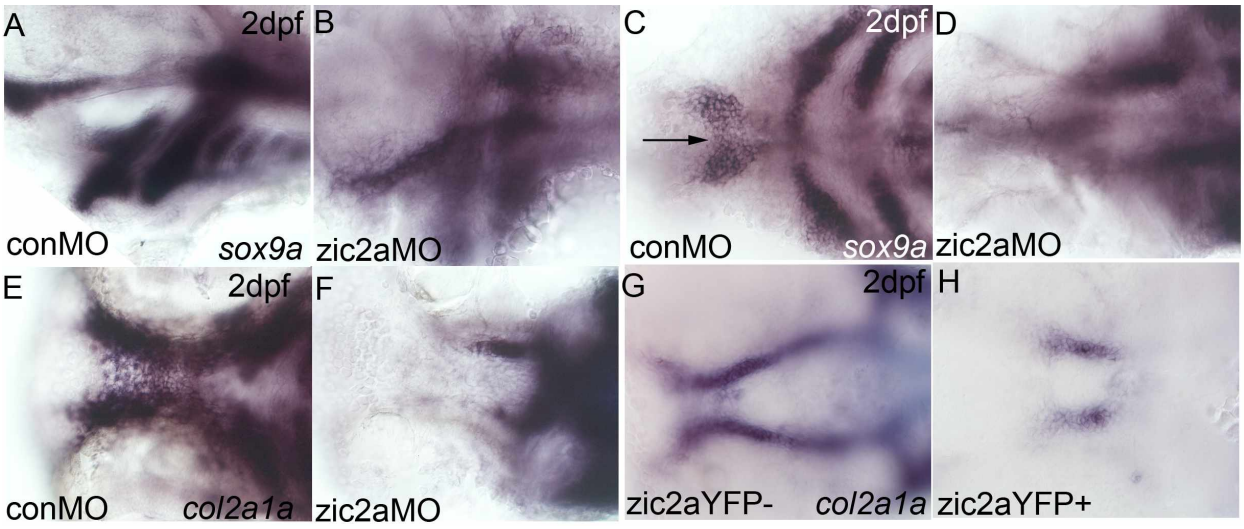

Fig. 3. *Zic2a regulates patterning of anterior chondrogenic condensations.* 2dpf zic2a morphants (A-F) and overexpressors (G,H) stained by ISH for *col2a1a* or *sox9a*. (A,B) *Sox9a* expression is reduced in the posterior PAs of Zic2a-depleted embryos (18/20, 1 exp.). (C,D) Zic2a morphants have shortened trabeculae (18/20, 1 exp.) and lack the medial ethmoid plate (12/20, 1 exp., arrow in 3C). (E,F) Expression of *col2a1a* reiterates the shortened trabeculae and lack of ethmoid plate in Zic2a-depleted embryos (43/43, 2 exp). (G,H) *Col2a1a* expression in wild-type siblings shows the bilateral trabeculae and ethmoid plate (67/107, 2 exp.). (H) The ethmoid plate is ablated and trabeculae are shortened by Zic2aYFP misexpression induced at 10hpf (38/67, 2 exp). A,B are lateral views. C-H are ventral views, anterior to the left.

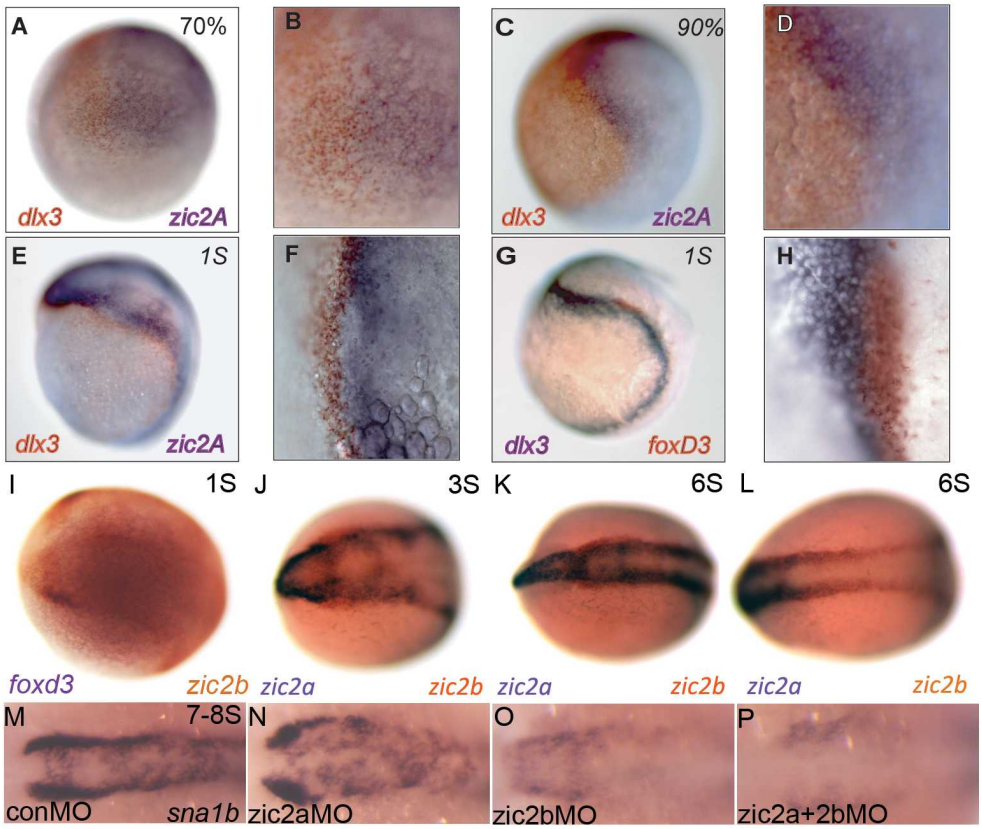

Fig. 4. *Zic2b promotes timely neural crest induction*. (A-L) Wild-type embryos stained by two-color ISH for expression of *dlx3b*, *foxd3*, *zic2a* and *zic2b*. (A,B) At 70% epiboly, weak expression of *dlx3b* (orange) and *zic2a* (purple) form two adjacent domains. (C,D) These domains are stronger by 90% epiboly but continue to overlap, suggesting the neural plate border is not completely formed. (E,F) At 1S, *dlx3b* (orange) and *zic2a* (purple) begin to separate. (G,H) *Foxd3* (orange) straddles the border beginning at 1S, overlapping neural and non-neural (*dlx3b*, purple) markers. (I) At 1S, NC marker *foxd3* (orange) and *zic2b* (purple) overlap at the neural plate border. (J,K) From 3-6S, *zic2b* (orange) is expressed in two anterior, bilateral domains from which *zic2a* (purple) is excluded. (L) *Zic2b* expression at the neural plate border extends into the posterior neural keel. (M,N) *Sna1b* expression is unchanged in zic2a morphants during early

somitogenesis (37/48, 5 exp.). (O) Zic2b morphants have reduced (19/47, 5 exp.) or absent (16/47, 5 exp.) NC domains. (P) The *sna1b* domain is reduced (11/38, 5 exp.) or more frequently absent (24/38, 5 exp.) in double zic2 morphants. A,C,E,G are lateral views, anterior to the right. B, D, F and H are high magnification images of A, C, E and G, respectively. I-P are dorsal views with anterior to the left.

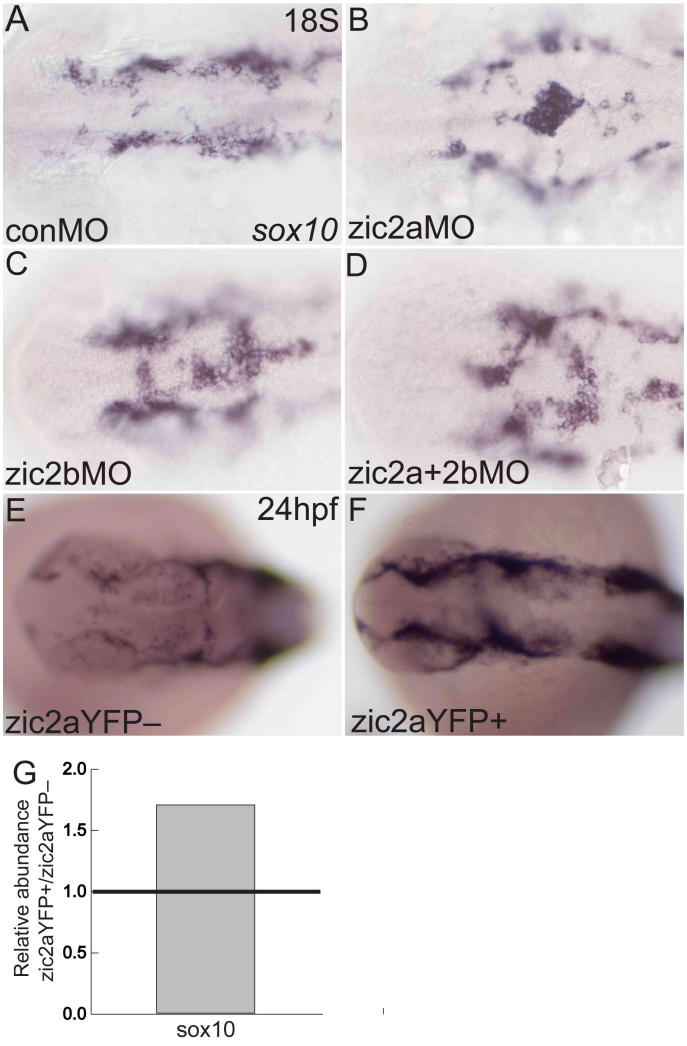

Fig. 5. *Zic2a and zic2b regulate neural crest migratory onset.* Morphant (A-D) or overexpressing embryos (E-F) stained by ISH for *sox10*. (A) At 18S, *sox10* is expressed in NC cells, which have exited the neural tube in control morphants (17/21, 3 experiments). (B,C) Single knockdown of Zic2a or Zic2b results in NC cells abnormally localized to the dorsal neural tube (8/12 zic2a morphants, 2 exp.; 14/32 zic2b morphants, 3 exp.). (D) Double Zic2 depletion causes a similar buildup of *sox10*-positive cells on the dorsal neural tube (7/10 embryos, 2 exp.). (E,F) Transgenic embryos were heat shocked at 10hpf to induce Zic2aYFP expression. Embryos

expressing the zic2aYFP fusion protein have wild-type localization of NC cells, but increased *sox10* expression (20/30, 2 exp.). (G) Quantitative real-time PCR for *sox10* in 24hpf embryos after 10hpf HS. Relative abundance of *sox10* transcript averaged across two biological replicates. A-F are dorsal views, anterior to the left.

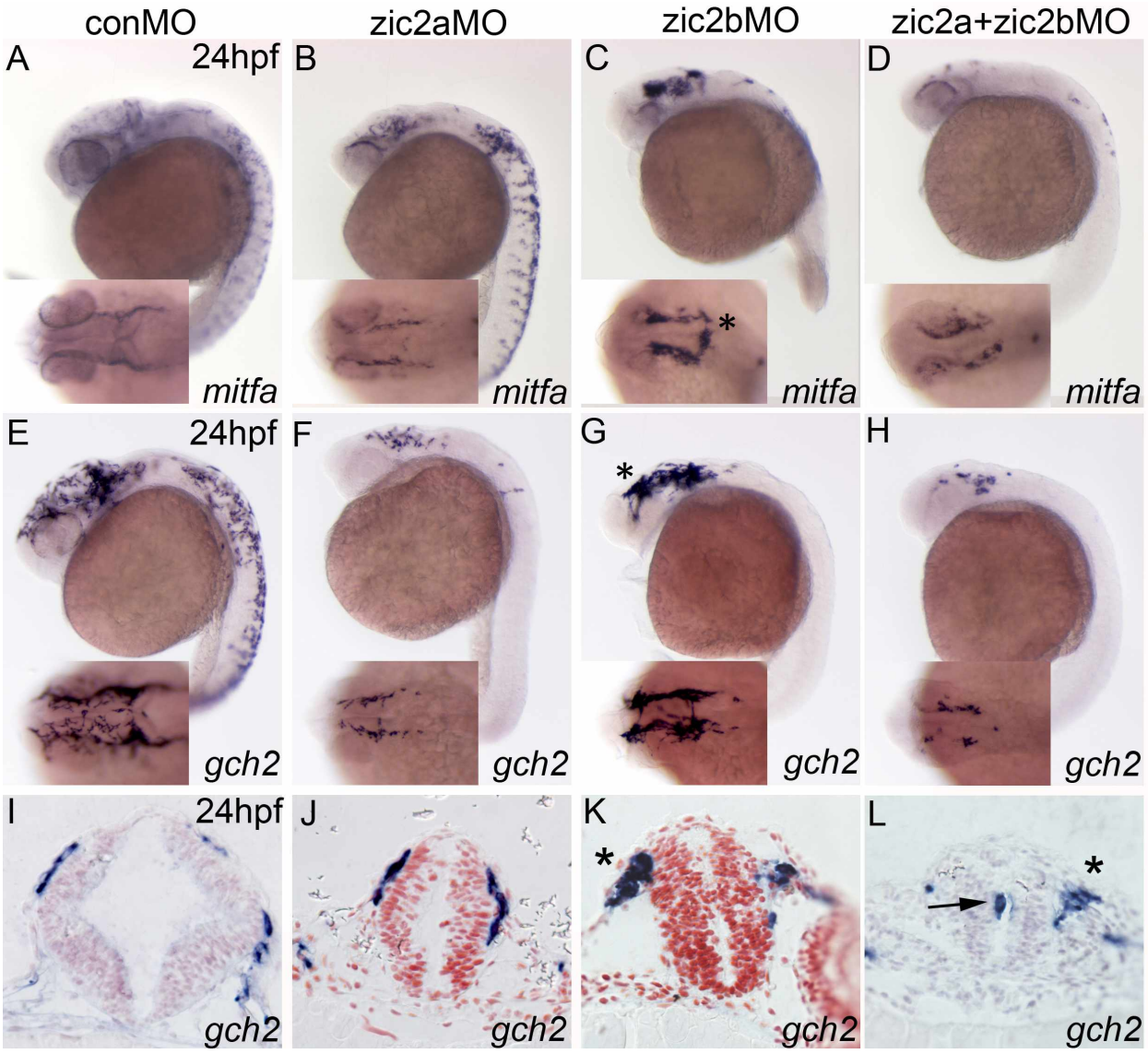

Fig. 6. *Zic2a and zic2b promote chromatophore development.* Zic2 morphant embryos stained by ISH for *mitfa* and *gch2* at 24hpf. (A,B) Zic2a knockdown causes a mild reduction of cranial melanophore progenitors, marked by *mitfa* expression (21/35, 3 exp.). (C) Zic2b knockdown dramatically reduces *mitfa* expression in the trunk (24/27, 3 exp.). (D) Knockdown of both Zic2 proteins reduces melanophores in both cranial and trunk regions (22/29, 3 exp.) and causes NC aggregation in the cranial region (12/24, 3 exp.). (E,F) Zic2a knockdown reduces xanthophore precursors, marked by *gch2*

expression, in the cranial region (13/20, 3 exp.) and trunk region (16/22, 3 exp.). (G) Zic2b knockdown reduces trunk xanthophores (27/28, 3 exp.). (H) Double Zic2 knockdown decreases *gch2* at both cranial and trunk axial levels (17/20 affected, 3 exp.). (I,J) *Gch2*-expressing cells migrating on the midbrain are wild-type in zic2a morphants (3/3, 1 exp.). (K,L) Large aggregates of migrating NC cells are observed after Zic2b knockdown (1/3, 1 exp.; asterisks in C,G,K) and double Zic2 knockdown (2/3, 1 exp.; asterisk in 7L). A-H are lateral views with anterior to the left, with insets showing dorsal views of the same embryos. I-J are transverse sections through the midbrain.

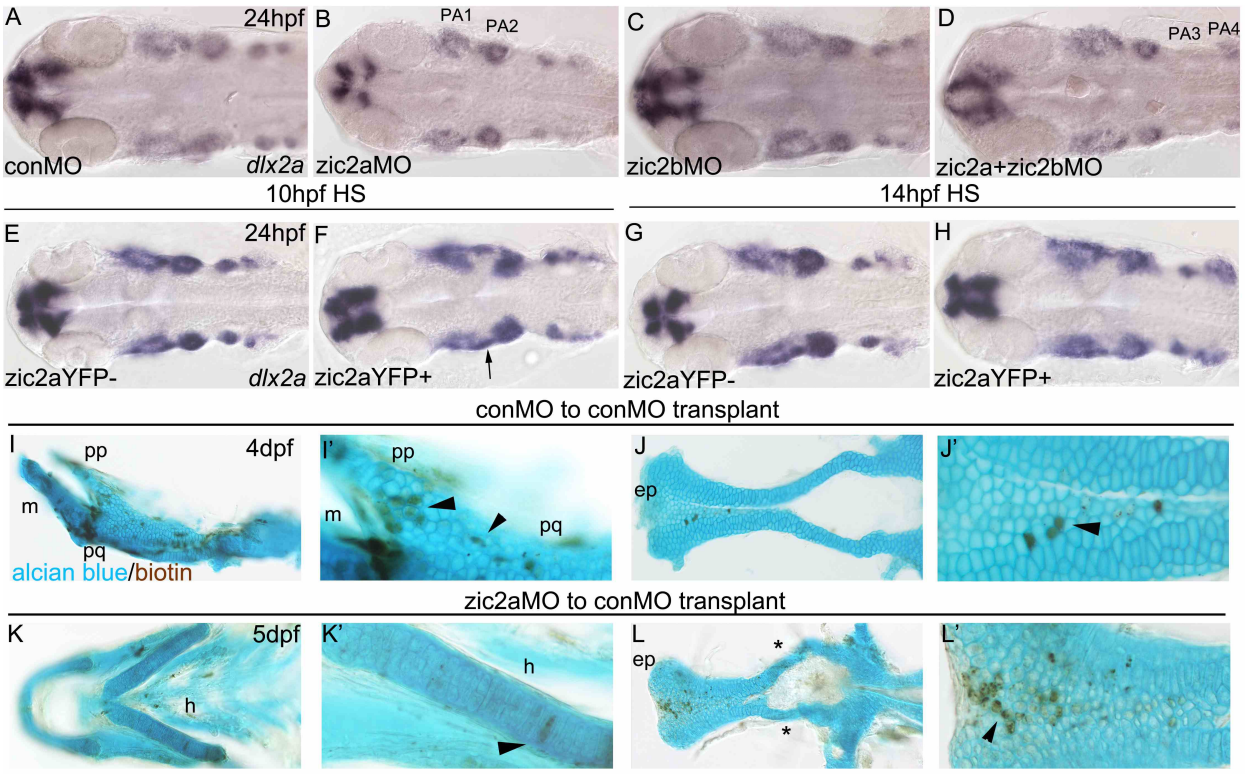

Fig. 7. *Pharyngeal arch primordia are mispatterned in response to changes in Zic2a levels.* (A-H) Embryos stained by ISH for *dlx2a.* (A) Four streams of NC cells that populate the pharyngeal arches express *dlx2a* (42/44, 3 exp.). (B) The *dlx2a* domain is reduced in PA1 and 2 of zic2a morphants (13/30, 3 exp.). (C) Zic2b knockdown has no effect on *dlx2a* expression in the PAs (40/44, 3 exp.). (D) The first two pharyngeal arches are reduced in some double morphants (15/46, 3 exp.), while other embryos have a reduction of *dlx2a* in PA3 and PA4 (11/46, 3 exp., shown in D) or all four PAs (10/46, 3 exp.). (E,F) After HS induction at 10hpf, some Zic2aYFP-positive embryos are wild-type (13/64 embryos, 3 exp.), some have an elongated PA1 (21/64, see arrow in F) and some have reduced *dlx2a* staining in the arches (28/64). (G,H) *Dlx2a* expression remains unchanged after Zic2aYFP induction at 14hpf (15/17, 1 exp.). (I-L) Transplant host embryos stained for biotin and alcian blue at 4dpf. (I,J) Transplanted control

morphant cells incorporated in the pterygoid process, palatoquadrate, and ethmoid plate of control morphant embryos (see arrowheads). (K,L) Transplanted Zic2a-deficient cells incorporated into the hyoid arch and the ethmoid plate of control morphant embryos. (L) Some control morphant host embryos develop with abnormal trabecular cartilages (see asterisks). A-H are dorsal views with anterior to the left. I-L are dissected pharyngeal and neurocranial cartilages. I',J',K' and L' are close-up views of I-L. Abbreviations: ep – ethmoid plate, h – hyoid, m - mandibular, pp – pterygoid process, pq – palatoquadrate.

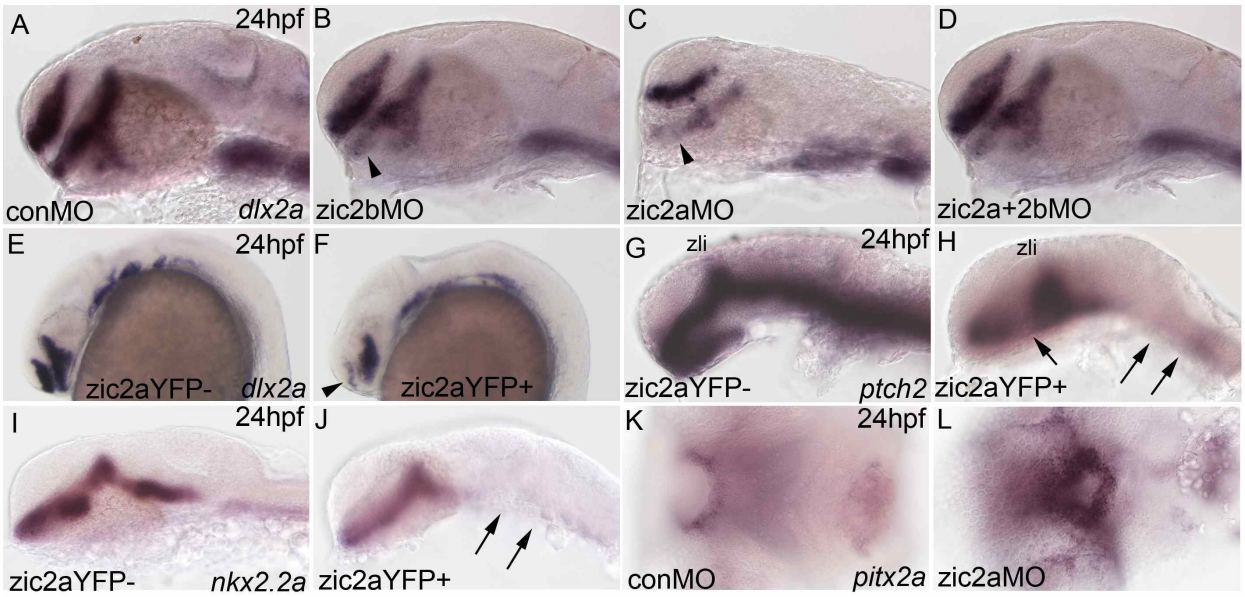

Fig. 8. *Zebrafish Zic2 patterns the ventral forebrain primordium.* Embryos stained by ISH for *dlx2a*, *nkx2.2a*, and *ptch2* at 24hpf and *pitx2a* at 3 dpf. (A) *Dlx2a* marks the telencephalon, prethalamus and hypothalamus in the developing forebrain of control morphants (42/44, 3 exp.). (B) Zic2b knockdown reduces *dlx2a* staining in the prethalamus (18/35, 3 exp., see arrowhead). (C) Zic2a knockdown reduces *dlx2a* in the prethalamus and hypothalamus, as previously described (see Sanek et al., 2008; 39/43, 3 exp.). (D) Double zic knockdown causes patterning defects similar to single Zic2a knockdown (46/46, 3 exp.). (E,F) Zic2aYFP induction at 10hpf strongly reduces *dlx2a* expression in the telencephalon (arrowhead in F) and hypothalamus (61/92, 4 exp.). (G,H) *Ptch2* expression is ablated in the hindbrain and spinal cord and reduced in the medial diencephalon of Zic2aYFP-expressing embryos, but maintained in the ZLI (49/57, 2 exp., see arrows in H). (I,J) Zic2aYFP induction between 10 and 11hpf ablates *nkx2.2a* expression in the hindbrain (35/35 embryos, 2 exp., arrows in J). (K,L) The stomodeum of zic2a morphants is decreased in size (55/56, 4 exp.). A-J are lateral

views, K, L are ventral views, anterior to the left. Abbreviations: zli – zona limitans intrathalamica.

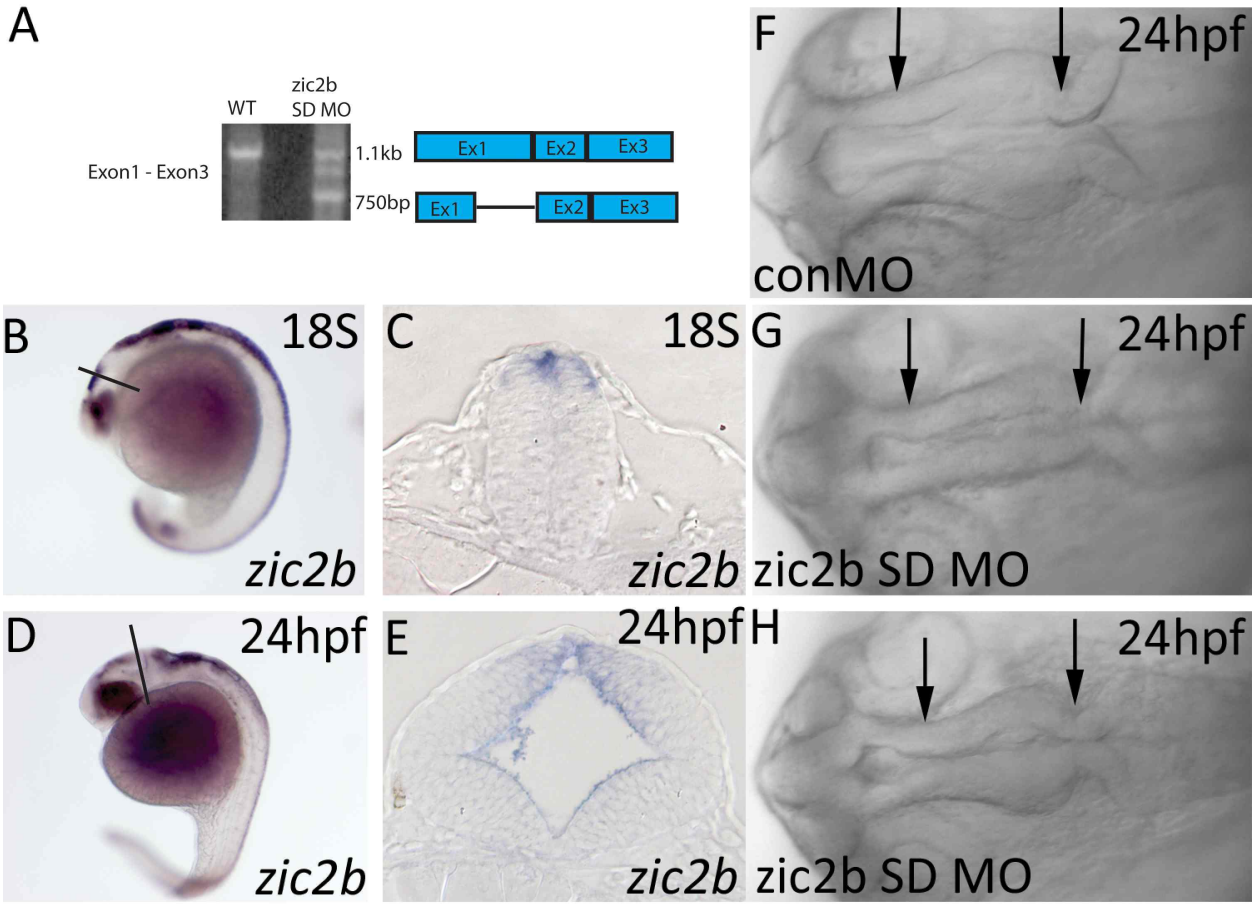

Supplemental Fig. 1. *Zic2b expression and knockdown.* (A) Embryos injected with zic2b splice-blocking MO express reduced levels of full-length *zic2b* transcript, and several mis-spliced transcript variants. (B,D) Wild-type embryos stained by ISH show expression of *zic2b* in the diencephalon, midbrain and hindbrain. (C,E) Restriction of *zic2b* expression to the dorsal neural tube is seen in transverse sections through the midbrain. (F-H) A midbrain neurulation defect is observed in zic2b morphants (midbrain primordium located between arrows in F-H). Zic2b morphants develop with small (35/104, 6 exp., see 1H) and closed midbrain ventricles by 24hpf (33/104, 6 exp., see 1G). B,D are lateral views, anterior to the left. C,E are transverse sections through the midbrain. F-H are dorsal views, anterior to the left.

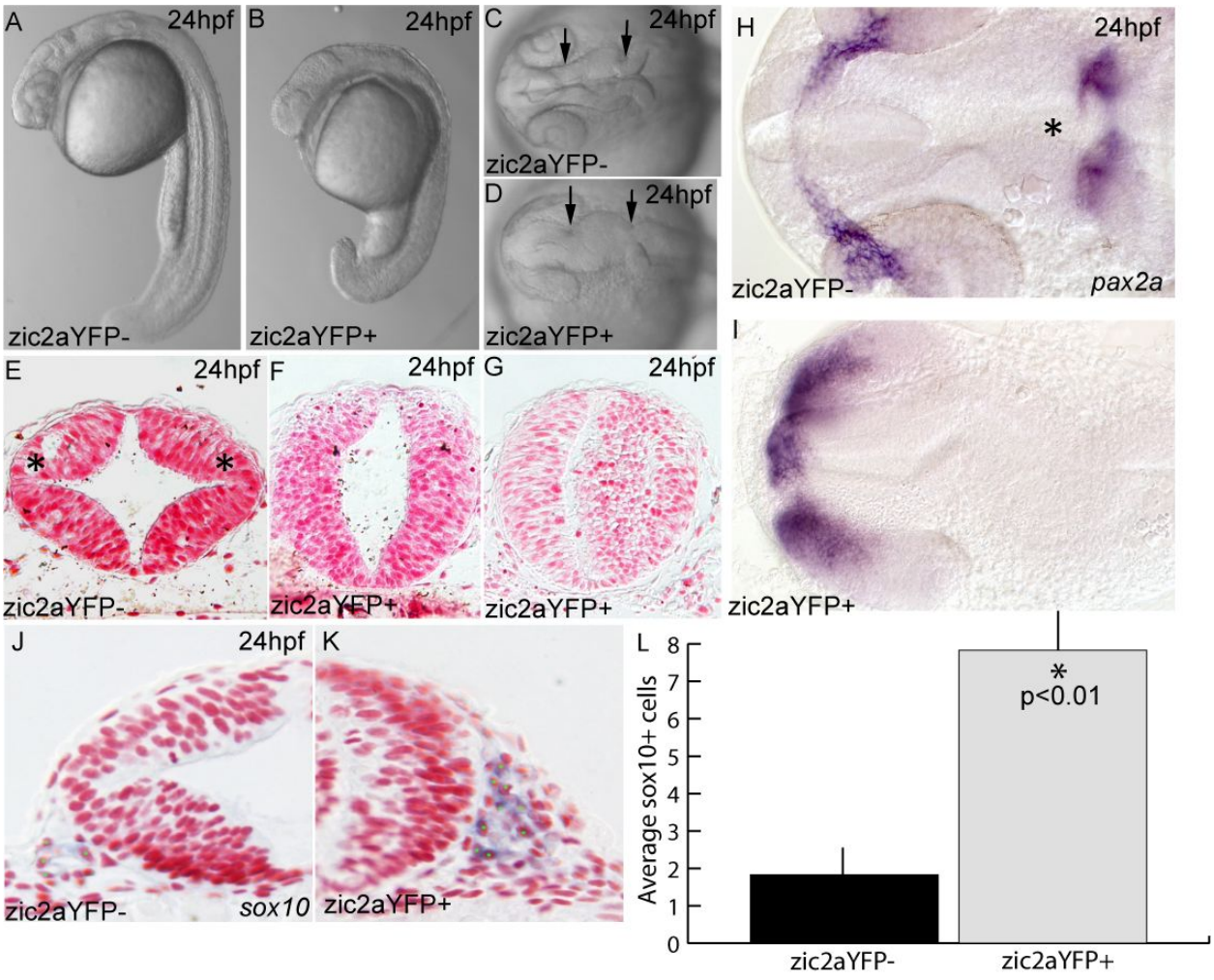

Supplemental Fig. 2. *Expression of a zic2aYFP fusion protein causes developmental defects.* (A-D) Embryos induced by heat shock to express the zic2aYFP fusion protein at 10hpf have a shortened anterior-posterior axis and a characteristic kinked neural tube with a closed midbrain ventricle (located between arrows in C,D; 75/87, 4 exp.). (E) Zic2aYFP-negative siblings have distinct dorsolateral hinge points in the midbrain (asterisks in E; 2/2, 2 exp.). (F,G) Zic2aYFP induction at 10hpf does not always preclude lumen formation, but does eliminate dorsolateral hinge points (4/4, 2 exp.). (H,I) Expression of *pax2a* reveals patterning defects in the retina, optic stalks and mid-hindbrain boundary of Zic2aYFP-expressing embryos (asterisk in H, 8/10, 1 exp). (J,K)

Zic2aYFP-expressing embryos have more sox10-positive cells lateral to the midbrain. (L) Comparison of average numbers of sox10-positive cells in half of the neural tube in a single section (averaged from 3 randomly selected midbrain-level sections per embryo, 2 embryos per condition, 1 exp). Error bars are standard error and significance was tested with a Student's t-test. A,B are lateral views, anterior to the left. C,D,H,I are dorsal views, anterior to the left. E-G are transverse sections through the midbrain.

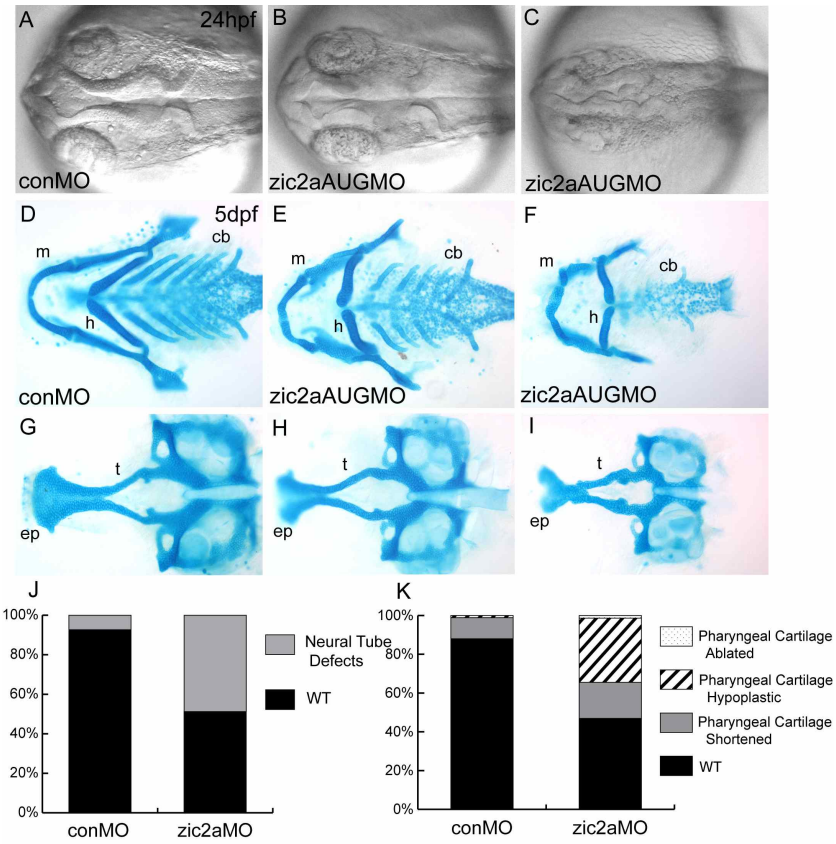

Supplemental Fig. 3. *Zic2a knockdown with non-overlapping zic2a morpholinos causes craniofacial defects.* (A-C) Zic2a morphants display variable neurulation defects, from wild-type (82/160, 5 exp.; shown in B) to closed or twisted midbrain ventricles (77/160, 5 exp.; shown in C). (D,G) Control morphants have mostly wild-type pharyngeal and neurocranial cartilages (242/275, 5 exp.), but a small proportion develops with mildly shortened cartilages. (E,F) Zic2a morphants display a range of craniofacial defects, including shortened pharyngeal cartilages (27/145, 5 exp.; shown in E) and hypoplastic pharyngeal cartilages with an incorrectly angled hyoid arch (48/145, 5 exp.; shown in F). (H,I) Neurocranial cartilage defects include mildly shortened and abnormally proximal trabeculae (shown in I) and correlate with the presence of pharyngeal cartilage defects. (J,K) Penetrance of neural tube defects at 24 hpf (J) and cartilage defects at 5 dpf (K)

following injection of control or zic2a translation-blocking morpholino. A-C are dorsal views, anterior to the left. D-F are dissected pharyngeal cartilages, ventral views, anterior to the left. G-I are dissected neurocranial cartilages, dorsal views, anterior to the left. Abbreviations: cb – ceratobranchials, ep – ethmoid plate, h – hyoid arch, m – mandibular arch, t – trabecular cartilages.

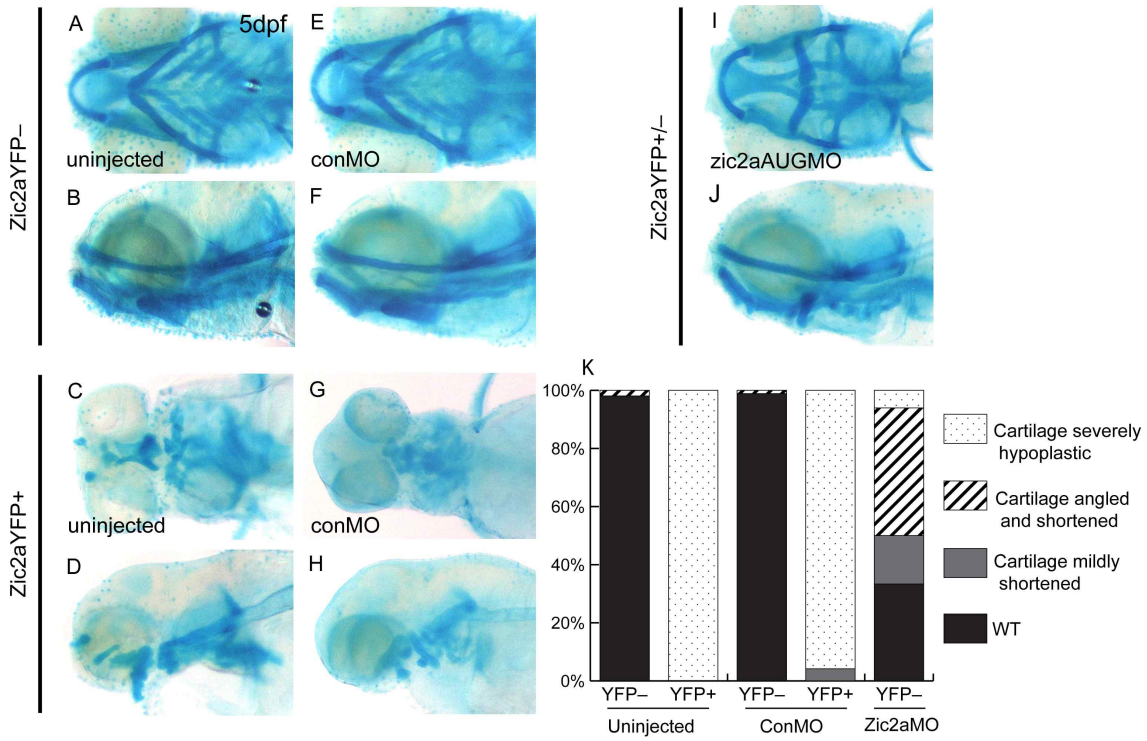

Supplemental Fig. 4. *Zic2a translation-blocking morpholino rescues craniofacial defects associated with elevated Zic2a levels.* Alcian blue-stained cartilage in heat-shocked *Tg(hsp70l:Gal4VP16);Tg(11XUAS:zic2aYFP)* embryos at 5dpf. (A-D) HS-induced expression of Zic2aYFP at 10 hpf results in severely shortened and hypoplastic anterior cartilages in uninjected embryos (67/67 embryos, 1 exp.; shown in C,D). (E-H) Zic2aYFP misexpressing control morphants display severe shortening and hypoplasia comparable to uninjected siblings (23/24, 2 exp.; shown in G,H). (I,J) Zic2aYPF misexpressing embryos injected with Zic2a morpholino were either wild-type (28/135, 2 exp.) or displayed variable craniofacial defects including shortening of anterior cartilages with an incorrectly angled hyoid arch (58/136, 2 exp.; shown in I,J) or more severe hypoplasia (12/136, 2 exp.; not shown). Zic2a overexpressor morphants did not display detectable amounts of the induced Zic2aYFP fusion protein (132/136, 2 exp.). (K)

Penetrance of cartilage defects at 5 dpf following zic2aAUGMO injection and Zic2aYFP induction at 10 hpf. A,C,E,G,I are ventral views anterior to the left. B,D,F,H,J are lateral views.

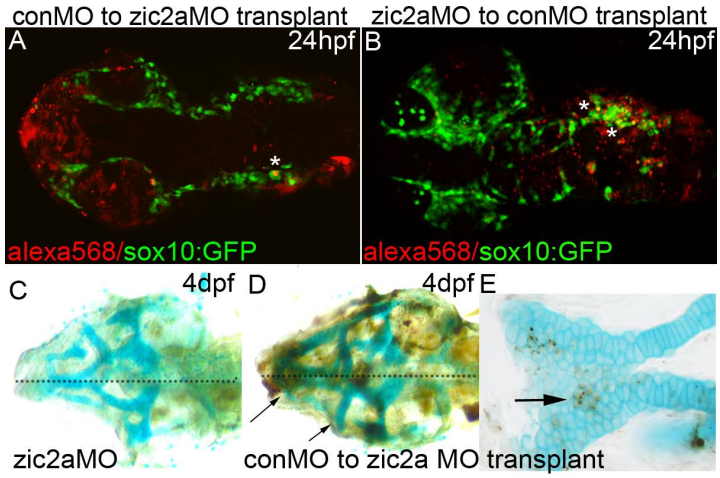

Supplemental Fig. 5. *Transplanted cells contribute to neural crest migratory streams.* Eight micron confocal Z-stacks of host sox10:GFP+ embryos with alexa568+ transplanted cells. (A) Transplanted control morphants cells colocalize with sox10:GFP-positive cells in migratory streams in 5/7 embryos analyzed. (B) Transplanted zic2a morphant cells colocalize with sox10:GFP-positive cells in migratory streams in 3/5 embryos analyzed. (C–E) 4 dpf embryos stained for alcian blue and biotin. (C) Zic2a morphant embryos have typical bilateral defects in the pharyngeal cartilages. (D) Zic2a morphant embryos that receive transplanted control morphant cells frequently display more severe defects on one side (see arrows, 9/15, 1 exp.). (E) Biotin-positive control morphant cell incorporation in the ethmoid plate of a zic2a morphant host embryo (see arrow, 2/15, 1 exp.).

Embryo	Overall distribution of transplanted cells	Pharyngeal cartilages	Neurocranial cartilages	Biotin incorporation in CF cartilages
E1	Forebrain Left retina Stomodeum	WT	WT	No
E2	Deep FB Retinas	WT	WT	No
E3**	Deep FB Stomodeum	WT	WT	Mandibular
E4**	Deep FB Stomodeum	WT	WT	Ethmoid plate
E5**	Deep FB Stomodeum	WT	WT	Hyosymplectic and palatoquadrate
E6	NA	WT	WT	No
E7**	NA	WT	WT	Ethmoid plate

Supplemental Table 1. *Summary of transplants from control morphant donor to control morphant host.* Donor cells were labeled with 3% dextran-conjugated biotin. Biotin/alcian blue staining was performed on embryos fixed at 4dpf. **Asterisks indicate embryos with biotin incorporation in craniofacial cartilages. NA – not assayed.

Embryo	Overall distribution of transplanted cells	Pharyngeal cartilages	Neurocranial cartilages	Biotin incorporation in CF cartilages	Biotin proximal to defective CF?
Experiment 1					
E1	Ventro-nasal retina Nasal placodes Dorsal midbrain	WT	WT	No	+
E2	Retina Nasal placodes	Abnormal	WT	No	NA
E3	Mosaic in retina Nasal placodes	WT	WT	No	NA
E4	Deep forebrain	WT	WT	No	+
E5	Mosaic in forebrain	WT	WT	No	+
Experiment 2					
E1	Right retina Dorsal midbrain	WT	WT	No	+
E2	Left retina	WT	WT	No	+
E3	Right retina	WT	Abnormal	No	+
E4	Dorsal brain Forebrain	WT	WT	No	+
E5	Stomodeum Nasal placodes	WT	WT	No	-
E6	Nasal placodes	WT	WT	No	-
E7**	Stomodeum Anterior forebrain Nasal placodes	Abnormal	Abnormal	Medial ethmoid plate	+
E8	Left retina Stomodeum	WT	Abnormal	No	+
E9	Right retina Nasal placodes	WT	Abnormal	No	+
E10	Stomodeum Forebrain Nasal placodes Midbrain	WT	Abnormal	No	+
E11	Left temporal retina Nasal placodes Forebrain	WT	WT	No	NA
E12	Retina Dorsal midbrain	WT	WT	No	-
E13**	Forebrain Nasal placodes Stomodeum	WT	WT	Hyoid	+
E14**	Anterior forebrain	WT	WT	Medial ethmoid plate Anterior basal commissure	+

Supplemental Table 2. *Summary of transplants from zic2aMO donor embryos to conMO host embryos.* Transplanted cells were labeled with 3% dextran-conjugated biotin. Biotin/alcian blue staining was performed on embryos fixed at 4dpf. **Asterisks indicate embryos with biotin incorporation in craniofacial cartilages. NA – not assayed.

Embryo	Overall distribution of transplanted cells	Transplanted neural crest?	Location of transplanted neural crest
E1**	Anterior forebrain Retinas Left of neural tube	Yes	Migratory streams
E2**	Dorsal midbrain/hindbrain Right of neural tube at midbrain/hindbrain axial level	Yes	Migratory streams Dorsal neural tube
E3	Anterior forebrain Left retina Dorsal midbrain	No	
E4	Forebrain Retinas Mosaic throughout neural tube	No	
E5**	Left forebrain Left retina Midbrain Mosaic in hindbrain	Yes	Migratory streams

Supplemental Table 3. *Summary of transplants from zic2a morphant donors to control morphant hosts.* Donor cells were labeled with 2% dextran-conjugated alexa-568. Donor and host embryos were Tg(sox10:GFP), and NC cells were visualized by GFP fluorescence. Confocal analysis was performed on embryos fixed at 24hpf. ** Asterisks indicate embryos with donor-derived NC cells.

Embryo	Overall distribution of transplanted cells	Transplanted neural crest?	Location of transplanted neural crest
E1**	Forebrain Retinas Midbrain Mid-hindbrain boundary	Yes	Migratory streams
E2**	Forebrain Left retina	Yes	Migratory streams
E3	Anterior forebrain Mosaic in retinas	No	
E4**	Forebrain Retinas Mosaic in midbrain	Yes	Migratory streams
E5**	Anterior forebrain Mosaic in midbrain	Yes	Migratory streams Dorsal neural tube
E6	Mosaic in forebrain Retinas Midbrain Hindbrain	No	
E7**	Forebrain Retinas Left neural tube	Yes	Migratory streams

Supplemental Table 4. *Summary of transplants from control morphant donors to zic2a morphant hosts.* Donor cells were labeled with 2% dextran-conjugated alexa-568. Donor and host embryos were Tg(sox10:GFP), and NC cells were visualized by GFP fluorescence. Confocal analysis was performed on embryos fixed at 24hpf. ** Asterisks indicate embryos with donor-derived NC cells.

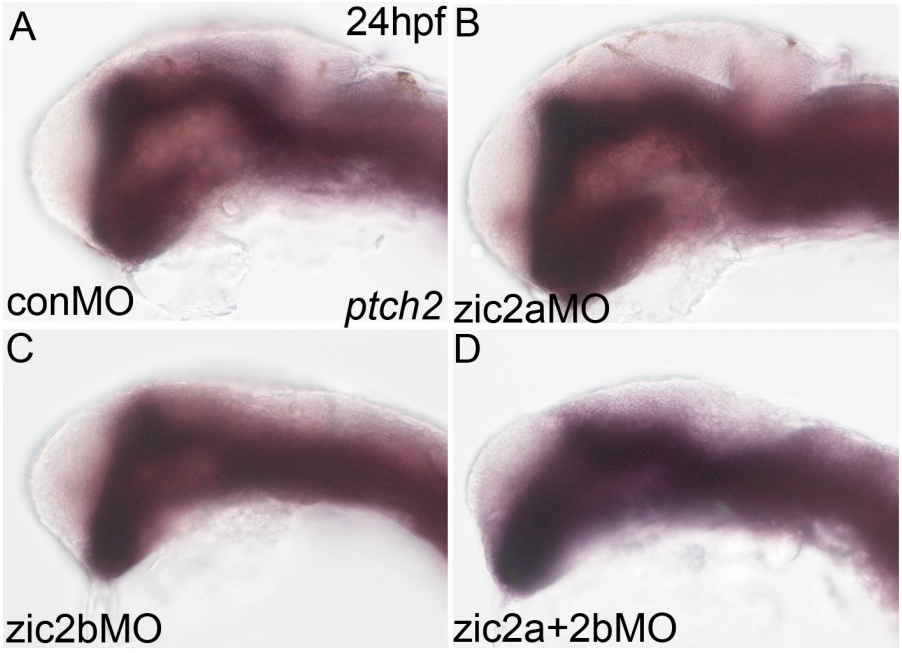

Supplemental Fig. 6. *Zic2b is not required for patterning the Hh target ptch2.* Zic2 morphant embryos stained by ISH for *ptch2* at 24hpf. (A,B) Zic2a knockdown does not affect expression of *ptch2* (see Sanek et al., 2008; 16/18, 1 exp.). (C,D) *Ptch2* expression is similarly unaffected in zic2b morphants (15/16, 1exp.) and double zic2 morphants (13/15, 1 exp.). A-D are lateral views, anterior to the left.

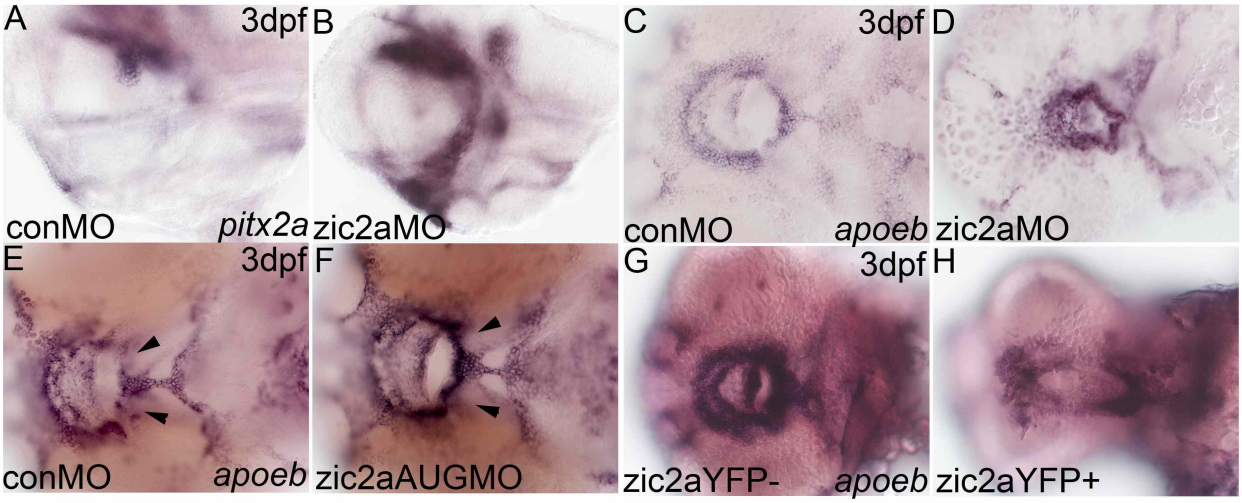

Supplemental Fig. 7. *The oropharynx is mildly mispatterned in zic2a morphants.* Embryos stained by ISH for *pitx2a* or *apoeb* at 3dpf. (A,B) *Pitx2a* expression is increased in the pharyngeal epithelium following Zic2a knockdown (49/56, 4 exp.). (C,D). *apoeb*, another marker of the oropharyngeal epithlium, shows a similar reduction in stomodeal size in moderately affected zic2a morphants (6/23, 2 exp.), while more severely affected embryos have no *apoeb* expression in the oropharnx (15/23, not shown). (E,F) *apoeb* is mildly mispatterned in zic2aAUGMO-injected embryos, either with increased, continual expression in the ventral stomodeum (8/48, 2 exp, arrows in F) or elongation of the stomodeum (25/48, 2 expt., not shown). (G,H) After Zic2aYFP induction at 10hpf, the stomodeal *apoeb* expression domain is variably mispatterned: narrowed and lengthened (14/49, 2 exp., see H), tightened into a smaller ring (7/49, 2 exp.) or fused into a single spot (25/49, 2 exp.). A,B are lateral views. C-H are ventral views, anterior to the left.

Chapter 3:

Rsph9 depletion is associated with a ciliary transposition defect and aberrant neural development

Abstract

Motile cilia are required to generate fluid flow in a number of organs, including the central nervous system (CNS). Here we provide a description of the putative motile cilia in the developing anterior CNS and begin to investigate their structure and function. Each of the three subdivisions of the embryonic brain harbors a distinct subpopulation of cilia in the floorplate. The ventral mid- and hindbrain have both primary cilia and motile cilia that grow in length throughout neurulation, while the forebrain has only short primary cilia. The motile ciliogenic gene program expressed in the neural tube is restricted ventrally and includes *rsph9*, a structural component of motile 9+2 cilia. We confirm that an Rsph9 fusion protein localizes to known 9+2 cilia in the pronephric ducts as well as to long ventral cilia in the cranial neural tube. In humans, *Rsph9* mutations cause primary ciliary dyskinesia, a disorder of motile cilia that manifests as impaired mucociliary clearance, infertility, and occasionally hydrocephalus. In zebrafish, Rsph9 depletion leads to hydrocephalus and ciliary ultrastructural defects. Transmission electron microscopy reveals a ciliary transposition phenotype, similar to that described in humans, in both the pronephric ducts and the neural tube of zebrafish embryos. Importantly, we find evidence of a mixed population composed predominantly of 9+0 as well as some 9+2 cilia in both the spinal canal and the cranial neural tube, suggesting that radial spokes may serve an unknown function in 9+0 cilia.

Introduction

Primary ciliary dyskinesia (PCD) is an autosomal recessive disorder with pleiotropic clinical manifestations. PCD affects as many as 1 in 15,000 births and presents as a mix of chronic respiratory infections, infertility, situs inversus and occasionally hydrocephalus (Knowles et al., 2013a). These symptoms are caused by structural defects in motile cilia that negatively impact their motility. To date, mutations in at least 30 genes have been identified as causative of PCD, accounting for about 70% of disease incidence (Antony et al., 2013; Austin-Tse et al., 2013; Hjeij et al., 2013; Horani et al., 2013; Knowles et al., 2013b; Kott et al., 2013; Moore et al., 2013; Onoufriadas et al., 2014). These genes encode cytoplasmic proteins important for cilia assembly and components of the inner and outer dynein arms, central pair, and radial spokes. Despite the recent advances in uncovering the genetic causes of PCD, there is much yet to learn about the biological function of motile cilia.

Cilia are microtubule-based organelles whose basic structure has been conserved across many organisms. Primary cilia are immotile and serve as signaling centers that integrate extracellular inputs. Motile, or secondary, cilia are found on more specialized tissues and provide mechanical force to generate extracellular fluid flow. Motile cilia have two basic structural arrangements of the axoneme. In the 9+2 arrangement, nine outer microtubule doublets encircle a central pair, and ciliary beating assumes a planar waveform. By contrast, 9+0 cilia lack the central pair and beat in a circular motion (Kramer-Zucker et al., 2005). Most vertebrate embryos have both 9+0

and 9+2 motile cilia at some point during development, sometimes together in the same organ, as is the case in the mouse embryonic CNS (Narita et al., 2012).

In the 9+2 cilium, each outer microtubule doublet is connected to the central pair via a structure called the radial spoke (reviewed in Pigino and Ishikawa, 2012). The T-shaped radial spoke is composed of 23 proteins that make up three subunits termed the stalk, the neck and the spoke head (Yang et al., 2006). The radial spokes of 9+2 cilia are highly organized. In human respiratory epithelial cells, as in most cell types, there are three subtypes of radial spokes that repeat themselves every 96nm. The stalk forms a stable connection to the A microtubule of the outer doublets, while the spoke head connects more transiently with the central pair (Afzelius, 1959; Warner and Satir, 1974). Thus far, three proteins of the spoke head have been associated with PCD in humans: *RSPH1, RSPH4A* and *RSPH9* (Castleman et al., 2009; Kott et al., 2013; Zietkiewicz et al., 2012). Patients with spoke head mutations all have some degree of ciliary transposition defects, characterized by a loss of the central pair and movement of one of the outer microtubule doublets into the center of the axoneme (Castleman et al., 2009). Airway cells from these patients show incompletely penetrant defects in ciliary motility, including a range of ciliary beat frequency from immotile to normal and a range of beat waveforms from planar to rotational (Kott et al., 2013).

Motile cilia serve a number of important functions during embryonic development. In the zebrafish, directional fluid flow in Kupferr's vesicle initiates L/R asymmetry, while motile cilia in the otic vesicle are required for appropriate otolith deposition (Essner et al., 2005; Yu et al., 2011). In the developing CNS, ependymal

cilia generate movement of the embryonic cerebrospinal fluid (CSF) (Kramer-Zucker et al., 2005). The role for eCSF, still poorly understood, is currently thought to be twofold. First, intralumenal pressure supports the rapid expansion of the ventricles and seems to provoke a response from the surrounding neural epithelium resulting in cell proliferation (Desmond and Jacobson, 1977). Second, trophic factors contained within CSF regulate neurepithelial cell fate, directing cell survival, proliferation and differentiation (Sawamoto et al., 2006; reviewed in Gato and Desmond, 2009).

Mutations causing dysmotile or dyskinetic cilia are associated with developmental defects. Disruption of the transcription factor *Foxj1* (*Hfh4*), a master regulator of motile ciliogenesis, ablates motile cilia in mammals, fish and amphibians (Brody et al., 2000; Hagenlocher et al., 2013; Yu et al., 2008). The loss of motile cilia-specific proteins such as *Hydin* (Davy et al., 2003) or *Mdnah5* (Ibanez-Tallon et al., 2004) results in dysmotile cilia in mice. The end result in all of these cases is an abnormal accumulation of CSF in the brain ventricles, termed hydrocephalus. Congenital hydrocephalus has serious implications for embryonic viability and long-term health.

Like most vertebrate epithelia, cells of the neural tube have cilia projecting from their apical surface into the lumen. In the CNS, study of motile cilia has been focused on the spinal canal, where they are reported to have a 9+0 arrangement (Kramer-Zucker et al., 2005). Cilia of the cranial neural tube remain relatively unstudied, due in part to the inaccessibility of the tissue. Here we undertake the first characterization of cilia in the anterior CNS of the zebrafish, and report that the mid- and hindbrain harbor a subpopulation of putative motile cilia in the floorplate. Presence of these long cilia

coincides with expression of genes in the motile ciliogenic pathway, including *rsph9*, which encodes structural component of 9+2 cilia.

We report a zebrafish model of PCD, achieved by knockdown of Rsph9, in which affected embryos develop with hydrocephalus and shortened motile cilia in several organs, including the ventral midbrain. The motile cilia in the cranial neural tube are a mixed population, with the majority being 9+0, and no function for radial spokes has ever been reported in a 9+0 cilium. Despite this, up to half of the cilia in the ventral midbrain of our PCD model have a ciliary transposition defect associated with loss of radial spokes in 9+2 cilia. This unexpected phenotype will be best studied in recently generated *rsph9* mutants, a promising model to dissect the relationships between motile cilia, fluid flow and embryonic morphogenesis.

Materials and Methods

Zebrafish strains and embryo manipulation

Adult zebrafish were maintained according to established methods (Westerfield, 2000). Embryos were obtained from natural matings and staged according to Kimmel et al. (1995). The following transgenic lines were used: *Tg(β-actin:mGFP)* (Cooper et al., 2004) and *Tg(β-actin:Arl13b-GFP)* (Borovina et al., 2010).

Gene-specific antisense oligonucleotide morpholinos were purchased from GeneTools (Philomath, OR) and included Rsph9 translation-blocking morpholino (rsph9MO, Castleman et al., 2009), p53 MO and standard control MO (conMO). Rsph9 and control MOs (2-4ng/nl) were diluted with p53MO (4-6ng/nl) in HEPES/KCl buffer and 1-2nl injected into the cell at the 1-2 cell stage. Ventricles were injected just behind the mid-hindbrain boundary with 2-4nl of 3% alexa-568 dextran in 100mM KCl and images were processed as described in Gutzman and Sive, 2009.

Immunohistochemistry, histology and in situ hybridization (ISH)

Embryos were fixed in 4% paraformaldehyde in PBS and stained with the following antibodies: anti-acetylated tubulin (1:400, Sigma), anti-gamma tubulin (1:1000, Sigma). Primary antibodies were detected fluorescently with Alexa-labeled goat anti-mouse or goat anti-rabbit secondary antibodies (1:1000, Molecular Probes). Nuclei were counterstained with DAPI (Invitrogen). Embryos were dissected and mounted in 3% methylcellulose for imaging on an Olympus IX81 inverted confocal microscope with

Fluoview 1000 confocal package. Cilia length was measured in Image J (NIH) (Jaffe et al., 2010). Averages were compiled from 20 cilia picked from 10um stacks of the dorsal- and ventral-most regions of the neural tube.

ISH was carried out as previously described (Gillhouse et al., 2004). Stained embryos were embedded in Eponate 12 (Ted Pella) and 5-7μm sections were cut with a steel blade on an American Optical Company microtome. Antisense digoxigenin-labeled RNA probes were transcribed using the MAXIscript kit (Ambion).

Probes for cilia genes were generated by transcription from a plasmid template (*foxj1a*, Hellman et al., 2010), or by PCR from genomic cDNA (*rsph4a* and *rsph9*) or full-length sequence purchased from Open Biosystems (*efhc1*) followed by TA cloning into pGEMT-Easy (Promega). Primers used were as follows: *efhc1* (Sense: 5'-CCT GCC AGG AAA CAC ATT TCG CG-3', Antisense: 5'-GGG TCC GTG GCG TGT CTG AGT GA-3'), *rsph4a* (Sense: 5'-ATGGAGATTACAGGTGAAGCG-3', Antisense: 5'-TTTGGCACTGATGCAGATGG-3'), *rsph9* (Sense: 5'-ATGGACTCTGATTCTCTG-3', Antisense: 5'-GATTGTGTCGCTGAAGTC-3').

Fusion protein localization and rescue assays

Full-length human and zebrafish *rsph9* sequences were purchased from Open Biosystems. A missense mutation in zebrafish *rsph9* was altered to match the published *rsph9* sequence (www.ensembl.org, Zv9) using site-directed mutagenesis (E225G) with the following primers (Sense: 5'-CGAAGACATTCTCAAAGGGTCATGGAGCCTGCAGC-3', Antisense: 5'-

GCTGCAGGCTCCATGACCCTTTGAGAATGTCTTCG-3'). The Rsph9-tRFP fusion protein construct was first generated by In-Fusion cloning into the NcoI site of a Gateway middle entry clone containing TagRFP (Kwan et al., 2007). Primers were designed to introduce a linker region of three glycines between the rsph9 and tagRFP sequences. Zebrafish rsph9-tRFP, tagRFP alone and human *rsph9* were subsequently cloned into the BamHI site of the pCS2+ vector using the Infusion kit (Clontech) and the following primers: tagRFP (CS2 BamHI tRFP F: 5'-TCTTTTTGCAGGATCCGGCTGGACCATGGTGTCTAA-3', CS2 BamHI tRFP R: 5'-CGAATCGATGGGATCCTCAATTAAGTTTGTGCCCCAGTTTG-3'), rsph9-tRFP (CS2 BamHI rsph9 F: 5'-TCT TTT TGC AGGATC CAT GGA CTC TGA TTC TCT GCA TTA C-3', CS2 BamHI tRFP R), human rsph9 (CS2 BamHI HS rsph9 F: 5'-TCTTTTTGCAGGATCCTGAGCGGAGCCGCTGACCTGAT-3', CS2 BamHI HS rsph9 R: 5'-CGAATCGATGGGATCCACATCCAGGCTGGCTCCCATTCTAT-3'). Messenger RNA was transcribed using the mMessage Machine kit (Ambion) and 25-50pg of RNA was injected into *Tg(β-actin:Arl13b-GFP)* embryos.

Transmission electron microscopy

Yolk cells of segmentation-stage embryos were injected with 6-8nl of 40mM AMP-PNP and yolk was expelled several minutes later using tweezers and a fine-gauge needle (adapted from Langenberg et al., 2003). Embryos were then transferred to a glass petri dish with glutaraldehyde fix in 200mM phosphate buffer, dissected in two just behind the otic placode and processed for TEM according to Jaffe et al., 2010.

CRISPR mutagenesis and high-resolution melt analysis (HRMA)

The target site in exon 2 of *rsph9* was selected using the ZiFiT Targeter website (http://zifit.partners.org/) with the criteria: 5'-GG-(N)18-NGG-3'. Guide RNA expression vectors were constructed and transcribed as described in Hwang et al., 2013 with the target sequence 5'-GGACGAGGCTACACATGAAG-5'. 2 nL of a mix containing 25 ng/μL sgRNA and 450 ng/μL Cas9 mRNA was injected into 1-cell embryos. Genomic DNA was extracted from single embryos or adult fish tail clips. qPCR amplification was performed on a StepOnePlus system (Life Technologies). Each 20 μL reaction contained a final concentration of 0.2 μM primers, 1X MeltDoctor HRM Master Mix (Life Technologies), and 2 μL gDNA. Primers were designed using the PrimerExpress software (Life Technologies) to amplify a 105 base region spanning the 3' end of exon 2. Primer pairs were tested for efficiency as in Sanek et al., 2009. Each sample was loaded with three technical replicates on a single plate. *rsph9* ex2 CRISPR primer sequences were 5'-ACCCGTCCCATGAGTACGA-3' in *rsph9* exon 2 and 5'-GCCCATCTGTGTGGTGTAAGG-3' in *rsph9* intron 2-3 (IDT). Melt curve analysis was performed using the MeltDoctor High Resolution Melt v3.0 Software. Melt profiles were automatically sorted into variant groups by the software based on melting temperature and melt curve shape. Samples were manually determined to be wild-type, heterozygous, or homozygous mutant at the *rsph9* locus.

Results

Ciliary length in the ventral anterior neural epithelium is dynamic during neurulation

Study of cilia present on the neural epithelium has largely been confined to those in the spinal canal, with little attention paid to cilia of the cranial NT, where morphogenesis is more complex and varied. To begin to understand the role of cilia during cranial neurulation, we characterized the cilia in the ventral and dorsal regions of the three early brain subdivisions, the forebrain (FB), midbrain (MB) and hindbrain (HB) in fixed tissue. Between 12S and 24S, about six hours of development, the cranial neural tube progresses from a closed rod with no lumen, to an open tube with the first of the folds and constrictions that are the precursors of the complex adult brain. We observe that cilia project from the apical surface of neurectodermal cells by at least 12S (Fig. 1A). Cilia in the ventral FB remain uniform and unchanged in length during neurulation (Fig.1B-D). Cilia in the ventral MB and HB are already longer than primary cilia at 12S, and increase in length progressively as neurulation proceeds (Fig.1E-H) (Fig.1I-K). Cilia in the dorsal neurepthelium of all three subdivisions are a uniformly short population, characteristic of primary cilia, and unchanging over the course of time observed here (Supplementary Fig. 1). The cilia in each compartment of the cranial NT are thus distinct from one another, with subpopulations of elongating cilia in the ventral MB and HB.

The motile ciliogenic program in the ventral anterior NT includes rsph9

To further characterize the newly identified ventral cilia population, we examined neural expression of genes known to be part of the motile ciliogenic program in other tissues. *Foxj1a*, a transcriptional regulator of motile ciliogenesis, and *efhc1*, a marker of cells bearing motile cilia (Yu et al., 2008), are both expressed in the same ventral MB domain that harbors long cilia during neurulation (Fig. 2B-D). To provide insight into the possible structure of these floorplate cilia, we generated probes against two genes thought to encode structural proteins specific to cilia with a 9+2 arrangement, *rsph9* and *rsph4a*. These genes were previously uncharacterized in zebrafish. *Rsph9* transcript is localized to a similar floorplate domain as *foxj1a* and *efhc1* (Fig. 2E,F). As expected, *rsph9* and *rsph4a* are expressed in other organs with motile cilia, including Kupferr's vesicle, the pronephric ducts and the spinal canal (Fig. 2G-I, Supp. Fig. 2). Interestingly, cilia in the posterior neural tube are reported to have a 9+0 arrangement, while radial spoke head proteins are thought to play a role only in 9+2 cilia.

We next sought to confirm that Rsph9 protein localizes to anterior floorplate cilia. In transient assays, an Rsph9-tRFP fusion protein localizes to 9+2 cilia in the pronephric ducts (Fig. 3A,B), to the uncharacterized cilia in the ventral MB (Fig. 3C,D) and to the 9+2 cilia in Kupferr's vesicle (Fig. 3E,F). Ciliary localization is not observed in the dorsal MB, where there are only short primary cilia, nor does tRFP alone localize to cilia (Supp. Fig. 3).

Rsph9-depleted embryos develop hydrocephalus and have ciliary defects

Humans with abnormal or absent ciliary motility (PCD) develop with defects in a number of organ systems. Rsph9 knockdown in zebrafish results in complete ablation of Rsph9-tRFP expression and hyperinflated ventricles at 24hpf (Fig. 4A,B, Supp. Fig. 4) followed by hydrocephalus clearly visible at 48hpf (Fig. 4C,D). To tie this gross morphological phenotype back to a structural requirement for Rsph9 in cilia, we examined motile cilia populations for abnormal phenotypes in several tissues of rsph9 morphants. Indeed, the cilia of Kupferr's vesicle are shortened following Rsph9 depletion, when compared with control morphant cilia (Fig. 4E,F). We observed a similar effect in the ventral MB and pronephric ducts of rsph9 morphants (Fig. 4G-J). There is evidence for additional cilia-related phenotypes in rsph9 morphants, including defects of the L/R axis, as heart looping is randomized following Rsph9 knockdown (Supp. Fig. 5). The hydrocephalus observed following Rsph9 knockdown thus correlates with abnormal motile cilia.

In humans with PCD, abnormal ciliary motility on respiratory epithelial cells is attributed to defects in ultrastructure, namely a transposition defect where the central pair of a 9+2 cilium is lost and an outer doublet is 'transposed' to the center of the axoneme. We sought to clarify whether the phenotypes observed in zebrafish rsph9 morphants could be due to a similar defect in ciliary ultrastructure. Our initial characterization of cilia in the ventral MB revealed that most wild-type axonemes are in a 9+0 arrangement, as has been found in the spinal canal (Fig. 5A). Note the outer dynein arms visible on the electron micrograph, indicating that these cilia are likely motile (Fig. 5, see arrowheads). There is some evidence for a small population of 9+2

cilia comingled with the 9+0 cilia (Fig. 5B; Table 1). In rsph9 morphant embryos, we observed a significant number of cilia with a classical ciliary transposition defect, i.e. an 8+1 configuration (Fig. 5C,D). This was somewhat surprising, given that the majority of cilia present in the ventral MB were 9+0, and no function for radial spokes has ever been reported in 9+0 cilia. Similarly, wild-type cilia in the spinal canal appear to be a mixed population, skewed heavily towards the 9+0 arrangement (Fig. 5E,F). Rsph9 knockdown results in ciliary transposition defects in the spinal canal as well (Fig. 5G,H). Finally, the pronephric duct cilia are almost exclusively 9+2, with a small proportion of cilia with more than two central microtubules (Fig. I,J; Table 1). We did not observe any 8+1 cilia in the kidneys of rsph9 morphants, but there were a substantial number of 9+0 cilia and a seemingly increased proportion of cilia in a 9+3 or 9+4 configuration (Fig. K,L). Rsph9 knockdown recapitulates the ciliary transposition defects of PCD patients with *RSPH9* mutations, and suggests that Rsph9 and radial spokes may serve a previously unreported and unknown function in 9+0 cilia.

Targeted mutagenesis of rsph9 using the CRISPR-Cas9 system

Because knockdown technologies are limited in their ability to faithfully recapitulate loss-of-function phenotypes, we next sought to generate an rsph9 mutant. The CRISPR-Cas9 system for targeted mutagenesis was recently successfully adapted for use in zebrafish, and has been reported as quite efficient (Hwang et al., 2013). We designed CRISPR guide RNAs against two sites at the *rsph9* locus (Fig. 6A) and verified the presence of induced mutations in injected embryos by high resolution melt

analysis (HRMA). We identified two stably transmitted alleles at the exon 2 site (Fig. 6B), which were sequenced and revealed as an 8bp deletion (*rsph9*^{208}) and an indel with net gain of 2bp (*rsph9*^{212}), both of which resulted in an early stop codon (Fig. 6C). These mutant lines will be used to interrogate the biological function of Rsph9 in a more carefully controlled system. Extremely preliminary analysis of zygotic homozygous *rsph9* mutants from both stable lines indicates at least one difference between knockdown and mutant models, in that we have not observed hydrocephalus in mutant embryos.

Discussion

Rsph9, a structural component of motile 9+2 cilia, is mutated in humans with PCD. Here we use the comparative accessibility of the zebrafish cranial neural tube to examine ciliary biology in the embryonic brain, as well specific aspects of PCD disease progression. We successfully model some aspects of PCD in zebrafish by knocking down Rsph9 protein levels. In particular, we recapitulate ciliary ultrastructural defects observed in humans, and show that these are associated with hydrocephalus. We further posit that our data raises the possibility of a role for the radial spoke in elongated 9+0 cilia of the ventral neural tube.

Significance of elongated cilia in the floorplate during neurulation

Our examination of the anterior neural tube is the earliest characterization of ciliary dynamics in this organ. We find a population of presumptive motile cilia in the ventral mid- and hindbrain at 12S (about 15hpf), long before the lumen opens and begins to fill with eCSF. These cilia bear dynein arms, the hallmark of motility, and continue to elongate during neurulation, until at least 24S (about 21hpf). We do not define when these cilia begin to beat, and the physiological significance of motile cilia at this stage is unclear. Indeed, even at older stages, the study of ependyma and choroid plexus function has thus far not been able to characterize the full importance of motile cilia on these tissues, and how their dysmotility can lead to defects such as hydrocephalus.

Elongating cilia in the neural rod may have multiple purposes, becoming motile when they are required to generate fluid flow, but also serving a sensory function. Our understanding of motile ciliary function is gradually widening to encompass a growing number of mechano- and chemosensory roles. For example, cilia of the respiratory epithelium are able to sense fluid flow and respond by maintaining their beat frequency despite increasing viscosity (Lorenzo et al., 2008). Recent evidence points to a sensory-motor response circuit mediated by motile cilia themselves and common to respiratory, oviductal and ependymal epithelia (reviewed in Bloodgood, 2010).

There is also evidence that cilia populations in the brain transition between different structures and states of motility as the tissues they populate mature. The choroid plexus of the perinatal swine and mouse harbors a heterogeneous population of cilia, with both motile and previously motile, and 9+0 and 9+2 cilia (Narita et al., 2012). As a group, these cilia seem to be in transition from a transiently motile phase to an adult immotile state. Elongating cilia in the early floorplate may be similarly in transition from immotile to motile, accounting for variability in structure. A recent time course of ependymal development in *Xenopus* reveals that each cell initially bears a single elongating cilium, then transitions gradually to a multiciliated state (Hagenlocher et al., 2013).

Transverse sections reveal that *foxj1a* likely drives motile ciliogenic gene expression in the anterior floorplate, as it does in other ciliated tissues throughout the zebrafish (Yu et al., 2008). This is not surprising, since the *foxj1* genes have been identified as master regulators of motile cilia in almost every organism to date (reviewed

in Choksi et al., 2014). Since we observe a mixed population of 9+0 and 9+2 cilia in the *foxj1a* domain, it does highlight the fact that we don't yet know what drives formation of each of these specific cilia types. Importantly, each compartment of the brain has a distinct mix of cilia as early as the neural rod stage (12S), from only primary cilia in the forebrain, to presumptive motile cilia of differing lengths between the mid- and hindbrain. This points towards region-specific cofactors regulating ciliogenesis differently in each subdivision of the neural tube.

Motile cilia and hydrocephalus

In zebrafish, the lumen of the cranial neural tube begins to open at 18hpf. Over the next six hours, the neural epithelium acquires a little of the complexity of shape inherent to the adult brain. Along the anterior-posterior axis, transverse strictures form and delineate the fore-, mid- and hindbrain compartments, each with an associated ventricle. Dorsolateral hinge points bisect the dorsal-ventral axis. By 24hpf, ventricles are filled with eCSF (Lowery and Sive, 2009), although the organ primarily responsible for CSF production in the adult, the choroid plexus, does not mature until 144hpf (Garcia-Lecea et al., 2008).

Our data demonstrate that relatively subtle defects in ciliary structure are associated with very early hydrocephalus, arising as early as we know eCSF is present in the ventricles. Hydrocephalus can occur via overproduction or impaired reabsorption of CSF, or by blockage of one of the narrow foramina connecting the ventricles (frequently the cerebral aqueduct). Mutant analysis suggests that cilia can contribute to

hydrocephalus in at least two ways. *Dnah5* mutant mice have dysmotile cilia and reduced CSF flow velocity, which subsequently leads to an occlusion of the cerebral aqueduct and fluid buildup (Ibanez-Tallon, 2002). By contrast, mutations in the *Ift88* gene cause hydrocephalus that begins before ciliary motility defects lead to impaired CSF flow (Banizs et al., 2005). In these mutants, the cilia of the choroid plexus are malformed and unable to perform the mechanosensory function that allows them to relay information about how much CSF to generate. This study, however, did not examine when cilia of the anterior floorplate begin beating. In order to differentiate between the two established modes of hydrocephalus formation as a result of ciliary defects, this will need to be established.

It is also important to note that in a preliminary analysis of the gross morphology in zygotic homozygous *rsph9* mutant zebrafish embryos, there is no indication of hydrocephalus, in contrast to what we observe in response to Rsph9 knockdown. One possible explanation for this observation would be maternally deposited mRNA. Hyperinflated ventricles are apparent within 24 hours of fertilization, well within the time frame during which maternal gene products may act. While it is not known whether *rsph9* mRNA is maternally deposited, the translation-blocking morpholino used in this study would presumably effectively knock down both protein translated from both zygotic and any maternal transcripts. In order to test this, it will be necessary to look for *rsph9* mRNA in pre-MBT embryos and to generate a maternal zygotic-null embryo.

Structure of floorplate cilia in the anterior neural tube

Our data show that the presumptive motile cilia in the cranial floorplate are likely to be a mixed population of 9+2 and 9+0, skewed towards the 9+0 arrangement. About half of anterior ventral neural tube cilia in the wild-type context have an electron-dense center, but no single cross-section was at the perfect angle to observe a central pair clearly. This difficulty is due in part to the relatively few cilia present in this region during neurulation.

We demonstrate that an Rsph9-tRFP fusion protein localizes to well-characterized 9+2 cilia in Kupferr's vesicle and the pronephric ducts, as well as the mixed population in the ventral midbrain. It is possible that Rsph9-tRFP is present in 9+0 cilia, which would be a novel finding. A second possibility is that the Rsph9-tRFP localization we observe in the ventral midbrain may be only to those cells with a 9+2 axoneme. If this were true, the Rsph9 fusion protein would provide the first *in vivo* 9+2-specific marker. This may well be the case, as Rsph9 localization has been shown to be heterogeneous in the neonate choroid plexus. Within a single multiciliated choroid plexus cell, Rsph9 localizes to some cilia and not to others (Nonami et al., 2012). It is also worth noting that there is a pattern of mutual exclusion of Arl13b-GFP and Rsph9-tRFP observed in transient assays. This may be an artifact of multiple fluorophore-tagged proteins attempting to localize to the same cilium, or Rsph9-tRFP might delineate a specific subpopulation of cells (i.e. the 9+2 cilia).

Role of the radial spoke

Our data show that the disruption of a radial spoke head protein, Rsph9, causes classical 9+2 ciliary transposition defects in a region sporting mostly 9+0 cilia. One explanation for this observation is that only those cilia with a 9+2 structure display the transposition defects. Although the proportion of ciliary transposition defects is greater than the proportion of 9+2 cilia, we cannot rule out this possibility. However, we find this explanation unsatisfactory for a number of reasons. First, TEM evidence for cilia with a central pair is as yet inconclusive, as outlined above. Second, the penetrance of transposition defects in the total cilia population is such that essentially every 9+ED cilium would have this phenotype. In humans with radial spoke head mutations, the proportion of cilia with transposition defects is frequently only around 10%, making this unlikely (Burgoyne et al., 2014).

An alternative explanation is that radial spokes have a previously unreported function in 9+0 cilia. Radial spokes regulate the motility of 9+2 cilia, at least in part by transducing signals from the central pair to the outer doublets, where asymmetrical dynein activity is responsible for driving ciliary beating (Salathe et al., 2007). The presence of motile 9+0 cilia in the spinal canal and mammalian node demonstrates that radial spokes are not required for motility, but they are thought instead to exert local control over the phosphorylation state of dyneins and thereby influence the waveform, which in 9+2 cilia is usually planar (Choksi et al., 2014). There are, however, atypical examples, such as the zebrafish Kupferr's vesicle, where cilia are 9+2 but beat with a rotational waveform (Kramer-Zucker et al., 2005). There is still much to understand about how radial spokes regulate ciliary motility.

What data exists on the structure-function relationship of individual radial spoke proteins comes from work in alga *Chlamydomonas reinhardtii*. In fact, only a few of the genes encoding radial spoke proteins have been identified as such in vertebrates, including just four in zebrafish. Several proteins have domains suggesting a role in calcium signal transduction. For example, RSP2 and RSP23 of the neck have calmodulin-binding motifs (Yang et al., 2006) while RSP20 of the stalk belongs to the calmodulin family. RSP9 itself contains no known motifs. Two other spoke head proteins, RSP1 and RSP10 are predicted to have multiple MORN (membrane occupation and recognition nexus) motifs, which are thought to play a role in intracellular calcium signaling (Yang et al., 2006). Interestingly, during a recent surge in the discovery of PCD-associated mutations, three radial spoke head proteins were identified, but no components of other radial spoke subunits (Knowles et al., 2013a).

In summary, the cilia of the cranial floorplate are heterogeneous, divided into subpopulations specific to each brain compartment, and dynamic in length throughout neurulation. We show that these cilia are required for early ventricle inflation. We also demonstrate that specific aspects of PCD such as ciliary ultrastructural defects can be modeled in a genetically tractable organism with great potential for dissecting the roles of radial spoke components.

Acknowledgements

We would like to thank Danielle Grotjahn for help imaging cilia and Abby Keller for her work generating rsph9 mutant fish lines.

References

Afzelius, B. 1959. Electron microscopy of the sperm tail; results obtained with a new fixative. J Biophys Biochem Cytol. 5, 269-78.

Antony, D., Becker-Heck, A., Zariwala, M. A., Schmidts, M., Onoufriadis, A., Forouhan, M., Wilson, R., Taylor-Cox, T., Dewar, A., Jackson, C. et al. 2013. Mutations in CCDC39 and CCDC40 are the major cause of primary ciliary dyskinesia with axonemal disorganization and absent inner dynein arms. Hum Mutat. 34, 462-72.

Austin-Tse, C., Halbritter, J., Zariwala, M. A., Gilberti, R. M., Gee, H. Y., Hellman, N., Pathak, N., Liu, Y., Panizzi, J. R., Patel-King, R. S. et al. 2013. Zebrafish Ciliopathy Screen Plus Human Mutational Analysis Identifies C21orf59 and CCDC65 Defects as Causing Primary Ciliary Dyskinesia. Am J Hum Genet. 93, 672-86.

Banizs, B., Pike, M. M., Millican, C. L., Ferguson, W. B., Komlosi, P., Sheetz, J., Bell, P. D., Schwiebert, E. M. and Yoder, B. K. 2005. Dysfunctional cilia lead to altered ependyma and choroid plexus function, and result in the formation of hydrocephalus. Development. 132, 5329-39.

Bloodgood, R. A. 2010. Sensory reception is an attribute of both primary cilia and motile cilia. J Cell Sci. 123, 505-9.

Borovina, A., Superina, S., Voskas, D. and Ciruna, B. 2010. Vangl2 directs the posterior tilting and asymmetric localization of motile primary cilia. Nat Cell Biol 12, 407-12.

Brody, S. L., Yan, X. H., Wuerffel, M. K., Song, S. K. and Shapiro, S. D. 2000. Ciliogenesis and left-right axis defects in forkhead factor HFH-4-null mice. *Am J Respir Cell Mol Biol.* 23, 45-51.

Burgoyne, T., Lewis, A., Dewar, A., Luther, P., Hogg, C., Shoemark, A. and Dixon, M. 2014. Characterizing the ultrastructure of primary ciliary dyskinesia transposition defect using electron tomography. Cytoskeleton (Hoboken). 71, 294-301.

Castleman, V. H., Romio, L., Chodhari, R., Hirst, R. A., de Castro, S. C., Parker, K. A., Ybot-Gonzalez, P., Emes, R. D., Wilson, S. W., Wallis, C. et al. 2009. Mutations in radial spoke head protein genes RSPH9 and RSPH4A cause primary ciliary dyskinesia with central-microtubular-pair abnormalities. Am J Hum Genet. 84, 197-209.

Choksi, S. P., Lauter, G., Swoboda, P. and Roy, S. 2014. Switching on cilia: transcriptional networks regulating ciliogenesis. Development. 141, 1427-41.

Cooper, M. S., Szeto, D.P., Sommers-Herival, G., Topczewski, J., Solnica-Krezel, L., Kang, H.C., Johnson, I., Kimelman, D. 2005. Visualizing morphogenesis in transgenic zebrafish embryos using BODIPY TR methyl ester dye as a vital counterstain for GFP. Dev Dyn.

232:359-68.

Davy, B. E. and Robinson, M. L. 2003. Congenital hydrocephalus in hy3 mice is caused by a frameshift mutation in Hydin, a large novel gene. Hum Mol Genet. 12, 1163-70.

Desmond, M. E. and Jacobson, A. G. 1977. Embryonic brain enlargement requires cerebrospinal fluid pressure. Dev Biol. 57, 188-98.

Essner, J. J., Amack, J. D., Nyholm, M. K., Harris, E. B. and Yost, H. J. 2005. Kupffer's vesicle is a ciliated organ of asymmetry in the zebrafish embryo that initiates left-right development of the brain, heart and gut. Development. 132, 1247-60.

Garcia-Lecea, M., Kondrychyn, I., Fong, S. H., Ye, Z. R. and Korzh, V. 2008. In vivo analysis of choroid plexus morphogenesis in zebrafish. PLoS One. 3, e3090.

Gato, A. and Desmond, M. E. 2009. Why the embryo still matters: CSF and the neuroepithelium as interdependent regulators of embryonic brain growth, morphogenesis and histiogenesis. Dev Biol. 327, 263-72.

Gillhouse, M., Wagner Nyholm, M., Hikasa, H., Sokol, S. Y. and Grinblat, Y. 2004. Two Frodo/Dapper homologs are expressed in the developing brain and mesoderm of zebrafish. Dev Dyn. 230, 403-9.

Gutzman, J. H. and Sive, H. 2009. Zebrafish brain ventricle injection. J Vis Exp. 26.

Hagenlocher, C., Walentek, P., C, M. L., Thumberger, T. and Feistel, K. 2013. Ciliogenesis and cerebrospinal fluid flow in the developing Xenopus brain are regulated by foxj1. Cilia. 2, 12.

Hjeij, R., Lindstrand, A., Francis, R., Zariwala, M. A., Liu, X., Li, Y., Damerla, R., Dougherty, G. W., Abouhamed, M., Olbrich, H. et al. 2013. ARMC4 mutations cause primary ciliary dyskinesia with randomization of left/right body asymmetry. Am J Hum Genet. 93, 357-67.

Horani, A., Brody, S. L., Ferkol, T. W., Shoseyov, D., Wasserman, M. G., Ta-shma, A., Wilson, K. S., Bayly, P. V., Amirav, I., Cohen-Cymberknoh, M. et al. 2013. CCDC65 mutation causes primary ciliary dyskinesia with normal ultrastructure and hyperkinetic cilia. PLoS One. 8, e72299.

Hwang, W. Y., Fu, Y., Reyon, D., Maeder, M. L., Tsai, S. Q., Sander, J. D., Peterson, R. T., Yeh, J. R. and Joung, J. K. 2013. Efficient genome editing in zebrafish using a CRISPR-Cas system. Nat Biotechnol. 31, 227-9.

Ibanez-Tallon, I., Gorokhova, S. and Heintz, N. 2002. Loss of function of axonemal dynein Mdnah5 causes primary ciliary dyskinesia and hydrocephalus. Hum Mol Genet. 11, 715-21.

Ibanez-Tallon, I., Pagenstecher, A., Fliegauf, M., Olbrich, H., Kispert, A., Ketelsen, U. P., North, A., Heintz, N. and Omran, H. 2004. Dysfunction of axonemal dynein heavy chain Mdnah5 inhibits ependymal flow and reveals a novel mechanism for hydrocephalus formation. Hum Mol Genet. 13, 2133-41.

Jaffe, K. M., Thiberge, S. Y., Bisher, M. E. and Burdine, R. D. 2010. Imaging cilia in zebrafish. Methods Cell Biol. 97, 415-35.

Kimmel, C. B., Ballard, W. W., Kimmel, S. R., Ullmann, B. and Schilling, T. F. 1995. Stages of embryonic development of the zebrafish. Dev Dyn. 203, 253-310.

Knowles, M. R., Daniels, L. A., Davis, S. D., Zariwala, M. A. and Leigh, M. W. 2013a. Primary ciliary dyskinesia. Recent advances in diagnostics, genetics, and characterization of clinical disease, Am J Respir Crit Care Med. 188, 913-22.

Knowles, M. R., Ostrowski, L. E., Loges, N. T., Hurd, T., Leigh, M. W., Huang, L., Wolf, W. E., Carson, J. L., Hazucha, M. J., Yin, W. et al. 2013b. Mutations in SPAG1 cause primary ciliary dyskinesia associated with defective outer and inner dynein arms. Am J Hum Genet. 93, 711-20.

Kott, E., Legendre, M., Copin, B., Papon, J. F., Dastot-Le Moal, F., Montantin, G., Duquesnoy, P., Piterboth, W., Amram, D., Bassinet, L. et al. 2013. Loss-of-function mutations in RSPH1 cause primary ciliary dyskinesia with central-complex and radial-spoke defects. Am J Hum Genet. 93, 561-70.

Kramer-Zucker, A. G., Olale, F., Haycraft, C. J., Yoder, B. K., Schier, A. F. and Drummond, I. A. (2005) 'Cilia-driven fluid flow in the zebrafish pronephros, brain and Kupffer's vesicle is required for normal organogenesis', Development 132(8): 1907-21.

Kwan, K. M., Fujimoto, E., Grabher, C., Mangum, B. D., Hardy, M. E., Campbell, D. S., Parant, J. M., Yost, H. J., Kanki, J. P. and Chien, C. B. 2007. The Tol2kit: a multisite gateway-based construction kit for Tol2 transposon transgenesis constructs. Dev Dyn. 236, 3088-99.

Lorenzo, I. M., Liedtke, W., Sanderson, M. J. and Valverde, M. A. 2008. TRPV4 channel participates in receptor-operated calcium entry and ciliary beat frequency regulation in mouse airway epithelial cells. Proc Natl Acad Sci USA. 105, 12611-6.

Lowery, L. A. and Sive, H. 2009. Totally tubular: the mystery behind function and origin of the brain ventricular system. Bioessays. 31, 446-58.

Moore, D. J., Onoufriadis, A., Shoemark, A., Simpson, M. A., zur Lage, P. I., de Castro, S. C., Bartoloni, L., Gallone, G., Petridi, S., Woollard, W. J. et al. 2013. Mutations in ZMYND10, a gene essential for proper axonemal assembly of inner and outer dynein arms in humans and flies, cause primary ciliary dyskinesia. Am J Hum Genet. 93, 346-56.

Narita, K., Kozuka-Hata, H., Nonami, Y., Ao-Kondo, H., Suzuki, T., Nakamura, H., Yamakawa, K., Oyama, M., Inoue, T. and Takeda, S. 2012. Proteomic analysis of multiple primary cilia reveals a novel mode of ciliary development in mammals. Biol Open. 1, 815-25.

Nonami, Y., Narita, K., Nakamura, H., Inoue, T. and Takeda, S. 2013. Developmental changes in ciliary motility on choroid plexus epithelial cells during the perinatal period. Cytoskeleton (Hoboken). 70, 797-803.

Onoufriadis, A., Shoemark, A., Munye, M. M., James, C. T., Schmidts, M., Patel, M., Rosser, E. M., Bacchelli, C., Beales, P. L., Scambler, P. J. et al. 2014. Combined exome and whole-genome sequencing identifies mutations in ARMC4 as a cause of primary ciliary dyskinesia with defects in the outer dynein arm. J Med Genet. 51, 61-7.

Pigino, G. and Ishikawa, T. 2012. Axonemal radial spokes: 3D structure, function and assembly. Bioarchitecture. 2, 50-58.

Salathe, M. 2007. Regulation of mammalian ciliary beating. Annu Rev Physiol. 69, 401-22.

Sanek, N. A., Taylor, A. A., Nyholm, M. K. and Grinblat, Y. 2009. Zebrafish zic2a patterns the forebrain through modulation of Hedgehog-activated gene expression. Development. 136, 3791-800.

Sawamoto, K., Wichterle, H., Gonzalez-Perez, O., Cholfin, J. A., Yamada, M., Spassky, N., Murcia, N. S., Garcia-Verdugo, J. M., Marin, O., Rubenstein, J. L. et al. 2006. New neurons follow the flow of cerebrospinal fluid in the adult brain. Science. 311, 629-32.

Warner, F. D. and Satir, P. 1974. The structural basis of ciliary bend formation. Radial spoke positional changes accompanying microtubule sliding. J Cell Biol. 63, 35-63.

Westerfield, M. 2000. The zebrafish book. A guide for the laboratory use of zebrafish (Danio rerio). 4th ed., Univ. of Oregon Press, Eugene.

Yang, C. and Yang, P. 2006. The flagellar motility of Chlamydomonas pf25 mutant lacking an AKAP-binding protein is overtly sensitive to medium conditions. Mol Biol Cell. 17, 227-38.

Yang, P., Diener, D. R., Yang, C., Kohno, T., Pazour, G. J., Dienes, J. M., Agrin, N. S., King, S. M., Sale, W. S., Kamiya, R. et al. 2006. Radial spoke proteins of Chlamydomonas flagella. J Cell Sci. 119, 1165-74.

Yu, X., Lau, D., Ng, C. P. and Roy, S. 2011. Cilia-driven fluid flow as an epigenetic cue for otolith biomineralization on sensory hair cells of the inner ear. Development. 138, 487-94.

Yu, X., Ng, C. P., Habacher, H. and Roy, S. 2008. Foxj1 transcription factors are master

regulators of the motile ciliogenic program. Nat Genet. 40, 1445-53.

Zietkiewicz, E., Bukowy-Bieryllo, Z., Voelkel, K., Klimek, B., Dmenska, H., Pogorzelski, A., Sulikowska-Rowinska, A., Rutkiewicz, E. and Witt, M. 2012. Mutations in radial spoke head genes and ultrastructural cilia defects in East-European cohort of primary ciliary dyskinesia patients. PLoS One. 7, e33667.

Figures

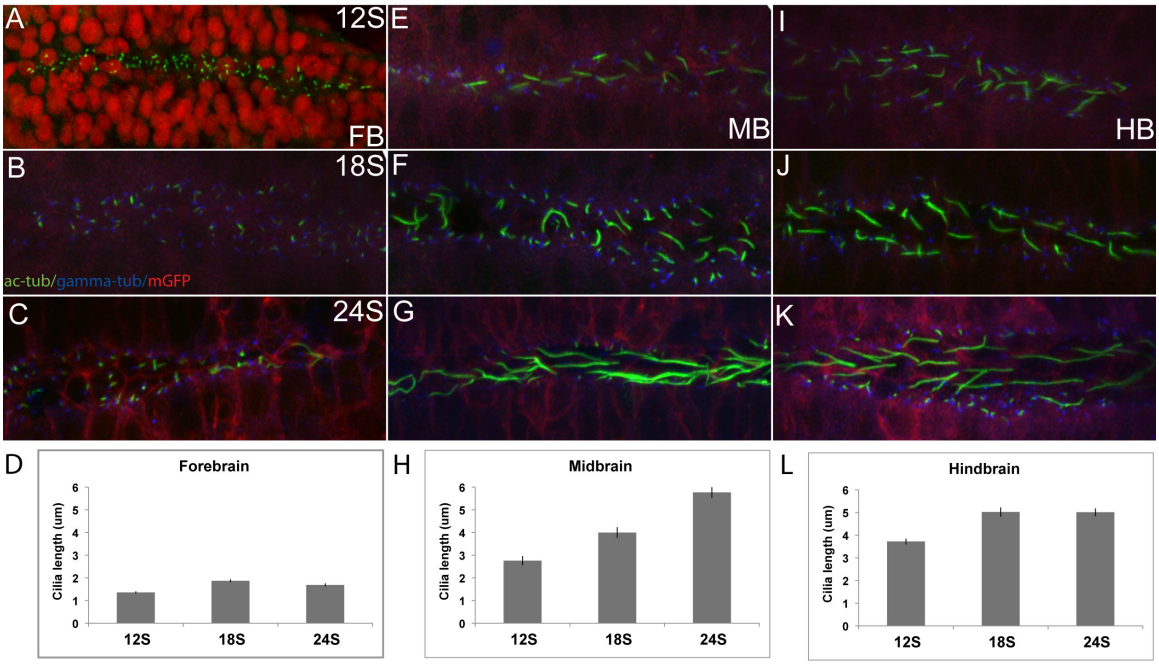

Figure 1. Distinct subpopulations of ventral cilia in each brain subdivision are dynamic in length during neurulation. *Tg(β-actin:mGFP)* embryos stained with antibodies against acetylated α-tubulin and γ-tubulin. (A-C) Cilia in the ventral FB do not change in length over time. (D) Averaged length of ventral FB cilia at 12S (1.36μm), 18S (1.87μm) and 24S (1.69μm). (E-G) Ventral MB cilia are longer than primary cilia on average and increase in length over time. (H) Averaged length at 12S (2.76μm), 18S (4μm) and 24S (5.77μm). (I-K) Ventral HB cilia are longer than MB cilia at 12S and increase in length over time. (L) Averaged length at 12S (3.72μm), 18S (5.02μm) and 24S (5.01μm). A-C, E-G, I-K are stacked confocal images with anterior to the left. Error bars represent standard error of the mean.

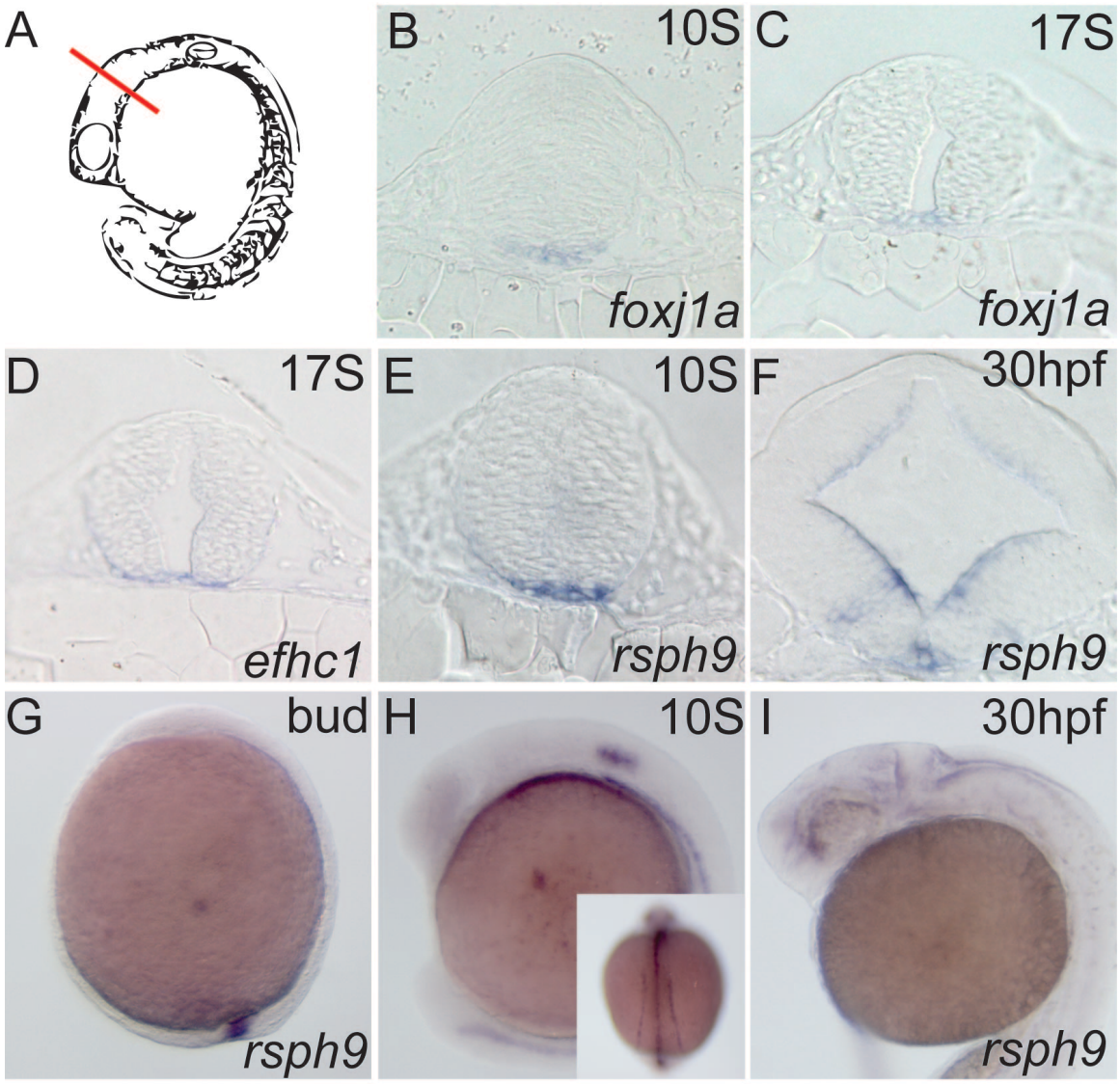

Figure 2. *Rsph9* is part of the motile ciliogenic program in the ventral midbrain.

Wild-type embryos stained by ISH for *efhc1, foxj1a* and *rsph9*. (A) Cartoon showing transverse sections through the midbrain. (B,C) *Foxj1a* is expressed in the floorplate of the midbrain throughout neurulation. (D) *Efhc1* expression in midbrain floorplate. (E,F) *Rsph9* transcript is localized to a floorplate domain similar to other motile ciliogenic genes until at least 30hpf. (G) During early neurulation, *rsph9* is expressed in Kupferr's vesicle and (H) the otic placodes, spinal canal and pronephric ducts. (I) After neurulation

is complete, *rsph9* continues to be expressed in the neural tube. B-F are transverse sections through the midbrain. G-I are lateral views with anterior to the left. H' is a dorsal view with anterior up.

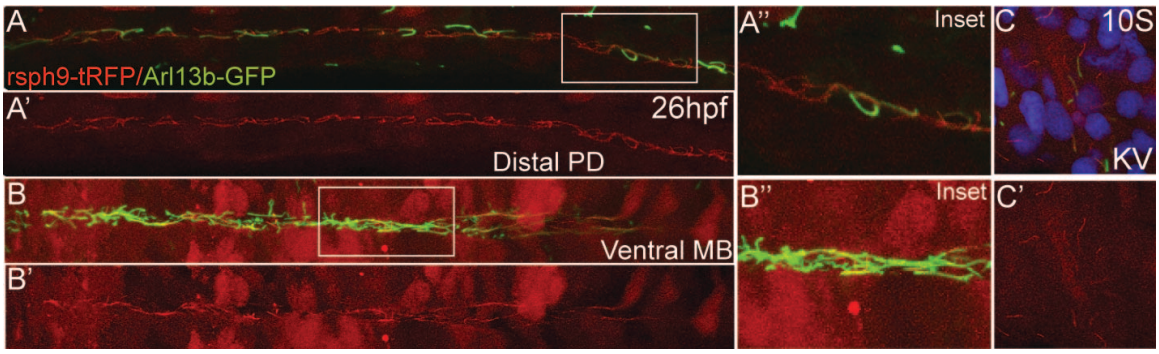

Figure 3. An rsph9 fusion protein localizes to motile cilia. *Tg(β-actin:Arl13b-GFP)* embryos injected with rsph9-tRFP mRNA. (A) Rsph9-tRFP fusion protein localizes to cilia in the pronephric ducts. (B) Rsph9-tRFP fusion protein localizes to long cilia in the ventral midbrain. (A'',B'') Inset views of A and B. (C,C') Rsph9-tRFP fusion protein localizes to the cilia of Kupferr's vesicle. A',B',C' are tRFP fluorescence alone. All images are confocal Z-stacks.

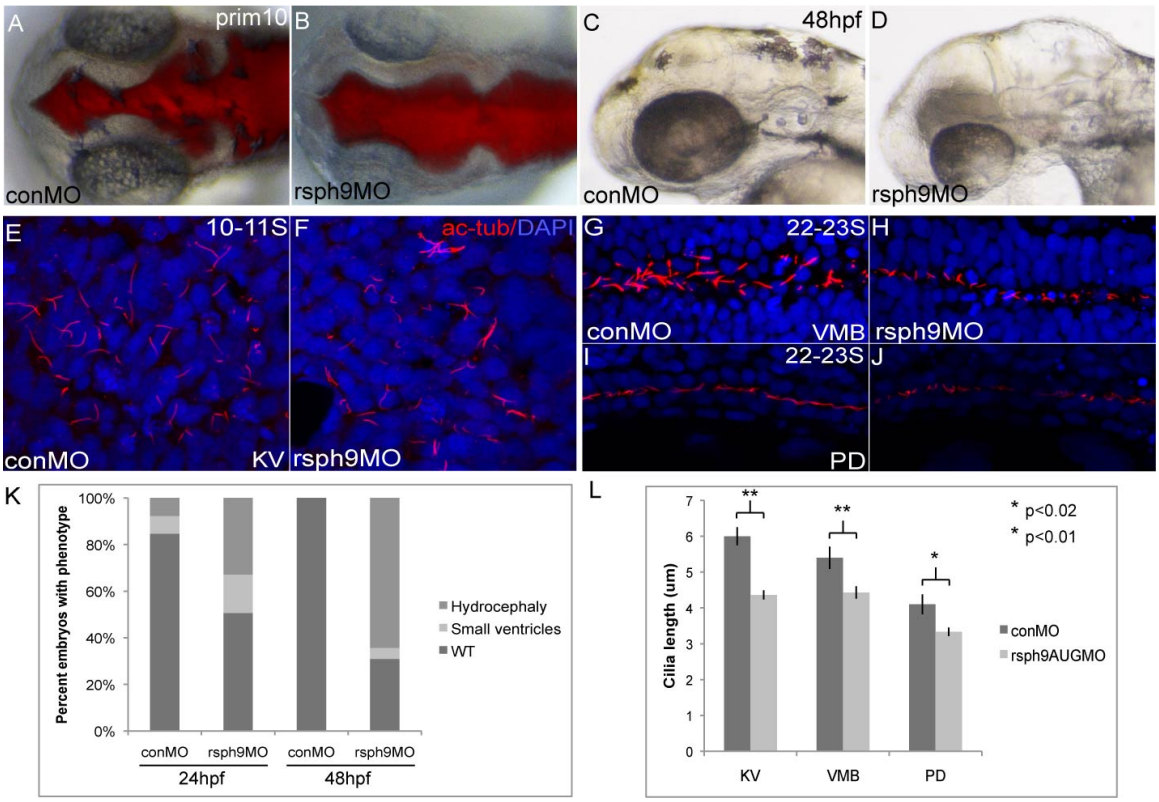

Figure 4. Rsph9 depletion causes hydrocephalus and defects in motile cilia. (A,B) Control and rsph9 morphant embryos injected with a ventricle-filling dye. Expanded ventricles in some rsph9 morphants is observable by 24hpf (26/79, 4 exp.). (C,D) Prominent hydrocephaly in 48hpf morphant embryos (27/42, 2 exp.). (E,F) Cilia of the Kupferr's vesicle are shortened in rsph9 morphants. (G,H) Cilia are also shortened in the ventral MB and (I,J) pronephric ducts of rsph9 morphants. (K) Penetrance of hydrocephalus in rsph9 morphants. (L) Average length of motile cilia in organs affected by Rsph9 knockdown. A,B are dorsal views, anterior to the left. C,D are lateral views, anterior to the left. E-J are confocal Z-stacks.

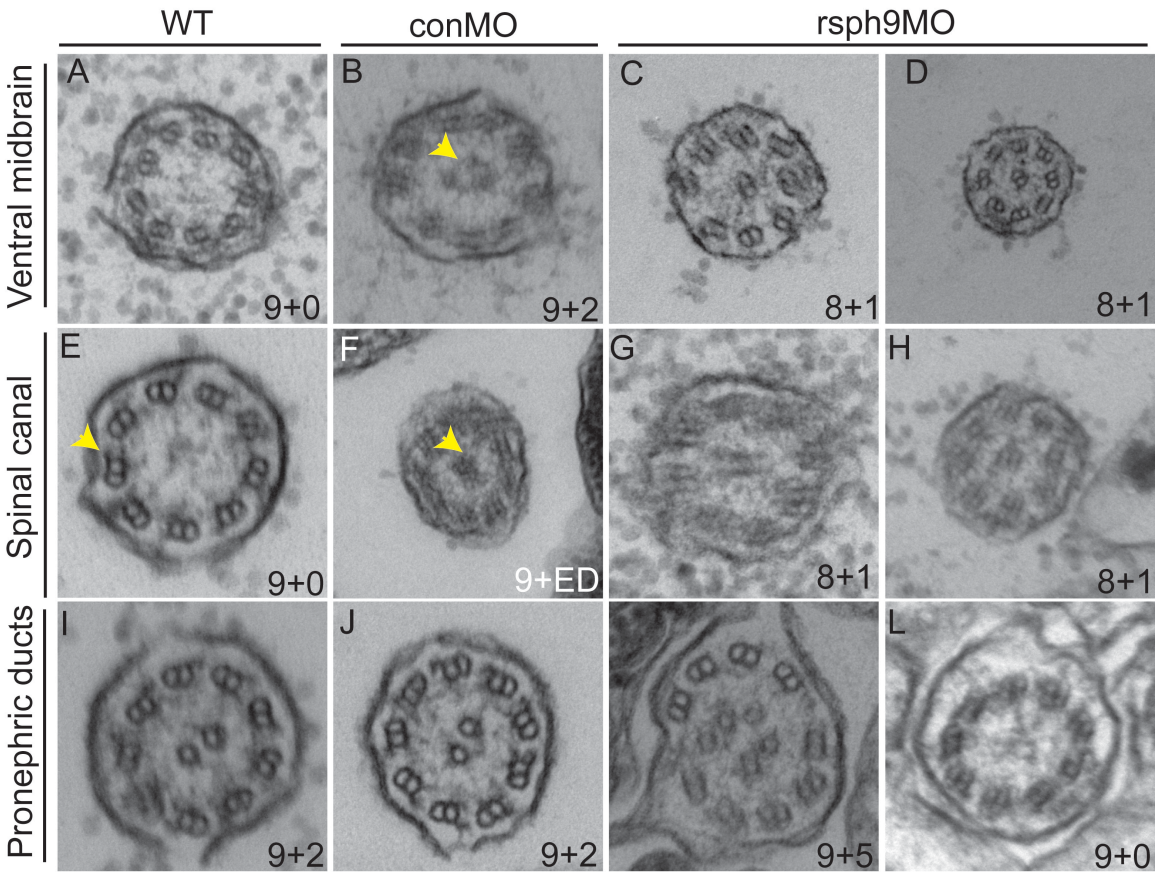

Figure 5. Ultrastructural defects in cilia following Rsph9 depletion. (A-L) Representative TEM images of wild-type, control and rsph9 morphant embryo cilia. (A,B) Most cilia in the ventral MB are 9+0, but there is evidence of some cilia with a central pair (see yellow arrow in B). (C,D) Two cilia with ciliary transposition defects in the ventral MB (E) Most cilia in the spinal canal are 9+0, and have outer dynein arms (see arrow in E). (F) Some cilia have an electron dense center (see arrow in F). (G,H) Ciliary transposition defects in two cilia of the spinal canal. (I,J) Kidney cilia in the 9+2 arrangement. (K,L) Some cilia in the rsph9 morphants have supernumerary central microtubules or loss of the central pair (see L). ED - electron dense.

Ventral MB	9+2 or 9+ED	9+0	8+1 or 8+ED	Total
WT	7	7	1	**15**
conMO	5	10	1	**16**
rsph9AUGMO	4	6	5	**15**
Ventral SC	**9+2 or 9+ED**	**9+0**	**8+1 or 8+ED**	**Total**
WT	0	3	0	**3**
conMO	1	0	0	**1**
rsph9AUGMO	0	1	2	**3**
Kidney	**9+2 or 9+ED**	**9+0**	**Other**	**Total**
WT	18	0	2	**20**
conMO	16	0	0	**16**
rsph9AUGMO	10	5	7	**22**

Table 1. Distribution of ciliary microtubule arrangements. Summary of microtubule arrangements under wild-type, control and rsph9 knockdown conditions in the ventral midbrain, spinal canal, and pronephric ducts. ED – electron dense. Other – 9+1,9+4,9+5 arrangements.

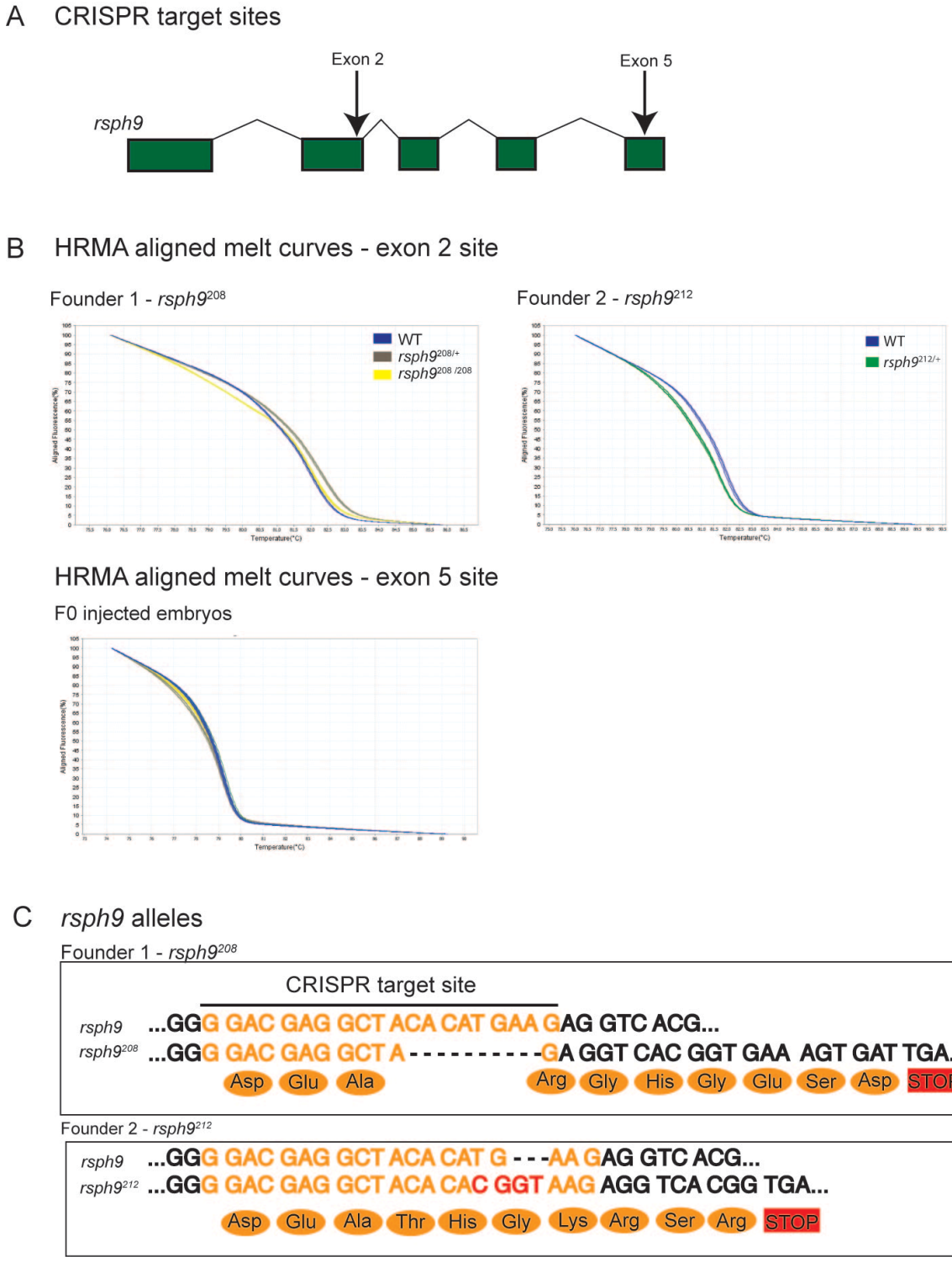

Figure 6. Generation of rsph9 mutant alleles using the CRISPR/Cas system. (A) Cartoon of *rsph9* with CRISPR sgRNA target sites in exon 2 and exon 5. (B) Aligned melts curves from high resolution melt analysis showing different melting profiles for

wild-type, heterozygous, and homozygous mutant embryos at the *rsph9* locus. The *rsph9* exon 5 mutant allele has not yet been sequenced and named. (C) The indels generated by CRISPR mutagenesis in each of two exon 2 alleles both lead to a premature stop codon.

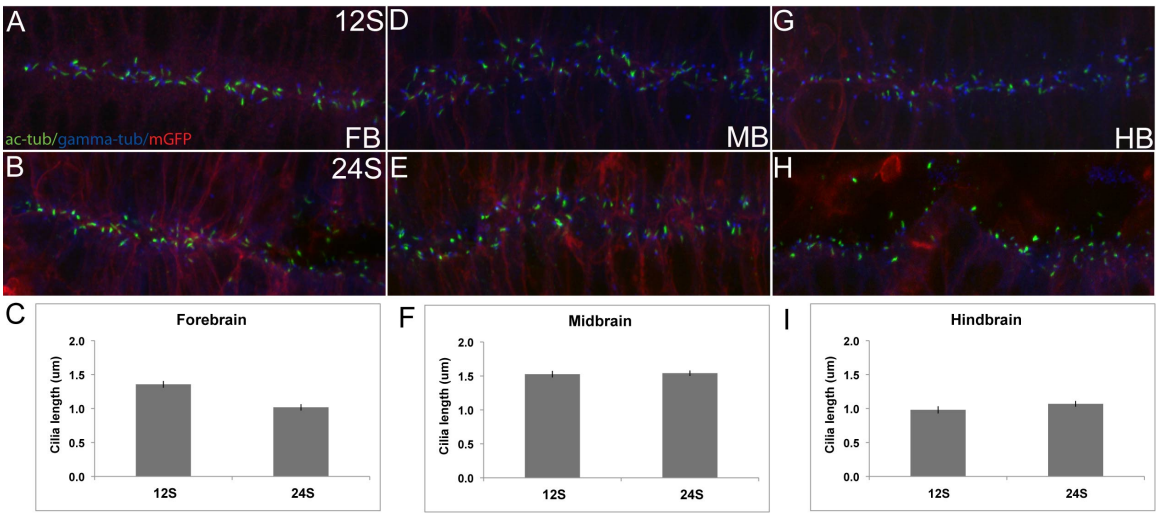

Supplementary Figure 1. Dorsal cilia are uniform across brain subdivisions and throughout neurulation. Fixed *Tg(β-actin:mGFP)* embryos stained with antibodies against acetylated α-tubulin and gamma-tubulin. (A,B) Cilia in the dorsal FB do not change in length over time. (C) Averaged length of dorsal FB cilia at 12S (1.36μm), and 24S (1.02μm). (D,E) Dorsal MB cilia remain unchanged over time. (F) Averaged length at 12S (1.53μm) and 24S (1.54μm). (G,H) Dorsal HB cilia remain unchanged over time. (I) Averaged length at 12S (0.98μm) and 24S (1.07μm). A-B, D-E, G-H are stacked confocal images with anterior to the left. Error bars represent standard error of the mean.

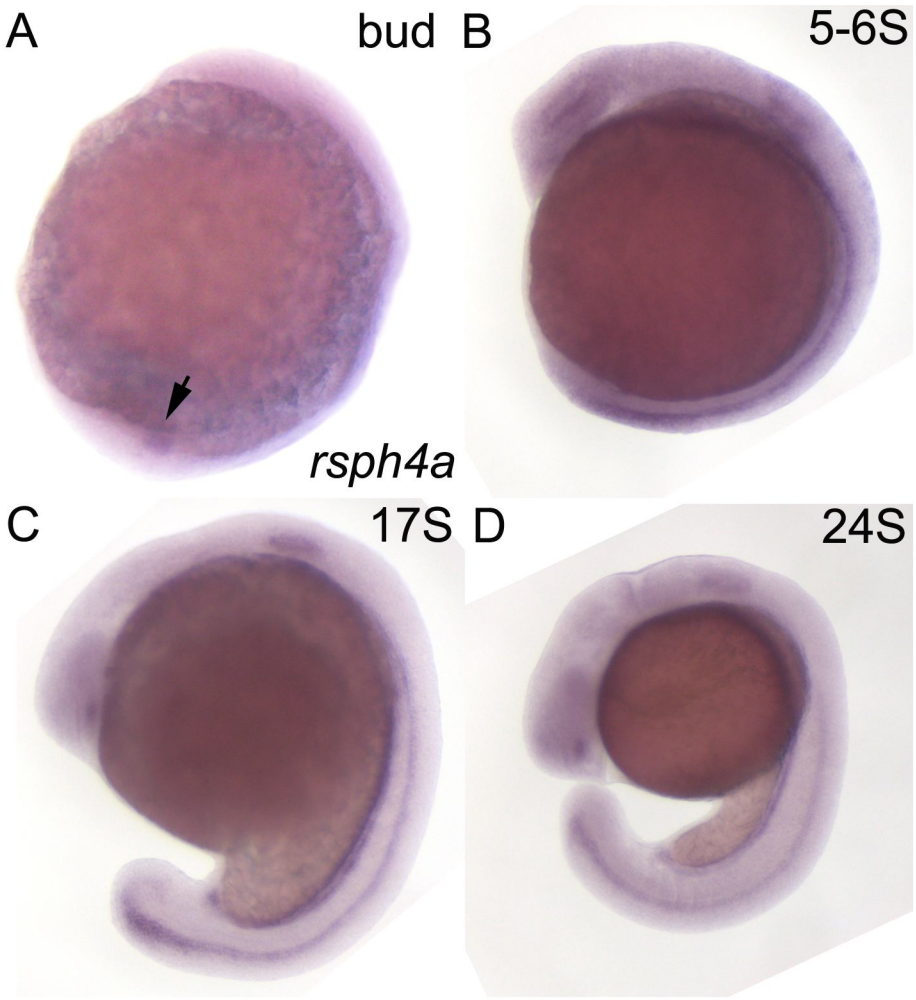

Supplementary Figure 2. *Rsph4a* is expressed in the cranial neural floorplate. Wild-type embryos stained by ISH for *rsph4a.* (A) During early neurulation, *rsph4a* transcript is expressed in Kupferr's vesicle (see arrow). (B-D) Beginning during early neurulation, *rsph4a* is expressed in the pronephric ducts, spinal canal and ventral cranial neural tube. A-D are lateral views with anterior to the left.

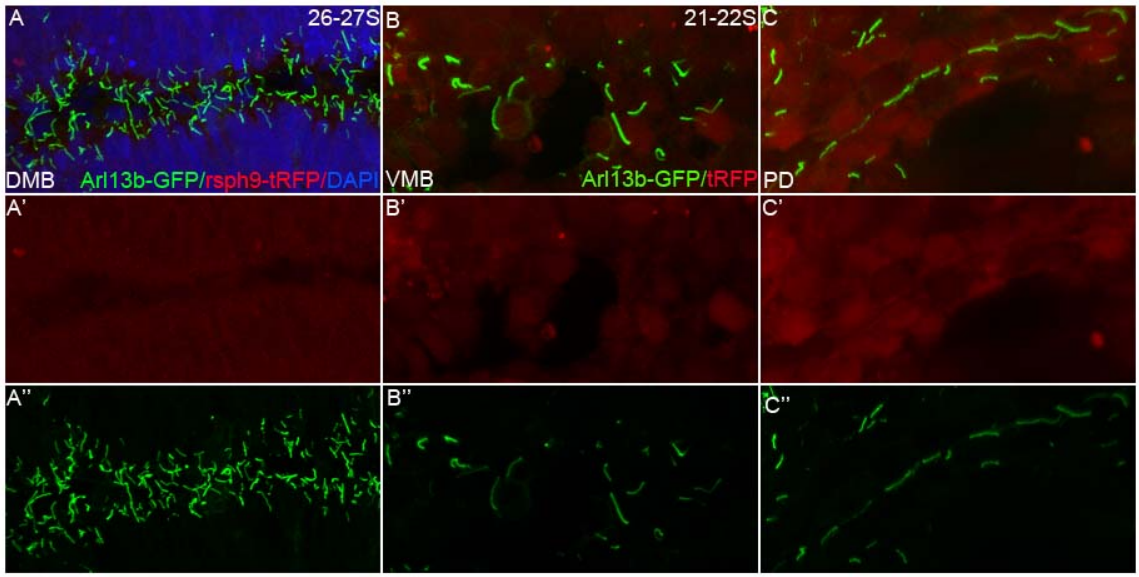

Supplemental Figure 3. Rsph9-tRFP localization to motile cilia is specific. *Tg(β-actin:Arl13b-GFP)* embryos injected with rsph9-tRFP mRNA (A) or tRFP RNA (B,C). (A) Rsph9-tRFP fusion protein does not localize to cilia of the dorsal MB. (B) TagRFP alone does not localize to cilia in the ventral MB. (C) tRFP protein does not localize to cilia in the pronephric ducts. A-C are confocal Z-stacks taken from the dorsal (A'-C') and (A''-C'') are red and green channels alone, respectively. (A), ventral (B) and lateral (C) views.

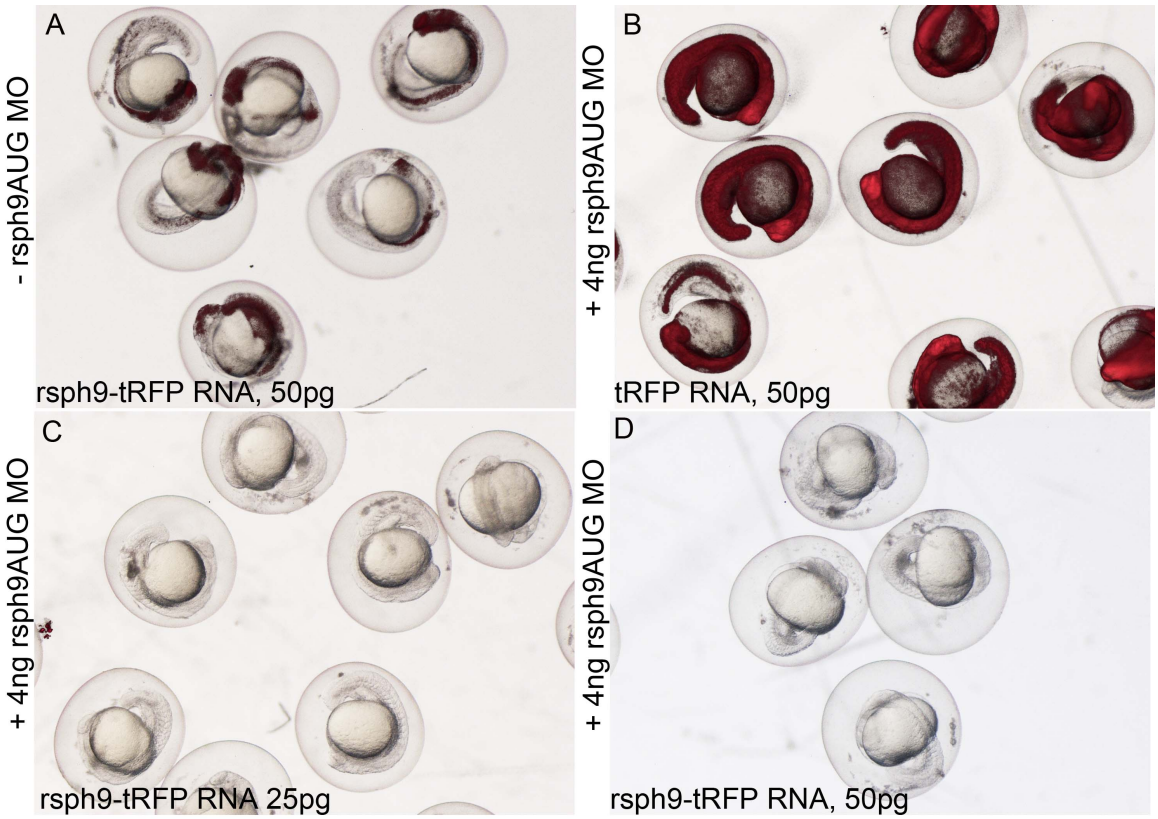

Supplemental Figure 4. Rsph9 knockdown is effective. Wild-type embryos injected with different combinations of rsph9MO and mRNA. (A) Injection of rsph9-tRFP mRNA alone results in tRFP fluorescence at varying levels among embryos. (B) Co-injection of rsph9MO with tRFP mRNA does not prevent tRFP fluorescence. (C,D) Co-injection of rsph9MO with rsph9-tRFP mRNA containing the binding site of the rsph9MO ablates tRFP expression.

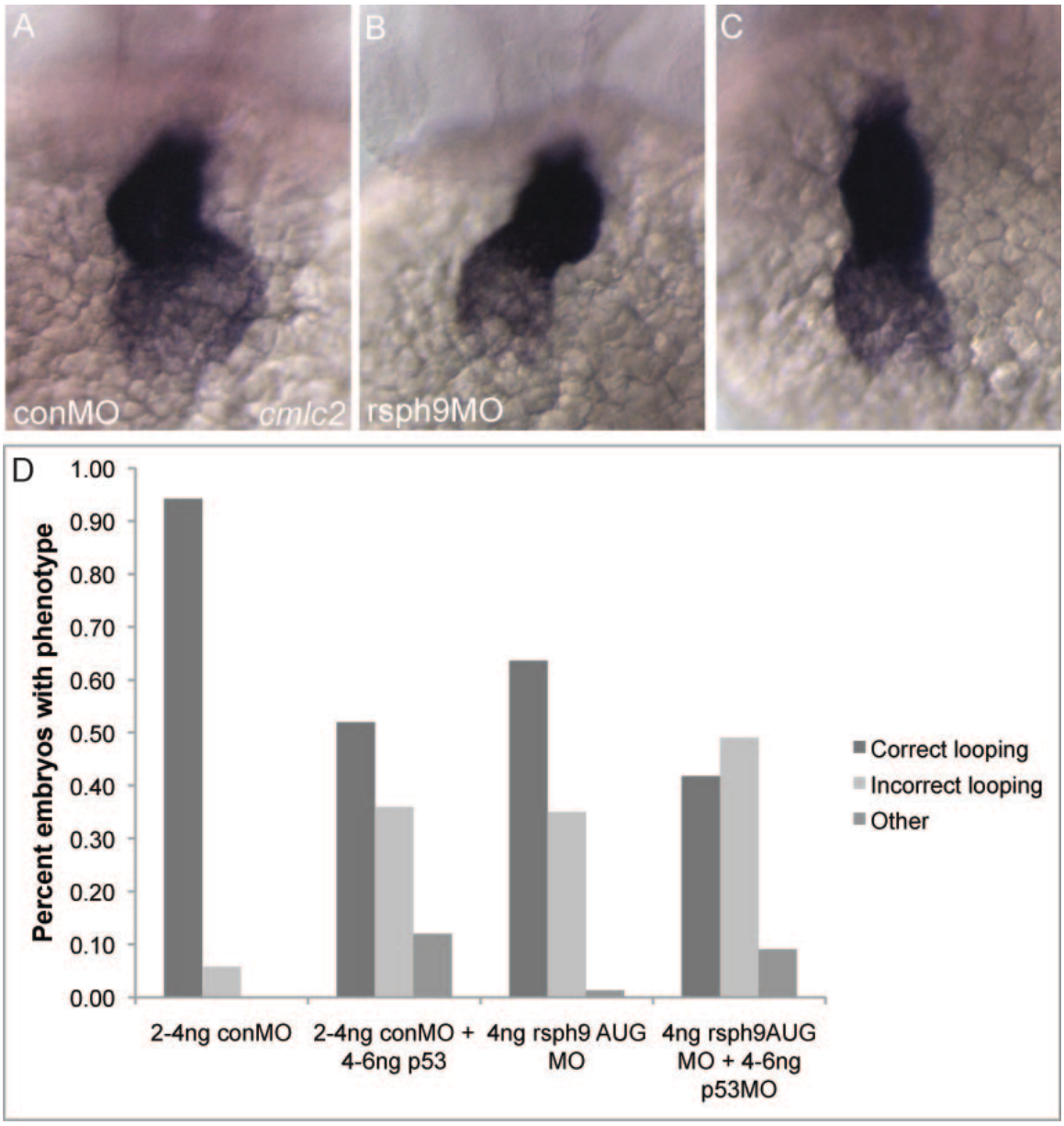

Supplemental Figure 5. Rsph9 knockdown causes heart looping defects. Control and rsph9 morphants stained by ISH for *cmlc2*. (A) The majority of control morphant hearts loop appropriately to the left. (B,C) Rsph9 morphant heart looping is randomized, with many exhibiting mirror looping or no looping. (D) The prevalence of looping defects with and without p53MO co-injection.

Chapter 4:

Future Directions

In the preceding chapters, I discussed two genetic controls governing disparate aspects of embryonic neural development. First, I identified a previously uncharacterized role for the *zic2* paralogs, *zic2a* and *zic2b*, in regulating craniofacial development. I showed that Zic2a knockdown results in a more severe loss of craniofacial cartilages than Zic2b, and defined the temporal window of requirement (before 17hpf). Somewhat surprisingly, the craniofacial dysmorphology observed in zic2a morphants was not entirely attributable to defects in neural crest development, as we initially hypothesized. Instead, I showed that *zic2b*, and not *zic2a*, is expressed in the presumptive neural crest and plays a larger role in timely specification. Both *zic2* genes promote the exit of non-ectomesenchymal neural crest from the neural tube, but the data as a whole is suggestive that this phenotype (1) does not affect the chondrogenic neural crest as strongly, if at all, and (2) is not sufficient to explain the massive defects in pharyngeal and neurocranial cartilages observed in Zic2a loss and gain-of-function assays. I therefore suggested that Zic2a has a second, parallel role in patterning the forebrain and surrounding tissues that act as important signaling centers during craniofacial development. This work represents the first investigation into *zic2b* function, as well as the first examination of how the zebrafish *zic2* paralogs have divided the functions of the single mammalian *Zic2* during neural crest development. More broadly, it provides insight into the complexity of interaction between forebrain, neural crest and craniofacial development, and places *zic2* into the hierarchy of genes directing these processes.

Next, I presented a zebrafish model of the human motile ciliopathy primary ciliary dyskinesia (PCD). I defined a population of presumptive motile cilia in the ventral mid- and hindbrain, and showed that Rsph9, a radial spoke head protein, localizes to these cilia. Depletion of Rsph9 resulted in shortened cilia in multiple organs, and transmission electron microscopy (TEM) revealed a ciliary transposition defect that recapitulates the phenotype observed in humans with radial spoke head mutations. This is the first characterization of cilia in the wild-type cranial neural tube during the vital process of neurulation. Recently generated *rsph9* mutants will provide an important tool for studying the role of radial spoke head proteins and motile cilia during development and disease progression. In this final chapter, I discuss some of the most pressing questions raised by this work and suggest the best avenues for further experimentation.

Seeking mechanisms for *zic* roles during CNS development

Zic mutant lines are required for a deeper analysis of zic functions

The experiments reported in previous chapters were carried out using antisense morpholino oligonucleotides designed to target specific mRNAs and reduce corresponding protein levels. The use of morpholino knockdown techniques in zebrafish has been both a boon and a curse. Morpholinos are a fast and effective reverse genetic system, but they often have off-target effects and it can be difficult to parse the specific from the non-specific phenotypes (Gerety et al., 2011; Robu et al., 2007). In addition, many experiments require a temporally stable null background for

interpretable results (see the Appendix). Much time and effort in the Grinblat lab has been put forth in the search for zebrafish *zic* mutants generated by the previously available random mutagenesis techniques. With the exception of a line with a gene-breaking transposon inserted into exon 1 of *zic2a* (*zic2a*^{GBT133}), we have had little success until recently (Clark et al., 2011). Homozygous *zic2a*^{GBT133} fish have no overt phenotype, but this is not necessarily surprising as many single gene mutations have no phenotype in zebrafish.

It has only recently become possible to deliberately target genes for mutation in zebrafish. Over the last few years, zinc finger nucleases, TALENs, and the CRISPR-Cas9 methods have all come to fruition in the zebrafish (Dahlem et al., 2012; Foley et al., 2009; Hwang et al., 2013). We have chosen to pursue both TALEN and CRISPR-mediated mutagenesis to obtain *zic* mutants. In addition to the *zic2a*^{GBT133} line, we currently have stable lines with mutations in *zic2b* and *zic5*. We are in the process of identifying compound *zic2a;zic5* mutants, and already have adult heterozygous *zic2a*^{GBT133}*;zic2b*^{1127} fish. All alleles identified so far encode truncated proteins and are predicted to be null. Preliminary analysis of compound homozygous embryos has revealed that they recapitulate some of the phenotypes observed in zic2a and zic2b morphants, and will provide an essential tool for assessing Zic function moving forward.

An unbiased screen for mediators of Zic2 function

One of the most important questions not yet addressed is the matter of how Zic2a interacts with Hh signaling to regulate craniofacial development. Three reports

from the Grinblat lab have now implicated Zic2a in patterning the forebrain and optic stalk tissues, likely by interacting with Hh signaling in a non-cell autonomous manner (Sanek and Grinblat, 2008; Sanek et al., 2009; TeSlaa et al., 2013 and Chapter 2). Collectively, the data implicate Zic2a as negative modulator of Hh signaling targets, but the existence of an Hh agonist or antagonist directly regulated by Zic2a is merely hypothesized. Because *zic2a* is a transcription factor, the most direct way to address how it exerts its role in the forebrain is to identify downstream effectors.

Previously, we carried out a microarray looking for Zic effectors using a knockdown assay (see Appendix for further discussion). This was an inherently flawed experiment for a number of reasons, including the efficacy and specificity of morpholinos. With mutants in hand, it is now possible to take an unbiased approach towards identifying Zic2 targets. Currently underway in the lab is an RNA-seq experiment using compound homozygous *zic2a*^{GBT133}*;zic2b*^{1127} embryos. Total RNA will be isolated from individual embryos at several stages during neurulation and eye morphogenesis and subjected to high-throughput sequencing without pooling. Sequencing data from compound homozygous embryos will be compared with stage-matched wild-type embryos, and transcripts that are differentially expressed in mutants will be identified as potential downstream effectors of Zic2a and/or Zic2b.

In the future, it may be advantageous to look for tissue-specific effectors of Zic2. The *Tg(pax6b:GFP)* line expresses GFP in the optic stalk, beginning at about 22S (Delporte et al., 2008). By crossing this line into the compound mutant line, we would be able to use flow cytometry to collect only GFP-positive cells from which to isolate

RNA for sequencing. This technique should enrich for the Zic2 targets important for its function in patterning the optic stalk/retinal interface (Sanek et al., 2009). Similarly, FACS could be used to collect RFP-positive cells from the compound mutant line, as the transposon used to generate the *zic2a*^{GBT133} line encodes mRFP. Fluorophore expression recapitulates most aspects of the endogenous *zic2a* domain, with the exception of the optic stalk. This strategy should enrich for Zic2a effectors important in the dorsal neural tube.

Zic2 target validation

Once we have a list of potential targets, it becomes important to validate data obtained in the RNA-seq experiment. Initial validation can be done using quantitative real-time PCR and *in situ* hybridization. These two techniques have complimentary advantages, in that real-time PCR is excellent at quantifying changes in gene expression in the whole embryo, while *in situ*s show tissue-specific changes in a qualitative manner. These techniques could also be used to separate targets specific to either *zic2a* or *zic2b* by comparing single and double mutants. The *zic* family shares high sequence similarity in the zinc finger region as well as overlapping expression domains, making it likely that there will be significant overlap in downstream effectors as well. In order to further pursue candidate effectors, we will need to know more about the biology of the genes identified by RNA-seq.

Eph/ephrins are potential zic2 effectors

In zic2a morphants, several lineages of neural crest cells fail to initiate migration and instead remain in the neural tube or are extruded into the lumen (Chapter 2). One important question raised by the work reported above is the matter of how Zic2 exerts its control over the onset of neural crest migration. The Eph/Ephrin family of transmembrane guidance molecules are likely candidates for Zic2 effectors, based on what we already know of Zic2 function and hints from the microarray presented in the Appendix. Eph/ephrin signaling mediates adhesion and cytoskeletal changes that impact neural crest cell morphology and migration during embryonic development (Santiago and Erickson, 2002). Specifically, Ephs and Ephrins are upstream of molecules such as Rho, Rac and Cdc42, via their regulation of GEFs and GAPs, whose activity is required for localized changes in cytoskeletal contraction (reviewed in Noren and Pasquale, 2004). These properties make them attractive candidates for mediating the neural crest retention phenotype observed in Zic2 knockdown assays.

The published literature supports a connection between Zic2 and Ephs. Zic2 is required for ipsilateral projection of mouse retinal ganglion cell axons via its regulation of EphB1 expression in the RGCs themselves (Garcia-Frigola et al., 2008; Lee et al., 2008). More recently, Zic2 has also been shown to induce EphA4 in dorsospinal neurons to maintain axon ipsilaterality (Escalante et al., 2013). Additionally, three ephrins expressed in the dorsal brain (*efna2*, *efna3b*, and *efnb3b*) were identified as downregulated in response to Zic2a depletion (see Appendix).

In order to test this relationship in zebrafish, the *zic2a;zic2b* and *zic2a;zic5* compound mutant lines can first be assessed for NC deficits and neural tube retention,

as in the morphants. Live imaging using the *Tg(sox10:GFP)* line combined with the F-actin biosensor mCherry-Utrophin-CH would offer an initial look at actin dynamics in mutant NC cells during delamination (Burkel et al., 2007; Nyholm et al., 2009). If the stereotyped behaviors associated with migratory initiation are affected, one could next ask whether they can be rescued by manipulating levels of specific Ephs or Ephrins. The expression pattern of EphB1 has not yet been characterized in zebrafish, but cloning an *in situ* probe against this gene would be an excellent place to start looking for a Zic2 downstream effector in this context.

My data also revealed that Zic2a likely contributes to craniofacial development by early patterning of one or more anterior tissues, required for chondrogenic neural crest migration or condensation. Possibilities include the forebrain, optic stalk and retina, all of which are important for neural crest invasion of the head. Since the Eph/ephrin signaling modality frequently provides repulsive or attractive cues during cell migration, one could test for a role during anterior neural crest migration. In fact, *efna3b* is specifically reduced in the nasal retina of zic2a morphants, a place where it may normally be required to provide guidance cues to cranial neural crest cells (see Appendix). This requirement could be tested using one of several identified fish lines with mutations in *efna3b* (www.zfin.org).

Zic2 interaction with Wnt signaling

Another possible mediator of *zic2*'s function during neural crest development is the Wnt signaling pathway. Canonical Wnt signaling directly activates *zic2a/zic5*

transcription via a shared regulatory region, and Wnt signaling is an important regulator of several aspects of neural crest development including delamination and pigment cell specification (Nyholm et al., 2007). Recent studies have shown that Zic2 and Zic3 proteins are both capable of inhibiting Wnt signaling in human cell lines via their physical interaction with Tcf factors (Fujimi et al., 2011; Pourebrahim et al., 2011). Collectively, these data suggest that some aspects of the Zic knockdown phenotype might be mediated by its interaction with Wnt signaling.

The nature of this network could be queried in several ways. The effect of Zic2a and/or Zic2b knockdown on Wnt signaling could be assessed in the *Tg(TOP:dGFP)* line, in which GFP expression is driven by four Lef binding sites (Dorsky et al., 2002). If Wnt signaling is altered in response to a reduction in Zic2a levels, expression of a Wnt antagonist using *Tg(hsp:dkk1b-GFP)* or activation of the canonical Wnt pathway with the *Tg(hsp:β-catenin-GFP)* fish lines could be induced at specific time points to test for rescue of the zic2a morphant neural crest phenotype (Caron et al., 2012). The relationship between *zic2* and Wnt signaling may be quite complex, as current data from human cell lines and *Xenopus* suggest that *zic*s inhibit Wnt-driven transcription, but Wnt signaling is though to promote neural crest migration and pigment cell specification, which are reduced in zic morphants (Lewis et al., 2004).

Pursuing Zic2 function in mutants

In parallel with the effort to elucidate downstream effectors of Zic2, it makes sense to pursue characterization of the mutant alleles we now have at our disposal.

Initial assays will look to confirm which phenotypes observed in morphants are present in mutants. Preliminary evidence indicates that coloboma, observed in Zic2a morphants, is also present in *zic2a*$^{GBT133-/-}$*;zic2b*$^{1127-/-}$ embryos. The development of the choroid fissure is an area of active study, and this mutant line offers a novel opportunity to image aberrant eye development *in vivo* (Kwan et al., 2012). Optic vesicle morphogenesis can be imaged on the tissue-wide level using *Tg(β-actin:mGFP)* embryos, or at the cellular level by mosaic expression of cytoskeletal biosensors. Then, if there are likely candidates for downstream Zic2 effectors during choroid fissure morphogenesis based on expression or function, these factors can be supplied as RNA or as exogenous protein (if they are secreted signaling molecules) to determine if they restore wild-type cell behaviors.

Zic2 morphants also develop with defects of the neural tube and disrupted integrity of important apical components (Nyholm et al., 2009). I have demonstrated that Zic2b knockdown causes midbrain ventricle defects very similar to those described in zic2a/zic5 morphants. This phenotype should therefore be assessed in both *zic2a*^{GBT133}*;zic2b*^{1127} and *zic2a;zic5* mutants with the use of cytoskeletal and junctional polarity markers such as phalloidin (an F-actin marker), phosphorylated myosin light chain (indicative of active actomyosin contraction), ZO-1 (a tight junction marker) and aPKC (a polarity determinant). If this phenotype is preserved in zic mutants, we can proceed to testing candidate effectors identified in the RNA-seq experiment to see if they are able to restore apical integrity and organization.

Phenotypes that may arise after morpholinos have lost their efficacy are of particular interest. Previous work in the lab has demonstrated that Zic2a and Zic5 have a mitogenic role in the midbrain, and the consensus in the field is that Zics have pro-proliferative roles that regulate the balance between multipotency and differentiation in both embryonic stem cells and the brain. If this is the case for Zic2 and/or Zic5 in zebrafish, we might expect to see reduced proliferation in the CNS of mutants, and premature exit of neural progenitors from the cell cycle. This can be tested in neurons and glia using antibodies against HuC/Elavl3 and GFAP, respectively.

Finally, there is some evidence that *ZIC2* mutation in humans can have serious long-term consequences for mental health. One report identified a human schizophrenia patient with a *ZIC2* mutation that disrupted its transcriptional activity (Hatayama et al., 2011). They characterized a set of behavioral deficits in hypomorphic *Zic2* mutant mice, including decreased pre-pulse inhibition in an acoustic startle challenge, a deficit frequently observed in humans with schizophrenia. This is an assay that can be replicated in larval zebrafish *zic* mutants, to determine whether they too have difficulty filtering superfluous sensory input (Burgess and Granato, 2007a). If this is indeed the case, zebrafish may provide an important model for mental health disorders going forward.

The role of motile cilia during neural development and disease

Regulation of ciliogenesis in the cranial neural tube

A time course of ciliary development in the cranial neural tube revealed several intriguing things. First, a population of ventral cilia in the MB and HB is already elongated at 12S, a point when the neural epithelium in zebrafish consists of a closed rod with no lumen (Hong and Brewster, 2006). These cilia have dynein arms, and thus are likely motile or become motile at some point, and continue to elongate over the course of the six hours of development observed. This finding raises several questions: (1) How is ciliogenesis regulated in the cranial floorplate, and (2) What is the physiological purpose of these presumptive motile cilia?

Second, cilia populations in each of the three compartments of the brain are distinct from one another. The FB has no elongating cilia, while the MB and HB harbor long, presumptive motile cilia, but of significantly different lengths. This result suggests that the motile cilia in each subdivision are differentially regulated. As so little is known about how ciliary diversity is generated, it will be extremely interesting to pursue an understanding of tissue-restricted specifiers of motile ciliogenesis.

Finally, the cilia population *within* each brain compartment seems to harbor some diversity. TEM data indicates that the motile cilia of the cranial floorplate are a mixed population, composed mainly of 9+0 cilia, as in the spinal canal, but with some evidence of 9+2 cilia as well. This phenomenon is not well-reported in the literature, but there is evidence that the cilia of the perinatal mouse choroid plexus are heterogeneous in structure and beating waveform (Narita et al., 2012). Additionally, a single choroid plexus cell can bear multiple types of motile cilia, as Rsph9 localizes to only a subset of cilia on a single cell (Nonami et al., 2013).

The preponderance of evidence indicates that *foxj1* (*foxj1a* and *foxj1b* in zebrafish) is the master regulator of motile ciliogenesis in essentially every vertebrate tissue examined to date (reviewed in Choksi et al., 2014). *Foxj1* is upstream, sometimes directly upstream, of a whole host of genes specific to motile cilia (Stubbs et al., 2008; Yu et al., 2008). We have shown that *foxj1a* is expressed in the floorplate of the MB and HB, where there are motile cilia, but not in the FB, which lacks motile cilia, suggesting that this regulatory relationship is likely preserved in the cranial NT as well. This can easily be tested by using published morpholinos to knock down *foxj1a* and then examining (1) markers of motile cilia such as *rsph9, dnahc9* and *efhc1* and (2) presence of elongated cilia during neurulation (Hellman et al., 2010). It will likely also be important to test the role of *foxj1b* by knocking it down both alone and together with *foxj1a*, as duplicated genes in the teleost lineage frequently share some functional redundancy.

Perhaps more interesting would be to determine what lies upstream of *foxj1* regulation of cranial cilia. *Rfx* genes are transcription factors that also regulate ciliogenesis, but are thought to regulate both primary and motile cilia (reviewed in Choksi et al., 2014). We have generated several mutant alleles of *rfx4* by CRISPR/Cas mutagenesis, which could be used to test the regulatory relationship between *rfx4* and *foxj1* in the ventral brain. However, thus far *rfx4* has only been linked with immotile ciliogenesis, so it may be necessary to include other *rfx* genes in this analysis (Ashique et al., 2009). *Rfx2* and *Rfx3* have each been explicitly associated with motile cilia, making them possible candidates as well (Chung et al., 2012; El Zein et al., 2009).

Only a few signaling pathways have been identified as upstream of motile ciliogenesis. The Fgf receptor *fgfr1* is required cell-autonomously in Kupferr's vesicle and the pronephric ducts of zebrafish, as well as several *Xenopus* tissues, to regulate cilia length, likely through *fgf8* and *fgf24* (Neugebauer et al., 2009). Interestingly, starting by 14S, *fgfr1a* is expressed in the ventral MB and HB (Thisse and Thisse, 2005). Preservation of this regulatory relationship could be tested in the cranial neural tube by using morpholino knockdown of the receptor, a dominant-negative Fgfr1 (Neugebauer et al., 2009), or pharmacological inhibition of Fgf signaling (SU5402, Millimaki et al., 2007).

A second pathway implicated in regulation of motile ciliogenesis is canonical Wnt signaling, which is a direct transcriptional regulator of *foxj1a* (Caron et al., 2012). Disruption of the Wnt pathway results in shortened cilia in Kupferr's vesicle and the pronephric ducts, downstream of Fgf signaling. However, Wnt inhibition has no effect on *foxj1a* expression in the posterior floorplate. Hedgehog (Hh) signaling is also thought to be upstream of *foxj1a* expression and motile ciliogenesis, specifically in the zebrafish and mouse spinal canal (Yu et al., 2008; Cruz et al., 2010). Numerous reagents exist to manipulate Hh signaling in zebrafish, including the small molecule inhibitor cyclopamine, which confers temporal control, published morpholinos targeting Gli mRNA (England et al., 2011), and RNA encoding a truncated Gli3 that functions as a repressor (Huang and Schier, 2009). Dampening of Hh signaling followed by examination of expression of *foxj1* genes, *rfx* genes, and characterization of ventral cilia

will provide an answer as to whether Hh regulates motile ciliogenesis in the cranial neural tube.

One intriguing possibility for a cell type-specific code regulating ciliogenesis is HSPG sulfation (Neugebauer et al., 2013). The 3-OST-5 enzyme is required in the cells of Kupferr's vesicle to regulate cilia length, in cooperation with Fgf signaling, while the 3-OST-6 enzyme acts in the same tissue to regulate ciliary motility. The authors of this paper suggest that various sulfotranserase enzymes carry out tissue-specific functions that generate an extracellular 'glycocode' on ciliated cells, regulating access of secreted ligands to their receptors on the cell surface. Examination of the expression pattern of the O-sulfotransferase enzymes would provide a starting point for those that could be important for regulating ciliogenesis in the cranial floorplate (Cadwallader and Yost, 2006).

Ciliary motility in the cranial floorplate

Our data indicates that ciliary length is dynamic during neurulation. However, fixed characterization is clearly not the ideal method for examining the biology of motile cilia. It is therefore imperative that we add live imaging of cranial cilia to our investigation of the role of motile cilia in the developing CNS.

The first objective is simply to ascertain when cranial cilia become motile. This may be possible at low resolution by imaging *Tg(β-actin:Arl13b-GFP)* embryos (Borovina et al., 2010). A second method is available as soon as the ventricles begin opening (at 18hpf), when we can inject fluorescent microspheres into the open lumen

and image their motility as a proxy. Individual beads can be tracked in order to get an idea of what type of flow is generated by ventral cilia (Supatto and Vermot, 2011). It is likely that cilia do not begin beating until the ventricles are filled with embryonic CSF, which occurs sometime between 18 and 24hpf.

These methods will be sufficient to examine ciliary beating in the cranial neural tube on a crude level, but higher resolution imaging to determine beat frequency and waveform will require a different approach. Although zebrafish are optically transparent, imaging the ventral mid- and hindbrain presents considerable challenges because of the depth of the tissue. In order to visualize waveform, ciliary motility should be viewed from the top down, rendering the ventral neural tube mostly inaccessible by current video microscopy techniques. Rather than imaging in an intact embryo, it may be necessary to isolate cranial neural tissue, remove the yolk, and culture it briefly to capture the floorplate cilia beating (Langenberg et al., 2003). Given the protein localization and TEM data suggesting that radial spoke components localize to 9+0 cilia, the question of what waveform these potentially atypical cilia assume becomes quite important.

Motile cilia and primary ciliary dyskinesia

One way to better understand the role of cilia during development is to characterize the breakdown of their function during disease. It has recently become quite common to identify a gene associated with PCD in humans via whole exome sequencing, and then examine the phenotype in a zebrafish knockdown model (see

Knowles et al., 2013; Zariwala et al., 2013 for examples, among many others). New human loci susceptible to mutations causing PCD have also been identified in a forward manner by screening for candidates in zebrafish (Austin-Tse et al., 2013). These rapid advances in the genetics of PCD leave us with a need for model organisms to truly understand how these mutations interact with disease progression (reviewed in Yuan and Sun, 2013). Zebrafish, a genetically tractable organism in which ciliary motility can be imaged directly *in vivo*, present an advantageous system within which to work.

Rsph9 mutants as a zebrafish PCD model

To this end, it will be very important to characterize ciliary phenotypes in recently established *rsph9*^{208} and *rsph9*^{212} mutant lines, which both have indels in exon 2 leading to premature stop codons (Chapter 3). Although a stable line has not yet been retrieved, we have also successfully targeted a second site in exon 5 of *rsph9*, which will hopefully allow us to uncover any off-target effects generated by CRISPR mutagenesis. Thus far, neither mutant allele has shown any evidence of hydrocephalus, a prominent developmental defect observed in Rsph9-depleted embryos. However, knockdown of zebrafish Rsph9 does recapitulate other aspects of PCD, most notably the precise ciliary transposition defect observed in airway cells taken from humans with mutations in any of three radial spoke head genes.

Although the *rsph9* mutant lines do not have hydrocephalus, that does not mean they do not have ciliary defects, as humans with mutations in motile cilia genes only occasionally develop hydrocephalus. The first task will be to analyze cilia as in the

morphants, by using the anti-acetylated tubulin antibody to examine length and TEM to look at ultrastructure. Another way to get a better look at ciliary structure is by scanning EM (SEM). We attempted SEM on rsph9 morphant embryos, but the temporal limitations of the morpholino meant that embryos were too small to mount with the setup available to us, a problem that is solved by the use of mutant lines. We expect to observe shortened cilia in the floorplate, but the added 3D resolution of SEM may provide more information on ciliary structure in mutants.

Live imaging of cranial floorplate cilia in mutants is a good long-term goal, but as discussed above may require some significant troubleshooting and advances in technology. We will therefore focus on assessing ciliary motility in other affected organs (Drummond, 2009). The spinal canal and the nasal placodes are both easily accessible. In the nasal placodes, which have 9+2 cilia, we would except to see a shift from planar to rotational waveform, something observed in the airway cells of humans with radial spoke mutations. In the spinal canal, which has many 9+0 cilia and perhaps a few 9+2 cilia, it is not clear what will happen to ciliary beat frequency or waveform. If there were a change in ciliary beating, it would add to the evidence that radial spokes have a novel role in 9+0 cilia.

Rsph9 knockdown resulted in shortened cilia in the neural tube, pronephric ducts, and Kupferr's vesicle. As mentioned above, the major phenotype observed in the primitive brain is not recapitulated in mutants. However, it is certainly worth investigating what happens to other ciliated organs. Morphant assays were suggestive of left-right axis defects, as shown by the randomized heart looping. Mutant analysis of

heart looping can be paired with *in situ* hybridization for expression of early markers of asymmetry such as *lefty2* (Bisgrove et al., 1999). These assays in mutants will provide a definitive answer as to the requirement for radial spoke heads during zebrafish establishment of the left-right axis.

Occasionally, PCD patients are reported to have corneal or retinal anomalies, and cystic kidney disease (reviewed in Ibanez-Tallon et al., 2003). Dysfunctional motile cilia can cause cystic kidneys, and the presence of kidney cysts can be assessed in larval zebrafish with histology and thin sectioning (Sullivan-Brown et al., 2008). While deafness has not previously been associated with PCD, motile cilia are required for otolith deposition in zebrafish (Yu et al., 2011). In order to assess the effect of radial spoke head mutations on eye and ear function, we can use behavioral assays. The acoustic and visual startle responses have been well characterized in wild-type larvae (Burgess and Granato, 2007b). If there are changes in acoustic or visual startle responses, the genesis of these defects might lie in one of several places. First, dysmotile cilia of the retina or otic placodes might be directly responsible for generating defects in the larval eye or ear. Alternatively, dysmotile cilia in the cranial neural tube may not effectively support distribution of eCSF and the trophic molecules it contains, leading to abnormal neuronal development and a secondary processing defect that prevents appropriate behavioral responses to external stimuli.

A role for radial spokes in 9+0 cilia?

Our data show that, in transient assays, an Rsph9-tRFP fusion protein localizes to motile cilia in the anterior floorplate, the pronephric ducts and in Kupferr's vesicle. At the stage examined, cilia in the spinal canal are reported to be primarily 9+0, which is also what we observe in the cranial floorplate (Kramer-Zucker et al., 2005). Together, these data suggest that a radial spoke head protein may localize to 9+0 cilia, which are generally thought to lack radial spokes as well as the central pair. This would be a novel finding, if true, and deserves careful investigation.

The most native assay would be to perform immuno-TEM using an Rsph9 antibody, and show its specific localization to cilia with a 9+0 structure in cross section. There are a few anti-human Rsph9 antibodies commercially available, but these work only infrequently in zebrafish whole-mount immunostaining, so it is worth considering alternatives. One possibility is to inject human *rsph9* mRNA and subsequently use immuno TEM with a human Rsph9 antibody. Another possibility is to fuse zebrafish Rsph9 with an electron-dense tag that allows visualization by TEM without immunostaining (Diestra et al., 2009). Finally, the presence of radial spokes in 9+0 cilia could be conclusively demonstrated by electron tomography (Burgoyne et al., 2014). While our data are suggestive that some radial spoke proteins may localize to 9+0 cilia, it is unclear what their role there would be.

One possibility is that radial spokes can influence ciliary waveform even in the absence of the central pair. Thus far there are no reports of 9+0 cilia with planar waveform, but there are some suggestions they may exist in the neural epithelium, raising the question of whether the central pair is required for that particular waveform.

This question would have to be assessed by live imaging *in vivo* markers that localize specifically to radial spokes or the central pair. Although Rsph9-tRFP may be such a marker, much further characterization is required to know definitively. Fluorophore fusions with other radial spoke or central pair components could be tested for 9+2 specificity as well.

Characterization of the radial spokes

I have presented data on *rsph9* expression and protein localization, the only one of 23 spoke proteins identified in *Chlamydomonas* that has been characterized in zebrafish (see Chapter 3; Castleman et al., 2009). In fact, very few vertebrate orthologs of radial spoke genes have been identified as such. In zebrafish, four of the five spoke head genes are annotated (*rsph1, rsph4a*, *rsph9* and *rsph10b*) and two stalk genes (*rsph3* and *ropn1l*). A third spoke gene, *dnajb13*, was characterized in mice (Guan et al., 2010). Very little is known about the structure of cilia in specific vertebrate tissues, and whether there is any specialization of radial spoke components for different compartments. It would therefore be useful to (1) identify the zebrafish orthologs of the remaining spoke genes, and (2) catalog their expression profiles. Zebrafish would provide a superb model within which to dissect tissue-specific structural aspects of motile cilia by systematically targeting spoke components via knockdown and CRISPR mutagenesis. This in-depth analysis will be justified if we identify a role for radial spokes during development using the *rsph9* mutant model.

Very little is known about the functional domains of radial spoke proteins, and which are required for ciliary beating. This could be assayed in zebrafish by injection of RNA encoding radial spoke components with disruptive mutations in conserved domains followed by live imaging of motile cilia in an accessible tissue. For example, the only known functional motifs in any spoke head protein are the MORN domains in RSP1 and RSP10. If these domains were preserved in vertebrate orthologs, mutational analysis would allow us to test their putative role in calcium signaling, and determine their impact on ciliary beat frequency and waveform.

The ciliated neural epithelium – looking into the future

Data presented in Chapter 3 are limited to cilia during the first 24 hours post fertilization. While these data are both interesting and valuable, one of the most exciting aspects of having mutants in hand is the ability to study later development of motile cilia. As the neural epithelium matures, it generates a specialized epithelium in each ventricle called the choroid plexus, which secretes embryonic CSF, as well as multiciliated ependymal cells that the ventricles and create laminar flow of the CSF across the ventricles. The choroid plexus is a vital tissue that is implicated in normal development as well as disease progression. It is at least transiently populated with motile cilia, and interestingly enough expresses both *zic*s and *rsph9* (Inoue et al., 2008; Narita et al., 2012). Moving forward, we would like to characterize both what happens to the floorplate cilia, and follow the rise of multiciliated cells.

A useful tool for tracking the presence of motile cilia is the gene trap line T2BGSZ10 (Tian et al., 2009), which carries a transgenic insertion in the first intron of *foxj1b*. Using *foxj1b*-driven expression of GFP, we can first assess when and which cells of the neural epithelium bear motile cilia as development proceeds past 24hpf. This can be done in fixed tissue with antibodies, as in Chapter 3, as well as by scanning EM. In *Xenopus* embryos, ependymal cells begin with a single elongating cilium, and then gradually become multiciliated over time (Hagenlocher et al., 2013). If this is also the case in zebrafish, it will be interesting to query the structure of that initial elongating cilium, ask whether it is itself motile, and determine whether this pilot cilium is required for subsequent multiciliation.

An important aspect of PCD in humans is the difficulty of diagnosis. Nasal nitric oxide measurements have been touted as a quick, efficient method. The most thorough method is thought to be TEM on multiciliated respiratory epithelial cells. However, both of these methods have recently been shown to have an unacceptable number of false negatives, as some mutations that cause PCD have nasal nitric oxide measurements within the normal range and a number of them have incompletely penetrant or no ultrastructural defects (Knowles et al., 2014). Therefore, identification of further phenotypes could provide hints for new diagnostic techniques in humans.

We are only beginning to scratch the surface of understanding the role of motile cilia during neuronal development. There is mounting evidence that while motile ciliopathies may sometimes have obvious phenotypes such as situs inversus, infertility, or mucociliary clearance defects, they are likely also involved in a host of much more

subtle brain anomalies that are only revealed in the neonate or even in the adult organism. For example, dyslexia candidate gene *dyx1c1*, strongly linked to dyslexia and verbal short-term memory, is expressed in motile ciliated organs, and its knockdown results in loss of the inner and outer dynein arms (Chandrasekar et al., 2013). *Dyx1c1* knockdown in rats disrupts neuronal migration and ultimately auditory processing and spatial learning (Szalkowski et al., 2013). Additionally, a major study of schizophrenia-associated genes in humans turned up at least one candidate locus near *CCDC39*, another motile cilia-associated gene whose loss disrupts inner dynein arms and causes PCD (Antony et al., 2012; Schizophrenia Working Group, 2014).

References

Antony, D., Becker-Heck, A., Zariwala, M. A., Schmidts, M., Onoufriadis, A., Forouhan, M., Wilson, R., Taylor-Cox, T., Dewar, A., Jackson, C. et al. 2013. Mutations in CCDC39 and CCDC40 are the major cause of primary ciliary dyskinesia with axonemal disorganization and absent inner dynein arms. Hum Mutat. 34, 462-72.

Ashique, A. M., Choe, Y., Karlen, M., May, S. R., Phamluong, K., Solloway, M. J., Ericson, J. and Peterson, A. S. 2009. The Rfx4 transcription factor modulates Shh signaling by regional control of ciliogenesis. Sci Signal. 2, ra70.

Austin-Tse, C., Halbritter, J., Zariwala, M. A., Gilberti, R. M., Gee, H. Y., Hellman, N., Pathak, N., Liu, Y., Panizzi, J. R., Patel-King, R. S. et al. 2013. Zebrafish Ciliopathy Screen Plus Human Mutational Analysis Identifies C21orf59 and CCDC65 Defects as Causing Primary Ciliary Dyskinesia. Am J Hum Genet. 93, 672-86.

Bisgrove, B. W., Essner, J. J. and Yost, H. J. 1999. Regulation of midline development by antagonism of lefty and nodal signaling. Development. 126, 3253-62.

Borovina, A., Superina, S., Voskas, D. and Ciruna, B. 2010. Vangl2 directs the posterior tilting and asymmetric localization of motile primary cilia. Nat Cell Biol. 12, 407-12.

Burgess, H. A. and Granato, M. 2007a. Sensorimotor gating in larval zebrafish. J Neurosci. 27, 4984-94.

Burgess, H. A. and Granato, M. 2007b. Modulation of locomotor activity in larval zebrafish during light adaptation. J Exp Biol. 210, 2526-39.

Burgoyne, T., Lewis, A., Dewar, A., Luther, P., Hogg, C., Shoemark, A. and Dixon, M. 2014. Characterizing the ultrastructure of primary ciliary dyskinesia transposition defect using electron tomography. Cytoskeleton (Hoboken). 71, 294-301.

Burkel, B. M., von Dassow, G. and Bement, W. M. 2007. Versatile fluorescent probes for actin filaments based on the actin-binding domain of utrophin. *Cell Motil Cytoskeleton.* 64, 822-32.

Cadwallader, A. B. and Yost, H. J. 2006. Combinatorial expression patterns of heparan sulfate sulfotransferases in zebrafish: I. The 3-O-sulfotransferase family. Dev Dyn. 235, 3423-31.

Caron, A., Xu, X. and Lin, X. 2012. Wnt/beta-catenin signaling directly regulates Foxj1 expression and ciliogenesis in zebrafish Kupffer's vesicle. Development. 139, 514-24.

Castleman, V. H., Romio, L., Chodhari, R., Hirst, R. A., de Castro, S. C., Parker, K. A., Ybot-Gonzalez, P., Emes, R. D., Wilson, S. W., Wallis, C. et al. 2009. Mutations in radial spoke

head protein genes RSPH9 and RSPH4A cause primary ciliary dyskinesia with central-microtubular-pair abnormalities. Am J Hum Genet. 84, 197-209.

Chandrasekar, G., Vesterlund, L., Hultenby, K., Tapia-Paez, I. and Kere, J. 2013. The zebrafish orthologue of the dyslexia candidate gene DYX1C1 is essential for cilia growth and function. PLoS One. 8, e63123.

Choksi, S. P., Lauter, G., Swoboda, P. and Roy, S. 2014. Switching on cilia: transcriptional networks regulating ciliogenesis. Development. 141, 1427-41.

Chung, M. I., Peyrot, S. M., LeBoeuf, S., Park, T. J., McGary, K. L., Marcotte, E. M. and Wallingford, J. B. 2012. RFX2 is broadly required for ciliogenesis during vertebrate development. Dev Biol. 363, 155-65.

Clark, K. J., Urban, M. D., Skuster, K. J. and Ekker, S. C. 2011. Transgenic zebrafish using transposable elements. Methods Cell Biol. 104, 137-49.

Cruz, C., Ribes, V., Kutejova, E., Cayuso, J., Lawson, V., Norris, D., Stevens, J., Davey, M., Blight, K., Bangs, F. et al. 2010. Foxj1 regulates floor plate cilia architecture and modifies the response of cells to sonic hedgehog signaling. Development. 137, 4271-82.

Dahlem, T. J., Hoshijima, K., Jurynec, M. J., Gunther, D., Starker, C. G., Locke, A. S., Weis, A. M., Voytas, D. F. and Grunwald, D. J. 2012. Simple methods for generating and detecting locus-specific mutations induced with TALENs in the zebrafish genome. PLoS Genet. 8, e1002861.

Delporte, F. M., Pasque, V., Devos, N., Manfroid, I., Voz, M. L., Motte, P., Biemar, F., Martial, J. A. and Peers, B. 2008. Expression of zebrafish pax6b in pancreas is regulated by two enhancers containing highly conserved cis-elements bound by PDX1, PBX and PREP factors. BMC Dev Biol 8, 53.

Diestra, E., Fontana, J., Guichard, P., Marco, S. and Risco, C. 2009. Visualization of proteins in intact cells with a clonable tag for electron microscopy. J Struct Biol. 165, 157-68.

Dorsky, R. I., Sheldahl, L. C. and Moon, R. T. 2002. A transgenic Lef1/beta-catenin-dependent reporter is expressed in spatially restricted domains throughout zebrafish development. Dev Biol. 241, 229-37.

Drummond, I. 2009. Studying cilia in zebrafish. Methods Cell Biol. 93, 197-217.

El Zein, L., Ait-Lounis, A., Morle, L., Thomas, J., Chhin, B., Spassky, N., Reith, W. and Durand, B. 2009. RFX3 governs growth and beating efficiency of motile cilia in mouse and controls the expression of genes involved in human ciliopathies. J Cell Sci. 122, 3180-9.

England, S., Batista, M. F., Mich, J. K., Chen, J. K. and Lewis, K. E. 2011. Roles of Hedgehog pathway components and retinoic acid signalling in specifying zebrafish ventral spinal cord neurons. Development. 138, 5121-34.

Escalante, A., Murillo, B., Morenilla-Palao, C., Klar, A. and Herrera, E. 2013. Zic2-dependent axon midline avoidance controls the formation of major ipsilateral tracts in the CNS. Neuron. 80, 1392-406.

Foley, J. E., Maeder, M. L., Pearlberg, J., Joung, J. K., Peterson, R. T. and Yeh, J. R. 2009. Targeted mutagenesis in zebrafish using customized zinc-finger nucleases. Nat Protoc. 4, 1855-67.

Fujimi, T. J., Hatayama, M. and Aruga, J. 2012. Xenopus Zic3 controls notochord and organizer development through suppression of the Wnt/beta-catenin signaling pathway. Dev Biol. 361, 220-31.

Garcia-Frigola, C., Carreres, M. I., Vegar, C., Mason, C. and Herrera, E. 2008. Zic2 promotes axonal divergence at the optic chiasm midline by EphB1-dependent and -independent mechanisms. Development. 135, 1833-41.

Gerety, S. S. and Wilkinson, D. G. 2011. Morpholino artifacts provide pitfalls and reveal a novel role for pro-apoptotic genes in hindbrain boundary development. Dev Biol. 350, 279-89.

Guan, J., Ekwurtzel, E., Kvist, U., Hultenby, K. and Yuan, L. 2010. DNAJB13 is a radial spoke protein of mouse '9+2' axoneme. Reprod Domest Anim. 45, 992-6.

Hagenlocher, C., Walentek, P., C, M. L., Thumberger, T. and Feistel, K. 2013. Ciliogenesis and cerebrospinal fluid flow in the developing Xenopus brain are regulated by foxj1. Cilia. 2, 12.

Hatayama, M., Ishiguro, A., Iwayama, Y., Takashima, N., Sakoori, K., Toyota, T., Nozaki, Y., Odaka, Y. S., Yamada, K., Yoshikawa, T. et al. 2011. Zic2 hypomorphic mutant mice as a schizophrenia model and ZIC2 mutations identified in schizophrenia patients. Sci Rep. 1, 16.

Hellman, N. E., Liu, Y., Merkel, E., Austin, C., Le Corre, S., Beier, D. R., Sun, Z., Sharma, N., Yoder, B. K. and Drummond, I. A. 2010. The zebrafish foxj1a transcription factor regulates cilia function in response to injury and epithelial stretch. Proc Natl Acad Sci USA. 107, 18499-504.

Hong, E. and Brewster, R. 2006. N-cadherin is required for the polarized cell behaviors that drive neurulation in the zebrafish. Development. 133, 3895-905.

Huang, P. and Schier, A. F. 2009. Dampened Hedgehog signaling but normal Wnt signaling in zebrafish without cilia. Development. 136, 3089-98.

Hwang, W. Y., Fu, Y., Reyon, D., Maeder, M. L., Tsai, S. Q., Sander, J. D., Peterson, R. T.,

Yeh, J. R. and Joung, J. K. 2013. Efficient genome editing in zebrafish using a CRISPR-Cas system. Nat Biotechnol. 31, 227-9.

Ibanez-Tallon, I., Heintz, N. and Omran, H. 2003. To beat or not to beat: roles of cilia in development and disease. Hum Mol Genet. 12, R27-35.

Inoue, T., Ogawa, M., Mikoshiba, K. and Aruga, J. 2008. Zic deficiency in the cortical marginal zone and meninges results in cortical lamination defects resembling those in type II lissencephaly. J Neurosci. 28, 4712-25.

Knowles, M. R., Ostrowski, L. E., Loges, N. T., Hurd, T., Leigh, M. W., Huang, L., Wolf, W. E., Carson, J. L., Hazucha, M. J., Yin, W. et al. 2013. Mutations in SPAG1 cause primary ciliary dyskinesia associated with defective outer and inner dynein arms. Am J Hum Genet. 93, 711-20.

Knowles, M. R., Ostrowski, L. E., Leigh, M. W., Sears, P. R., Davis, S. D., Wolf, W. E., Hazucha, M. J., Carson, J. L., Olivier, K. N., Sagel, S. D. et al. 2014. Mutations in RSPH1 cause primary ciliary dyskinesia with a unique clinical and ciliary phenotype. Am J Respir Crit Care Med. 189, 707-17.

Kramer-Zucker, A. G., Olale, F., Haycraft, C. J., Yoder, B. K., Schier, A. F. and Drummond, I. A. 2005. Cilia-driven fluid flow in the zebrafish pronephros, brain and Kupffer's vesicle is required for normal organogenesis. Development. 132, 1907-21.

Kwan, K. M., Otsuna, H., Kidokoro, H., Carney, K. R., Saijoh, Y. and Chien, C. B. 2012. A complex choreography of cell movements shapes the vertebrate eye. Development. 139, 359-72.

Langenberg, T., Brand, M. and Cooper, M. S. 2003. Imaging brain development and organogenesis in zebrafish using immobilized embryonic explants. Dev Dyn. 228, 464-74.

Lee, R., Petros, T. J. and Mason, C. A. 2008. Zic2 regulates retinal ganglion cell axon avoidance of ephrinB2 through inducing expression of the guidance receptor EphB1. *J Neurosci.* 28, 5910-9.

Lewis, J. L., Bonner, J., Modrell, M., Ragland, J. W., Moon, R. T., Dorsky, R. I. and Raible, D. W. 2004. Reiterated Wnt signaling during zebrafish neural crest development. Development. 131, 1299-308.

Millimaki, B. B., Sweet, E. M., Dhason, M. S. and Riley, B. B. 2007. Zebrafish atoh1 genes: classic proneural activity in the inner ear and regulation by Fgf and Notch. Development. 134, 295-305.

Narita, K., Kozuka-Hata, H., Nonami, Y., Ao-Kondo, H., Suzuki, T., Nakamura, H., Yamakawa,

K., Oyama, M., Inoue, T. and Takeda, S. 2012. Proteomic analysis of multiple primary cilia reveals a novel mode of ciliary development in mammals. Biol Open. 1, 815-25.

Neugebauer, J. M., Amack, J. D., Peterson, A. G., Bisgrove, B. W. and Yost, H. J. 2009. FGF signalling during embryo development regulates cilia length in diverse epithelia. Nature. 458, 651-4.

Neugebauer, J. M., Cadwallader, A. B., Amack, J. D., Bisgrove, B. W. and Yost, H. J. 2013. Differential roles for 3-OSTs in the regulation of cilia length and motility. Development. 140, 3892-902.

Nonami, Y., Narita, K., Nakamura, H., Inoue, T. and Takeda, S. 2013. Developmental changes in ciliary motility on choroid plexus epithelial cells during the perinatal period. Cytoskeleton (Hoboken). 70, 797-803.

Noren, N. K. and Pasquale, E. B. 2004. Eph receptor-ephrin bidirectional signals that target Ras and Rho proteins. Cell Signal. 16, 655-66.

Nyholm, M. K., Wu, S. F., Dorsky, R. I. and Grinblat, Y. 2007. The zebrafish zic2a-zic5 gene pair acts downstream of canonical Wnt signaling to control cell proliferation in the developing tectum. Development. 134, 735-46.

Nyholm, M. K., Abdelilah-Seyfried, S. and Grinblat, Y. 2009. A novel genetic mechanism regulates dorsolateral hinge-point formation during zebrafish cranial neurulation. J Cell Sci. 122, 2137-48.

Pourebrahim, R., Houtmeyers, R., Ghogomu, S., Janssens, S., Thelie, A., Tran, H. T., Langenberg, T., Vleminckx, K., Bellefroid, E., Cassiman, J. J. et al. 2011. Transcription factor Zic2 inhibits Wnt/beta-catenin protein signaling. J Biol Chem. 286, 37732-40.

Robu, M. E., Larson, J. D., Nasevicius, A., Beiraghi, S., Brenner, C., Farber, S. A. and Ekker, S. C. 2007. p53 activation by knockdown technologies. PLoS Genet. 3, e78.

Sanek, N. A. and Grinblat, Y. 2008. A novel role for zebrafish zic2a during forebrain development. Dev Biol. 317, 325-35.

Sanek, N. A., Taylor, A. A., Nyholm, M. K. and Grinblat, Y. 2009. Zebrafish zic2a patterns the forebrain through modulation of Hedgehog-activated gene expression. Development. 136, 3791-800.

Santiago, A. and Erickson, C. A. 2002. Ephrin-B ligands play a dual role in the control of neural crest cell migration. Development. 129, 3621-32.

Schizophrenia Working Group of the Psychiatric Genomics Consortium. 2014. Biological

insights form 108 schizophrenia-associated loci. Nature. 511, 421-427.

Stubbs, J. L., Oishi, I., Izpisua Belmonte, J. C. and Kintner, C. 2008. The forkhead protein Foxj1 specifies node-like cilia in Xenopus and zebrafish embryos. Nat Genet. 40, 1454-60.

Sullivan-Brown, J., Schottenfeld, J., Okabe, N., Hostetter, C. L., Serluca, F. C., Thiberge, S. Y. and Burdine, R. D. 2008. Zebrafish mutations affecting cilia motility share similar cystic phenotypes and suggest a mechanism of cyst formation that differs from pkd2 morphants. Dev Biol. 314, 261-75.

Supatto, W. and Vermot, J. 2011. From cilia hydrodynamics to zebrafish embryonic development. Curr Top Dev Biol. 95, 33-66.

Szalkowski, C. E., Booker, A. B., Truong, D. T., Threlkeld, S. W., Rosen, G. D. and Fitch, R. H. 2013. Knockdown of the candidate dyslexia susceptibility gene homolog dyx1c1 in rodents: effects on auditory processing, visual attention, and cortical and thalamic anatomy. Dev Neurosci. 35, 50-68.

Teslaa, J. J., Keller, A. N., Nyholm, M. K. and Grinblat, Y. 2013. Zebrafish Zic2a and Zic2b regulate neural crest and craniofacial development. Dev Biol. 380, 73-86.

Thisse, C., and Thisse, B. 2005. High Throughput Expression Analysis of ZF-Models Consortium Clones. ZFIN Direct Data Submission (http://zfin.org)

Tian, T., Zhao, L., Zhao, X., Zhang, M. and Meng, A. 2009. A zebrafish gene trap line expresses GFP recapturing expression pattern of foxj1b. J Genet Genomics. 36, 581-9.

Yu, X., Lau, D., Ng, C. P. and Roy, S. 2011. Cilia-driven fluid flow as an epigenetic cue for otolith biomineralization on sensory hair cells of the inner ear. Development. 138, 487-94.

Yu, X., Ng, C. P., Habacher, H. and Roy, S. 2008. Foxj1 transcription factors are master regulators of the motile ciliogenic program. Nat Genet. 40, 1445-53.

Yuan, S. and Sun, Z. 2013. Expanding horizons: ciliary proteins reach beyond cilia. Annu Rev Genet. 47, 353-76.

Zariwala, M. A., Gee, H. Y., Kurkowiak, M., Al-Mutairi, D. A., Leigh, M. W., Hurd, T. W., Hjeij, R., Dell, S. D., Chaki, M., Dougherty, G. W. et al. 2013. ZMYND10 is mutated in primary ciliary dyskinesia and interacts with LRRC6. Am J Hum Genet. 93, 336-45.

Appendix:

Searching for downstream effectors of *zic* genes

Introduction

The Zic family of zinc finger transcription factors plays a number of important roles during neural development (reviewed in Merzdorf, 2007 and Aruga and Mikoshiba, 2011). The *zic*s are some of the earliest genes expressed in the neural ectoderm, which they help to pattern. They regulate the balance between neural proliferation and differentiation. Finally, Zics are required for the physical reshaping of the neural plate into the neural tube (Nyholm et al., 2009). Although the *zic* genes are transcription factors, and likely exert their influence over tissue specification and morphogenesis via regulation of target gene expression, very few direct targets have been identified. Elucidating downstream effectors of *zic* genes will provide insight into how patterning, proliferation and morphogenesis are coordinated during neural development.

Work in the Grinblat lab has established several critical roles for Zics during segmentation stages. First, the *zic2a-zic5* gene pair promotes proliferation in the developing tectum, downstream of canonical Wnt signaling (Nyholm et al., 2007). Second, Zic2a and Zic5 function together upstream of important cellular aspects neurulation, such as junction integrity and actomyosin contraction at the apical seam of the neural tube (Nyholm et al., 2009). When these Zics are depleted, zebrafish embryos undergo aberrant cranial neurulation and have neural crest defects (TeSlaa et al., 2013). This closely resembles what has been observed in the *Zic2* mouse knockout, which develops with spina bifida and pigment abnormalities that are neural crest in origin (Elms et al., 2003). Much attention is currently focused on understanding the pro-proliferative aspect of Zic function. How Zics control the cellular mechanisms of tissue

morphogenesis remains more mysterious. They may directly regulate the genes responsible for controlling the cytoskeleton or junction integrity, for example Rho kinases or their regulators, or these processes might be much more distal to *zic* genes' primary targets.

A third embryonic function for Zic2a exists in patterning several tissue boundaries. Zic2a is critical for eye morphogenesis and development, restricting expression of several genes at the interface of the retina and optic stalk. Zic2a morphants display forebrain deficits and coloboma (Sanek and Grinblat, 2008; Sanek et al., 2009). This phenotype is reminiscent of both *Zic2* mouse mutants as well as humans, where mutations in *ZIC2* are associated with holoprosencephaly and mild craniofacial dysmorphology (Nagai et al., 2000; Solomon et al., 2010). Additionally, a patterning role at the neural plate border is well established, and disruption of Zic2 or Zic5 function reduces the neural crest domain (Brewster et al., 1998; Inoue et al., 2004; Nakata et al., 2000). However, the specific genetic program Zics drive remains unknown.

Already identified targets offer few insights into the mechanisms by which Zics regulate neural development. Several targets validated in human neuronal cell lines, such as the dopamine receptor D_{1a}, *CamKII*α and *ApoE*, have clear roles in the adult CNS, but their function during embryonic brain development, particularly as early as neurulation, are ill defined (Sakurada et al., 2005; Salero et al., 2001; Yang et al., 2000). Slightly better fleshed out is a role for Zics in maintenance of progenitor state. Zic1 represses the proneural bHLH gene *Atoh1* (or *Math1*) (Ebert et al., 2003). Zic3 directy

activates *Nanog* in ESCs, and Zic3 loss-of-function upregulates gene expression programs associated with neuronal differentiation (Lim et al., 2010; Winata et al., 2013). Zic2 was recently identified as a cofactor of Oct4 that drives embryonic stem cells from naïve to primed pluripotency (Buecker et al., 2014).

Zic genes occupy an interesting nexus during embryonic development, in that they are players in early neural patterning, neuronal proliferation and differentiation, and neural tube morphogenesis. Study of the Zic family therefore offers the possibility of a deeper understanding of how the embryo integrates these three vital processes at a transcriptional level, as it must in order to accomplish the monumental task of achieving the mature adult form. To identify downstream effectors and potentially direct targets of Zic2 and Zic5, we performed a microarray comparing gene expression in control morphant embryos with gene expression in Zic morphant embryos. Here I identify candidate downstream effectors of Zic2a and Zic5, validate their response to Zic2a depletion, and discuss a pitfall of traditional reverse genetic methods in zebrafish.

Materials and Methods

Fish husbandry and embryo manipulations

Adult zebrafish were maintained according to established methods (Westerfield, 2000). Embryos were obtained from natural matings and staged according to Kimmel et al. (1995). Heterozygous *Tg(HS:GFP-Δtcf)* embryos (Lewis et al., 2004) were heat-shocked at 37°C for 30 minutes, then recovered at 28.5°C, sorted for presence of GFP

and fixed for ISH. *Tg(11XUAS:Zic2aYFP)* fish were mated with *Tg(HSP70l:Gal4)* fish and the resulting embryos were heat shocked at bud stage in a 37°C water bath for 1 hour, recovered at room temp, sorted for YFP and fixed for ISH (see Chapter 2). Heat-shocked YFP-negative siblings were used as controls.

MO knockdown and overexpression assays

The following antisense MOs were purchased from GeneTools: *zic2a* and *zic5* splice blocking MOs, *zic2a* translation blocking MO (Nyholm et al., 2007), *rfx4* translation blocking MO (5'-CTCCTCTGAGAAAATGGCTCCGTGC-3'), standard p53MO, standard conMO. MOs were diluted in 1X Danieau buffer (Nasevicius and Ekker, 2000) to 1-2ng/nl (zic2a+5MO), 1-2ng/nl (rfx4MO), and 2-4ng/nl (conMO) and 0.5-1nl was injected at the one-cell stage. p53MO was added at 1.5X the concentration of the specific morpholino to control for nonspecific effects, where noted.

Microarray and data analysis

Single-celled AB-type embryos were injected with either conMO or zic2a+5MO (Nyholm et al., 2007). Embryos were allowed to develop to 16-somites, just before morphants begin to show ventricle defects, at which point embryos were bisected at the level of the otic vesicle and anterior halves were harvested into TriZol for total RNA extraction (Life Technologies). Samples were processed and the microarray performed in the laboratory of Shawn Burgess (NHGRI, Bethesda, MD). cRNA was hybridized to a custom chip containing 34,231 probes representing approximately 19,000 genes.

Those genes altered significantly by at least two fold were identified for further analysis using the DAVID bioinformatics resource (Huang et al., 2009).

Quantitative real-time PCR

RNA was isolated from whole embryos using Trizol (Life Technologies) and cDNA was generated with the High Capacity cDNA archive kit from 1ug of input RNA (Applied Biosystems). Each 20ul reaction contained a final concentration of 0.2uM primers, 1X Power SYBR Green dye and 2ul of a 1:20 dilution of template cDNA. Each biological replicate was loaded as three technical replicates on the plate. Primers in Table 3 were designed using the PrimerExpress software (Applied Biosystems) and tested for efficiency as in Sanek et al., 2009. qPCR was performed on an Applied Biosystems 7500 StepOne Plus machine using the $\Delta\Delta$Ct method.

In situ hybridization and histology

Antisense digoxigenin-labeled RNA probes were transcribed using the MAXIscript kit (Ambion) from the following plasmid or PCR templates: *dkk1b* (Untergasser et al., 2011), *efna2* (a gift from Andrew Waskiewicz), *efna3b* (eu35), *efnb3b* (eu323), *foxj1a* (Hellman et al., 2010), *foxj1b* (Hellman et al., 2010) *nr2e1* and *nr2f5* (Bertrand et al., 2007), *pou3f2b* (eu83), *rsph9* (see Chapter 3), *sfrp1a* (Tendeng and Houart, 2006), *sox19b* (cb174), *tektin1* (Yu et al., 2008). ISH was carried out as previously described (Gillhouse et al., 2004). Stained embryos were embedded in

Eponate 12 (Ted Pella) and 5-7μm sections were cut with a steel blade on an American Optical Company microtome.

In situ probes for three genes were cloned from wild-type cDNA using the following primers:*efhc1* (Forward: 5'-CCT GCC AGG AAA CAC ATT TCG CG-3'; Reverse: 5'-GGG TCC GTG GCG TGT CTG AGT GA-3'), *rfx4* (Forward: 5'-GGG AAC TGA GGA GGG GGA GTC CT-3'; Reverse: 5'-TGG CAG GAG AGT AGG GTC CAG GTG-3'), *wdr16* (5'-AAC TCT GCG TGT GTG GGA AC-3'; Reverse: 5'-CGA TGC CAA CAT GGG TCA CT-3').

Results

Microarray for downstream effectors of the zic transcription factors

The *zic* genes are transcription factors, but very few direct targets have been identified. We performed a microarray analysis on zic2a/zic5 morphants to identify downstream effectors. Of the loci represented on the chip, 242 were identified as altered at least 2-fold, some of which were present on the chip multiple times (Table 1). Of these, 15 gene records have since been discontinued and 37 transcribed loci were not associated with a known gene. We used the online bioinformatics tool DAVID to annotate these genes and sort them into categories based on gene ontology (Fig. 1; Huang et al., 2009). An additional 12 genes did not map to a known DAVID identifier. Of the enriched GO terms, most were associated with either trunk development or cell cycle arrest, which are likely artifacts of the experimental design (see Table 1).

However, genes associated with transcription and DNA binding were significantly overrepresented in morphants, suggesting *zic2a* and *zic5* might regulate the expression of other transcription factors. Additionally, within the list of significantly altered transcripts, there were many encoded by genes that we might expect to find based on what we know about *zic2a* and *zic5* function. These included genes involved in adhesion and cytoskeletal regulation (ephrins), eye development (nuclear receptors), Wnt signaling modulation (*sfrp1a* and *dkk1b*), and neural proliferation (*pou3f2b, pou3f3b, sox19b*). Genes were chosen for further validation by qPCR or *in situ* based on biological relevance, expression pattern, or magnitude of response to Zic depletion (summarized in Table 2). To simplify the system, we confirmed the microarray results for 12 genes by qPCR using knockdown of Zic2a alone (Fig. 2). Since these results largely recapitulated transcript changes observed in double morphants, we continued to use single zic2a morphants when pursuing other interesting genes identified in the microarray.

Ephrins and nuclear hormone receptors: shared expression domains with zics

The microarray showed reduced transcript abundance of three ephrins in Zic-depleted embryos: *efna2*, *efna3b*, and *efnb3b*. Ephrins and their receptors, the Eph tyrosine kinases, are important regulators of a number of aspects of development; most notably cell sorting and boundary maintenance, and axon guidance (reviewed in Pasquale, 2005). Quantitative PCR confirmed the reduction of *efna2* and *efna3b* transcripts in zic2a morphants, but there was no significant change in *efnb3b*

expression (Fig. 2). In control embryos, *efna2* was strongly expressed in the forebrain (FB) – midbrain (MB) boundary, the MB itself, and the mid-hindbrain boundary (MHB). Following Zic2a knockdown, *efna2* expression was reduced in both the FB and MB domains (Fig. 3A,B). Interestingly, expression was more strongly reduced and even ablated in the dorsal MB, where *zic2a* is co-expressed, and less affected in the ventral MB. *Efna3b* was expressed in the MHB as well as the nasal retina. Zic2a depletion reduced expression specifically in the nasal retinal domain while having little effect on the MB domain (Fig.3C,D, see arrowhead). *Efnb3b*, whose expression is distributed more broadly throughout the developing CNS, remained unchanged in zic2a morphants (Fig.3E,F).

Nuclear hormone receptors are a large family of transcription factors that regulate an array of processes in adults as well as some aspects of development. Of these, one of the best studied is *Tlx*, or *nr2e1* in zebrafish, which has important roles in neural stem cells (reviewed in Gui et al., 2011). Many of these nuclear receptors are 'orphans' with unknown ligands, including the three nuclear receptors whose expression was shown by the microarray to be downregulated in zic morphants: *nr2e1*, *nr2f1b* and *nr2f5*. *Nr2e1* is expressed in the zebrafish embryonic FB and tectum. In zic2a morphants, FB expression of *nr2e1* is unaffected, while MB expression is reduced or ablated (Fig. 4A,B). *Nr2f5* is broadly expressed in the CNS, and, surprisingly, its expression domains in the retina and MB appear expanded in response to Zic2a depletion (Fig. 4C,D). *Nr2f1b* transcript levels, although identified in the microarray as reduced, remained

unchanged in zic2a morphants when measured by qPCR and by *in situ* (data not shown).

The Wnt signaling pathway: dkk1b and sfrp1a

Transcript abundance of two members of the Wnt signaling pathway was significantly altered in response to Zic depletion. *Dkk1b* expression was increased in zic morphants while *sfrp1a* expression was decreased, a result confirmed by qPCR (Fig. 2). Both genes were originally identified as Wnt antagonists, although *sfrp1a*'s influence over Wnt signaling has been shown to be context-dependent (reviewed in Bovolenta et al., 2008). By *in situ, dkk1b* expression is activated in many ectopic locations throughout the NT in embryos depleted of Zic2a (Fig. 5A,B). *Sfrp1a* transcript level is strongly reduced in ventral MB and HB domains, both by Zic2a depletion and by global expression of a Zic2aYFP fusion protein (Fig. 5C-F). In embryos with reduced Wnt signaling, *sfrp1a* restriction is lost and its expression domain is expanded into the dorsal NT (Fig. 5G,H).

Transcription factors of the central nervous system: pou3f2b and sox19b

Pou3f2b, broadly expressed in the zebrafish CNS, was identified by the microarray as reduced in zic morphant embryos. It belongs to a large family of POU domain-containing transcription factors that bind a specific octameric DNA sequence. We observed a downregulation of *pou3f2b* in the cranial NT by *in situ* hybridization (Fig. 6A,B). Microarray results also showed decreased *sox19b* transcript abundance in

response to Zic depletion. *Sox19b* is a member of the SoxB1 family of transcription factors, which are important for specifying the neural ectoderm in zebrafish (Okuda et al., 2010). In zebrafish, *sox19b* is expressed in the developing CNS, with exception of the boundary between FB and MB and the MHB. This result was confirmed by *in situ* hybridization, which showed a mild downregulation of *sox19b* in the cranial NT of zic2a morphant embryos (Fig. 6C,D).

In the context of human and mouse melanomas, *Pou3f2* promotes proliferation under the direct control of Wnt/β-catenin signaling via a Tcf/Lef consensus site in its promoter (Goodall et al., 2004). *Sox19b* mediates events downstream of Wnt signaling during neural induction in zebrafish (Shih et al., 2010). Given the interaction of these genes with Wnt signaling, we examined their expression following inhibition of the Wnt/β-catenin pathway in *Tg(HS:GFP-Δtcf)* embryos. At 24S, *pou3f2b* exhibits localized reduced expression in the dorsal MB (Fig. 6E,F), while *sox19b* is slightly reduced throughout the cranial NT (Fig. 6G,H), indicating they may respond to Wnt signaling within the zebrafish neural tube as well.

Zic2a expression in the dorsal neural tube is driven by Wnt signaling and restricted ventrally at the dorsolateral hinge points (DLHPs) of the MB via an unknown mechanism (Nyholm et al., 2009). No gene with a complimentary expression domain restricted ventral to the DLHPs has been identified. Since *sfrp1a*, *pou3f2b* and *sox19b* all appeared to be expressed in the ventral MB at 18S, we examined their expression relative to the DLHPs. *Sfrp1a* is expressed in the ventral MB and its dorsal limit is found at the mature DLHPs (Fig. 7A,B, see arrows). Interestingly, Zic2a depletion greatly

reduces expression of *sfrp1a* ventral to the hinge points (Fig. 7C,D). Although it is difficult to tell in whole mount embryos, we found *pou3f2b* to be restricted to the ventral MB at 18S (Fig. 7E). *Sox19b*, on the other hand, is expressed both dorsal and ventral to developing hinge points (Fig. 7G). Neither *pou3f2b* nor *sox19b* domains in the MB appear significantly affected by Zic2a knockdown on thin sections (Fig. 7F,H).

Transcriptional regulation of ciliogenesis: rfx4

Rfx4 is a winged-helix transcription factor that was identified in the microarray as downregulated in zic morphants. Many members of the *rfx* family regulate both primary and motile ciliogenesis, and *rfx4* has been shown to be particularly important in the vertebrate cranial neural tube (Ashique et al., 2008). Although there is no obvious reduction in *rfx4* expression in zic2a morphants by *in situ* or qPCR (Fig. 8A,B and data not shown), a bilateral diencephalic domain is mispatterned after Zic2a depletion (see arrowheads and insets). Misexpression of a Zic2aYFP fusion protein does cause a decrease in *rfx4* expression throughout the cranial neural tube (Fig. 8C,D). Rfx4 knockdown causes a curved phenotype reminiscent of mutants deficient in Hedgehog signaling and consistent with a role for zebrafish Rfx4 in primary ciliogenesis (Fig. 8E,F). Rfx4 morphant embryos also have smaller ventricles, suggesting a neurulation defect (see insets, Fig. 8E,F).

Motile ciliogenesis and p53-dependent apoptosis: efhc1, rsph9, tektin1 and wdr16.

The motile ciliogenic gene network has been well defined in several zebrafish tissues. We noted that the expression of a number of genes associated with motile cilia was increased in Zic-depleted embryos (Fig. 2). These included *efhc1*, which encodes a microtubule-associated protein that binds alpha-tubulin; *rsph9*, a structural component of 9+2 cilia; *tektin1*, an alpha-helical protein that assembles into rods that associate closely with the ciliary axoneme; and *wdr16*, which is expressed in kinocilia-bearing cells and encodes a protein of unknown function. We generated *in situ* probes for these genes and examined their expression patterns, which in the case of *rsph9* was previously uncharacterized (see Chapter 3). We found them to be expressed in organs bearing motile cilia, including Kupferr's vesicle, the pronephric ducts, the otic vesicle and the floorplate of the neural tube. We also confirmed their upregulation in zic2a morphants, both in their native expression domains, as well as in ectopic locations, particularly the dorsal midbrain (Fig. 9A-H, see arrowheads in D,H).

The upregulation of genes associated with motile cilia in the dorsal brain of zic2a morphants suggested that Zic2a might repress the formation of motile cilia in the dorsal brain. To look more closely at this possibility, we examined expression of *foxj1a* and *foxj1b*, two transcription factors sufficient for driving motile ciliogenesis in zebrafish. Zic2a depletion has no effect on *foxj1a* expression (Fig. 10A,B), but causes ectopic expression of *foxj1b* in the dorsal MB and elsewhere in the NT (Fig. 10D,E), similar to the other cilia genes characterized in zic2a morphants, such as *rsph9* (Fig. 10G,H). This effect, however, was rescued by the concomitant knockdown of p53, which inhibits the p53-dependent apoptotic pathway (Fig. 10C,F,I). This is a frequent source of

nonspecific morpholino toxicity in zebrafish, and activation of this pathway has been reported in the community (although not yet published) to be associated with *de novo* generation of motile cilia (Robu et al., 2007). Although it appears that the ectopic expression of motile cilia genes in the dorsal NT is therefore not a specific response to Zic2a knockdown, there are a few further pieces of data that muddy the waters. First, Zic2a knockdown with a second, non-overlapping MO produces an identical effect on *foxj1b* and *rsph9* expression (Fig. 10, see insets). Although observation of the same phenotype with two or more MOs is considered a standard test of specificity, ectopic expression is again ablated by p53MO co-injection. Second, global expression of a Zic2aYFP fusion protein ablates expression of *rsph9* and *foxj1b* in the cranial neural tube and greatly reduces expression of *foxj1a* and *foxj1b* in the spinal cord (Fig. 11A-H). This is not necessarily an expected result if ectopic expression of motile cilia-associated genes were caused by nonspecific activation of pro-apoptotic genes downstream of p53.

Conclusions and Future Directions

Here we report the results of a microarray designed to identify a list of candidates for proximal downstream effectors of the transcription factors Zic2a and Zic5. Several inadequacies of the experimental design were brought home by analysis of the list of significantly altered transcripts. First, potential targets were enriched for transcripts expressed in the trunk, rudimentary heart, and yolk syncytial layer (Table 1). This is likely an artifact resulting from the dissection of the embryos. Zic morphants tend to be

smaller than controls, and likely carried more post-otic tissue with them when dissected. Second, genes involved in cell death were also enriched among potential targets. As mentioned previously, morpholinos can cause non-specific, p53-dependent apoptosis. This result is still surprising, as none of the phenotypes attributed to Zic2a/Zic5 knockdown and published by the Grinblat lab are p53-dependent (Nyholm et al., 2007; Sanek and Grinblat, 2008). Zic morphant-enriched GO terms encompassed trunk musculature and somite development, along with cell cycle arrest, further highlighting the flaws inherent in the experimental design.

However, there were several promising aspects of the microarray. First, transcripts of the eye and neural tube were enriched among potential targets. Second, we identified one of the known targets of Zic2a, *apoea*, as increased by four-fold in zic2a morphants. This result was confirmed by qPCR (Fig. 2). The repressive relationship suggested by our zebrafish data is in contrast to a human glioblastoma cell line, where Zic2 binds the proximal promoter and activates *APOE* transcription (Salero et al., 2001). Finally, a microarray for downstream effectors of Zic1 identified *aqp3b* as upregulated in response to Zic1 depletion in *Xenopus*, while in this microarray, *aqp12* transcript levels are increased in zic morphants (Cornish et al., 2009).

If it were desirable to pursue any candidate effectors identified by this microarray further, it would make sense to pick those with transcripts enriched in tissues where *zic2a* is also expressed. For example, there was a relatively rich list of differentially regulated transcripts expressed in the retina and optic tectum, two tissues where Zic2a plays an important role (Table 1). It may also be possible to screen candidate targets

by searching for promoters with the Zic binding site identified by Salero et al. in the *apoea* proximal promoter.

There are a few other genes that might be worth pursuing now that we have zic mutants in hand (see Chapter 4). *Rdh12* is a member of the retinoic acid signaling pathway, which is known to interact with *zic* genes and was upregulated on the microarray (Drummond et al., 2013; Maurus and Harris, 2009). The si:ch211-89f7.1 locus, a homolog of mammalian *SEC14L2*, and *snx14* are both part of the secretory pathway, and were increased in zic morphants. These genes are interesting candidates for mediating the Zic2a/Zic5 role in regulating midbrain apical organization and neural crest delamination. Work done on another zinc finger transcription factor of the CNS, *ovo1*, showed that its knockdown results in a neural crest retention phenotype very similar to that observed in zic morphants. A microarray for targets further revealed that *ovo1* regulates genes in the secretory pathway, and thereby affects protein trafficking to the membrane (Piloto and Schilling, 2010). If they regulate genes important for vesicle trafficking, Zics could similarly affect trafficking of junction components or regulators of the cytoskeleton to the apical surface of the neural tube.

Wnt signaling

There is ample evidence that Zics interact with canonical Wnt signaling. Work in the Grinblat lab has demonstrated that *zic2a* is likely a direct target of Wnt signaling, while work in other labs has shown that Zic2 interacts with Tcf/Lef factors to inhibit Wnt signaling (Fujimi et al., 2011; Nyholm et al., 2007; Pourebrahim et al., 2011). We

showed that both Zic2a knockdown and overexpression reduce *sfrp1a* expression in the ventral midbrain. Although this relationship is likely not direct, *sfrp1a* is the first gene we have identified whose ventral restriction by the dorsolateral hinge points mirrors *zic2a*'s dorsal restriction. *Sfrp1* was originally reported as a Wnt antagonist, but recent data indicates it can act to potentiate or repress Wnt signaling depending on the context (Esteve et al., 2011; Holly et al., 2014). It will be interesting to determine in the future if *sfrp1a* is also required for DLHP bending, as Zic2a is, and whether Wnt signaling has a role in this process.

Cell proliferation and differentiation

We demonstrated that *pou3f2b* and *sox19b* expression is mildly reduced in response to Zic2a knockdown. *Pou3f2b*, in particular, is expressed in a ventral MB domain at 18S that nicely complements that of *zic2a* in the dorsal MB. Again, it is unlikely that Zics directly activate *pou3f2b* or *sox19b*, since they are not expressed in the same domains. Rather, it is likely that Zic proteins play a role in regulating the balance between proliferation and differentiation in the neural progenitor population, and when that balance is disrupted, so is the expression of other genes involved in maintenance of progenitor state, such as *pou3f2b* and *sox19b*.

In human cell lines, SoxB1 proteins (of which Sox19b is a member) act in concert with other transcription factors to regulate various cell states in populations of embryonic stem cells and neural progenitors. Members of the class III POU transcription factor family frequently interact with SoxB1 proteins, and specific interactions are specific to

different populations of pluripotent cells within the developing embryo. In neural progenitor cells, Pou3f2 (or Brn1.2) is the main interacting partner of Sox2, and together they bind distal enhancer regions to promote expression of genes important for neural progenitor cell identity (Lodato et al., 2013). In zebrafish, the *soxB1* genes regulate expression of genes associated with a number of different signaling pathways, including RA and Nodal signaling, and also maintain expression of repressor-type bHLH genes that maintain the progenitor stage. Collectively, Zics, POU domain transcription factors, and SoxB1 proteins are similarly positioned to integrate cell fate decisions with patterning and morphogenesis in the developing embryo.

A group of genes that are co-expressed with *zic2a* and make excellent sense as potential downstream effectors are the nuclear hormone receptors *nr2e1*, *nr2f1b*, and *nr2f5*. These genes are involved in two aspects of neural development that correlate well with Zic2a function. First, we showed that *nr2e1* expression is ablated in the dorsal midbrain domain of zic2a morphants. *Nr2e1* is important for maintenance of self-renewing neural stem cells in adult mice, and regulates cell-cycle progression in embryonic mouse brain (Shi et al., 2003; Zhao et al., 2009). Second, all three of these nuclear receptor genes are expressed in various subdomains of the forebrain and developing eye. In eye-specific *Nr2f1*;*Nr2f2* knockout mice, the neural progenitors of the eye fail to differentiate as they should, ultimately compromising the morphogenesis of the optic vesicle and leading to coloboma, among other things (Tang et al., 2010). It will be interesting to see if *nr2f1b* or any of the other nuclear receptor genes mentioned lie downstream of the requirement for Zic2a during eye development.

Cilia, morpholinos and apoptosis – a cautionary tale

Analysis of *rfx4*, a transcriptional regulator of ciliogenesis, showed that although globally unchanged in zic2a morphants, a specific bilateral diencephalic domain of expression was mispatterned. Unpublished data from the lab shows that *rfx4* shares this expression domain with *rsph9* and *zic2a*. This suggests these FB cells are ciliated, although it is unclear what tissue arises from this domain and what its function might be. *Rfx4* is required for development of the subcommissural organ and modulates Hh signaling in the ventral neural epithelium via its regulation of primary ciliogenesis (Ashique et al., 2009; Blackshear et al., 2003). Preliminary evidence from rfx4 morphants confirmed that this role is preserved in zebrafish embryos, which display axis curvature defects reminiscent of Hh pathway mutants in response to Rfx4 knockdown.

Although well defined in other zebrafish tissues, including the caudal neural tube, the expression program associated with motile ciliogenesis in the cranial neural tube remains unstudied. It was therefore of great interest when we noted the upregulation of a number of genes associated with motile cilia in Zic-depleted embryos. These motile cilia genes were ectopically expressed in the dorsal brains of zic2a morphants, leading us to hypothesize that they are normally repressed by Zic2a. However, subsequent co-injection of a p53 morpholino revealed that the upregulated of the motile ciliogenic gene program was likely nonspecific.

There is some evidence that motile ciliogenesis is a generalized response to injury in organs with fluid flow. Hellman et al., 2010 demonstrated that *foxj1a* is

upregulated after mechanical obstruction of the kidney, only in the tubule upstream of the blockage (i.e. in response to ‘epithelial stretch’ specifically). Injury to the spinal cord caused similarly increased foxj1a expression, leading to ectopic motile cilia. If this were also the case in the cranial neural tube, it would be interesting to determine whether motile cilia respond to the epithelial stretch caused by ventricle overinflation in a zebrafish hydrocephalus model. Such a mechanism would have important implications for disease progression in humans.

References

Aruga, J. and Mikoshiba, K. 2011. Role of BMP, FGF, calcium signaling, and Zic proteins in vertebrate neuroectodermal differentiation. Neurochem Res. 36, 1286-92.

Ashique, A. M., Choe, Y., Karlen, M., May, S. R., Phamluong, K., Solloway, M. J., Ericson, J. and Peterson, A. S. 2009. The Rfx4 transcription factor modulates Shh signaling by regional control of ciliogenesis. Sci Signal. 2, ra70.

Bertrand, S., Thisse, B., Tavares, R., Sachs, L., Chaumot, A., Bardet, P. L., Escriva, H., Duffraisse, M., Marchand, O., Safi, R. et al. 2007. Unexpected novel relational links uncovered by extensive developmental profiling of nuclear receptor expression. PLoS Genet. 3, e188.

Blackshear, P. J., Graves, J. P., Stumpo, D. J., Cobos, I., Rubenstein, J. L. and Zeldin, D. C. 2003. Graded phenotypic response to partial and complete deficiency of a brain-specific transcript variant of the winged helix transcription factor RFX4. Development. 130, 4539-52.

Bovolenta, P., Esteve, P., Ruiz, J. M., Cisneros, E. and Lopez-Rios, J. 2008. Beyond Wnt inhibition: new functions of secreted Frizzled-related proteins in development and disease. J Cell Sci. 121, 737-46.

Brewster, R., Lee, J. and Ruiz i Altaba, A. 1998. Gli/Zic factors pattern the neural plate by defining domains of cell differentiation. Nature. 393, 579-83.

Buecker, C., Srinivasan, R., Wu, Z., Calo, E., Acampora, D., Faial, T., Simeone, A., Tan, M., Swigut, T. and Wysocka, J. 2014. Reorganization of enhancer patterns in transition from naive to primed pluripotency. Cell Stem Cell. 14, 838-53.

Cornish, E. J., Hassan, S. M., Martin, J. D., Li, S. and Merzdorf, C. S. 2009. A microarray screen for direct targets of Zic1 identifies an aquaporin gene, aqp-3b, expressed in the neural folds. Dev Dyn. 238, 1179-94.

Drummond, D. L., Cheng, C. S., Selland, L. G., Hocking, J. C., Prichard, L. B. and Waskiewicz, A. J. 2013. The role of Zic transcription factors in regulating hindbrain retinoic acid signaling. BMC Dev Biol. 13, 31.

Ebert, P. J., Timmer, J. R., Nakada, Y., Helms, A. W., Parab, P. B., Liu, Y., Hunsaker, T. L. and Johnson, J. E. 2003. Zic1 represses Math1 expression via interactions with the Math1 enhancer and modulation of Math1 autoregulation. Development. 130, 1949-59.

Elms, P., Siggers, P., Napper, D., Greenfield, A. and Arkell, R. 2003. Zic2 is required for neural crest formation and hindbrain patterning during mouse development. Dev Biol. 264, 391-406.

Esteve, P., Sandonis, A., Ibanez, C., Shimono, A., Guerrero, I. and Bovolenta, P. 2011.

Secreted frizzled-related proteins are required for Wnt/beta-catenin signalling activation in the vertebrate optic cup. Development. 138, 4179-84.

Fujimi, T. J., Hatayama, M. and Aruga, J. 2012. Xenopus Zic3 controls notochord and organizer development through suppression of the Wnt/beta-catenin signaling pathway. Dev Biol. 361, 220-31.

Gillhouse, M., Wagner Nyholm, M., Hikasa, H., Sokol, S. Y. and Grinblat, Y. 2004. Two Frodo/Dapper homologs are expressed in the developing brain and mesoderm of zebrafish. Dev Dyn. 230, 403-9.

Goodall, J., Martinozzi, S., Dexter, T. J., Champeval, D., Carreira, S., Larue, L. and Goding, C. R. 2004. Brn-2 expression controls melanoma proliferation and is directly regulated by beta-catenin. Mol Cell Biol. 24, 2915-22.

Gui, H., Li, M. L. and Tsai, C. C. 2011. A tale of tailless. Dev Neurosci. 33, 1-13.

Hellman, N. E., Liu, Y., Merkel, E., Austin, C., Le Corre, S., Beier, D. R., Sun, Z., Sharma, N., Yoder, B. K. and Drummond, I. A. 2010. The zebrafish foxj1a transcription factor regulates cilia function in response to injury and epithelial stretch. Proc Natl Acad Sci USA. 107, 18499-504.

Holly, V. L., Widen, S. A., Famulski, J. K. and Waskiewicz, A. J. 2014. Sfrp1a and Sfrp5 function as positive regulators of Wnt and BMP signaling during early retinal development. Dev Biol. 388, 192-204.

Huang da, W., Sherman, B. T. and Lempicki, R. A. 2009. Systematic and integrative analysis of large gene lists using DAVID bioinformatics resources. Nat Protoc. 4, 44-57.

Inoue, T., Hatayama, M., Tohmonda, T., Itohara, S., Aruga, J. and Mikoshiba, K. 2004. Mouse Zic5 deficiency results in neural tube defects and hypoplasia of cephalic neural crest derivatives. Dev Biol. 270, 146-62.

Kimmel, C. B., Ballard, W. W., Kimmel, S. R., Ullmann, B. and Schilling, T. F. 1995. Stages of embryonic development of the zebrafish. Dev Dyn. 203, 253-310.

Lewis, J. L., Bonner, J., Modrell, M., Ragland, J. W., Moon, R. T., Dorsky, R. I. and Raible, D. W. 2004. Reiterated Wnt signaling during zebrafish neural crest development. Development. 131, 1299-308.

Lim, L. S., Hong, F. H., Kunarso, G. and Stanton, L. W. 2010. The pluripotency regulator Zic3 is a direct activator of the Nanog promoter in ESCs. Stem Cells. 28, 1961-9.

Lodato, M. A., Ng, C. W., Wamstad, J. A., Cheng, A. W., Thai, K. K., Fraenkel, E., Jaenisch, R. and Boyer, L. A. 2013. SOX2 co-occupies distal enhancer elements with distinct POU factors

in ESCs and NPCs to specify cell state. PLoS Genet. 9, e1003288.

Maurus, D. and Harris, W. A. 2009. Zic-associated holoprosencephaly: zebrafish Zic1 controls midline formation and forebrain patterning by regulating Nodal, Hedgehog, and retinoic acid signaling. Genes Dev. 23, 1461-73.

Merzdorf, C. S. 2007. Emerging roles for zic genes in early development Dev Dyn. 236, 922-40.

Nagai, T., Aruga, J., Minowa, O., Sugimoto, T., Ohno, Y., Noda, T. and Mikoshiba, K. 2000. Zic2 regulates the kinetics of neurulation. Proc Natl Acad Sci USA. 97, 1618-23.

Nakata, K., Koyabu, Y., Aruga, J. and Mikoshiba, K. 2000. A novel member of the Xenopus Zic family, Zic5, mediates neural crest development. Mech Dev. 99, 83-91.

Nasevicius, A. and Ekker, S. C. 2000. Effective targeted gene 'knockdown' in zebrafish. Nat Genet. 26, 216-20.

Nyholm, M. K., Abdelilah-Seyfried, S. and Grinblat, Y. 2009. A novel genetic mechanism regulates dorsolateral hinge-point formation during zebrafish cranial neurulation. J Cell Sci. 122, 2137-48.

Nyholm, M. K., Wu, S. F., Dorsky, R. I. and Grinblat, Y. 2007. The zebrafish zic2a-zic5 gene pair acts downstream of canonical Wnt signaling to control cell proliferation in the developing tectum. Development. 134, 735-46.

Okuda, Y., Ogura, E., Kondoh, H. and Kamachi, Y. 2010. B1 SOX coordinate cell specification with patterning and morphogenesis in the early zebrafish embryo. PLoS Genet. 6, e1000936.

Pasquale, E. B. 2005. Eph receptor signalling casts a wide net on cell behaviour. Nat Rev Mol Cell Biol. 6, 462-75.

Piloto, S. and Schilling, T. F. 2010. Ovo1 links Wnt signaling with N-cadherin localization during neural crest migration. Development. 137, 1981-90.

Pourebrahim, R., Houtmeyers, R., Ghogomu, S., Janssens, S., Thelie, A., Tran, H. T., Langenberg, T., Vleminckx, K., Bellefroid, E., Cassiman, J. J. et al. 2011. Transcription factor Zic2 inhibits Wnt/beta-catenin protein signaling. J Biol Chem. 286, 37732-40.

Robu, M. E., Larson, J. D., Nasevicius, A., Beiraghi, S., Brenner, C., Farber, S. A. and Ekker, S. C. 2007. p53 activation by knockdown technologies. PLoS Genet. 3, e78.

Sakurada, T., Mima, K., Kurisaki, A., Sugino, H. and Yamauchi, T. 2005. Neuronal cell type-specific promoter of the alpha CaM kinase II gene is activated by Zic2, a Zic family zinc finger

protein. Neurosci Res. 53, 323-30.

Salero, E., Perez-Sen, R., Aruga, J., Gimenez, C. and Zafra, F. 2001. Transcription factors Zic1 and Zic2 bind and transactivate the apolipoprotein E gene promoter. J Biol Chem. 276, 1881-8.

Sanek, N. A. and Grinblat, Y. 2008. A novel role for zebrafish zic2a during forebrain development. Dev Biol. 317, 325-35.

Sanek, N. A., Taylor, A. A., Nyholm, M. K. and Grinblat, Y. 2009. Zebrafish zic2a patterns the forebrain through modulation of Hedgehog-activated gene expression. Development. 136, 3791-800.

Shi, Y., Chichung Lie, D., Taupin, P., Nakashima, K., Ray, J., Yu, R. T., Gage, F. H. and Evans, R. M. 2004. Expression and function of orphan nuclear receptor TLX in adult neural stem cells. Nature. 427, 78-83.

Shih, Y. H., Kuo, C. L., Hirst, C. S., Dee, C. T., Liu, Y. R., Laghari, Z. A. and Scotting, P. J. 2010. SoxB1 transcription factors restrict organizer gene expression by repressing multiple events downstream of Wnt signaling. Development. 137, 2671-81.

Solomon, B. D., Lacbawan, F., Mercier, S., Clegg, N. J., Delgado, M. R., Rosenbaum, K., Dubourg, C., David, V., Olney, A. H., Wehner, L. E. et al. 2010. Mutations in ZIC2 in human holoprosencephaly: description of a novel ZIC2 specific phenotype and comprehensive analysis of 157 individuals. J Med Genet. 47, 513-24.

Tang, K., Xie, X., Park, J. I., Jamrich, M., Tsai, S. and Tsai, M. J. 2010. COUP-TFs regulate eye development by controlling factors essential for optic vesicle morphogenesis. Development. 137, 725-34.

Tendeng, C. and Houart, C. 2006. Cloning and embryonic expression of five distinct sfrp genes in the zebrafish Danio rerio. Gene Expr Patterns. 6, 761-71.

Teslaa, J. J., Keller, A. N., Nyholm, M. K. and Grinblat, Y. 2013. Zebrafish Zic2a and Zic2b regulate neural crest and craniofacial development. Dev Biol. 380, 73-86.

Untergasser, G., Martowicz, A., Hermann, M., Tochterle, S. and Meyer, D. 2011. Distinct expression patterns of dickkopf genes during late embryonic development of Danio rerio. Gene Expr Patterns. 11, 491-500.

Westerfield, M. 2000. The zebrafish book. A guide for the laboratory use of zebrafish (Danio rerio). 4th ed., Univ. of Oregon Press, Eugene.

Winata, C. L., Kondrychyn, I., Kumar, V., Srinivasan, K. G., Orlov, Y., Ravishankar, A.,

Prabhakar, S., Stanton, L. W., Korzh, V. and Mathavan, S. 2013. Genome wide analysis reveals Zic3 interaction with distal regulatory elements of stage specific developmental genes in zebrafish. PLoS Genet. 9, e1003852.

Yang, Y., Hwang, C. K., Junn, E., Lee, G. and Mouradian, M. M. 2000. ZIC2 and Sp3 repress Sp1-induced activation of the human D1A dopamine receptor gene. J Biol Chem. 275, 38863-9.

Yu, X., Ng, C. P., Habacher, H. and Roy, S. 2008. Foxj1 transcription factors are master regulators of the motile ciliogenic program. Nat Genet. 40, 1445-53.

Zhao, C., Sun, G., Li, S. and Shi, Y. 2009. A feedback regulatory loop involving microRNA-9 and nuclear receptor TLX in neural stem cell fate determination. Nat Struct Mol Biol. 16, 365-71.

Figures

Table 1. Significantly altered transcripts. See Excel file. Sheet 1: List of genes significantly altered at least two-fold. Sheet 2: GO terms and ZFIN anatomy terms enriched in zic morphants. Sheet 3: Clusters of related annotation terms significantly enriched in zic morphants.

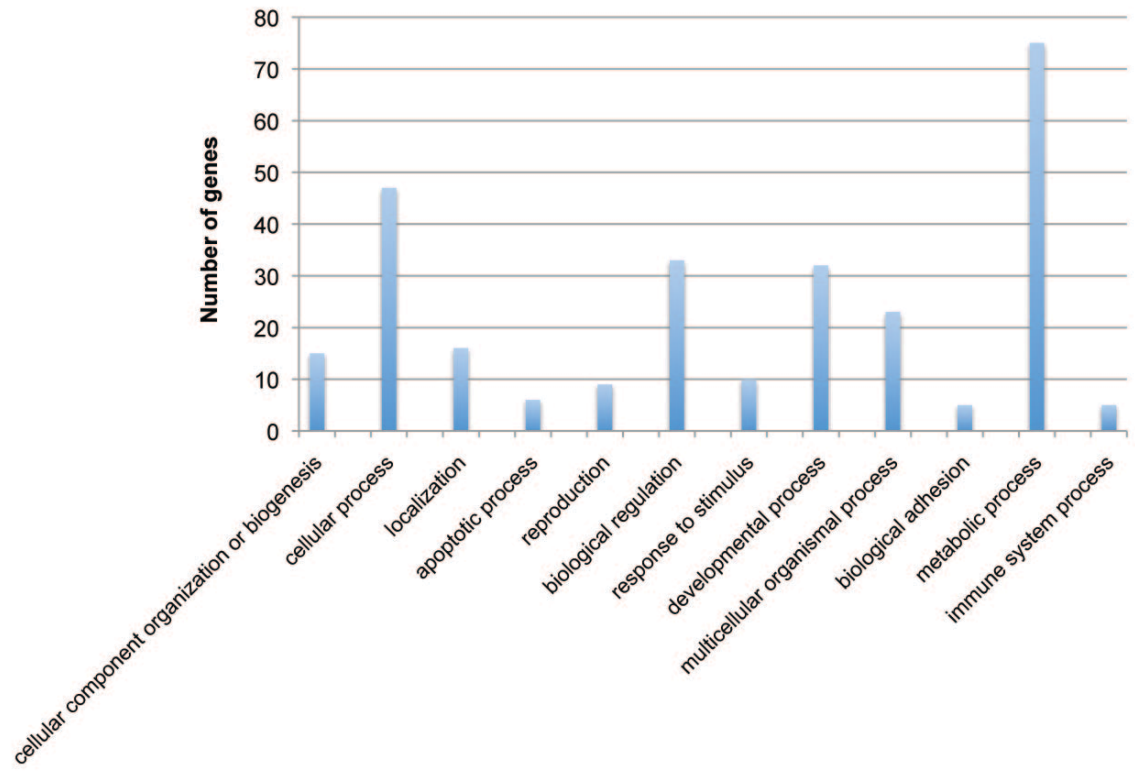

Figure 1. Distribution of significantly altered genes based on gene ontology terms.

Gene	Fold change on microarray	Fold change by q-RT-PCR	Biological replicates	p-value	Change in expression by in situ	Biological replicates	Stage	Probe	Reason for validation
apoea*	4	1.98	3	p<0.05	-	-	-	-	Known target
arpc5b	1.98	2.1	1	-	-	-	-	-	Cytoskeleton
ctsc	2.94	1.71	1	-	-	-	-	-	Altered more than 3-fold
dkk1b*	2.57	1.98	2	p<0.02	7/7 upregulated	1	18S	Dorsky	Wnt signaling
efhc1*	2.1	2.61	2	p<0.04	35/39 upregulated	2	18-21S	JT	Cilia
lgmn	2.25	1.51	1	-	-	-	-	-	Available primers
mmp13a	2.29	1.84	1	-	-	-	-	-	Available primers
mpp1	2.86	-	-	-	3/5 upregulated	1	25S	ZIRC	Available probe
mtp	2.12	1.55	1	-	-	-	-	-	Heart relevance
necap1*	2.5	2.17	2	p<0.02	-	-	-	-	Vesicle trafficking
raf1a	2.27	1.38	1	-	-	-	-	-	Heart relevance
rasd1	3.68	1.26 and 2.68	2	Not sig	-	-	-	-	Altered more than 3-fold
rdh12*	3.08	2.4	2	p<0.01	-	-	-	-	Altered more than 3-fold/RA signaling
rsph9*	2.03	2.57	2	p<0.05	89/104 ectopic upregulation	5	21-23S	MN/MS	Cilia
snx11l	2.02	3.83 and 1.63	2	Not sig	-	-	-	-	Vesicle trafficking
tektin1*	2.52	-	-	-	23/40 upregulated	2	18S	Roy	Clia
wdr16*	3	3.31 and 1.35	2	Not sig	15/39 upregulated	2	21-22S	MZ	Altered more than 3-fold/cilia

Gene	Fold change on microarray	Fold change by q-RT-PCR	Biological replicates	p-value	Change in expression by in situ	Biological replicates	Stage	Probe	Reason for validation
aspm	0.35	0.46	1	-	-	-	-	-	Cytoskeleton
efna2*	0.45	0.05 and 0.19	2	Not sig	15/25 reduced in FB/MB	2	18-20S	Waskiewicz	Midbrain expression/adhesion
efna3b*	0.51	0.32	2	p<0.02	16/17 reduced in retina	2	18S	ZIRC genomic primers	Midbrain expression/adhesion
gap43	0.52	0.43	1	-	7/21 reduced in MB/HB	1	27S	Udvadia	Neural crest
gch2*	0.47	-	-	-	15/20 reduced	3	18S and 24hpf	ZIRC genomic primers	Neural crest
mpz	0.39	-	-	-	4/11 reduced; 10/11 HB mispatterned	1	20-21S	Halpern	Altered more than 3-fold/midbrain expression
nr2e1*	0.518	0.49, 0.77 and 1.1	3	Not sig	9/9 reduced	1	18S	Thisse	Midbrain expression
nr2f1b	0.357	0.32, 0.71 and 0.97	3	Not sig	-	-	-	Thisse	Midbrain expression
nr2f5	0.357	No change	-	-	5/6 upregulated	1	19S	Thisse	Midbrain expression
pbp	0.465	0.48, 0.69	2	Not sig	-	-	-	-	Heart relevance
pou3f2b*	0.545	-	-	-	19/19 reduced	2	18S	ZIRC genomic primers	Midbrain expression
rfx4	0.475	0.57	1	-	42/47 FB domains mispatterned	2	18S and 24hpf	JT	Cilia/midbrain expression
sfrp1a*	0.345	0.47	2	p<0.05	11/17 reduced	1	18S	Houart	Wnt signaling/midbrain expression
sox19b*	0.525	0.59	1	-	5/10 reduced	2	18S	ZIRC	Midbrain expression
stmn1a*	0.545	-	-	-	9/9 reduced	1	18S	ZIRC	Cytoskeleton

Table 2. List of validated genes

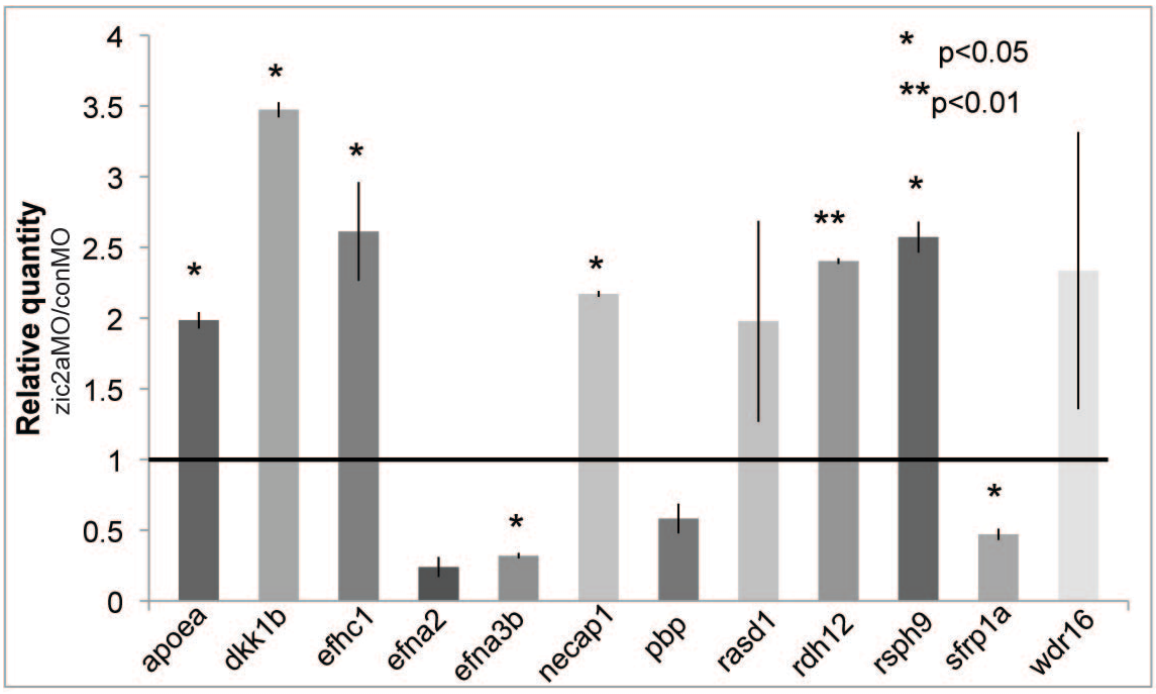

Figure 2. qPCR validation of microarray. Relative quantity of each transcript in zic2a morphants as compared to control morphants, averaged over at least two independent experiments. Significance is shown when it holds across multiple experiments, but differences in gene expression for the transcripts shown were always significant within the individual experiments.

Gene Name	Primer sequence (5'-3')
apoea sense	AGC TGA GGA AAT GAG GGA CAA C
apoea antisense	TGC TGT CAG AGA TCA GTG TGT CTA AT
ef1α sense	CTT CTC AGG CTG ACT GTG C
ef1α antisense	CCG CTA GCA TTA CCC TCC
dkk1b sense	GCA GCA ATG GTG TTT GCA TT
dkk1b antisense	CGA TGG ACA CGA ACT CTT CCA
efhc1 sense	GAA CAC ACA CTC TCT TCA CTC AGA CA
efhc1 antisense	CAG CTT CAT CAC ACT CTG GAT GTA
efna2 sense	TCG GAG AAG TTT CAG CTC TTC AC
efna2 antisense	GGG ATG AGG AGA GGA GAT GTA ATA AT
efna3b sense	CGG AGC TGC CTG AGA TTA AGA
efna3b antisense	GGC TGA GGC TCA TCA TCT GAA
necap1 sense	TTC TAA TAC GGT GGT TCA GTC CAA
necap1 antisense	GAA GCA GGA ACA GAG CTT GCA
pbp sense	GCT GGC CAT GAC TGA TCC A
pbp antisense	GAT GCC ATT CCC GAA ATT TG
rasd1 sense	ATC AGC TGG ATA TTT TGG ATA CTT CA
rasd1 antisense	CAC ATC ACC GGT CAG AAT GG
rdh12 sense	GGC GCT CAG ACC TCC ATC TA
rdh12 antisense	CGC AGT CAC TGA AAT GTT TGC
rsph9 sense	CCA CGT GGT GCA TTC ATC AA
rsph9 antisense	GGA TGA AGG CCT CCA AAG CT
sfrp1a sense	AAT GAA AAT GGA TGT GAT TCT GGA T
sfrp1a antisense	CCC GCT TGA CCT CTT GGA
wdr16 sense	GTG GCA CTG ACA GAA AGA TTG G
wdr16 antisense	AGC CCT CAA GTT CTC TGA TTG C

Table 3. List of qPCR primers.

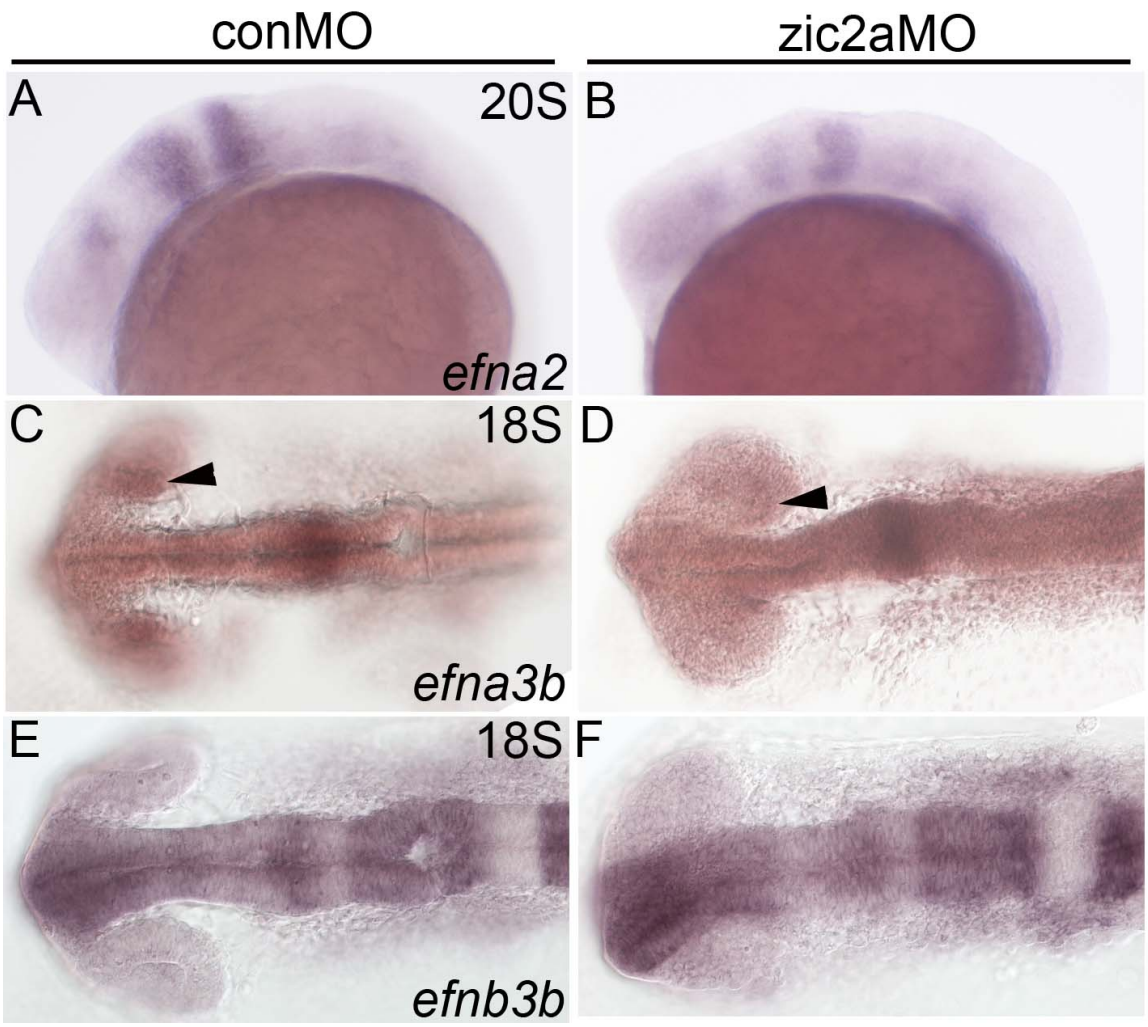

Figure 3. Expression of ephrin genes validated by *in situ* in zic2a morphants.

(A,B) Expression of *efna2* is reduced in the dorsal midbrain following Zic2a depletion (15/23, 2 exp.). (C,D) Expression of *efna3b* is reduced in the nasal retinal domain of zic2a morphants (16/17, 2 exp., see arrowheads). (E,F) Neural tube expression of *efnb3b* remains unchanged in zic2a morphants by *in situ* (6/6 embryos, 1 exp.). A,B are lateral views, C-F are dorsal views with anterior to the left.

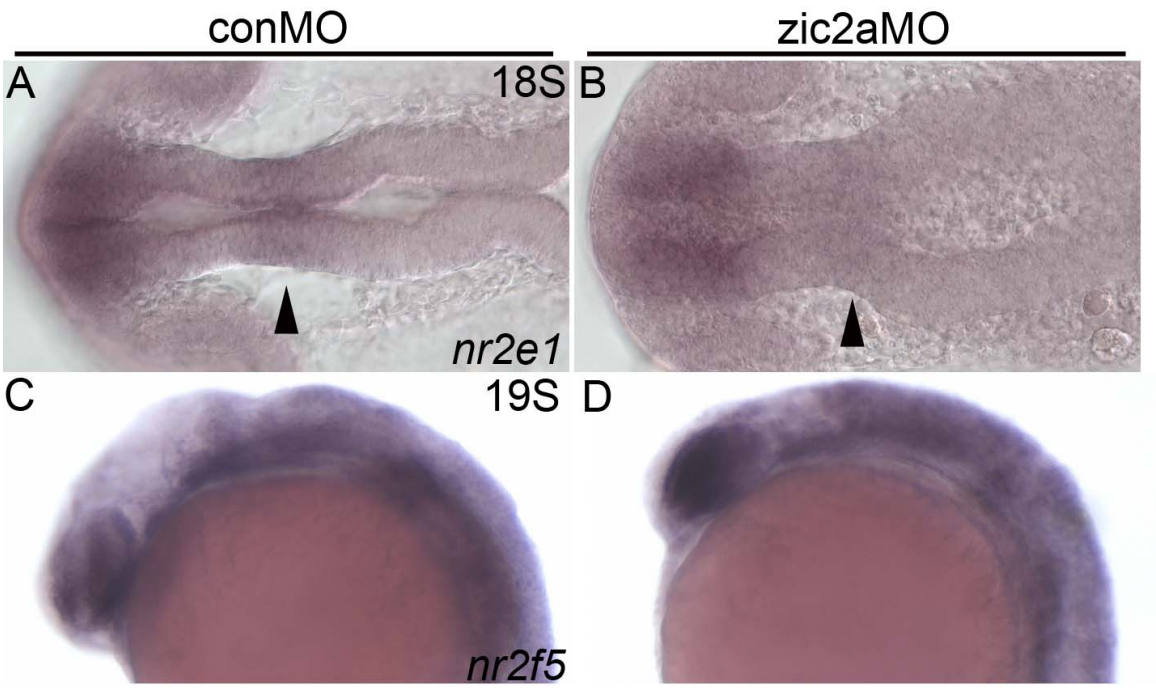

Figure 4. Expression of nuclear receptor genes in zic2a morphants. (A,B) Expression in the midbrain domain of *nr2e1* is reduced (2/9) or ablated (7/9, 2 exp.) in embryos depleted of Zic2a (see arrowheads). (C,D) *Nr2f5* expression is upregulated in the neural tube of zic2a morphants (5/6, 1 exp). A,B are dorsal views, C,D are lateral views with anterior to the left.

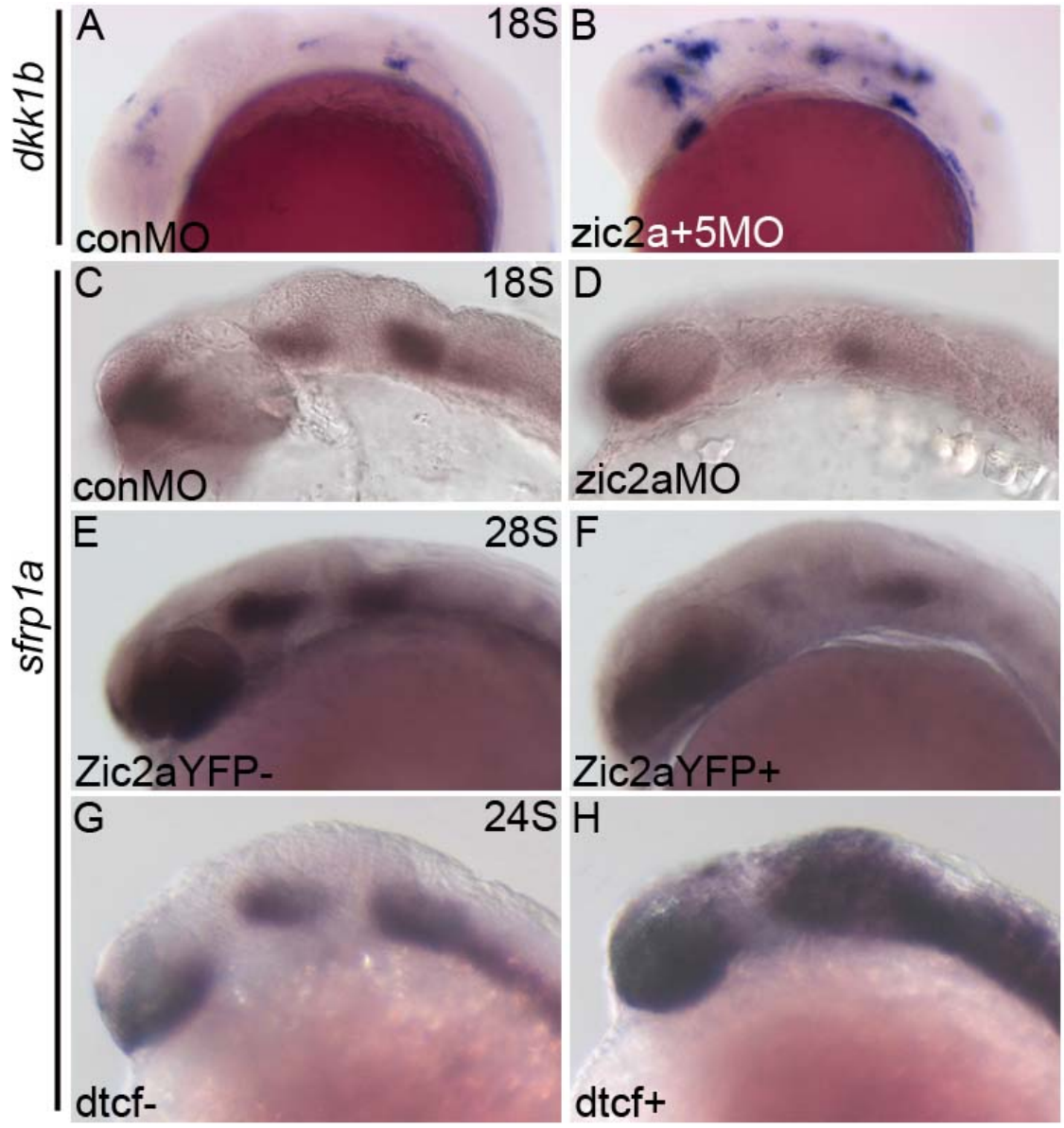

Figure 5. Expression of secreted Wnt pathway members in embryos with depleted or misexpressed Zic2a. (A,B) *Dkk1b* transcript is expressed in ectopic locations following depletion of Zic2a alone or together with Zic5 (29/31, 4 exp.). (C,D) *sfrp1a* expression is reduced in the ventral MB of zic morphants (17/23, 1 exp.). (E,F) Expression of Zic2aYFP also results in reduction of *sfrp1a* transcripts in the ventral MB and hindbrain (19/19, 1 exp.). (G,H) Following inhibition of Wnt signaling, *sfrp1a*

expression expands into the dorsal brain (23/23, 2 exp.). All views are lateral with anterior to the left.

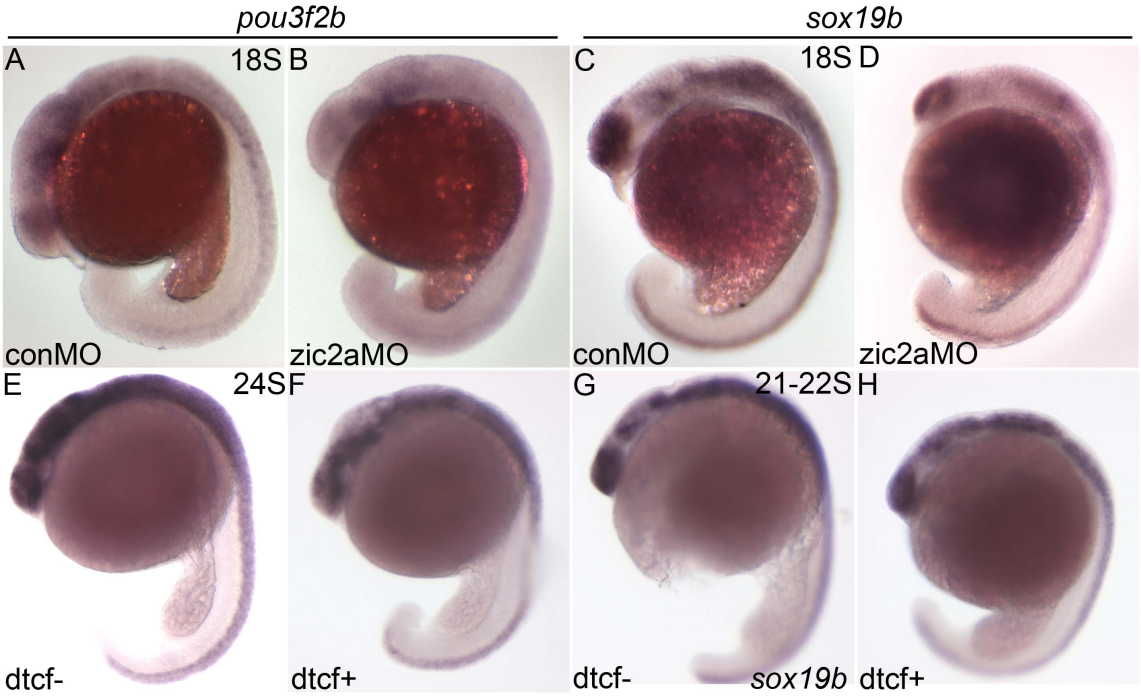

Figure 6. Expression of pro-proliferation transcription factors in zic2a morphants. (A,B) Expression of *pou3f2b* is mildly downregulated following Zic2a depletion (21/21, 2 exp.). (C,D) *Sox19b* expression is mildly downregulated following Zic2a depletion (5/10, 2 exp.). (E,F) Inhibition of Wnt signaling also causes a reduction in dorsal MB expression of *pou3f2b* (7/9, 1 exp.). (G,H) Inhibition of Wnt signaling results in reduced expression of *sox19b* (13/16, 1 exp.). All views are lateral with anterior to the left.

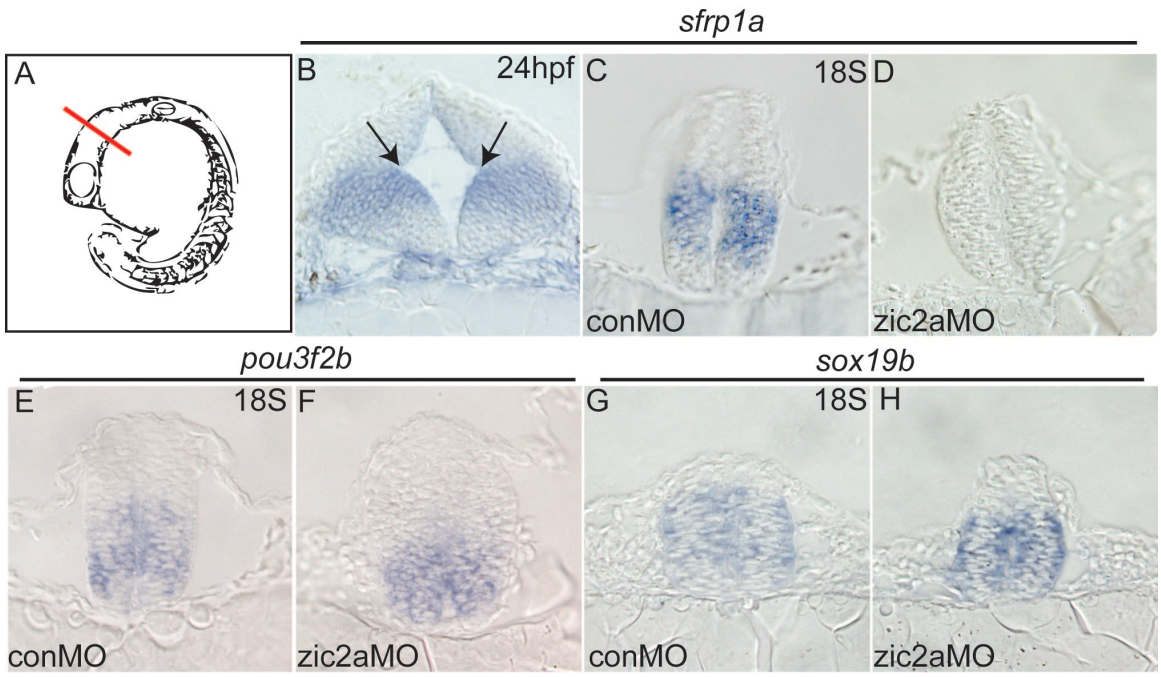

Figure 7. Restriction of several Wnt pathway interacting genes along the dorsal-ventral axis of the neural tube. (A) Cartoon demonstrating transverse sections through the midbrain. (B) *Sfrp1a* expression is restricted ventral to DLHPs in the MB (3/3, 1 exp.). (C,D) Zic2a depletion reduces *sfrp1a* expression in the ventral MB (2/3, 1 exp.). (E,F) *Pou3f2b* expression is restricted to the ventral MB in control morphants (2/2, 1 exp.). Zic2a depletion has no effect on *pou3f2b* transcript levels in the MB (3/3, 1 exp.). (G,H) *Sox19b* is expressed throughout the MB of control morphants, excluding the alar and floor plate (1/1, 1 exp.). *Sox19b* expression is variably affected in zic2a morphants (reduced in 1/2, 1 exp.).

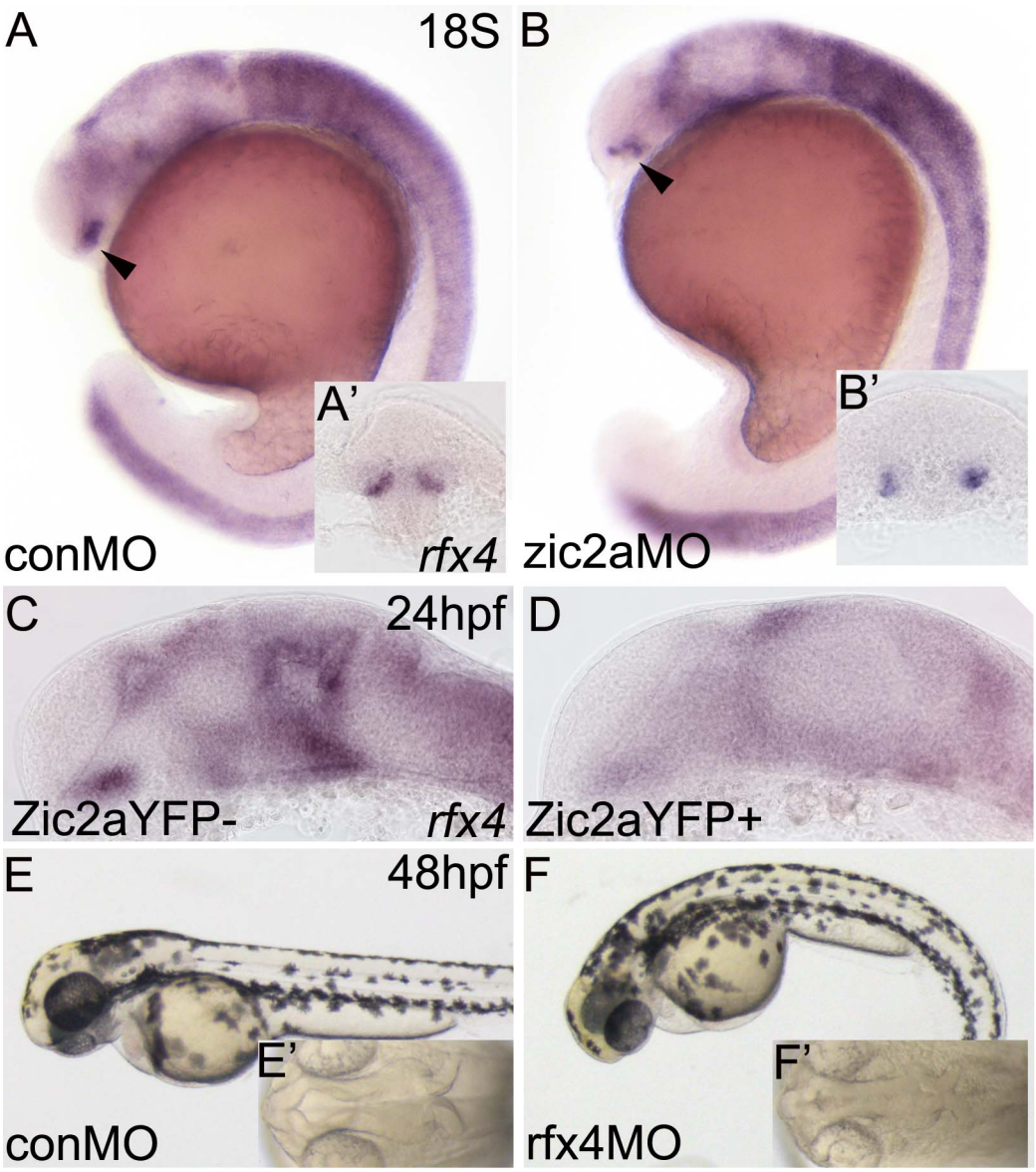

Figure 8. *Rfx4* expression and knockdown phenotype. (A,B) Expression of *rfx4* is mildly reduced in some embryos (20/73), (A',B') but more frequently mispatterned in the diencephalon (58/70, 3 exp.). (C,D) Forebrain expression of *rfx4* is reduced (6/23) or ablated (16/23, 2 exp.) in embryos expressing Zic2aYFP. (E,F) Rfx4 knockdown causes a curvature along the A/P axis (50/74, 4 exp.) and (E',F') occasionally defects in

ventricle shape (11/73, 4 exp.). A-F are lateral views, E',F' are dorsal views with anterior to the left. A', B' are transverse sections through the forebrain.

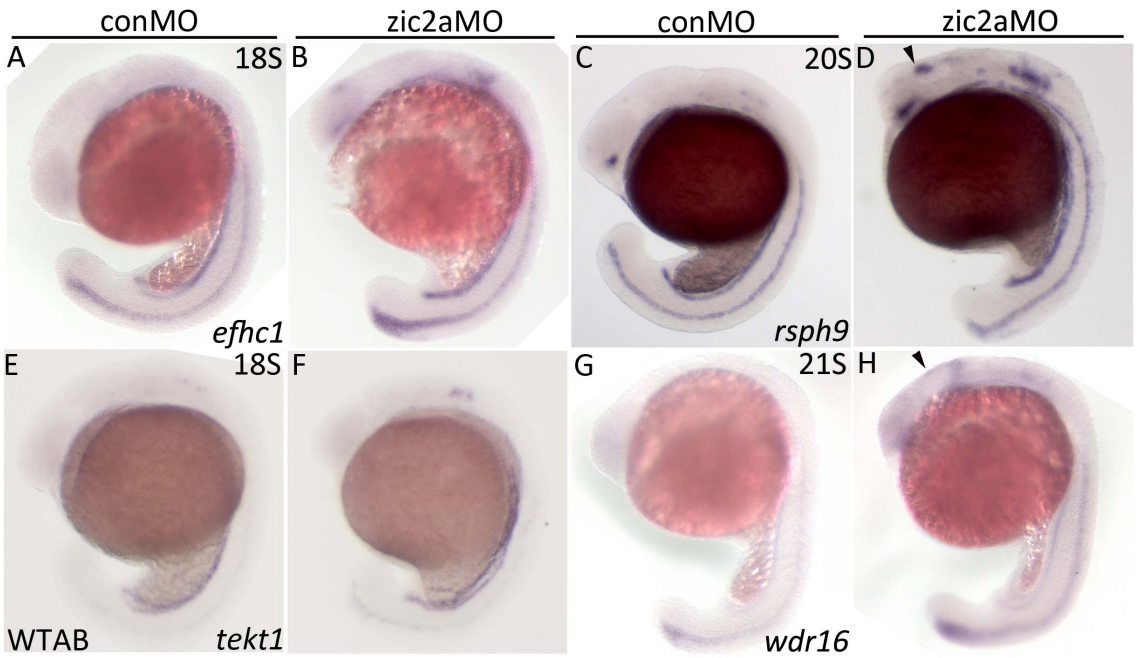

Figure 9. The motile ciliogenic program in zic2a morphants. (A,B) *Efhc1* is upregulated (35/39) and ectopically expressed (21/39, 2 exp.) in zic morphants. (C,D) *Rsph9* is upregulated and ectopically expressed (89/104, 5 exp.) in zic2a morphants. (E,F) *Tekt1* expression is increased in zic2a/zic5 morphants (23/40, 2 exp.). (G,H) *Wdr16* is upregulated in endogenous domains (14/39) and expressed ectopically (15/39, 2 exp.) in zic2a morphants. All views are lateral with anterior to the left.

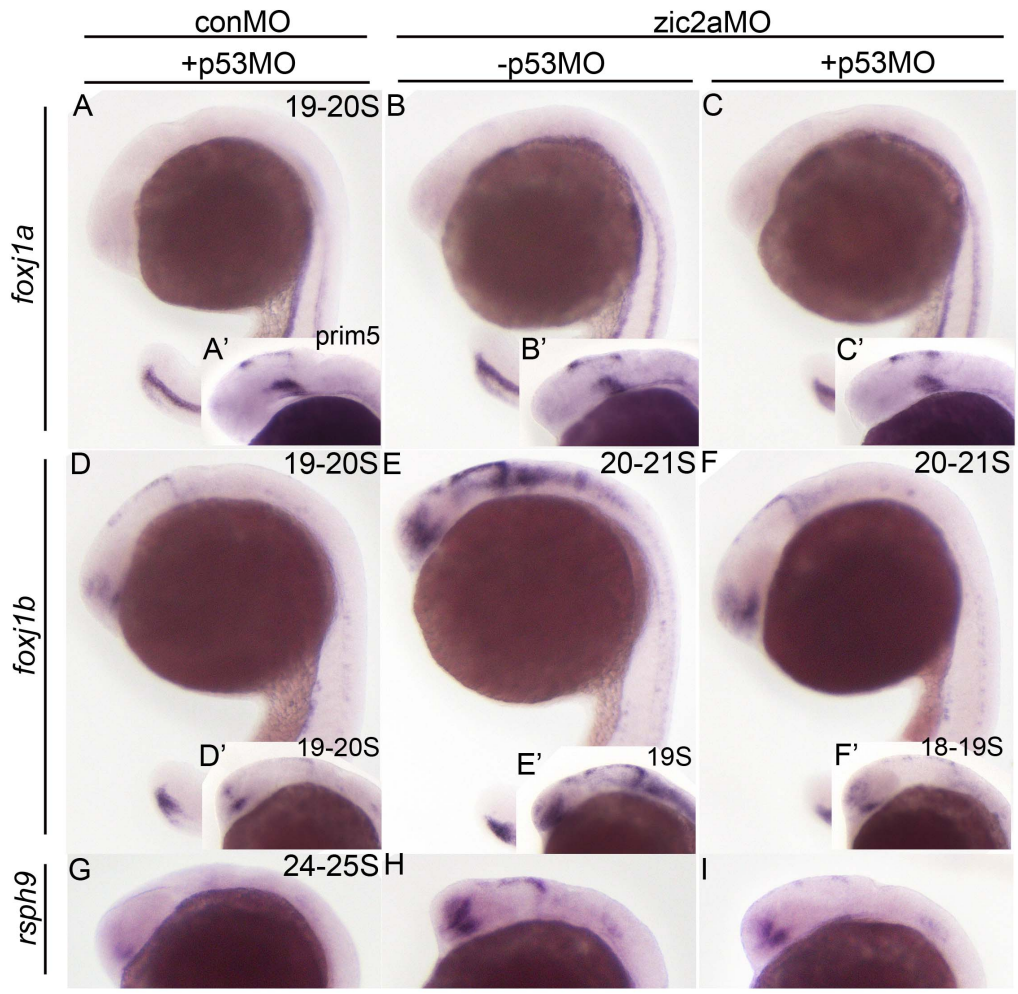

Figure 10. *Foxj1* transcription factors in zic2a morphants. (A-C) Zic2a depletion does not cause ectopic *foxj1a* expression, regardless of p53MO coinjection (-p53MO: 24/24 WT, +p53MO: 19/19 WT, 2 exp). (A'-C') *Foxj1a* is similarly unchanged in embryos injected with zic2aMO targeting the translational start site (-p53MO: 12/20 WT; +p53MO: 21/21 WT, 1exp.). (D-F) *Foxj1b* expression is strongly increased in zic2a morphants alone (85/85, 5 exp.). In the presence of p53MO, that response is reduced (25/62, 4 exp.). (D'-F') *Foxj1b* expression is strongly increased in zic2a morphants injected with translation-blocking MO (35/35, 2 exp.), a response that is prevented by coinjection of p53MO (24/29 WT, 2 exp.). (G-I) The ectopic expression of *rsph9*

transcript in zic2a morphants is reduced by coinjection of p53MO (-p53MO: 15/104 WT, 5 exp., +p53MO: 33/36 WT, 2 exp.). All views are lateral with anterior to the left.

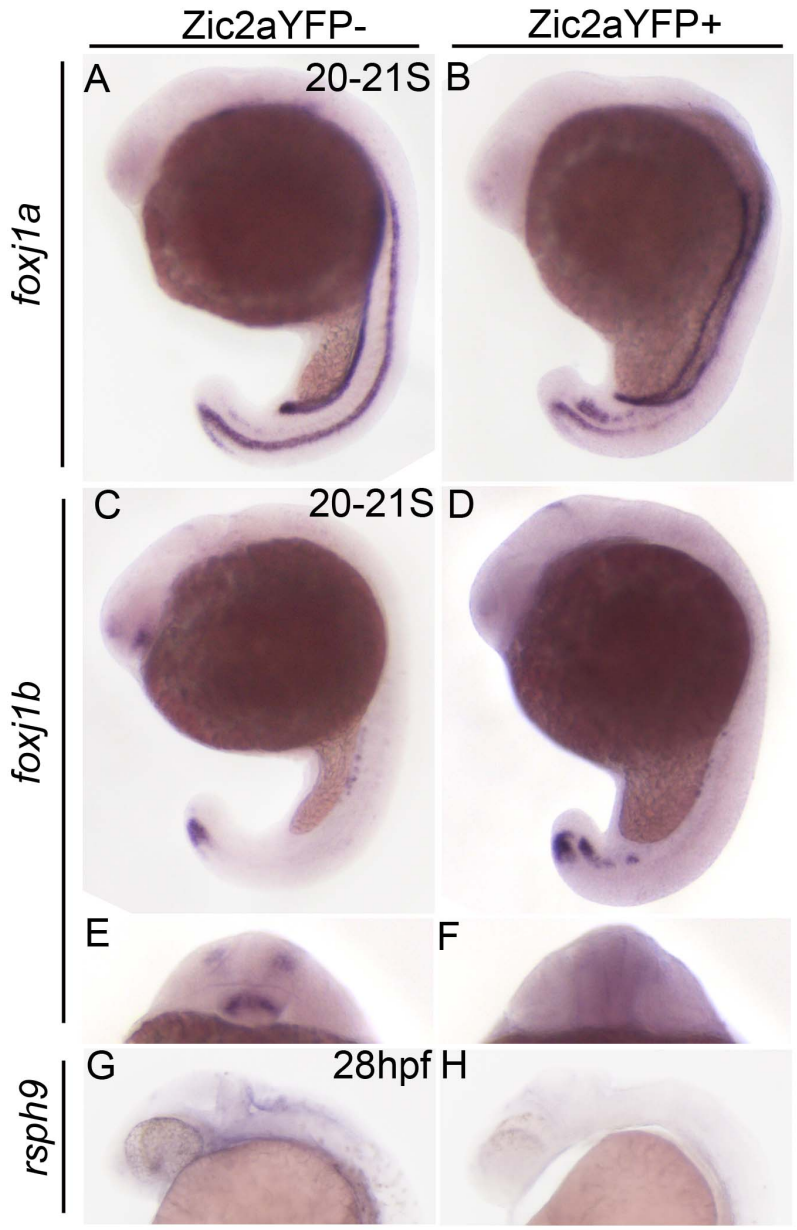

Figure 11. Motile cilia gene expression is reduced in embryos misexpressing Zic2aYFP. (A,B) *Foxj1a* expression is reduced throughout the ventral brain of Zic2aYFP-expressing embryos (22/22, 1 exp.). (C-F) *Foxj1b* expression is reduced in the forebrain and ectopically expressed in the posterior tail bud region of Zic2aYFP-expressing embryos (11/15, 1 exp.). (G,H) *Rsph9* expression is reduced (9/48) or

ablated in Zic2aYFP-expressing embryos (37/48, 3 exp.). A-D, G,H are lateral views with anterior to the left. E,F are transverse cross sections through the forebrain.